



UNIFORMED SERVICES UNIVERSITY OF THE HEALTH SCIENCES
F. EDWARD HÉBERT SCHOOL OF MEDICINE
4301 JONES BRIDGE ROAD
BETHESDA, MARYLAND 20814-4799



GRADUATE PROGRAMS IN
THE BIOMEDICAL SCIENCES
AND PUBLIC HEALTH

Ph.D. Degrees

Interdisciplinary
-Emerging Infectious Diseases
-Molecular & Cell Biology
-Neuroscience

Departmental
-Clinical Psychology
-Environmental Health Sciences
-Medical Psychology
-Medical Zoology

Physician Scientist (MD/Ph.D.)

Doctor of Public Health (Dr.P.H.)

Master of Science Degrees

-Public Health

Masters Degrees

-Military Medical History
-Public Health
-Tropical Medicine & Hygiene

Graduate Education Office

Eleanor S. Metcalf, Ph.D., Associate Dean
Bettina Arnett, Support Specialist
Roni Bull, Support Specialist

Web Site

<http://www.usuhs.mil/graded/>
http://usuhs.mil/geo/gradpgm_index.html

E-mail Address

graduateprogram@usuhs.mil

Phone Numbers

Commercial: 301-295-9474
Toll Free: 800-772-1747
DSN: 295-9474
FAX: 301-295-6772

August 13, 2009

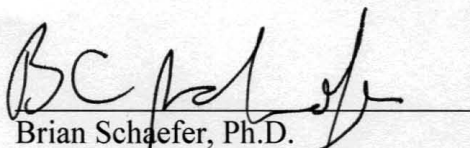
DISSERTATION APPROVAL SHEET
FOR THE DOCTORAL DISSERTATION
IN THE EMERGING INFECTIOUS DISEASES
GRADUATE PROGRAM

Title of Dissertation: "Investigating the Anti-apoptotic Effects of
Shigella flexneri Infection in Epithelial Cells"

Name of Candidate: Christina S. Faherty
Doctor of Philosophy Degree
8/26/09

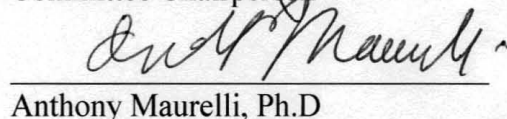
DISSERTATION AND ABSTRACT APPROVED:

DATE:


Brian Schaefer, Ph.D.

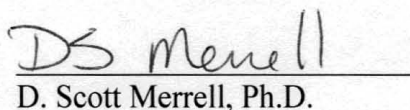
Department of Microbiology and Immunology
Committee Chairperson

8/26/09


Anthony Maurelli, Ph.D.

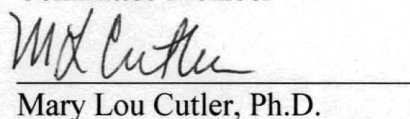
Department of Microbiology and Immunology
Dissertation Advisor

08-26-09


D. Scott Merrell, Ph.D.

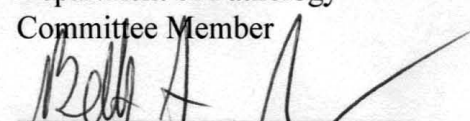
Department of Microbiology and Immunology
Committee Member

8/26/09


Mary Lou Cutler, Ph.D.

Department of Pathology
Committee Member

8/26/09


Beth McCormick, Ph.D.

University of Massachusetts Medical School
Department of Molecular Genetics and Microbiology
Committee Member

8/26/09

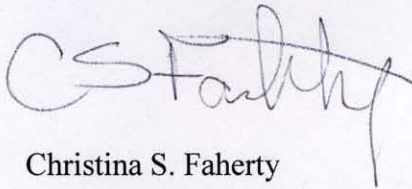
Report Documentation Page				Form Approved OMB No. 0704-0188	
Public reporting burden for the collection of information is estimated to average 1 hour per response, including the time for reviewing instructions, searching existing data sources, gathering and maintaining the data needed, and completing and reviewing the collection of information. Send comments regarding this burden estimate or any other aspect of this collection of information, including suggestions for reducing this burden, to Washington Headquarters Services, Directorate for Information Operations and Reports, 1215 Jefferson Davis Highway, Suite 1204, Arlington VA 22202-4302. Respondents should be aware that notwithstanding any other provision of law, no person shall be subject to a penalty for failing to comply with a collection of information if it does not display a currently valid OMB control number.					
1. REPORT DATE 13 AUG 2009		2. REPORT TYPE		3. DATES COVERED 00-00-2009 to 00-00-2009	
4. TITLE AND SUBTITLE Investigating The Anti-apoptotic Effects Of Shigella Flexneri Infection In Epithelial Cells				5a. CONTRACT NUMBER	
				5b. GRANT NUMBER	
				5c. PROGRAM ELEMENT NUMBER	
6. AUTHOR(S)				5d. PROJECT NUMBER	
				5e. TASK NUMBER	
				5f. WORK UNIT NUMBER	
7. PERFORMING ORGANIZATION NAME(S) AND ADDRESS(ES) Uniformed Services University of the Health Sciences,4301 Jones Bridge RD,Bethesda,MD,20814				8. PERFORMING ORGANIZATION REPORT NUMBER	
9. SPONSORING/MONITORING AGENCY NAME(S) AND ADDRESS(ES)				10. SPONSOR/MONITOR'S ACRONYM(S)	
				11. SPONSOR/MONITOR'S REPORT NUMBER(S)	
12. DISTRIBUTION/AVAILABILITY STATEMENT Approved for public release; distribution unlimited					
13. SUPPLEMENTARY NOTES					
14. ABSTRACT Shigella flexneri is a Gram-negative, facultative intracellular pathogen that causes bacillary dysentery by invading the colonic epithelium. Previous research has shown that Shigella induces a rapid cell death in macrophages. In infected epithelial cells however only a stress response is observed and the eukaryotic cells remain viable during infection. Since S. flexneri utilizes epithelial cells for replication and survival, the hypothesis of this dissertation is that S. flexneri inhibits apoptosis in epithelial cells in order to establish a replicative niche inside the host. An apoptosis assay was developed by adding staurosporine, a chemical inducer of the intrinsic pathway of apoptosis, to the standard invasion assay.					
15. SUBJECT TERMS					
16. SECURITY CLASSIFICATION OF:			17. LIMITATION OF ABSTRACT Same as Report (SAR)	18. NUMBER OF PAGES 308	19a. NAME OF RESPONSIBLE PERSON
a. REPORT unclassified	b. ABSTRACT unclassified	c. THIS PAGE unclassified			

Copyright Statement

The author hereby certifies that the use of any copyrighted material in the thesis manuscript entitled:

“Investigating the Anti-Apoptotic Effects of *Shigella flexneri* Infection in Epithelial Cells”

is appropriately acknowledged and, beyond brief excerpts, is with the permission of the copyright owner.

A handwritten signature in dark ink, appearing to read 'CS Faherty', with a stylized, cursive script.

Christina S. Faherty

Department of Microbiology and Immunology

Uniformed Services University of the Health Sciences

Abstract

Title of Dissertation:

Investigating the Anti-Apoptotic Effects of *Shigella flexneri* Infection in
Epithelial Cells

Christina S. Faherty, Doctor of Philosophy, 2009

Thesis directed by:

Anthony T. Maurelli, Ph.D.

Professor, Department of Microbiology and Immunology

Shigella flexneri is a Gram-negative, facultative intracellular pathogen that causes bacillary dysentery by invading the colonic epithelium. Previous research has shown that *Shigella* induces a rapid cell death in macrophages. In infected epithelial cells however, only a stress response is observed and the eukaryotic cells remain viable during infection. Since *S. flexneri* utilizes epithelial cells for replication and survival, the hypothesis of this dissertation is that *S. flexneri* inhibits apoptosis in epithelial cells in order to establish a replicative niche inside the host. An apoptosis assay was developed by adding staurosporine, a chemical inducer of the intrinsic pathway of apoptosis, to the standard invasion assay. Results from the apoptosis assay demonstrated that *S. flexneri* consistently prevents apoptosis in HeLa cells by inhibiting caspase-3 activation in the

presence of staurosporine, despite the detection of both cytochrome *c* release from the mitochondria and caspase-9 activation. *S. flexneri* is the first bacterial pathogen identified to be able to inhibit caspase-3 activation directly. In order to compare the changes in apoptosis-specific gene expression in infected and uninfected cells, both in the presence and absence of staurosporine, a microarray analysis was performed. *S. flexneri* induces many pro-survival changes upon infection including increasing the expression of nuclear factor κ B, the jun oncogene, several members of the inhibitor of apoptosis gene family, and genes important for inhibiting the extrinsic pathway of apoptosis. The results indicated that *S. flexneri* blocks apoptosis at multiple checkpoints along both pathways to prevent apoptosis. Finally, this dissertation identified the *Shigella* factor responsible for apoptosis inhibition. A $\Delta spa15$ mutant is unable to inhibit apoptosis, and Spa15 secretion was detected for the first time in the Congo red secretion assay by constructing C-terminal hemagglutinin tags on *spa15*. Spa15 secretion is dependent on the type-III secretion system, and occurs during infection. The data presented here provide the basis for future experiments that will continue to demonstrate the unique ability of *S. flexneri* to inhibit apoptosis and will also serve as a basis to determine how *Shigella* differentiates between macrophages and epithelial cells. The inhibition of apoptosis is vital for pathogens, especially *Shigella*, to survive *in vivo*.

Investigating the Anti-Apoptotic Effects of *Shigella flexneri*

Infection in Epithelial Cells

By

Christina Suzanne Faherty

Dissertation submitted to the Faculty of the
Emerging Infectious Diseases Interdisciplinary Graduate Program
of the Uniformed Services University of the Health Sciences

F. Edward Hèbert School of Medicine

in partial fulfillment of the
requirements for the degree of

Doctor of Philosophy 2009

Dedications

To my husband, William, for all of your love, support, and laughter.

I could not have done this without you.

*To my parents, John and Suzanne Clark,
for always encouraging me to reach for the stars.*

*In loving memory of my grandfather, Joseph J. Selitto,
who shared my passion for science.*

Acknowledgements

To my thesis advisor, Dr. Anthony Maurelli, and to my thesis committee, thank you for your support, encouragement, and guidance.

To the members of the Maurelli lab, thank you for your assistance, advice, and the numerous jokes that helped me get through the many long days.

To my friends and fellow graduate students, thank you for your friendship, support, and laughter on this long journey.

To my family, especially my husband William and my parents, thank you for everything.

I really cannot thank you enough for all that you have done for me.

Table of Contents

APPROVAL SHEET	i
COPYRIGHT STATEMENT	ii
ABSTRACT	iii
TITLE PAGE.....	v
DEDICATIONS	vi
ACKNOWLEDGEMENTS.....	vii
LIST OF TABLES.....	xiii
LIST OF FIGURES	xiv
INTRODUCTION	1
<i>SHIGELLA FLEXNERI</i>	<i>1</i>
<i>The organism.....</i>	<i>1</i>
<i>Disease impact and transmission</i>	<i>3</i>
<i>Infection and pathogenicity.....</i>	<i>4</i>
<i>Treatment and vaccine development</i>	<i>8</i>
APOPTOSIS	10
APOPTOSIS AND INFECTION.....	15
<i>Protection of the mitochondria and prevention of cytochrome c release</i>	<i>21</i>
<i>Activation of cell survival pathways</i>	<i>23</i>
<i>Interaction with caspases.....</i>	<i>27</i>

<i>SHIGELLA FLEXNERI</i> AND APOPTOSIS.....	28
HYPOTHESIS AND SPECIFIC AIMS	30
REFERENCES	31
<i>SHIGELLA FLEXNERI</i> INHIBITS STAUROSPORINE-INDUCED APOPTOSIS IN EPITHELIAL CELLS	55
ABSTRACT	55
INTRODUCTION.....	56
MATERIALS AND METHODS	58
<i>Bacterial strains and growth conditions.....</i>	<i>58</i>
<i>Mutant construction.....</i>	<i>60</i>
<i>Apoptosis assay</i>	<i>62</i>
<i>Immunofluorescence.....</i>	<i>62</i>
<i>Protein sample preparation and Western blot analysis.....</i>	<i>63</i>
<i>Statistical analysis.....</i>	<i>65</i>
RESULTS.....	65
<i>Shigella flexneri inhibits staurosporine-induced apoptosis.....</i>	<i>65</i>
<i>Shigella flexneri prevents the activation of caspase-3 in the presence of staurosporine.....</i>	<i>69</i>
<i>Shigella flexneri does not prevent cytochrome c release or caspase-9 activation in the presence of staurosporine.....</i>	<i>73</i>
<i>HeLa cell protection from STS-induced apoptosis requires S. flexneri invasion,</i>	

<i>secretion, and MxiE-regulated gene products.....</i>	78
DISCUSSION.....	81
ACKNOWLEDGEMENTS.....	86
REFERENCES	87

**MICROARRAY ANALYSIS OF *SHIGELLA FLEXNERI*-INFECTED
EPITHELIAL CELLS IDENTIFIES HOST FACTORS IMPORTANT FOR
APOPTOSIS INHIBITION.....94**

ABSTRACT	94
BACKGROUND	95
RESULTS AND DISCUSSION	97

Uninfected HeLa cells with STS compared to uninfected HeLa cells..... 105

Shigella-infected HeLa cells compared to uninfected HeLa cells. 105

*Shigella-infected HeLa cells treated with STS compared to uninfected HeLa
cells treated with STS.....* 116

*Shigella-infected HeLa cells treated with STS compared to Shigella-infected
HeLa cells.* 125

In situ hybridization analysis to confirm the microarray results. 127

CONCLUSION..... 130

MATERIALS AND METHODS..... 132

Bacterial strains used and growth conditions. 132

Immunofluorescence analysis. 133

Apoptosis assay and RNA isolation. 133

<i>Microarray hybridization and analysis.</i>	134
<i>In situ hybridization analysis.</i>	135
ACKNOWLEDGEMENTS	138
REFERENCES	138
 SPA15 OF <i>SHIGELLA FLEXNERI</i> IS SECRETED THROUGH THE TYPE-III SECRETION SYSTEM AND PREVENTS STAUROSPORINE-INDUCED APOPTOSIS.220	
ABSTRACT	220
INTRODUCTION.....	221
MATERIALS AND METHODS	223
<i>Bacterial strains and growth conditions.</i>	223
<i>Strain and plasmid construction.</i>	223
<i>Virulence assays.</i>	228
<i>Congo red secretion assay.</i>	229
<i>Immunofluorescence and Western blot analysis.</i>	229
<i>Statistical analysis.</i>	230
RESULTS	231
<i>Identifying spa15 as the anti-apoptosis gene.</i>	231
<i>Spa15 is secreted into the cytoplasm of the host cell.</i>	239
<i>Spa15 secretion is delayed in the $\Delta mxiE$ mutant.</i>	247
DISCUSSION	251
ACKNOWLEDGEMENTS	259

REFERENCES	260
DISCUSSION	269
PREFACE.....	269
DISCUSSION AND SIGNIFICANCE OF FINDINGS.....	270
<i>Shigella flexneri</i> inhibits apoptosis in epithelial cells.	270
<i>The microarray analysis provides further insights into apoptosis inhibition.</i>	273
<i>Identification of the Shigella factor responsible for apoptosis inhibition.</i>	278
ADDITIONAL STUDIES	282
<i>The disparate response of Shigella to macrophages and epithelial cells</i>	282
<i>In vivo conditions and apoptotic stimuli.</i>	284
CONCLUSION.....	285
REFERENCES	287

List of Tables

Table 1. Classification of bacteria that inhibit apoptosis.....	17
Table 2. Strains and plasmids used in this study.....	59
Table 3. Primers used in this study.....	61
Table 4. Cell counts of apoptosis assay experiments.	68
Table 5. A selection of upregulated genes in wildtype-infected cells compared to uninfected cells.....	111
Table 6. A selection of upregulated genes in wildtype-infected cells with staurosporine compared to uninfected cells with staurosporine.	122
Table 7. Probes and sequences used for the in situ hybridization experiments.	137
Supplementary Table 1. Data for spots that show statistically significant differences in the indicated pairwise analyses.	156
Supplementary Table 2. Lists of genes in all comparisons categorized by function.	195
Table 8. Strains and plasmids used in this study.....	224
Table 9. Primers used in this study.....	226
Table 10. <i>Shigella</i> genes analyzed that had no effect on apoptosis protection.	233

List of Figures

Figure 1. The apoptosis pathways.	14
Figure 2. Mechanisms by which bacterial pathogens inhibit apoptosis at different points along the apoptotic pathway.	20
Figure 3. <i>Shigella flexneri</i> protects HeLa cells from staurosporine-induced apoptosis. ...	67
Figure 4. Activated caspase-3 is not present in <i>Shigella</i> -infected cells after staurosporine treatment.	70
Figure 5. Western blot analysis for the activation of caspase-3.....	72
Figure 6. Cytochrome <i>c</i> release occurs in infected cells after staurosporine treatment. ...	75
Figure 7. Western blot analysis of caspase-9 activation.	77
Figure 8. <i>Shigella flexneri</i> mutants analyzed in the apoptosis assay.....	80
Figure 9. Immunofluorescence analysis of HeLa cells treated with staurosporine.	99
Figure 10. Schematic of the infections and treatment conditions used in this study.	103
Figure 11. Cluster diagram of significant genes across treatment groups.	104
Figure 12. Model of apoptosis inhibition by <i>Shigella flexneri</i> at multiple checkpoints in epithelial cells.....	108
Figure 13. Infected cells resist apoptosis induction via the extrinsic pathway.	112
Figure 14. Venn diagram comparing Uninfected versus Wildtype-infected to Uninfected cells treated with staurosporine versus Wildtype-infected cells treated with staurosporine.	117

Figure 15. Comparison of the microarray and in situ hybridization results.	129
Figure 16. The $\Delta spa15$ mutant cannot prevent caspase-3 activation in HeLa monolayers treated with staurosporine.	235
Figure 17. BS902-infected cells are apoptotic upon normal infection.	236
Figure 18. Western blot analysis for caspase-3 activation.....	238
Figure 19. Spa15 is secreted in the Congo red secretion assay.....	241
Figure 20. Spa15 secretion requires the type-III secretion system.....	244
Figure 21. Spa15 is secreted into the cytoplasm of infected epithelial cells.	246
Figure 22. Spa15 secretion in the $\Delta mxiE$ mutant.....	250
Figure 23. Model of Spa15 function in the eukaryotic cell.	258

Chapter One

Introduction

Shigella flexneri

The organism

Shigella flexneri is a Gram-negative facultative intracellular bacterial pathogen that causes shigellosis or bacillary dysentery. The genus is comprised of four species, *S. dysenteriae* (serogroup A), *S. flexneri* (serogroup B), *S. boydii* (serogroup C), and *S. sonnei* (serogroup D). The O antigen on the lipopolysaccharide (LPS) defines the serogroups. *S. dysenteriae*, *S. flexneri*, and *S. boydii* are distinct from *S. sonnei* in that *S. sonnei* is positive in beta-D-galactosidase and ornithine decarboxylase reactions (76, 100). Kiyoshi Shiga isolated the first *Shigella* species, *S. dysenteriae* type 1, in Japan in 1896. Simon Flexner, J.S.K. Boyd, and Carl Sonne isolated similar organisms over the next 40 years, leading to the placement of the group in the genus *Shigella* by the 1950s (76). Prior to the 1960s, it was believed that *Shigella* caused infection by adhering to the surface of intestinal epithelial cells and induced damage through the use of an endotoxin (39). It was not until 1964 that LaBrec, et al. and Voino-Tasenetsky et al. established that *Shigella* penetrates the intestinal mucosa to cause disease (39, 58, 110). Extensive research attempted to identify the genetic basis of virulence throughout the 1960s and 1970s. The identification of the virulence plasmid and the demonstration that *Shigella* virulence requires this large plasmid occurred in the early 1980s (94-96). Since that time,

extensive studies have been performed to characterize the genes on the virulence plasmid (39, 100). The disease burden and global impact of shigellosis serve as the rationale for research that will enhance our understanding of the pathogen and the mechanisms by which it causes disease. The goal of these research efforts is to develop safe, effective treatments and vaccines.

From an evolutionary viewpoint, *Shigella* is highly related to *Escherichia coli*; and based on sequencing of housekeeping genes, *Shigella* species can be considered to be clones of *E. coli*. The *Shigella* species evolved from multiple *Escherichia coli* ancestors by obtaining the virulence plasmids and pathogenicity islands (86, 90). Following the acquisition of these factors, the different species of *Shigella* negatively selected (deleted or inactivated) many genes from the commensal *E. coli* ancestors that interfered with the new pathogenic potential of the organism. These alterations were independent events (20, 70). Therefore, the four species of *Shigella* result from independent, convergent evolution from *E. coli* to give rise to the current *Shigella* species classification (86, 90).

Interestingly, the pathogenic enteroinvasive *E. coli* (EIEC) is very similar to *Shigella*, and was originally classified under the *Shigella* genus (60). Both EIEC and *Shigella* harbor a virulence plasmid of approximately 220 kilobases (kb) and both utilize fewer substrates compared to commensal *E. coli* (60). Extensive analysis comparing housekeeping and virulence gene sequences have shown that both *Shigella* and EIEC can be classified as a distinct, invasive pathovar within *E. coli*. However, *Shigella* forms a distinct clustering group from EIEC (60). This distinction between EIEC and *Shigella* is supported by observations that most EIEC strains are less virulent and some EIEC strains have retained motility and the ability to ferment lactose (3, 9). In addition, EIEC can

ferment mucate and utilize L-serine, D-xylose, and sodium acetate (60). These distinctions, especially in regards to virulence, have kept *Shigella* separate from EIEC in taxonomic classifications.

Disease impact and transmission

Shigella causes a significant global health burden, especially in developing countries. There are approximately 165 million annual cases of bacillary dysentery leading to over 1 million deaths (45). Most cases take place in the developing world where 70 percent of infections occur in children under the age of 5 (98). However, during epidemics of *S. dysenteriae* type 1, adults are affected as much as children (76). Poor sanitation, malnutrition, contaminated food or water, and inadequate medical treatment are the main causes of the high incidence in the developing world. Fecal-oral transmission is the most common form of exposure to the bacteria, and transmission increases with poor hygiene and close contact (45). *Shigella* is highly contagious since as little as 10 to 100 bacilli can cause disease. However, most infections require an infectious dose of 500 organisms, which represents the inoculum that causes disease in 50% of volunteers (23). The majority of cases of shigellosis occur in endemic areas, and *S. flexneri* causes the most mortality in these regions (45). The predominant serotypes of *S. flexneri* in endemic areas are 1b, 2a, 3a, 4a, and 6 with serotype 2a causing 32 – 58% of the infections. In addition, *S. flexneri* serotype 2a most often occurs in outbreaks in industrialized nations (55). *S. sonnei* infection also occurs in industrialized countries and is responsible for 75% of the annual cases in the United States. *S. sonnei* is transmitted by the consumption of undercooked food and contaminated water (76). *S. dysenteriae* type 1 infection occurs in endemic regions in developing countries, but is responsible for most

of the epidemic outbreaks in Africa, Asia, and Central America. In these regions the population is susceptible to infection due to natural disasters or political turmoil, resulting in high rates of infection and death (55). Interestingly, *S. boydii* was originally isolated in India and rarely occurs in infections outside of India (76).

Infection and pathogenicity

Disease is due to the ability of the pathogen to invade the colonic epithelium. Clinical symptoms of disease include fever, watery diarrhea, fatigue, and malaise. Patients typically progress to dysentery where the symptoms become more severe and typically include bloody, mucoid stools and abdominal cramps (76). The organism generally does not disseminate and remains limited to the intestinal mucosa (93). Most infections resolve in 5 to 7 days, but life-threatening complications occur in malnourished children and include dehydration, hypoglycemia, and intestinal perforation (76).

The symptoms of dysentery are due to an intense inflammatory reaction to the bacteria. *Shigella* cannot invade the apical side of the colonic epithelium, and therefore, must first transit from the intestinal lumen through the microfold or membranous cells (M cells), which are specialized epithelial cells that collect antigens from the intestinal environment and deliver them to the underlying mucosal lymphoid tissue for antigen presentation to macrophages and lymphocytes (45). After transit through the M cells, the bacteria encounter the resident macrophages in the sub-mucosa, where the bacteria are engulfed by these immune cells. *Shigella* induces cell death to escape macrophage killing and concurrently causes the release of cytokines interleukin (IL)-1 β and IL-18 from the macrophages. IL-1 β triggers the recruitment of polymorphonuclear (PMN) cells to the site of infection while IL-18 promotes the production of interferon gamma (IFN- γ) by

natural killer (NK) cells and T lymphocytes (100). After escaping the macrophage, the bacteria can then invade the basolateral face of the colonic epithelium. In addition, recent evidence suggests that *Shigella* can disrupt the tight junctions between the colonic epithelial cells from the apical surface to gain access to the basolateral pole of the cells for invasion (92).

At the basolateral surface, *Shigella* requires genes on the 220-kb virulence plasmid to invade the host cells. Encoded in the *mxi-spa* operon on the plasmid is a type-III secretion system (T3SS) (100). The system is an effective means for delivering bacterial proteins from the cytoplasm of the bacterial cell across the inner membrane, periplasm, peptidoglycan layer, and outer membrane into the cytoplasm of host cells. The system is comprised of a needle complex that has a cytoplasmic C ring, a seven-ringed basal body, and a protruding needle (18, 100). The cytoplasmic C ring associates with the portion of the basal body that is located on the inner membrane of the cell wall to control the assembly of the needle, to provide energy for secretion, to mediate the recognition of substrates, to release chaperones from the substrates, and to unfold the substrates for secretion. The basal body has an average length of 32 nanometers (nm) and a diameter of approximately 20 to 40 nm (18, 100, 104). The basal body spans the inner membrane, periplasm, peptidoglycan layer, and outer membrane of the bacterial cell to provide support for the needle. The needle, which is assembled after the basal body is constructed, is a helical polymer approximately 45 to 60 nm in length with a diameter of 7 nm that extends into the extracellular space. The channel within the needle is 2 to 3 nm wide to allow the partially folded effector proteins to pass (18, 100, 104). Prior to contact with the colonic epithelium or in the absence of a secretion signal, the IpaB and IpaD

proteins associate at the tip of the needle and form a plug to block the secretion of proteins required for invasion until the host cell or a proper secretion signal are encountered (24, 72).

Expression of genes on the virulence plasmid is affected by many environmental changes with temperature being the predominant factor. Optimal expression also requires a neutral pH of 7.4 (22). The T3SS needle complex is synthesized and assembled at 37°C, the temperature shift that occurs upon entry into the host (100). The transcriptional activator VirF is encoded on the virulence plasmid and induced at 37°C. VirF in turn activates the second plasmid regulator VirB to induce the transcription of the *mxi-spa* operon, which results in the expression of the genes required for invasion (69, 106).

The secretion of proteins required for invasion of the colonic epithelium is induced upon contact of the bacteria with the host cells. This contact induces a conformational change in IpaD to allow the IpaB and IpaC proteins to associate with the host cell membrane (24, 84). The IpaB and IpaC proteins bind to the $\alpha_5\beta_1$ integrin and CD44 receptors on the host cell surface (101, 113). The IpaB/IpaC complex also forms pores in the host cell membrane to allow entry of additional bacterial proteins required for invasion (12). Along with IpaC, IpgB1 and VirA induce Rac1/Cdc-42-dependent actin polymerization to cause host membrane ruffles (40, 118). Meanwhile, IpaA binds to the host protein vinculin, which leads to the depolymerization of actin filaments (107). These host cytoskeletal rearrangements lead to the internalization of the bacteria through membrane engulfment (108). After engulfment, the bacteria are inside a vacuole that is subsequently lysed by IpaB, IpaC, and IpaD to allow the bacteria to enter the cytoplasm of the host cell. Once inside the cytoplasm, the bacteria utilize the IcsA protein to

mediate actin-based motility. IcsA localizes to one pole of the bacteria and induces actin polymerization. This polymerization allows the bacteria to spread within the epithelial cell and into adjacent cells without the need for the bacteria to enter the extracellular environment (8, 83). Furthermore, intracellular bacteria secrete additional proteins, termed T3SS effector proteins, through the T3SS into the cytoplasm of the epithelial cell to facilitate intracellular survival. The genes encoding these proteins are scattered throughout the 220-kb virulence plasmid, and only recently the function of these proteins inside the epithelial cell has started to be characterized (100).

Inside the epithelial cells, *Shigella* activates the ERK1/2 pathway through the *Shigella* effector proteins OspF and OspC1 to induce the expression of IL-8 and allow additional recruitment of PMNs to the site of infection (53, 71, 80, 122). The PMNs transit from the sub-mucosa and disrupt the tight junctions of the epithelial cells to enter the gut lumen. This PMN disruption, in conjunction with the tight junction disruption by *Shigella*, allows more bacteria to gain access to the basolateral pole of the epithelial cells for invasion (80, 92). The PMN infiltration is also what is responsible for the destruction of the colonic epithelium, which leads to the severe disease symptoms and impairs water and nutrient adsorption (45). The PMNs eventually kill extracellular bacteria to help resolve infection since the bacteria cannot escape the phagocytic vacuole of the PMNs (64). The IFN- γ produced by T cells and NK cells also facilitates bacterial clearance by activating macrophages. These activated macrophages are protected from *Shigella*-induced cell death and enhance macrophage killing of the pathogen (45, 114).

Treatment and vaccine development

Treatment of shigellosis requires oral rehydration therapy to prevent dehydration, and antibiotics are administered based on the susceptibility of the locally circulating strain (76). While antibiotic treatment is effective and reduces the amount of bacteria excreted from infected patients, increases in antibiotic resistance burden the limited health services in developing countries due to restricted availability of antibiotics (45). Historically, *S. flexneri* played an important role in the discovery of multiple drug resistance. By the middle of the 1940s, sulfonamides were most effective in treating *Shigella* infections in Japan, but by 1952 most isolates were resistant to the antibiotic. Extensive use of streptomycin, tetracycline, and chloramphenicol also led to highly resistant isolates of *Shigella*. Some of these isolates from Japan were even resistant to all four antibiotics by 1956. This high level of resistance led Tomoichiro Akiba and Kunitaro Ochiai to hypothesize that drug resistance was being transferred from *E. coli* to *Shigella* in the intestinal tracts of patients. At the time, it was believed that antibiotic resistance in bacteria was only due to genetic mutation and selection. The pivotal studies on *Shigella* by Akiba, et al. and Ochiai, et al. led Susumu Mitsuhashi, Tsutomu Watanabe, Rintaro Nakay, and their collaborators to demonstrate that resistance can occur by the transfer of genetic material, termed resistance or R factors, through bacterial conjugation (25). Today, resistance to sulfonamides, tetracyclines, and ampicillin occurs worldwide, and these drugs are not recommended for treatment of shigellosis. Despite the emergence of quinolone resistance, ciprofloxacin, levofloxacin, or norfloxacin can still be used to treat infections. Azithromycin can penetrate human cells, is effective against *Shigella in vitro*, and has been successful in treating infections (5, 34, 76).

Given the disease burden and the increase in antibiotic resistance, the development of a safe, effective vaccine is strongly desired. The major component of protective immunity to *Shigella* infection is a humoral immune response with most antibodies directed against the LPS and the Ipa proteins (45, 57, 82). Protection is mostly serotype specific since a majority of the anti-LPS antibodies are directed against the O antigen on the LPS, with serum immunoglobulin (Ig) G, serum IgM, and most importantly secretory IgA antibodies being the dominant antibodies generated (45, 82). Secretory IgA antibodies coat the outer membrane of the bacteria to prevent attachment and invasion to mucosal surfaces. Anti-LPS IgA has been detected in people recovering from *Shigella* infection. These antibodies have also been found in breast milk of convalescent mothers and most likely contribute to the reduction of disease severity in breast-fed infants (45). Unfortunately, natural infection does not provide long-term protection and is serotype specific due to the antibody response against LPS (82). Serum and mucosal antibodies directed against the *Shigella* Ipa invasion proteins have been detected in both adults and children. Interestingly, malnourished children with severe disease do not have mucosal IgA antibodies against the Ipa proteins, which suggests that these antibodies are important for reducing disease duration and severity (78).

Successful vaccines must induce a strong antibody response at the mucosal surface to generate long-lasting immunity (45). Early vaccine candidates were unsuccessful since they consisted of parenterally-injected inactivated bacteria and most likely failed to induce a strong mucosal response (45). Therefore, oral vaccination, which mimics the route of infection, is being used in the current attempts to generate a successful vaccine. At present, live attenuated vaccines in which mutations have been made in

metabolic and virulence genes in *Shigella* are being attempted with the belief that these strains can induce strong mucosal responses while not causing significant side effects (45, 57, 82). Other candidate vaccines include a subunit vaccine named Invaplex consisting of the IpaB protein, the IpaC protein, and LPS. Invaplex binds to mammalian cells and induces uptake to mimic invasive infection and generate a humoral response (109). In addition, current attempts are using mixtures of different *Shigella* serotypes with live, attenuated strains in order to generate a vaccine against multiple strains (57). As work toward a successful vaccine candidate continues, new insights into the pathogenesis of *Shigella* and the host immune response will guide researchers and eventually lead to the development of an effective vaccine.

Apoptosis¹

Apoptosis, or programmed cell death, is a natural phenomenon that occurs regularly in multicellular organisms during embryonic development. This form of cell death also removes damaged cells from tissues without causing an inflammatory response (44, 89). Apoptosis is characterized by DNA fragmentation, chromatin condensation, cytoplasmic shrinkage, and cell death without lysis or damage to neighboring cells. Apoptosis, which is activated by intrinsic and extrinsic pathways (Fig. 1), differs from other forms of cell death in that it does not cause damage to neighboring cells or induce an inflammatory response (27, 56). In the intrinsic pathway, certain apoptotic stimuli

¹ Excerpts taken from the review article: Faherty, C.S. and A.T. Maurelli. Staying alive: bacterial inhibition of apoptosis during infection. *Trends in Microbiology*. 2008 April;16(4):173-80.

alter the normal status of the Bcl-2 family of proteins. This family of proteins is defined by the presence of at least one Bcl-2 homology (BH) domain. The pro-survival proteins (Bcl-2, Bcl-x_L, Mcl-1, Bfl-1/A1, Bcl-w and Boo/Diva) comprise the Bcl-2 subfamily (19, 91). Bcl-2, Bcl-x_L and Bcl-w have a hydrophobic domain on the carboxyl terminus that targets the proteins to the cytoplasmic face of the outer mitochondrial membrane, the endoplasmic reticulum and the nuclear envelope. Bcl-2 is an integral membrane protein whereas Bcl-x_L and Bcl-w become tightly associated with these membranes only after a cytotoxic signal induces a conformational change in the proteins (19).

The pro-apoptotic proteins are broken down into two subfamilies: the Bax subfamily in which the proteins have multiple BH domains (Bax, Bak, Bok and Bcl-x_S) and the BH3-only subfamily, which comprise proteins with a single BH3 domain (Bid, Bad, Bmf, Bim, Bik, Puma, Hrk and Noxa) (19, 91). Both subfamilies of pro-apoptotic proteins are required for apoptosis initiation. The BH3-only proteins are direct antagonists and act by binding to and inhibiting the pro-survival proteins in response to apoptotic signals. Once the BH3-only proteins neutralize Bcl-2, Bcl-x_L and Bcl-w, the pro-apoptotic Bax and Bak proteins form heterodimers and homodimers within the mitochondrial membrane, which results in the release of cytochrome *c* and other pro-apoptotic factors (19, 91).

Once cytochrome *c* is released into the cytosol, it binds to the apoptosome (89), a complex of proteins made up of the apoptosis activating factor-1 (Apaf1) protein and the initiator caspase-9. A morphological change in the apoptosome results from cytochrome *c* binding, which causes caspase-9 to become activated. Caspase-9 activates caspase-3, leading to apoptosis (89). Caspase-3 is known as the executioner caspase, because it

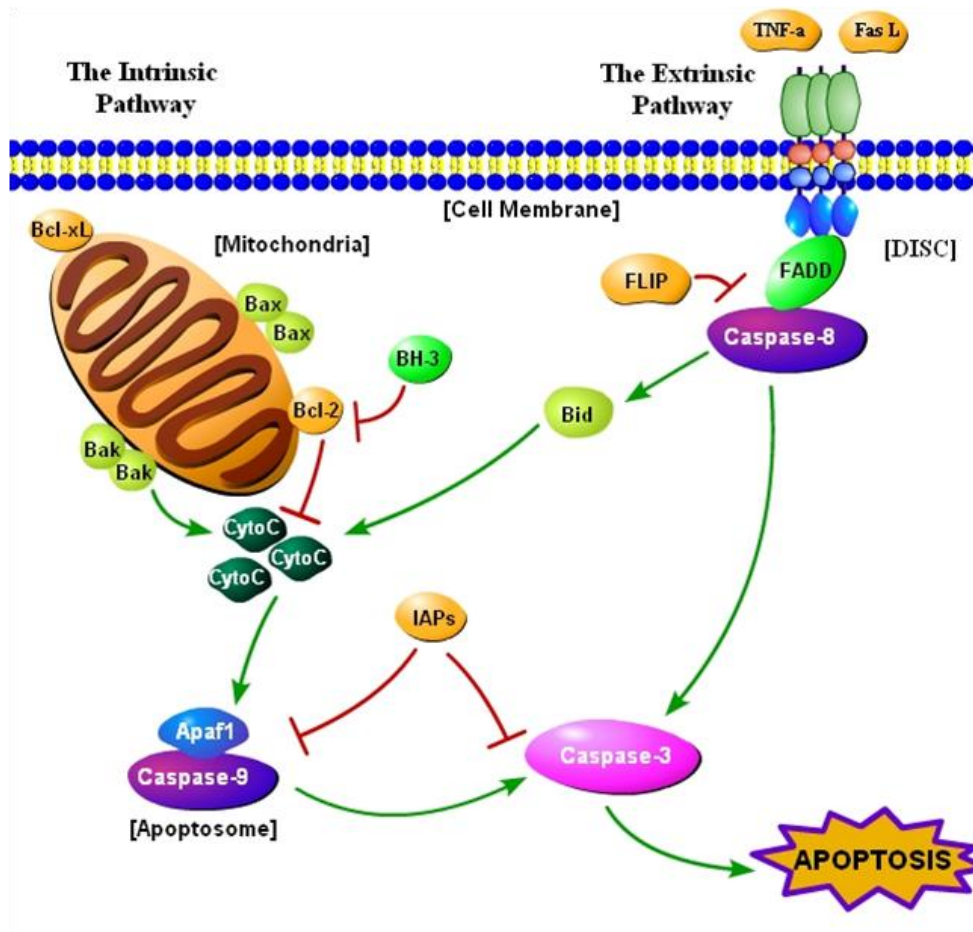
activates or cleaves various protein targets, which is detrimental to the cell and results in death (89). Activation of caspase-9 and caspase-3 is normally inhibited by a family of proteins known as the inhibitor of apoptosis proteins (IAPs), and XIAP (X-linked IAP) is the most potent IAP (89).

In the extrinsic pathway, ligands such as Fas ligand (FasL) or tumor necrosis factor α (TNF- α) bind to death receptors on the membrane of the host cell. Trimerization of the death receptors follows, forming what is known as the death-inducing signaling complex (DISC), which includes the Fas-associated death domain (FADD) adaptor protein, the Flice-like inhibitory protein (FLIP), and procaspase-8 (44). FLIP associates with caspase-8 at the DISC to inhibit activation. When caspase-8 is activated, it in turn directly activates caspase-3 (89). In addition, caspase-8 activates the pro-apoptotic protein Bid, which stimulates the intrinsic pathway to enhance the apoptotic signal, because Bid activation eventually leads to cytochrome *c* release (89).

Figure 1. The apoptosis pathways.

Apoptosis is activated by intrinsic and extrinsic pathways. In the intrinsic pathway, pro-apoptotic proteins (Bax and Bak) permeabilize the mitochondrial membrane, resulting in cytochrome *c* (CytoC) release. Cytochrome *c* binds to the apoptosome to cause caspase-9 activation. Caspase-9 in turn activates the caspase-3, leading to apoptosis. The inhibitor of apoptosis proteins (IAPs) can prevent activation of the caspases. In the extrinsic pathway, Fas ligand (FasL) and tumor necrosis factor α (TNF- α) bind to death receptors leading to the formation of the death-inducing signaling complex (DISC). The DISC contains the Fas-associated death domain (FADD) adaptor protein, the Flice-like inhibitory protein (FLIP), and procaspase-8. FLIP prevents caspase-8 activation. When caspase-8 is activated, it in turn directly activates caspase-3. In addition, caspase-8 activates the pro-apoptotic protein Bid, which causes cytochrome *c* release and activation of the intrinsic pathway. The green arrows indicate activation/progression of the pathways while the red lines indicate points of inhibition.

Figure 1. The apoptosis pathways.



Faherty and Maurelli (2008). Trends Microbiol. **16**:173-180.

*Apoptosis and Infection*²

Bacteria, viruses (41) and parasites (15) can either induce or prevent apoptosis to augment infection. Many bacterial pathogens that cause apoptosis target immune cells such as macrophages (120) and neutrophils (13) because these cells would otherwise kill the pathogens (35, 52). *Yersinia enterocolitica*, *Y. pestis*, and *Y. pseudotuberculosis* induce apoptosis in macrophages through the Yop T3SS effector proteins. The proteins inhibit cell survival pathways and activate caspases (35). Uropathogenic *E. coli* and *Mycobacterium tuberculosis* induce apoptosis in neutrophils by increasing reactive oxygen species, which is known to induce the intrinsic pathway of apoptosis (13, 81). Other bacterial pathogens can induce apoptosis in epithelial cells. For example, *Pseudomonas aeruginosa* induces apoptosis in the lung epithelium by upregulating the CD95 and CD95 ligand to cause caspase-8 and caspase-3 activation. Interestingly, the apoptosis in *P. aeruginosa* infection enhances the immune system clearance of the pathogen since CD95 or CD95 ligand deficient mice are unable to clear the bacteria and succumb to infection (35). Grassmé et al. hypothesized that the apoptosis induction by *P. aeruginosa* triggers the immune cells to phagocytose the apoptotic cells, which subsequently kills the bacteria (35). While *Pseudomonas*-induced apoptosis assists the host immune response to the infectious agent, most bacterial-induced apoptosis benefit the pathogen and enhance infection.

² Excerpts taken from the review article: Faherty, C.S. and A.T. Maurelli. Staying alive: bacterial inhibition of apoptosis during infection. *Trends in Microbiology*. 2008 April;16(4):173-80.

New research has shown that many bacterial pathogens can in fact prevent apoptosis during infection. This research grew out of the observations that some organisms induce cell death in one cell type but not in others (see below). It is becoming more evident that the ability to inhibit apoptosis during infection provides the bacterial pathogen with a survival advantage *in vivo*. Bacterial pathogens can be grouped into three classes (Table 1, Fig. 2) based on the mechanisms employed to inhibit apoptosis as outlined below.

Table 1. Classification of bacteria that inhibit apoptosis.

Pathogens grouped by class	Cell type ^a	Proposed or demonstrated mechanism	Ref.
Protection of mitochondria			
<i>Chlamydia sp.</i>	Hep2, HeLa	Bacterial CPAF protein inhibits and degrades pro-apoptotic proteins	21, 29, 36, 85, 87, 115
<i>Neisseria meningitidis</i>	HeLa	Bacterial PorB protein prevents cytochrome <i>c</i> release	67, 68
Activation of cell survival pathways			
<i>Neisseria gonorrhoeae</i>	UEC	Activates NF- κ B pathway	10, 11, 74
<i>Salmonella enterica</i>	HeLa, IEC-6	Bacterial SopB protein activates PI3/Akt pathway	51
<i>Anaplasma phagocytophilum</i>	Neutrophils	Activates p38 MAPK, ERK, PI3/Akt, NF- κ B pathways	17, 31, 61
<i>Ehrlichia chaffeensis</i>	THP-1	Activates NF- κ B and upregulates pro-survival genes	119
<i>Rickettsia rickettsii</i>	HUVEC	Activates NF- κ B and upregulates pro-survival genes	46, 47
<i>Bartonella sp.</i>	Mono Mac 6, HUVEC	Activates NF- κ B pathway, induces <i>cIAP-1</i> , <i>cIAP-2</i> expression	48, 50, 99
<i>Helicobacter pylori</i>	MKN45	Induces <i>cIAP-2</i> expression through	116

		NF- κ B activation	
<i>Porphyromonas gingivalis</i>	GEC	Activates PI3/Akt pathway	117
<i>Listeria monocytogenes</i>	J774	Activates PI3/Akt and NF- κ B pathways	65
<i>Coxiella burnetti</i>	HeLa, THP-1	Prevents cytochrome <i>c</i> release through the PI3/Akt and Erk1/2 pathways	63, 111, 112
Interaction with caspases			
<i>Legionella pneumophila</i>	U937	Exploits caspase-3 activation while preventing apoptosis through NF- κ B activation	1, 2, 59
Further investigation required			
<i>Wolbachia</i>	Neutrophils	Prevents caspase-3 activation	6, 79
<i>Mycoplasma fermentans</i>	U937	Inhibits TNF- α -induced apoptosis	32, 33
<i>Brucella suis</i>	THP-1	Upregulates pro-survival genes	37
<i>Escherichia coli</i> K1	THP-1, RAW 264.7	Upregulates pro-survival genes	102

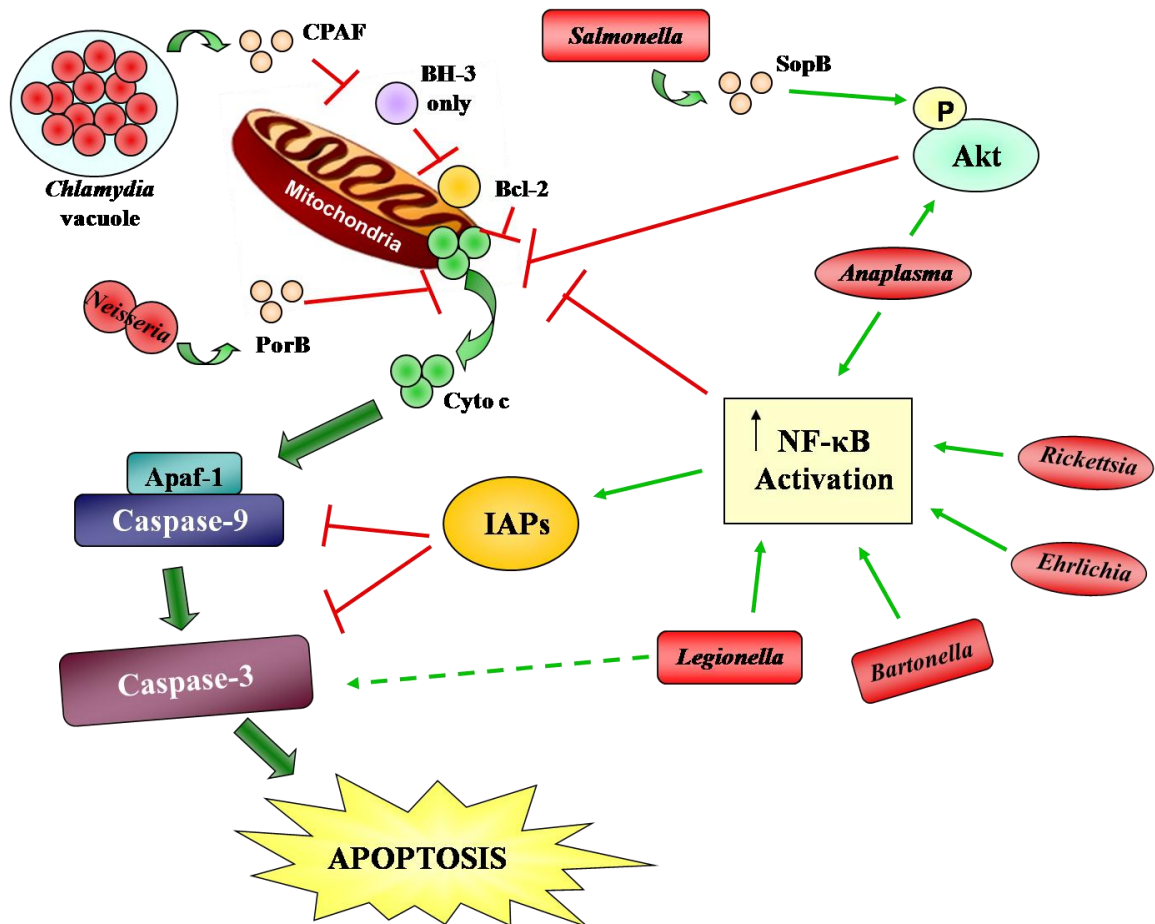
^a HeLa, UEC, IEC-6, GEC, and Hep2 are epithelial cell lines. MKN45 is a gastric adenocarcinoma cell line.

Mono Mac 6, THP-1, and U937 are monocytic cell lines. HUVEC are primary human umbilical vein endothelial cells. J774 and RAW 264.7 are macrophage cell lines.

Figure 2. Mechanisms by which bacterial pathogens inhibit apoptosis at different points along the apoptotic pathway.

Chlamydia secretes the chlamydial proteasome-like activity factor (CPAF) to inhibit and degrade the pro-apoptotic proteins with one BH3 domain. These pro-apoptotic proteins inhibit the pro-survival Bcl-2 proteins upon activation. The outer membrane protein porin PorB of *Neisseria meningitidis* and porin IB of *N. gonorrhoeae* prevent cytochrome *c* (CytoC) release. *Salmonella* secretes the effector SopB through a type III secretion system, resulting in the activation of the phosphatidylinositol 3-kinase/Akt (PI3K/Akt) pathway. This pathway prevents cytochrome *c* release. *Anaplasma* also activates the PI3K/Akt pathway in addition to activating nuclear factor kappa B (NF- κ B). NF- κ B prevents the release of cytochrome *c* and activates the inhibitor of apoptosis proteins (IAPs). *Bartonella*, *Ehrlichia*, and *Rickettsia* activate NF- κ B as well. *Legionella* directly activates some caspase-3 to enhance infection, but inhibits apoptosis through NF- κ B. Red lines indicate inhibition in the pathway while green arrows indicate activation. The bacterial proteins that specifically participate in apoptosis inhibition are shown, where known. The shapes of the bacteria, all shown in red, represent their morphology. P, phosphate.

Figure 2. Mechanisms by which bacterial pathogens inhibit apoptosis at different points along the apoptotic pathway.



Protection of the mitochondria and prevention of cytochrome c release

One mechanism utilized by *Chlamydia* and *Neisseria* to prevent apoptosis is the use of a secreted product that prevents cytochrome *c* release. This mechanism has been studied extensively in *Chlamydia* (38, 73, 121). Infected epithelial cells were exposed to either staurosporine (STS) or ultraviolet (UV) irradiation to determine if the bacteria can prevent apoptosis induced by these stimuli of the intrinsic pathway. Initially, it was discovered that *Chlamydia trachomatis* inhibits the pro-apoptotic host proteins Bax and Bak and prevents them from permeabilizing the mitochondrial membrane. Cytochrome *c* release and subsequent caspase activation are inhibited in infected cells (121). Further research indicated that *Chlamydia* targets pro-apoptotic proteins with a BH3 domain (i.e. Bik, Puma and Bim) for degradation (21, 29, 115). The chlamydial proteasome-like activity factor (CPAF), a protease that is secreted by *C. trachomatis*, was identified as the bacterial product required for the degradation of the pro-apoptotic proteins (85). In addition, *Chlamydia* could also upregulate the inhibitor of apoptosis proteins (IAPs) when tumor necrosis factor α (TNF- α) was used as an inducer of the extrinsic pathway of apoptosis (87). It is unknown if both CPAF and upregulation of the IAPs are required for the anti-apoptotic activity of *Chlamydia*. In addition to blocking apoptosis, *Chlamydia*-infected cells continue to undergo DNA synthesis and mitosis up to 40 h post-infection, which aids in establishing a persistent infection (36). Preventing apoptosis would help ensure that the eukaryotic cell continues to divide in the presence of apoptotic signals from the host (see below). Obligate intracellular pathogens like *Chlamydia* rely on the survival of the host cell. Therefore, it is important not only to inhibit apoptosis, but also

to ensure that the cell maintains the division cycle given that cell cycle arrest often leads to apoptosis.

Neisseria also inhibits apoptosis by preventing cytochrome *c* release (67, 68).

Neisseria meningitidis uses its outer membrane protein porin PorB to prevent apoptosis by targeting it to the mitochondria, which results in inhibition of cytochrome *c* release. When *Neisseria*-infected HeLa cells are incubated with STS, mitochondrial integrity remains, there is no cytochrome *c* release, and a normal mitochondrial membrane potential is maintained (68). In addition, when purified PorB is incubated with host cells for 24 h, PorB enters the cell and prevents STS-induced apoptosis. The mechanism of PorB entry into epithelial cells is poorly understood, but once inside the cells purified PorB localizes to the mitochondrial membrane (67). PorB co-immunoprecipitates with the mitochondrial protein voltage-dependent anionic channel (VDAC), which is a component of the mitochondrial permeability transition pore (PT). Massari et al. suggested that PorB interacts directly with the mitochondrial PT or indirectly with the PT by binding to VDAC, and that this interaction stabilizes the mitochondria in the presence of STS (67). Since Massari et al. published these findings however, additional studies on the PT and the role of VDACs (4, 30) suggest that VDACs might not be important for mitochondrial membrane permeabilization during cell death. Therefore, PorB may localize to some other protein in the PT and how PorB specifically interacts with the PT to prevent STS-induced apoptosis remains to be determined.

Muller et al. found that the PorB homolog in *Neisseria gonorrhoeae*, porin IB, also translocates to the mitochondria, but causes apoptosis in Jurkat T cells and HeLa cells (75). However, Massari et al. (67) speculated that differences in cell types or porin

purification explain the discrepancies between the results. In addition, serum deprivation was used by Muller et al., which makes the cells more sensitive to stress and apoptotic stimuli. Massari et al. repeated the experiments with PorB and porin IB with and without serum, and found the same anti-apoptotic results as he described for PorB. They concluded that *N. gonorrhoeae* has the same ability to stabilize the mitochondria through porin IB as *N. meningitidis* does with PorB (67, 68).

Other groups have found that porin IB might function differently to inhibit apoptosis. *N. gonorrhoeae* increases the expression of the host anti-apoptotic genes bfl-1, cIAP-2 and cox-2 through nuclear factor kappa B (NF- κ B) activation (10, 11). Bfl-1 interacts with pro-apoptotic proteins such as Bid and Bax to inhibit cytochrome *c* release, cIAP-2 prevents caspase-3 activation, and Cox-2 activates the phosphatidylinositol 3-kinase/Akt pathway (PI3K/Akt) (11). This pathway results in Akt phosphorylation, which in turn prevents pro-apoptotic proteins from permeabilizing the mitochondrial membrane (49). NF- κ B activation is required for the induced expression of the pro-survival genes, and MG-132, a cell-permeable proteasome inhibitor that therefore prevents I κ B degradation and NF- κ B activation, prevents upregulation of the genes (10). Finally, apoptosis is also inhibited in *N. gonorrhoeae*-infected human fallopian tube epithelial cells when TNF- α is used to induce apoptosis (74), indicating that *Neisseria* can also inhibit the extrinsic pathway, and therefore could possess several mechanisms to inhibit apoptosis.

Activation of cell survival pathways

The second mechanism by which bacteria inhibit apoptosis is through exploitation of the cell survival pathways naturally present in the host. *Salmonella*, *Anaplasma*,

Ehrlichia, *Rickettsia*, *Wolbachia* and *Bartonella* are examples of bacteria with this ability. *Salmonella enterica* serovar Typhimurium inhibits camptothecin-induced apoptosis in HeLa and rat small intestine epithelial cells by activating the PI3K/Akt pathway (51). This pathway prevents cytochrome *c* release, which inhibits activation of the caspase cascade. Akt phosphorylation and activation during infection occurs due to secretion of a type-III secretion system (T3SS) effector, SopB. A Δ *sopB* mutant is unable to prevent camptothecin-induced apoptosis, and Akt is not activated in cells infected with this mutant (51). Finally, it is interesting to note that *Salmonella* induces cell death in macrophages (28), which enables the bacteria to escape immune cells. Therefore, *Salmonella* infection of a eukaryotic cell leads to different outcomes depending on which cell type is infected.

Anaplasma phagocytophilum prevents apoptosis in neutrophils (17, 31, 61). No inducer of apoptosis is required because neutrophils isolated from human donors spontaneously undergo apoptosis by 24 h in cell culture, and *A. phagocytophilum* infection of these neutrophils prevents the spontaneous apoptosis normally observed (17). Protein and gene expression studies showed that the p38 mitogen-activated protein kinase (MAPK) pathway is activated by the bacteria during infection. p38 MAPK activation leads to the inhibition of caspase-3 activation, but other signaling pathways might also be involved (17). Not only is p38 MAPK upregulated, but the extracellular signal-regulated kinase (ERK), PI3K/Akt and NF- κ B pathways are also upregulated (61). A bacterial product has not been identified for this upregulation of cell-survival pathways, but active infection is required because heat-killed bacteria do not prevent neutrophil apoptosis as efficiently as live bacteria (61). In addition, *A. phagocytophilum* can inhibit the extrinsic

pathway of apoptosis by preventing caspase-8 cleavage (31), and therefore ensures its survival by blocking both pathways of apoptosis.

Three other obligate intracellular pathogens inhibit apoptosis by activating cell survival pathways. First, *Ehrlichia chaffeensis* inhibits apoptosis in the human monocyte cell line THP1 through upregulation of NF- κ B, as determined using microarray analysis. In addition, other pro-survival genes such as *Bcl-2* and *Bcl-2*-related genes are also induced during infection (119). *Rickettsia rickettsii* prevents apoptosis in endothelial cells in an NF- κ B-dependent manner, which results in the upregulation of pro-survival proteins, the down-regulation of pro-apoptotic proteins, and a lack of cytochrome *c* release and caspase activation (46, 47). It has not been determined exactly how infection leads to NF- κ B activation, or what bacterial products are required to inhibit apoptosis. Finally, *Wolbachia*, an endosymbiont of filarial nematode parasites, inhibits apoptosis in human neutrophils during infection (79). The presence of *Wolbachia* is important to the immune response to the parasite since PMN infiltration is absent when the bacteria are not present (14). The bacteria are exposed to human cells during death of the parasite (105), allowing the *Wolbachia* surface protein (WSP) to inhibit apoptosis in the neutrophils. Only the lack of caspase-3 activation was reported (6), and additional studies are needed to determine how the surface protein is anti-apoptotic.

Bartonella henselae activates NF- κ B leading to increased expression of cIAP-1 and cIAP-2 and inhibition of caspase-3 activation and apoptosis (48). Mitochondrial integrity and the presence or absence of cytochrome *c* release have not been tested. The *B. henselae* outer membrane adhesin A (BadA) is required for the inhibition of apoptosis (48). However, *B. henselae* and *Bartonella quintana* also inhibit apoptosis in vascular

endothelial cells through the BepA protein, which is secreted into host cells through the type IV secretion system (99). Although infection activates NF- κ B, ectopically expressed BepA translocates to the plasma membrane and increases the cyclic adenosine monophosphate (cAMP) levels in the cell, which results in the anti-apoptosis activity. cAMP increases the expression of cIAP-2, activates protein kinase A (PKA) to inhibit the pro-apoptotic Bad protein, and activates the ERK and p38 MAPK pathways (99). It was not determined if cIAP-2, PKA, ERK or p38 MAPK are affected by the BepA-dependent increase in cAMP levels. The different bacterial proteins identified between the two studies might be attributed to differences in cell types used, but future studies should determine if one or both of the *Bartonella* proteins (BadA and BepA) are required for protection.

B. henselae and *B. quintana* cause human infections in which angioproliferative lesions can occur. Interestingly, *Bartonella vinsonii*, *Bartonella elizabethae* and *Bartonella clarridgeiae* are not associated with disease and do not inhibit apoptosis in endothelial cells in the presence of actinomycin D, a chemical inducer of apoptosis (50). This observation further illustrates how bacterial pathogens have evolved to inhibit apoptosis to establish a replicative niche inside the host. *Bartonella*, along with *Salmonella*, *Anaplasma*, *Ehrlichia*, *Wolbachia* and *Rickettsia*, inhibit apoptosis through the utilization of the host cell survival pathways that normally function to block apoptosis. This strategy of apoptosis inhibition is an indirect but effective approach to prevent apoptosis during infection.

Interaction with caspases

Legionella pneumophila exploits the activation of caspase-3 during intracellular replication in macrophages while at the same time preventing apoptosis until the late stages of infection (2). *L. pneumophila* utilizes the Dot/Icm type IV secretion system to activate caspase-3, which in turn enables evasion of the endosomal-lysosomal pathway through an unidentified mechanism (2). *L. pneumophila* is then free to grow inside a replicative vacuole derived from the rough endoplasmic reticulum (2). The caspase-3 activation is independent of the intrinsic or extrinsic pathways of apoptosis. During late stages of infection, *L. pneumophila* escapes into the cytoplasm of the host cell, and then apoptosis facilitates bacterial egress (2). Apoptosis inhibition during early infection despite caspase-3 activation is achieved through the activation of NF- κ B, which is also dependent on the Dot/Icm system (1). Furthermore, the bacterial effector SdhA, which is secreted by the Dot/Icm system, is required for apoptosis inhibition. While the Δ *sdhA* mutant is unable to inhibit apoptosis, the role of SdhA in apoptosis inhibition remains unknown (59). *L. pneumophila* provides a fascinating example of a bacterial pathogen that exploits caspase-3 activation for replication while at the same time inhibiting cell death, until the bacteria no longer need the cell.

In conclusion, an emerging theme in bacterial pathogenesis is the ability of bacteria to inhibit apoptosis in eukaryotic cells to establish a replicative niche inside the host. Bacterial pathogens employ at least three different mechanisms to inhibit apoptosis. Mitochondrial permeabilization and subsequent cytochrome *c* release are important events in apoptosis and also serve as a means to differentiate the various mechanisms used to inhibit apoptosis. Bacterial pathogens can directly protect the mitochondria or

upregulate cell survival pathways to prevent cytochrome *c* release. Related organisms such as *A. phagocytophilum* and *E. chaffeensis* use similar methods to inhibit apoptosis, whereas other related organisms such as *N. meningitidis* and *N. gonorrhoeae* utilize different mechanisms to inhibit apoptosis. Clearly, the method employed by each bacterial strain does not have to be the same, and each method probably represents the most efficient means of inhibiting apoptosis for that pathogen in that particular cell type.

Shigella flexneri and Apoptosis

Shigella flexneri was the first bacterial pathogen found to be associated with apoptosis induction in macrophages (125). In murine J774 macrophages, invasive bacteria cause apoptosis, as measured by a chromium 51 release assay, DNA fragmentation, and electron microscope evaluation of infected cells (125). The bacteria need to escape from the phagolysosome of the macrophage and be present in the cytoplasm of the cell in order to induce cell death (124). The *S. flexneri* effector IpaB induces apoptosis in macrophages by binding and activating caspase-1, also known as interleukin-1 β converting enzyme (ICE) (16, 42, 123). Caspase-1 activation in macrophages leads to the secretion of interleukin (IL)-1 β and IL-18 to induce an inflammatory response (97, 123). IpaB alone is sufficient to induce cell death since microinjection of purified IpaB induces apoptosis in macrophages (16). Finally, the rabbit ileal loop model of infection demonstrated that apoptosis occurs *in vivo* since macrophages, T cells, and B cells are apoptotic upon *S. flexneri* infection (126).

The role of caspase-1 in apoptosis was once poorly understood; however, caspase-1 is now believed not to be involved in apoptosis. Caspase-1 is defined as an initiator

caspase, but there has never been a clear, distinct role for caspase-1 activation of caspase-3. Recent research suggested that caspase-1 is not involved in apoptosis. Caspase-1 null mice respond normally to apoptotic stimuli, and caspase-1 deficient cells have a normal response to apoptotic inducers (27, 62). A new paradigm has emerged among microbiologists defining pathogen-induced, caspase-1-mediated cell death as “pyroptosis” since apoptosis does not result in an inflammatory response (7, 27). With regards to *Shigella*-induced macrophage cell death, the term “apoptosis” was not used in several publications. For example, Fernandez-Prada, et al. verified that *Shigella* induce a rapid cell death, but defined the form of death as oncosis (26). Later, two separate studies defined the macrophage cell death induced by *S. flexneri* as necrosis (54, 77). Despite the differences in the description of the cell death observed in infected macrophages, the consensus is that *Shigella* induces a rapid cell death in macrophages that requires IpaB binding to and activating caspase-1. This consensus is due to the fact that caspase-1 knockout mice are not susceptible to *Shigella*-induced cell death, which verifies that caspase-1 is required for cell death in *Shigella*-infected macrophages (43). Also, there is no debate that the activation of caspase-1 is not only important for the bacteria to escape the detrimental environment of the macrophage, but it is also important for the induction of the inflammatory response that actually facilitates bacterial invasion of epithelial cells *in vivo*. These cell death descriptions occurred prior to the establishment of the pyroptosis definition; however, pyroptosis is now being used by *Shigella* researchers (103).

Epithelial cells, on the other hand, are not induced to undergo cell death during *Shigella* infection. Infected HeLa cells remain viable and intact for approximately four hours post-infection (66). Epithelial cells are metabolically stressed by the bacteria during

infection since the epithelial cells have decreases in nucleoside triphosphate levels, reduced protein synthesis (as measured by decreases in the ability to incorporate extracellular radiolabeled methionine), and increases in glucose uptake (66). Morphological examination of the infected epithelial cells demonstrates that the cells are not apoptotic. Interestingly, the bacteria appear in close proximity to the mitochondria upon electron microscopy examination of the infected epithelial cells (66). This publication alluded to the possibility that *S. flexneri* can inhibit apoptosis in epithelial cells. However, Mantis et al. did not analyze eukaryotic proteins in the apoptosis pathways in infected epithelial cells. While *in vivo* studies identified apoptotic cells during infection, only immune cells were described. For example, tissue samples from patients infected with *S. dysenteriae* type-1 have apoptotic immune cells in the rectal mucosa. However, the authors did not state whether or not the epithelial cells were apoptotic (88). In addition, Zychlinsky et al. only described immune cells as apoptotic from rabbit ileal loop infections with *S. flexneri* (126). Therefore, direct evidence for the ability of *S. flexneri* to inhibit apoptosis was missing. Since epithelial cells provide the replicative niche for the bacteria, it is important to determine if *S. flexneri* can inhibit apoptosis in epithelial cells in order to fully understand *Shigella* pathogenesis.

Hypothesis and Specific Aims

The goal of the studies described in this dissertation is to demonstrate that *Shigella flexneri* has the ability to inhibit apoptosis in epithelial cells and define the genetic and molecular mechanisms underlying this phenotype. The hypothesis of this work is that *S. flexneri* actively inhibits apoptosis in epithelial cells in order to establish a

replicative niche inside the host to enhance survival. The specific aims of this dissertation are to demonstrate that *S. flexneri* inhibits apoptosis in epithelial cells and to identify the point of inhibition in the apoptosis pathways during infection. These two aims are addressed in the second and third chapters. Finally, the last aim is to identify which *S. flexneri* genes are required for apoptosis inhibition in epithelial cells, and this aim is addressed in the fourth chapter.

References

1. **Abu-Zant, A., S. Jones, R. Asare, J. Suttles, C. Price, J. Graham, and Y. A. Kwaik.** 2007. Anti-apoptotic signalling by the Dot/Icm secretion system of *L. pneumophila*. *Cell Microbiol.* **9**:246-264.
2. **Abu-Zant, A., M. Santic, M. Molmeret, S. Jones, J. Helbig, and Y. Abu Kwaik.** 2005. Incomplete activation of macrophage apoptosis during intracellular replication of *Legionella pneumophila*. *Infect. Immun.* **73**:5339-5349.
3. **Andrade, A., J. A. Giron, J. M. Amhaz, L. R. Trabulsi, and M. B. Martinez.** 2002. Expression and characterization of flagella in nonmotile enteroinvasive *Escherichia coli* isolated from diarrhea cases. *Infect. Immun.* **70**:5882-5886.
4. **Baines, C. P., R. A. Kaiser, T. Sheiko, W. J. Craigen, and J. D. Molkenin.** 2007. Voltage-dependent anion channels are dispensable for mitochondrial-dependent cell death. *Nat. Cell. Biol.* **9**:550-555.

5. **Basualdo, W., and A. Arbo.** 2003. Randomized comparison of azithromycin versus cefixime for treatment of shigellosis in children. *Pediatr. Infect. Dis. J.* **22**:374-377.

6. **Bazzocchi, C., S. Comazzi, R. Santoni, C. Bandi, C. Genchi, and M. Mortarino.** 2007. *Wolbachia* surface protein (WSP) inhibits apoptosis in human neutrophils. *Parasite Immunol.* **29**:73-79.

7. **Bergsbaken, T., S. L. Fink, and B. T. Cookson.** 2009. Pyroptosis: host cell death and inflammation. *Nat. Rev. Micro.* **7**:99-109.

8. **Bernardini, M. L., J. Mounier, H. d'Hauteville, M. Coquis-Rondon, and P. J. Sansonetti.** 1989. Identification of *icsA*, a plasmid locus of *Shigella flexneri* that governs bacterial intra- and intercellular spread through interaction with F-actin. *Proc. Natl. Acad. Sci. U S A* **86**:3867-3871.

9. **Beutin, L., K. Gleier, I. Kontny, P. Echeverria, and F. Scheutz.** 1997. Origin and characteristics of enteroinvasive strains of *Escherichia coli* (EIEC) isolated in Germany. *Epidemiol. Infect.* **118**:199-205.

10. **Binnicker, M. J., R. D. Williams, and M. A. Apicella.** 2004. Gonococcal porin IB activates NF-kappaB in human urethral epithelium and increases the expression of host antiapoptotic factors. *Infect. Immun.* **72**:6408-6417.

11. **Binnicker, M. J., R. D. Williams, and M. A. Apicella.** 2003. Infection of human urethral epithelium with *Neisseria gonorrhoeae* elicits an upregulation of host anti-apoptotic factors and protects cells from staurosporine-induced apoptosis. *Cell. Microbiol.* **5**:549-560.

12. **Blocker, A., P. Gounon, E. Larquet, K. Niebuhr, V. Cabiaux, C. Parsot, and P. Sansonetti.** 1999. The tripartite type III secreton of *Shigella flexneri* inserts IpaB and IpaC into host membranes. *J. Cell. Biol.* **147**:683-693.

13. **Blomgran, R., L. Zheng, and O. Stendahl.** 2004. Uropathogenic *Escherichia coli* triggers oxygen-dependent apoptosis in human neutrophils through the cooperative effect of type 1 fimbriae and lipopolysaccharide. *Infect. Immun.* **72**:4570-4578.

14. **Brattig, N. W., D. W. Buttner, and A. Hoerauf.** 2001. Neutrophil accumulation around *Onchocerca* worms and chemotaxis of neutrophils are dependent on *Wolbachia* endobacteria. *Microbes Infect.* **3**:439-446.

15. **Bruchhaus, I., T. Roeder, A. Rennenberg, and V. T. Heussler.** 2007. Protozoan parasites: programmed cell death as a mechanism of parasitism. *Trends Parasitol.* **23**:376-383.

16. **Chen, Y., M. R. Smith, K. Thirumalai, and A. Zychlinsky.** 1996. A bacterial invasin induces macrophage apoptosis by binding directly to ICE. *EMBO J* **15**:3853-3860.
17. **Choi, K. S., J. T. Park, and J. S. Dumler.** 2005. *Anaplasma phagocytophilum* delay of neutrophil apoptosis through the p38 mitogen-activated protein kinase signal pathway. *Infect. Immun.* **73**:8209-8218.
18. **Cornelis, G. R.** 2006. The type III secretion injectisome. *Nat. Rev. Microbiol.* **4**:811-825.
19. **Cory, S., and J. M. Adams.** 2002. The Bcl2 family: regulators of the cellular life-or-death switch. *Nat. Rev. Cancer* **2**:647-656.
20. **Day, W. A., Jr., R. E. Fernandez, and A. T. Maurelli.** 2001. Pathoadaptive mutations that enhance virulence: genetic organization of the cadA regions of *Shigella* spp. *Infect. Immun.* **69**:7471-7480.
21. **Dong, F., M. Pirbhai, Y. Xiao, Y. Zhong, Y. Wu, and G. Zhong.** 2005. Degradation of the proapoptotic proteins Bik, Puma, and Bim with Bcl-2 domain 3 homology in *Chlamydia trachomatis*-infected cells. *Infect. Immun.* **73**:1861-1864.

22. **Dorman, C. J., and M. E. Porter.** 1998. The *Shigella* virulence gene regulatory cascade: a paradigm of bacterial gene control mechanisms. *Mol. Microbiol.* **29**:677-684.

23. **DuPont, H. L., M. M. Levine, R. B. Hornick, and S. B. Formal.** 1989. Inoculum size in shigellosis and implications for expected mode of transmission. *J. Infect. Dis.* **159**:1126-1128.

24. **Espina, M., A. J. Olive, R. Kenjale, D. S. Moore, S. F. Ausar, R. W. Kaminski, E. V. Oaks, C. R. Middaugh, W. D. Picking, and W. L. Picking.** 2006. IpaD localizes to the tip of the type III secretion system needle of *Shigella flexneri*. *Infect. Immun.* **74**:4391-4400.

25. **Falkow, S.** 1975. Infectious multiple drug resistance. Pion, London.

26. **Fernandez-Prada, C. M., D. L. Hoover, B. D. Tall, and M. M. Venkatesan.** 1997. Human monocyte-derived macrophages infected with virulent *Shigella flexneri* in vitro undergo a rapid cytolytic event similar to oncosis but not apoptosis. *Infect. Immun.* **65**:1486-1496.

27. **Fink, S. L., and B. T. Cookson.** 2005. Apoptosis, pyroptosis, and necrosis: mechanistic description of dead and dying eukaryotic cells. *Infect. Immun.* **73**:1907-1916.

28. **Fink, S. L., and B. T. Cookson.** 2006. Caspase-1-dependent pore formation during pyroptosis leads to osmotic lysis of infected host macrophages. *Cell. Microbiol.* **8**:1812-1825.
29. **Fischer, S. F., J. Vier, S. Kirschnek, A. Klos, S. Hess, S. Ying, and G. Hacker.** 2004. *Chlamydia* inhibit host cell apoptosis by degradation of proapoptotic BH3-only proteins. *J. Exp. Med.* **200**:905-916.
30. **Galluzzi, L., and G. Kroemer.** 2007. Mitochondrial apoptosis without VDAC. *Nat. Cell. Biol.* **9**:487-489.
31. **Ge, Y., and Y. Rikihisa.** 2006. *Anaplasma phagocytophilum* delays spontaneous human neutrophil apoptosis by modulation of multiple apoptotic pathways. *Cell. Microbiol.* **8**:1406-1416.
32. **Gerlic, M., J. Horowitz, S. Farkash, and S. Horowitz.** 2007. The inhibitory effect of *Mycoplasma fermentans* on tumour necrosis factor (TNF)-alpha-induced apoptosis resides in the membrane lipoproteins. *Cell. Microbiol.* **9**:142-153.
33. **Gerlic, M., J. Horowitz, and S. Horowitz.** 2004. *Mycoplasma fermentans* inhibits tumor necrosis factor alpha-induced apoptosis in the human myelomonocytic U937 cell line. *Cell. Death. Differ.* **11**:1204-1212.

34. **Gordillo, M. E., K. V. Singh, and B. E. Murray.** 1993. In vitro activity of azithromycin against bacterial enteric pathogens. *Antimicrob. Agents Chemother.* **37**:1203-1205.

35. **Grassme, H., V. Jendrossek, and E. Gulbins.** 2001. Molecular mechanisms of bacteria induced apoptosis. *Apoptosis.* **6**:441-445.

36. **Greene, W., Y. Xiao, Y. Huang, G. McClarty, and G. Zhong.** 2004. *Chlamydia*-infected cells continue to undergo mitosis and resist induction of apoptosis. *Infect. Immun.* **72**:451-460.

37. **Gross, A., A. Terraza, S. Ouahrani-Bettache, J. P. Liautard, and J. Dornand.** 2000. In vitro *Brucella suis* infection prevents the programmed cell death of human monocytic cells. *Infect. Immun.* **68**:342-351.

38. **Hacker, G., S. Kirschnek, and S. F. Fischer.** 2006. Apoptosis in infectious disease: how bacteria interfere with the apoptotic apparatus. *Med. Microbiol. Immunol.* **195**:11-19.

39. **Hale, T. L.** 1991. Genetic basis of virulence in *Shigella* species. *Microbiol. Rev.* **55**:206-224.

40. **Handa, Y., M. Suzuki, K. Ohya, H. Iwai, N. Ishijima, A. J. Koleske, Y. Fukui, and C. Sasakawa.** 2007. *Shigella* IpgB1 promotes bacterial entry through the ELMO-Dock180 machinery. *Nat. Cell. Biol.* **9**:121-128.

41. **Hay, S., and G. Kannourakis.** 2002. A time to kill: viral manipulation of the cell death program. *J. Gen. Virol.* **83**:1547-1564.

42. **Hilbi, H., Y. Chen, K. Thirumalai, and A. Zychlinsky.** 1997. The interleukin 1beta-converting enzyme, caspase 1, is activated during *Shigella flexneri*-induced apoptosis in human monocyte-derived macrophages. *Infect. Immun.* **65**:5165-5170.

43. **Hilbi, H., J. E. Moss, D. Hersh, Y. Chen, J. Arondel, S. Banerjee, R. A. Flavell, J. Yuan, P. J. Sansonetti, and A. Zychlinsky.** 1998. *Shigella*-induced apoptosis is dependent on caspase-1 which binds to IpaB. *J. Biol. Chem.* **273**:32895-32900.

44. **Hyer, M. L., T. Samuel, and J. C. Reed.** 2006. The FLIP-side of Fas signaling. *Clin. Cancer Res.* **12**:5929-5931.

45. **Jennison, A. V., and N. K. Verma.** 2004. *Shigella flexneri* infection: pathogenesis and vaccine development. *FEMS Microbiol. Rev.* **28**:43-58.

46. **Joshi, S. G., C. W. Francis, D. J. Silverman, and S. K. Sahni.** 2004. NF-kappaB activation suppresses host cell apoptosis during *Rickettsia rickettsii* infection via regulatory effects on intracellular localization or levels of apoptogenic and anti-apoptotic proteins. FEMS Microbiol. Lett. **234**:333-341.

47. **Joshi, S. G., C. W. Francis, D. J. Silverman, and S. K. Sahni.** 2003. Nuclear factor kappa B protects against host cell apoptosis during *Rickettsia rickettsii* infection by inhibiting activation of apical and effector caspases and maintaining mitochondrial integrity. Infect .Immun. **71**:4127-4136.

48. **Kempf, V. A., A. Schairer, D. Neumann, G. A. Grassl, K. Lauber, M. Lebidziejewski, M. Schaller, P. Kyme, S. Wesselborg, and I. B. Autenrieth.** 2005. *Bartonella henselae* inhibits apoptosis in Mono Mac 6 cells. Cell. Microbiol. **7**:91-104.

49. **Kennedy, S. G., E. S. Kandel, T. K. Cross, and N. Hay.** 1999. Akt/Protein kinase B inhibits cell death by preventing the release of cytochrome *c* from mitochondria. Mol. Cell. Biol. **19**:5800-5810.

50. **Kirby, J. E., and D. M. Nekorchuk.** 2002. *Bartonella*-associated endothelial proliferation depends on inhibition of apoptosis. Proc. Natl. Acad. Sci. U S A **99**:4656-4661.

51. **Knodler, L. A., B. B. Finlay, and O. Steele-Mortimer.** 2005. The *Salmonella* effector protein SopB protects epithelial cells from apoptosis by sustained activation of Akt. *J. Biol. Chem.* **280**:9058-9064.

52. **Kobayashi, S. D., K. R. Braughton, A. R. Whitney, J. M. Voyich, T. G. Schwan, J. M. Musser, and F. R. DeLeo.** 2003. Bacterial pathogens modulate an apoptosis differentiation program in human neutrophils. *Proc. Natl. Acad. Sci. U S A* **100**:10948-10953.

53. **Kohler, H., S. P. Rodrigues, and B. A. McCormick.** 2002. *Shigella flexneri* Interactions with the Basolateral Membrane Domain of Polarized Model Intestinal Epithelium: Role of Lipopolysaccharide in Cell Invasion and in Activation of the Mitogen-Activated Protein Kinase ERK. *Infect. Immun.* **70**:1150-1158.

54. **Koterski, J. F., M. Nahvi, M. M. Venkatesan, and B. Haimovich.** 2005. Virulent *Shigella flexneri* causes damage to mitochondria and triggers necrosis in infected human monocyte-derived macrophages. *Infect. Immun.* **73**:504-513.

55. **Kotloff, K. L., J. P. Winickoff, B. Ivanoff, J. D. Clemens, D. L. Swerdlow, P. J. Sansonetti, G. K. Adak, and M. M. Levine.** 1999. Global burden of *Shigella* infections: implications for vaccine development and implementation of control strategies. *Bull. World Health Organ.* **77**:651-666.

56. **Kroemer, G., L. Galluzzi, and C. Brenner.** 2007. Mitochondrial membrane permeabilization in cell death. *Physiol. Rev.* **87**:99-163.

57. **Kweon, M. N.** 2008. Shigellosis: the current status of vaccine development. *Curr. Opin. Infect. Dis.* **21**:313-318.

58. **LaBrec, E. H., H. Schneider, T. J. Magnani, and S. B. Formal.** 1964. Epithelial cell penetration as an essential step in the pathogenesis of bacillary dysentery. *J. Bacteriol.* **88**:1503-1518.

59. **Laguna, R. K., E. A. Creasey, Z. Li, N. Valtz, and R. R. Isberg.** 2006. A *Legionella pneumophila*-translocated substrate that is required for growth within macrophages and protection from host cell death. *Proc. Natl. Acad. Sci. U S A* **103**:18745-18750.

60. **Lan, R., M. C. Alles, K. Donohoe, M. B. Martinez, and P. R. Reeves.** 2004. Molecular evolutionary relationships of enteroinvasive *Escherichia coli* and *Shigella* spp. *Infect. Immun.* **72**:5080-5088.

61. **Lee, H. C., and J. L. Goodman.** 2006. *Anaplasma phagocytophilum* causes global induction of antiapoptosis in human neutrophils. *Genomics.* **88**:496-503.

62. **Li, P., H. Allen, S. Banerjee, S. Franklin, L. Herzog, C. Johnston, J. McDowell, M. Paskind, L. Rodman, J. Salfeld, and et al.** 1995. Mice deficient in IL-1 beta-converting enzyme are defective in production of mature IL-1 beta and resistant to endotoxic shock. *Cell*. **80**:401-411.

63. **Luhrmann, A., and C. R. Roy.** 2007. *Coxiella burnetii* inhibits activation of host cell apoptosis through a mechanism that involves preventing cytochrome c release from mitochondria. *Infect. Immun.* **75**:5282-5289.

64. **Mandic-Mulec, I., J. Weiss, and A. Zychlinsky.** 1997. *Shigella flexneri* is trapped in polymorphonuclear leukocyte vacuoles and efficiently killed. *Infect. Immun.* **65**:110-115.

65. **Mansell, A., N. Khelef, P. Cossart, and L. A. O'Neill.** 2001. Internalin B activates nuclear factor-kappa B via Ras, phosphoinositide 3-kinase, and Akt. *J. Biol. Chem.* **276**:43597-43603.

66. **Mantis, N., M. C. Prevost, and P. Sansonetti.** 1996. Analysis of epithelial cell stress response during infection by *Shigella flexneri*. *Infect. Immun.* **64**:2474-2482.

67. **Massari, P., Y. Ho, and L. M. Wetzler.** 2000. *Neisseria meningitidis* porin PorB interacts with mitochondria and protects cells from apoptosis. Proc. Natl. Acad. Sci. U S A **97**:9070-9075.

68. **Massari, P., C. A. King, A. Y. Ho, and L. M. Wetzler.** 2003. Neisserial PorB is translocated to the mitochondria of HeLa cells infected with *Neisseria meningitidis* and protects cells from apoptosis. Cell. Microbiol. **5**:99-109.

69. **Maurelli, A. T., B. Blackmon, and R. Curtiss, 3rd.** 1984. Temperature-dependent expression of virulence genes in *Shigella* species. Infect. Immun. **43**:195-201.

70. **Maurelli, A. T., R. E. Fernandez, C. A. Bloch, C. K. Rode, and A. Fasano.** 1998. "Black holes" and bacterial pathogenicity: a large genomic deletion that enhances the virulence of *Shigella* spp. and enteroinvasive *Escherichia coli*. Proc. Natl. Acad. Sci. U S A **95**:3943-3948.

71. **McCormick, B. A., A. M. Siber, and A. T. Maurelli.** 1998. Requirement of the *Shigella flexneri* virulence plasmid in the ability to induce trafficking of neutrophils across polarized monolayers of the intestinal epithelium. Infect. Immun. **66**:4237-4243.

72. **Menard, R., P. Sansonetti, and C. Parsot.** 1994. The secretion of the *Shigella flexneri* Ipa invasins is activated by epithelial cells and controlled by IpaB and IpaD. EMBO J. **13**:5293-5302.

73. **Miyairi, I., and G. I. Byrne.** 2006. *Chlamydia* and programmed cell death. Curr. Opin. Microbiol. **9**:102-108.

74. **Morales, P., P. Reyes, M. Vargas, M. Rios, M. Imarai, H. Cardenas, H. Croxatto, P. Orihuela, R. Vargas, J. Fuhrer, J. E. Heckels, M. Christodoulides, and L. Velasquez.** 2006. Infection of human fallopian tube epithelial cells with *Neisseria gonorrhoeae* protects cells from tumor necrosis factor alpha-induced apoptosis. Infect. Immun. **74**:3643-3650.

75. **Muller, A., D. Gunther, V. Brinkmann, R. Hurwitz, T. F. Meyer, and T. Rudel.** 2000. Targeting of the pro-apoptotic VDAC-like porin (PorB) of *Neisseria gonorrhoeae* to mitochondria of infected cells. EMBO J. **19**:5332-5343.

76. **Niyogi, S. K.** 2005. Shigellosis. J. Microbiol. **43**:133-143.

77. **Nonaka, T., T. Kuwabara, H. Mimuro, A. Kuwae, and S. Imajoh-Ohmi.** 2003. *Shigella*-induced necrosis and apoptosis of U937 cells and J774 macrophages. Microbiology. **149**:2513-2527.

78. **Oberhelman, R. A., D. J. Kopecko, E. Salazar-Lindo, E. Gotuzzo, J. M. Buysse, M. M. Venkatesan, A. Yi, C. Fernandez-Prada, M. Guzman, R. Leon-Barua, and et al.** 1991. Prospective study of systemic and mucosal immune responses in dysenteric patients to specific *Shigella* invasion plasmid antigens and lipopolysaccharides. *Infect. Immun.* **59**:2341-2350.

79. **Pannebakker, B. A., B. Loppin, C. P. Elemans, L. Humblot, and F. Vavre.** 2007. Parasitic inhibition of cell death facilitates symbiosis. *Proc. Natl. Acad. Sci. U S A* **104**:213-215.

80. **Perdomo, J. J., P. Gounon, and P. J. Sansonetti.** 1994. Polymorphonuclear leukocyte transmigration promotes invasion of colonic epithelial monolayer by *Shigella flexneri*. *J. Clin. Invest.* **93**:633-643.

81. **Perskvist, N., M. Long, O. Stendahl, and L. Zheng.** 2002. *Mycobacterium tuberculosis* promotes apoptosis in human neutrophils by activating caspase-3 and altering expression of Bax/Bcl-xL via an oxygen-dependent pathway. *J. Immunol.* **168**:6358-6365.

82. **Phalipon, A., L. A. Mulard, and P. J. Sansonetti.** 2008. Vaccination against shigellosis: is it the path that is difficult or is it the difficult that is the path? *Microbes Infect.* **10**:1057-1062.

83. **Philpott, D. J., J. D. Edgeworth, and P. J. Sansonetti.** 2000. The pathogenesis of *Shigella flexneri* infection: lessons from in vitro and in vivo studies. *Philos. Trans. R. Soc. Lond. B. Biol. Sci.* **355**:575-586.

84. **Picking, W. L., H. Nishioka, P. D. Hearn, M. A. Baxter, A. T. Harrington, A. Blocker, and W. D. Picking.** 2005. IpaD of *Shigella flexneri* is independently required for regulation of Ipa protein secretion and efficient insertion of IpaB and IpaC into host membranes. *Infect. Immun.* **73**:1432-1440.

85. **Pirbhai, M., F. Dong, Y. Zhong, K. Z. Pan, and G. Zhong.** 2006. The secreted protease factor CPAF is responsible for degrading pro-apoptotic BH3-only proteins in *Chlamydia trachomatis*-infected cells. *J. Biol. Chem.* **281**:31495-31501.

86. **Pupo, G. M., R. Lan, and P. R. Reeves.** 2000. Multiple independent origins of *Shigella* clones of *Escherichia coli* and convergent evolution of many of their characteristics. *Proc. Natl. Acad. Sci. U S A* **97**:10567-10572.

87. **Rajalingam, K., M. Sharma, N. Paland, R. Hurwitz, O. Thieck, M. Oswald, N. Machuy, and T. Rudel.** 2006. IAP-IAP complexes required for apoptosis resistance of *C. trachomatis*-infected cells. *PLoS Pathog.* **2**:e114.

88. **Raqib, R., C. Ekberg, P. Sharkar, P. K. Bardhan, A. Zychlinsky, P. J. Sansonetti, and J. Andersson.** 2002. Apoptosis in acute shigellosis is associated with increased production of Fas/Fas ligand, perforin, caspase-1, and caspase-3 but reduced production of Bcl-2 and interleukin-2. *Infect. Immun.* **70**:3199-3207.
89. **Reed, J. C.** 2000. Mechanisms of apoptosis. *Am. J. Pathol.* **157**:1415-1430.
90. **Rolland, K., N. Lambert-Zechovsky, B. Picard, and E. Denamur.** 1998. *Shigella* and enteroinvasive *Escherichia coli* strains are derived from distinct ancestral strains of *E. coli*. *Microbiology.* **144**(Pt 9):2667-2672.
91. **Roset, R., L. Ortet, and G. Gil-Gomez.** 2007. Role of Bcl-2 family members on apoptosis: what we have learned from knock-out mice. *Front. Biosci.* **12**:4722-4730.
92. **Sakaguchi, T., H. Kohler, X. Gu, B. A. McCormick, and H. C. Reinecker.** 2002. *Shigella flexneri* regulates tight junction-associated proteins in human intestinal epithelial cells. *Cell. Microbiol.* **4**:367-381.
93. **Sansonetti, P. J.** 2001. Rupture, invasion and inflammatory destruction of the intestinal barrier by *Shigella*, making sense of prokaryote-eukaryote cross-talks. *FEMS Microbiol. Rev.* **25**:3-14.

94. **Sansonetti, P. J., H. d'Hauteville, C. Ecobichon, and C. Pourcel.** 1983. Molecular comparison of virulence plasmids in *Shigella* and enteroinvasive *Escherichia coli*. *Ann. Microbiol. (Paris)* **134A**:295-318.
95. **Sansonetti, P. J., D. J. Kopecko, and S. B. Formal.** 1982. Involvement of a plasmid in the invasive ability of *Shigella flexneri*. *Infect. Immun.***35**:852-860.
96. **Sansonetti, P. J., D. J. Kopecko, and S. B. Formal.** 1981. *Shigella sonnei* plasmids: evidence that a large plasmid is necessary for virulence. *Infect. Immun.* **34**:75-83.
97. **Sansonetti, P. J., A. Phalipon, J. Arondel, K. Thirumalai, S. Banerjee, S. Akira, K. Takeda, and A. Zychlinsky.** 2000. Caspase-1 activation of IL-1[beta] and IL-18 are essential for *Shigella flexneri*-induced inflammation. *Immunity*. **12**:581-590.
98. **Sansonetti, P. J., G. Tran Van Nhieu, and C. Egile.** 1999. Rupture of the intestinal epithelial barrier and mucosal invasion by *Shigella flexneri*. *Clin. Infect. Dis.* **28**:466-475.
99. **Schmid, M. C., F. Scheidegger, M. Dehio, N. Balmelle-Devaux, R. Schulein, P. Guye, C. S. Chennakesava, B. Biedermann, and C. Dehio.** 2006. A

translocated bacterial protein protects vascular endothelial cells from apoptosis.
PLoS Pathog. **2**:e115.

100. **Schroeder, G. N., and H. Hilbi.** 2008. Molecular pathogenesis of *Shigella* spp.: controlling host cell signaling, invasion, and death by type III secretion. Clin. Microbiol. Rev. **21**:134-156.

101. **Skoudy, A., J. Mounier, A. Aruffo, H. Ohayon, P. Gounon, P. Sansonetti, and G. Tran Van Nhieu.** 2000. CD44 binds to the *Shigella* IpaB protein and participates in bacterial invasion of epithelial cells. Cell. Microbiol. **2**:19-33.

102. **Sukumaran, S. K., S. K. Selvaraj, and N. V. Prasadaraao.** 2004. Inhibition of apoptosis by *Escherichia coli* K1 is accompanied by increased expression of BclXL and blockade of mitochondrial cytochrome c release in macrophages. Infect. Immun. **72**:6012-6022.

103. **Suzuki, T., L. Franchi, C. Toma, H. Ashida, M. Ogawa, Y. Yoshikawa, H. Mimuro, N. Inohara, C. Sasakawa, and G. Nunez.** 2007. Differential regulation of caspase-1 activation, pyroptosis, and autophagy via Ipaf and ASC in *Shigella*-infected macrophages. PLoS Pathog. **3**:e111.

104. **Tamano, K., S. Aizawa, E. Katayama, T. Nonaka, S. Imajoh-Ohmi, A. Kuwae, S. Nagai, and C. Sasakawa.** 2000. Supramolecular structure of the

Shigella type III secretion machinery: the needle part is changeable in length and essential for delivery of effectors. EMBO J. **19**:3876-3887.

105. **Taylor, M. J., and A. Hoerauf.** 1999. *Wolbachia* bacteria of filarial nematodes. Parasitology Today. **15**:437-442.

106. **Tobe, T., S. Nagai, N. Okada, B. Adler, M. Yoshikawa, and C. Sasakawa.** 1991. Temperature-regulated expression of invasion genes in *Shigella flexneri* is controlled through the transcriptional activation of the *virB* gene on the large plasmid. Mol. Microbiol. **5**:887-893.

107. **Tran Van Nhieu, G., A. Ben-Ze'ev, and P. J. Sansonetti.** 1997. Modulation of bacterial entry into epithelial cells by association between vinculin and the *Shigella* IpaA invasin. EMBO J. **16**:2717-2729.

108. **Tran Van Nhieu, G., and P. J. Sansonetti.** 1999. Mechanism of *Shigella* entry into epithelial cells. Curr. Opin. Microbiol. **2**:51-55.

109. **Turbyfill, K. R., R. W. Kaminski, and E. V. Oaks.** 2008. Immunogenicity and efficacy of highly purified invasin complex vaccine from *Shigella flexneri* 2a. Vaccine. **26**:1353-1364.

110. **Voino-Tasenetsky, M. V., and T. N. Khavkin.** 1964. A study of the intraepithelial localization of dysentery-causing agents by means of fluorescent antibodies. *J. Microbiol.* **12**:98-100.
111. **Voth, D. E., and R. A. Heinzen.** 2009. Sustained activation of Akt and Erk1/2 is required for *Coxiella burnetii* antiapoptotic activity. *Infect. Immun.* **77**:205-213.
112. **Voth, D. E., D. Howe, and R. A. Heinzen.** 2007. *Coxiella burnetii* inhibits apoptosis in human THP-1 cells and monkey primary alveolar macrophages. *Infect. Immun.* **75**:4263-4271.
113. **Watarai, M., S. Funato, and C. Sasakawa.** 1996. Interaction of Ipa proteins of *Shigella flexneri* with alpha5beta1 integrin promotes entry of the bacteria into mammalian cells. *J. Exp. Med.* **183**:991-999.
114. **Way, S. S., A. C. Borczuk, R. Dominitz, and M. B. Goldberg.** 1998. An essential role for gamma interferon in innate resistance to *Shigella flexneri* infection. *Infect. Immun.* **66**:1342-1348.
115. **Xiao, Y., Y. Zhong, W. Greene, F. Dong, and G. Zhong.** 2004. *Chlamydia trachomatis* infection inhibits both Bax and Bak activation induced by staurosporine. *Infect. Immun.* **72**:5470-5474.

116. **Yanai, A., Y. Hirata, Y. Mitsuno, S. Maeda, W. Shibata, M. Akanuma, H. Yoshida, T. Kawabe, and M. Omata.** 2003. *Helicobacter pylori* induces antiapoptosis through nuclear factor-kappaB activation. *J. Infect. Dis.* **188**:1741-1751.
117. **Yilmaz, O., T. Jungas, P. Verbeke, and D. M. Ojcius.** 2004. Activation of the phosphatidylinositol 3-kinase/Akt pathway contributes to survival of primary epithelial cells infected with the periodontal pathogen *Porphyromonas gingivalis*. *Infect. Immun.* **72**:3743-3751.
118. **Yoshida, S., E. Katayama, A. Kuwae, H. Mimuro, T. Suzuki, and C. Sasakawa.** 2002. Shigella deliver an effector protein to trigger host microtubule destabilization, which promotes Rac1 activity and efficient bacterial internalization. *EMBO J.* **21**:2923-2935.
119. **Zhang, J. Z., M. Sinha, B. A. Luxon, and X. J. Yu.** 2004. Survival strategy of obligately intracellular *Ehrlichia chaffeensis*: novel modulation of immune response and host cell cycles. *Infect. Immun.* **72**:498-507.
120. **Zhang, Y., A. T. Ting, K. B. Marcu, and J. B. Bliska.** 2005. Inhibition of MAPK and NF-kappa B pathways is necessary for rapid apoptosis in macrophages infected with *Yersinia*. *J. Immunol.* **174**:7939-7949.

121. **Zhong, Y., M. Weininger, M. Pirbhai, F. Dong, and G. Zhong.** 2006.
Inhibition of staurosporine-induced activation of the proapoptotic multidomain
Bcl-2 proteins Bax and Bak by three invasive chlamydial species. *J. Infect.*
53:408-414.

122. **Zurawski, D. V., C. Mitsuhashi, K. L. Mumy, B. A. McCormick, and A. T. Maurelli.** 2006. OspF and OspC1 are *Shigella flexneri* type III secretion system
effectors that are required for postinvasion aspects of virulence. *Infect. Immun.*
74:5964-5976.

123. **Zychlinsky, A., C. Fitting, J. M. Cavaillon, and P. J. Sansonetti.** 1994.
Interleukin 1 is released by murine macrophages during apoptosis induced by
Shigella flexneri. *J. Clin. Invest.* **94**:1328-1332.

124. **Zychlinsky, A., B. Kenny, R. Menard, M. C. Prevost, I. B. Holland, and P. J. Sansonetti.** 1994. IpaB mediates macrophage apoptosis induced by *Shigella*
flexneri. *Mol. Microbiol.* **11**:619-627.

125. **Zychlinsky, A., M. C. Prevost, and P. J. Sansonetti.** 1992. *Shigella flexneri*
induces apoptosis in infected macrophages. *Nature.* **358**:167-169.

126. **Zychlinsky, A., K. Thirumalai, J. Arondel, J. R. Cantey, A. O. Aliprantis, and P. J. Sansonetti.** 1996. In vivo apoptosis in *Shigella flexneri* infections. Infect. Immun. **64**:5357-5365.

Chapter Two

Shigella flexneri Inhibits Staurosporine-Induced Apoptosis in Epithelial Cells

Published as: Clark, C.S. and Maurelli, A.T. *Shigella flexneri* inhibits staurosporine-induced apoptosis in epithelial cells. *Infection and Immunity*. 2007 May;75(5):2531-9.

Abstract

Shigella flexneri is a facultative intracellular organism that causes bacillary dysentery. The *Shigella* IpaB protein activates caspase-1 in macrophages, which eventually leads to apoptosis. In contrast, epithelial cells infected with *Shigella* undergo a stress response but do not die. Therefore, the objective of this study was to determine if *Shigella* has the ability to inhibit apoptosis in epithelial cells. A modified gentamicin protection assay was used to investigate if HeLa cells infected with *S. flexneri* are able to resist the induction of apoptosis following treatment with 4 μ M of staurosporine. Nuclear staining and immunofluorescence revealed that infected cells remained healthy while uninfected cells appeared apoptotic. Only uninfected cells had detectable levels of activated caspase-3 upon immunofluorescence, and this was verified by Western blot analysis. Despite interfering with caspase-3 activation, *Shigella*-infected cells treated with staurosporine did have cytochrome *c* release and caspase-9 activation, indicating that *Shigella* protects epithelial cells from apoptosis by inhibiting caspase-3 activation. Analysis of *S. flexneri* mutants showed that invasion and a functional type III secretion

system were required to block apoptosis. In addition, a mutant with a deletion in *mxiE*, which encodes a transcriptional activator for genes induced intracellularly, failed to inhibit apoptosis. Therefore, protection of epithelial cells from apoptosis by *S. flexneri* is regulated by one or more of the bacterial genes under the control of *mxiE*. We believe that *S. flexneri*, like other pathogens, inhibits apoptosis in epithelial cells but causes apoptosis in macrophages to ensure survival inside the host.

Introduction

Shigella flexneri is a gram-negative, facultative intracellular organism, the causative agent of bacillary dysentery, and generates a significant global burden (19). Infection with *Shigella* causes an intense acute inflammatory reaction that leads to the destruction of the colonic epithelium. Clinical symptoms include watery diarrhea, severe abdominal pain, and bloody, mucoid stools (14). These symptoms of dysentery are due to the penetration of *Shigella* into colonic epithelial cells, which provide an intracellular environment for the bacteria to multiply and spread to adjacent cells. Entry into epithelial cells is mediated by the Ipa proteins encoded on the 220-kb virulence plasmid. Secretion of these proteins is dependent on a type III secretion system (T3SS), which is encoded by 20 genes in the *mxi-spa* locus of the virulence plasmid (30).

Previous studies have shown that resident macrophages undergo apoptosis after phagocytosis of *Shigella* (5, 12, 36). Apoptosis, also known as programmed cell death, is a typical mechanism used during fetal development and in adult cell maintenance to eliminate cells without causing an inflammatory response. It has now been recognized that numerous bacteria and viruses exploit or interact with the apoptotic pathway to

enhance the infection process (4, 8, 24). Apoptosis consists of extrinsic and intrinsic pathways that can be utilized by cells. One feature that the two pathways have in common is the use of an effector cysteine aspartate-specific protease (caspase-3) that cleaves substrates like protein kinases, signal transduction proteins, and chromatin-modifying proteins such as poly(ADP-ribose) polymerase and DNA repair proteins, leading to cell death (28). Other important players in these pathways include pro-survival proteins, pro-apoptotic proteins, initiator caspases (e.g., caspase-8 and caspase-9), and cytochrome *c* release from the mitochondria (1).

Shigella was first recognized to be involved in apoptosis through its induction of the pathway in macrophages (36). Caspase-1 is activated in macrophages infected with *Shigella* through the binding of the *Shigella* effector IpaB. Caspase-1, also known as interleukin-1 β -converting enzyme, is responsible for activating the proinflammatory cytokines interleukin-1 β and interleukin-18. Caspase-1 is considered an initiator caspase; however, the role of caspase-1 in apoptosis has not been defined. There is some controversy as to whether macrophages undergo apoptosis or necrosis or if caspase-1 is even required for the killing of the macrophages (18, 25, 33). The fact of the matter is that *S. flexneri* is able to induce cell death in macrophages. In contrast, epithelial cells infected with *S. flexneri* undergo a stress response but do not die. Stress was measured by examining deoxynucleoside triphosphate levels and the ability to synthesize proteins and transport hexose. Although infected epithelial cells do not die, analysis for apoptosis has not been done (21).

The goal of this study was to determine if *S. flexneri* infection of epithelial cells protects the cells from apoptosis. We hypothesize that *S. flexneri* inhibits apoptosis in epithelial cells in order to ensure the bacterium's intracellular survival and replication. We found that *S. flexneri* is able to protect HeLa cells from staurosporine (STS)-induced apoptosis by preventing the activation of caspase-3 despite the presence of cytochrome *c* release and caspase-9 activation. Analysis of a $\Delta mxiE$ mutant revealed that this mutant was unable to protect epithelial cells from apoptosis to the same extent as wild-type *S. flexneri*. The protein products of the MxiE-regulated genes are effectors secreted through the T3SS, which are expressed during intracellular growth (15, 20). Therefore, one or several of the genes regulated by MxiE are important for protecting *Shigella*-infected epithelial cells from apoptosis.

Materials and Methods

Bacterial strains and growth conditions.

The strains of *S. flexneri* used are listed in Table 2. Bacteria were routinely cultured at 37°C either in Luria-Bertani broth (LB) with aeration or on tryptic soy broth (TSB) plates with 1.5% agar and 0.025% Congo red (Sigma). Antibiotics were used at the following concentrations: kanamycin, 50 µg/ml; streptomycin, 50 µg/ml; chloramphenicol, 5 µg/ml; and ampicillin, 100 µg/ml.

Table 2. Strains and plasmids used in this study.

Strain/Plasmid	Description	Source/Reference
<i>S. flexneri</i> strains		
2457T	Wild-type serotype 2a	11
M90T	Wild-type serotype 5	23
BS543	2457T/ Δ <i>icsA</i>	29
BS547	2457T/ Δ <i>mxiM-1::aphA-3</i>	31
BS567	M90T/ Δ <i>ipaB2::aphA-3</i>	23
BS611	2457T/ Δ <i>mxiE2::aphA-3</i>	15
BS758	BS543/ Δ <i>mxiE2::aphA-3</i>	this study
BS766	2457T transformed with pKM208	this study
BS826	2457T/ Δ <i>ipgD</i>	this study
BS828	BS543/ Δ <i>ipgD</i>	this study
Plasmids		
pKD3	oriR6K, <i>bla</i> , <i>cat</i>	7
pKM208	Temperature-sensitive <i>red</i> -, <i>gam</i> -, <i>lacI</i> - expressing plasmid driven by P_{Tac} promoter, <i>bla</i>	7
pCP20	FLP^+ λ cI857 ⁺ λ ρ_R Rep ^{ts} <i>bla cat</i>	6

Mutant construction.

BS758 was constructed by transduction of BS543 with P1L4 grown on BS611 with selection for kanamycin resistance. BS828 was constructed using the λ red linear recombination method as previously described (7) with the following modifications. PCR was used to amplify a chloramphenicol resistance cassette gene (*cat*) from pKD3 (Table 2) with 5' and 3' overhangs identical to the 5' and 3' regions of *ipgD* internal to the start and stop codons, respectively (Table 3). BS766 was grown overnight at 30°C, subcultured into LB, and grown to mid-log phase at 30°C. Isopropyl- β -D-thiogalactopyranoside (IPTG; 1 mM) was added to the medium to induce expression of the λ red recombination genes, and the bacteria were grown at 37°C for 30 min. The bacteria were then heat shocked at 42°C for 15 min, electroporated with the cleaned PCR product, recovered in SOC medium, and plated on tryptic soy broth plates containing Congo red and chloramphenicol. Positive recombinants were purified and screened via PCR using two sets of primers (Table 3). One set amplified *ipgD* in the wild-type control while also amplifying the *cat* gene in the mutants so that the sizes of the products could be compared. The second primer set amplified half of *ipgD* in the wild-type control and resulted in no product in the mutants because *ipgD* was not present. Next, this mutant was used as the donor strain for transduction of 2457T and BS543 using P1L4, and positive transductants were selected via chloramphenicol resistance. After PCR confirmation of the deletion in the wild-type and BS543 backgrounds, the *cat* cassette was removed by transforming pCP20 (Table 2) and incubating restreaked colonies at 42°C to generate BS826 and BS828. Control experiments were performed to ensure that BS826 and BS828 were invasive in HeLa cells.

Table 3. Primers used in this study.

Purpose	Forward Primer		Reverse Primer	
	Designation	Sequence	Designation	Sequence
Amplify	ipgDcatF	ACTAATTTGGGAT	ipgDcatR	GACGAATACCCT
<i>cat</i> cassette		TGCATCAGGTTTC		TTCACCATATTC
for <i>ipgD</i>		ATTTCAAAGCGG		CATATTTTTGGG
deletion		AGATTCCTATAAA		TCCCCTATTCTTT
		GTGTAGGCTGGA		CCATATGAATAC
		GCTGCTTC		CTCCTTAGT
Confirm	ipgDF	AGAGAACCCTGT	ipgDR	ATTAGCACATCA
<i>ipgD</i>		TGAATAAG		TCATCAAG
deletion				
Confirm	ipgDcenF	TTATATCAGCCTA	ipgDR	ATTAGCACATCA
<i>ipgD</i>		TGGATTG		TCATCAAG
deletion				

Apoptosis assay.

The HeLa cell invasion assay was performed as previously described (13), but modifications were made to measure the effect of STS on infected cells. Bacteria were subcultured from an overnight culture at 37°C into LB, grown at 37°C with shaking to mid-log phase, and standardized to an optical density at 600 nm of 0.72 in every experiment. The bacteria were then washed with 1X phosphate-buffered saline (PBS) prewarmed to 37°C, resuspended in prewarmed 1X Dulbecco's minimal essential medium (DMEM), and applied to semiconfluent monolayers of HeLa cells in six-well tissue culture plates. Next, the plates were centrifuged at 3,000 rpm for 10 min at 37°C to facilitate the invasion process by allowing the bacteria to make contact with the HeLa cells. The plates were incubated at 37°C with 5% CO₂ for 30 min. The cells were then washed with 1X PBS, prewarmed DMEM plus 50 µg/ml gentamicin was added, and the plates were incubated for 3 hours at 37°C with 5% CO₂. Cells were then washed again, and DMEM plus 50 µg/ml gentamicin and 4 µM STS (Sigma and Calbiochem) was added for an additional 3 hours. After the 6-hour invasion assay, cells were either fixed for immunofluorescence or scraped for Western blot analysis. For the Western blot assays, the initial DMEM incubation was extended to an hour and the incubation in DMEM plus 50 µg/ml gentamicin was reduced to 2.5 hours to increase the percentage of the monolayer that became infected.

Immunofluorescence.

After infection, cells (or uninfected controls) were fixed with 3% formaldehyde (36% stock; Sigma) and 0.2% glutaraldehyde (25% stock; Sigma) in 1X PBS for 5 min at 4°C. To visualize nuclei, 5 mg/ml of 4,6-diamido-2-phenylindole (DAPI; Molecular

Probes) was diluted 1:1,000 in 1X PBS and added to the monolayers for 20 min at room temperature in the dark.

For the activated caspase-3 staining, monolayers were blocked with 10% natural goat serum (NGS) and 0.1% saponin in 1X PBS for 20 min at room temperature. After washing, a rabbit anti-human cleaved caspase-3 antibody (Cell Signaling Technology) was added in a 1:500 dilution in 1X PBS with 10% NGS and 0.1% saponin for 1 h. After another round of washing, cells were incubated with the secondary antibody, a goat anti-rabbit immunoglobulin G antibody conjugated to Alexa 594 (Invitrogen), at a 1:1,000 dilution in 1X PBS with 10% NGS and 0.1% saponin for 45 min (32). DAPI staining was performed following the antibody staining.

For the cytochrome *c* staining, the STS incubation time in the apoptosis assay was adjusted to 2 hours in order to detect optimal levels of cytochrome *c* release. All other aspects of the assay remained the same. The staining procedures were followed as described in the protocol provided by Molecular Probes.

For all immunofluorescence experiments, antifade reagent (Molecular Probes) was added before coverslips were applied after the staining procedure. Samples were stored in the dark at 4°C and analyzed with an Olympus BX60 fluorescence microscope with an attached digital camera using X100 magnification.

Protein sample preparation and Western blot analysis.

Infected monolayers and uninfected controls were washed with 1X PBS after the modified invasion assay, and lysis solution consisting of 1% Triton X-100 and 1% protease inhibitor cocktail (Sigma) was immediately added to the monolayers. Cells were scraped on ice and then sonicated. Proteins in the whole-cell lysates were concentrated by

trichloroacetic acid precipitation. Protein pellets were resuspended in 100 μ l of sodium dodecyl sulfate (SDS) loading buffer. One microliter of each sample was diluted in 100 μ l 1X PBS to measure the final protein concentration at an optical density reading of 280 nm on a Nanodrop ND-1000 spectrophotometer in which samples were blanked against 1 μ l of SDS loading buffer diluted in 100 μ l 1X PBS.

Each sample was resolved by SDS-polyacrylamide gel electrophoresis (PAGE), and Coomassie blue staining verified equal loading of total protein for all samples. Proteins were transferred to a nitrocellulose membrane and blocked with 5% dry milk in Tris-buffered saline (TBS). Caspases were detected by applying anti-caspase-3 antibody or an anti-caspase-9 antibody (Cell Signaling Technology) at a concentration of 1:1,000 in TBS-Tween (TBST) with 5% dry milk overnight at 4°C. After washing, donkey anti-rabbit immunoglobulin G antibody conjugated to horseradish peroxidase (Amersham Biosciences) was added at a 1:1,000 concentration in TBST with 5% dry milk for 1 h. Prior to use in immunodetection, antibodies were adsorbed separately against wild-type *S. flexneri* to remove some cross-reactivity of the antibodies to the bacteria. Briefly, an acetone powder was prepared from a fresh culture of *S. flexneri* 2457T. Each antibody was diluted 1:1,000 in TBST and incubated with the powder for 30 min at 4°C with gentle rotation. Afterwards, each antibody dilution was centrifuged at $10,000 \times g$ for 10 min at 4°C. Each supernatant was removed and added to the 5% dry milk to be applied to the nitrocellulose membrane for the appropriate incubation times.

Western blots were developed using the Visualizer developing system (Upstate Cell Signaling Solutions) according to the protocol provided, and the blots were imaged using a Fuji Intelligent Dark Box with Fujinon lens and Image Reader LAS-3000

software (Fuji) on the chemiluminescence setting in increment mode at 10-second intervals. Densitometry comparisons were made using the Image Gauge V4.22 software provided, which determined the amount of inactivated and activated caspase-3 for each treatment condition.

Statistical analysis.

The data presented in Table 4 were analyzed using the Fisher exact test on the Strata Statistics/Data Analysis program, version 8.2 for Windows. The results for the three separate experiments were analyzed and then combined using the method of Fisher (10). The densitometry results for the Western blots were analyzed using Tukey's analysis of variance post hoc test on the SPSS program, version 12.0.1 for Windows.

Results

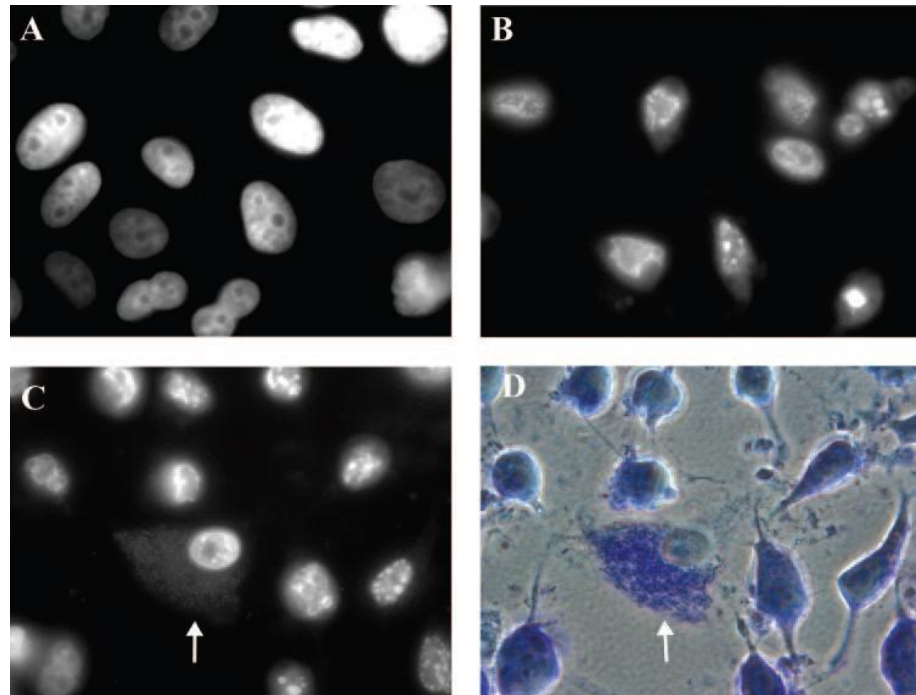
Shigella flexneri inhibits staurosporine-induced apoptosis.

The apoptosis assay was used to determine if *S. flexneri* has the ability to inhibit STS-induced apoptosis. STS inhibits protein kinases such as protein kinase C. Inhibition of protein kinase C allows the pro-apoptotic protein Bad to permeabilize the mitochondrial membrane, which leads to cytochrome *c* release and activation of the caspase cascade. A 3-hour incubation of 4 μ M STS was optimal for inducing apoptosis in uninfected HeLa cells (data not shown). Therefore, the gentamicin assay was modified as described in Materials and Methods. In addition, an Δ *icsA* mutant of *S. flexneri* (BS543), which invades and replicates intracellularly but is unable to spread from cell to cell, was used to keep the bacteria in the same HeLa cell throughout the course of the modified

assay. MIC experiments confirmed that 2457T and BS543 were able to replicate in the presence of up to 8 μ M STS in LB (data not shown).

Upon DAPI staining of the infected monolayer, the nuclei of infected cells appeared healthy with a normal shape and a visible nucleolus (Fig. 3C) similar to what is seen upon DAPI staining of healthy, normal HeLa cells (Fig. 3A). However, the nuclei of uninfected cells in the infected monolayer had the characteristic appearance of apoptotic nuclei, namely, DNA fragmentation and chromatin condensation as seen in the control experiments of an uninfected monolayer induced to undergo apoptosis using 4 μ M STS for 3 h (Fig. 3B). In addition, the cytoplasm of uninfected cells in the infected monolayer appeared to be shrinking while the cytoplasm of infected cells was able to maintain its shape (Fig. 3D). These results were reproducible in three separate experiments, and cell counts were performed as a method of quantitation. Out of a total of 983 cells, all uninfected cells (667) appeared apoptotic while all infected cells (316) appeared healthy (Table 4). In addition, cell counts were performed in experiments in which the STS incubation times were changed to 2 h or 4 h in the apoptosis assay. In these experiments, *S. flexneri* was still able to consistently protect HeLa cells from STS-induced apoptosis (data not shown).

Figure 3. *Shigella flexneri* protects HeLa cells from staurosporine-induced apoptosis.



A. DAPI stained image of a monolayer of normal, healthy HeLa cells.

B. DAPI stained monolayer of HeLa cells induced to undergo apoptosis using 4 μM STS for 3 hours.

C. DAPI stained monolayer infected with *S. flexneri* strain BS543 and treated with 4 μM STS. The arrow points to an infected cell in which the bacteria are also visible in the cytoplasm upon DAPI staining. This image is representative of cells observed in three independent experiments.

D. Phase-contrast view of panel C with Giemsa staining. The arrow points to the infected cell.

Table 4. Cell counts of apoptosis assay experiments.

Expt	No. of cells			
	<u>Infected</u>		<u>Uninfected</u>	
	Healthy ^b	Apoptotic ^c	Healthy ^b	Apoptotic ^c
First Experiment ^a	102 ^d	0	0	219
Second Experiment	125 ^d	0	0	224
Third Experiment	89 ^d	0	0	224
Average	105 ^d	0	0	222

^a = At least 300 cells were analyzed for each experiment.

^b= Defined as having a normal appearance of the nuclei (normal shape and visible nucleolus) in addition to having a normal appearance of the cytoplasm as compared to control HeLa cells without STS treatment.

^c= Defined as having a characteristic apoptotic nucleus (DNA fragmentation, chromatin condensation) in addition to having cytoplasmic shrinkage as compared to control HeLa cells with STS treatment.

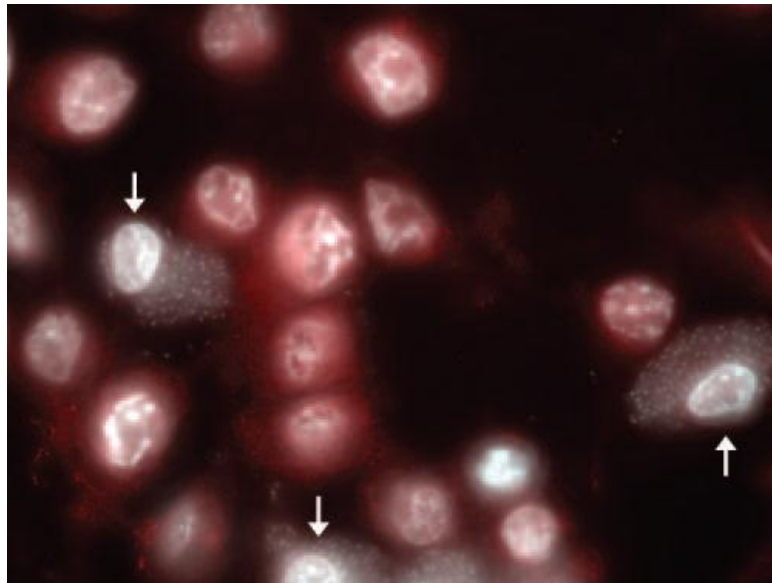
^d = P value <0.001 using Fisher's exact test. Results for the three separate experiments were combined using the method of Fisher (10).

Shigella flexneri prevents the activation of caspase-3 in the presence of staurosporine.

As a method to confirm the above observations, infected monolayers were stained for activated caspase-3. STS-treated uninfected cells stained positive for activated caspase-3 (red) in addition to possessing apoptotic nuclei (Fig. 4). However, STS-treated infected cells did not stain for activated caspase-3. This observation was consistent in three repeated experiments.

In order to confirm the immunofluorescence results, Western blot experiments were performed to measure the effect of *Shigella* infection on STS-induced activation of caspase-3. The apoptosis assay was adjusted to increase the percentage of the monolayer that became infected upon invasion with *S. flexneri*. Therefore, wild-type *S. flexneri* 2a (2457T) was used because the ability to spread from cell to cell was required to achieve optimal infection of the monolayer. In addition, the DMEM incubation was slightly increased as described in Materials and Methods. An anti-caspase-3 antibody, which recognizes the full-length (35-kDa), inactive form of caspase-3 in addition to the activated (17-kDa), cleaved form of the protein, was used. As seen in Fig. 5A, there was more inactive caspase-3 and there was less activated caspase-3 in the sample treated with STS and infected with 2457T (lane 4) than in the uninfected cells receiving STS treatment (lane 2). Densitometry analysis of the Western blot showed a significant induction in activated caspase-3 in uninfected cells treated with STS compared to infected cells treated with STS (Fig. 5B). These results verified that *S. flexneri* was able to inhibit STS-induced apoptosis in infected HeLa cells by affecting the activation of caspase-3.

Figure 4. Activated caspase-3 is not present in Shigella-infected cells after staurosporine treatment.



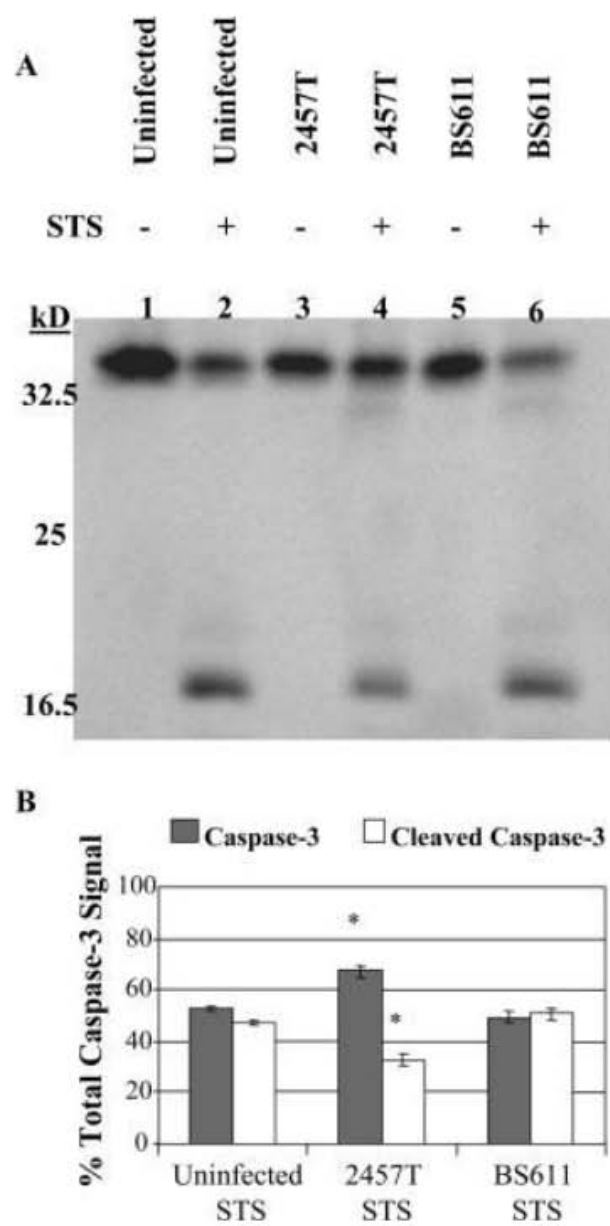
Immunofluorescence analysis of an infected monolayer stained for activated caspase-3 (red) in addition to DAPI staining (white) after STS treatment in the modified assay. The arrows point to infected cells. This image is representative of cells observed in three independent experiments.

Figure 5. Western blot analysis for the activation of caspase-3.

A. Whole-cell lysates were separated by SDS-PAGE and analyzed by immunoblotting with an anti-caspase-3 antibody, which recognizes the full-length, inactive form of caspase-3 (35 kDa) and the large fragment resulting from cleavage during activation (17 kDa). Lane 1, uninfected HeLa cells; lane 2, uninfected HeLa cells with STS treatment; lane 3, 2457T-infected cells; lane 4, 2457T-infected cells with STS treatment; lane 5, BS611-infected cells; lane 6, BS611-infected cells with STS treatment.

B. Results of densitometry analysis of the percentage of the total caspase-3 detected in the Western blot are divided into the inactive form (caspase-3) and the activated form (cleaved caspase-3). The average percentage of each form is shown, with error bars representing the standard deviations from three independent experiments. *, $P < 0.001$ using Tukey's analysis of variance post hoc test, showing a significant difference between the 2457T STS treatment group and the other two treatment groups.

Figure 5. Western blot analysis for the activation of caspase-3.



Shigella flexneri does not prevent cytochrome *c* release or caspase-9 activation in the presence of staurosporine.

In order to determine at which point in the apoptotic pathway *S. flexneri* inhibits apoptosis, we next determined if cytochrome *c* release occurred in infected cells. When stained for cytochrome *c* release, uninfected, healthy cells without STS treatment displayed weak, background staining since cytochrome *c* remains inside the mitochondria under normal conditions (Fig. 6A). However, STS treatment resulted in a very bright, positive signal for cytochrome *c* release in uninfected cells (Fig. 6B). When the staining procedure was applied to a *Shigella*-infected monolayer after STS treatment, infected cells also had a very bright signal for cytochrome *c* release (Fig. 6C and D). This observation was consistent in three repeated experiments. Western blot analysis for caspase-9 activation was next performed using an anti-caspase-9 antibody, which recognizes the inactive form of the protein (47 kDa) in addition to the two cleaved products (37 and 35 kDa). As seen in Figure 7, there is the same level of caspase-9 activation in all monolayers treated with STS. Densitometry analysis revealed that there was no significant difference in caspase-9 activation between *Shigella*-infected and uninfected monolayers treated with STS. Taken together, the results demonstrate that *S. flexneri* has the ability to protect HeLa cells from STS-induced apoptosis by inhibiting the activation of caspase-3 while not affecting any other aspect of the apoptosis pathway.

Figure 6. Cytochrome c release occurs in infected cells after staurosporine treatment.

A to D - Staining for cytochrome *c* release.

A. Healthy HeLa cells (no infection or STS treatment).

B. An uninfected HeLa cell after 2 hours of STS treatment.

C and D. Infected monolayer after 2 hours of STS treatment. Arrows point to infected cells. Images are representative fields from three experiments. Control experiments demonstrated that the cytochrome *c* antibody did not cross react with the *S. flexneri* surface or secreted proteins and that cytochrome *c* release does not occur in infected cells without STS treatment (data not shown).

E and F. Phase contrast images of panels C and D, respectively, showing bacteria inside infected cells.

Figure 6. Cytochrome *c* release occurs in infected cells after staurosporine treatment.

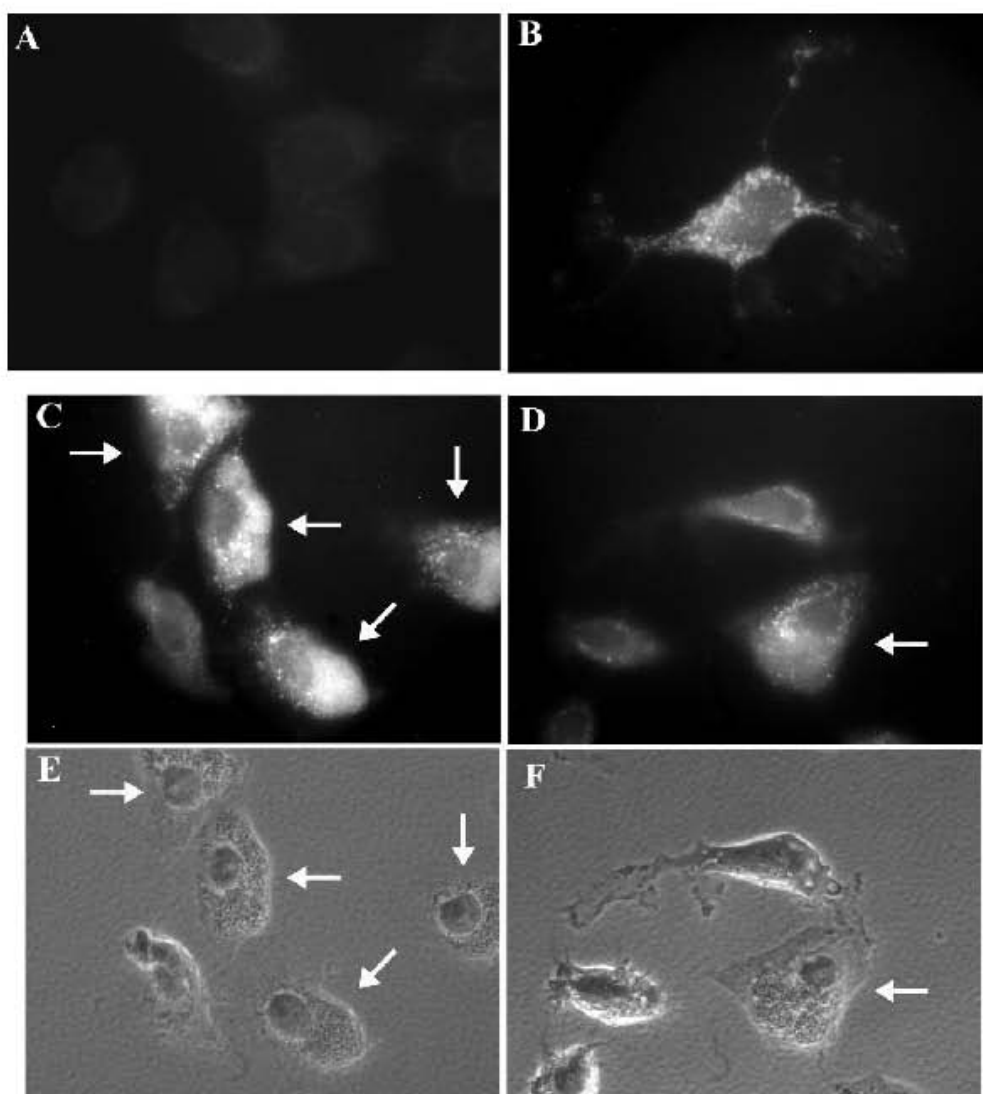
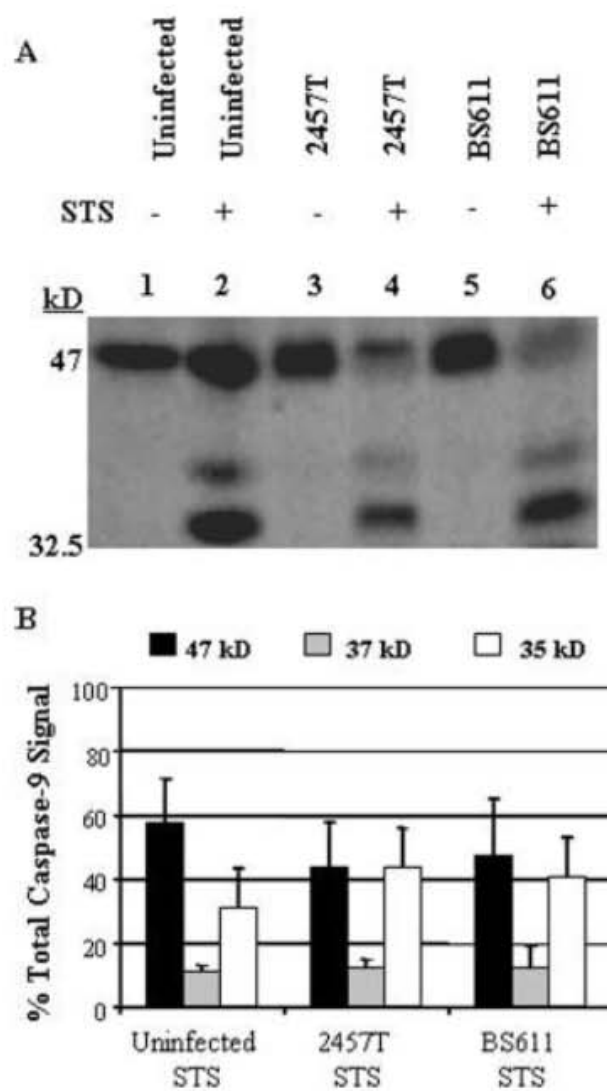


Figure 7. Western blot analysis of caspase-9 activation.

A. Whole-cell lysates were separated by SDS-PAGE and analyzed by immunoblotting with an anti-caspase-9 antibody, which recognizes the full-length, inactive form of caspase-9 (47 kDa) and the two fragments resulting from cleavage during activation (37 and 35 kDa). Lane 1, uninfected HeLa cells; lane 2, uninfected HeLa cells with STS treatment; lane 3, 2457T-infected cells; lane 4, 2457T-infected cells with STS treatment; lane 5, BS611-infected cells; lane 6, BS611-infected cells with STS treatment.

B. Results of densitometry analysis of the percentage of the total caspase-9 detected in the Western blot are divided into the inactive form (47 kDa) and the two activated forms (37 and 35 kDa). The average percentage of each form is shown, with error bars representing the standard deviations from three independent experiments.

Figure 7. Western blot analysis of caspase-9 activation.



HeLa cell protection from STS-induced apoptosis requires S. flexneri invasion, secretion, and MxiE-regulated gene products.

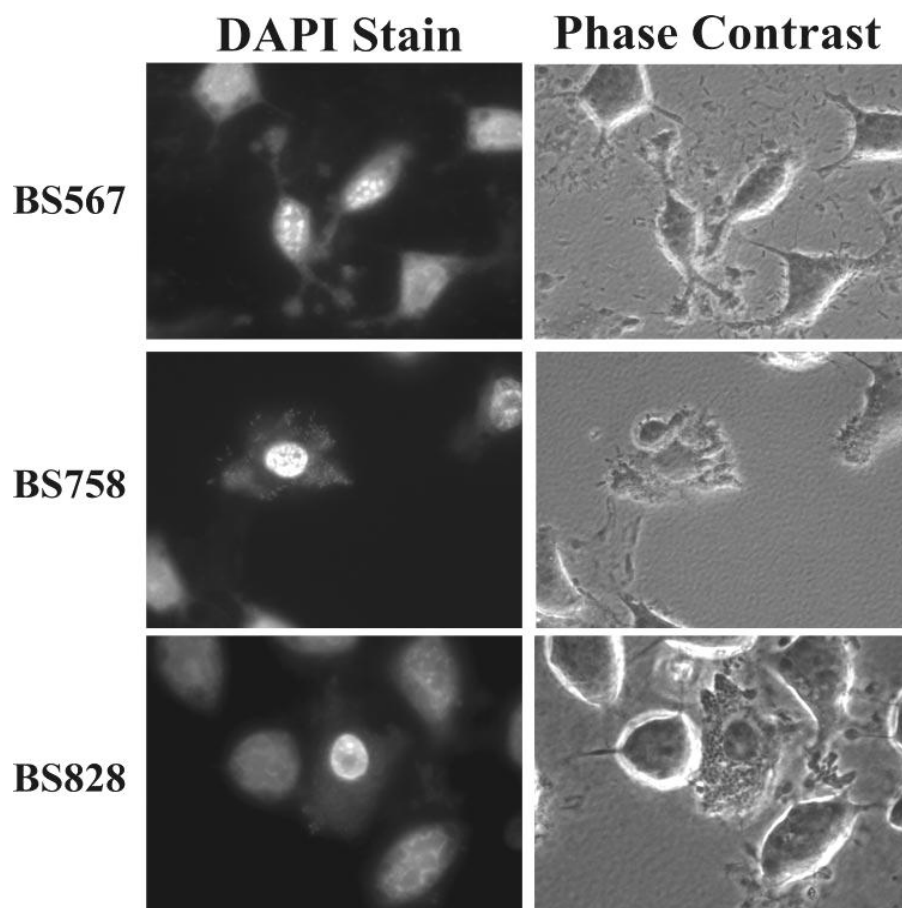
We first determined if invasion and a functional T3SS were important for protection by analyzing a $\Delta mxiM$ mutant (BS547), which has a dysfunctional T3SS, is unable to translocate the Ipa invasins, and is therefore noninvasive. Since this mutant is noninvasive, gentamicin was removed from the medium. The $\Delta mxiM$ mutant was unable to protect HeLa cells from apoptosis (data not shown). Additional experiments were performed with a $\Delta ipaB$ mutant (BS567) since this mutant is noninvasive but still has a functional T3SS. As seen in Figure 8, although the bacteria were present in the extracellular environment, the HeLa cells still became apoptotic after the STS treatment. As a result of the mutant analysis, we concluded that *S. flexneri* needed to express a functional T3SS inside of the host cytosol in order to protect HeLa cells from STS-induced apoptosis.

Based on the above observations, analysis was performed on a $\Delta mxiE$ mutant because MxiE regulates the expression of genes induced intracellularly. Some of the protein products of these genes are known to be secreted via the T3SS into the cytosol of the host cell. As seen in Figure 8, BS758 ($\Delta mxiE$ in an invasive but nonspreading $\Delta icsA$ background) was unable to protect HeLa cells from STS-induced apoptosis. Upon DAPI staining, distorted nuclei of the infected cells were evident and the nucleoli were no longer visible despite the presence of intracellular bacteria. In addition, the cytoplasm of the cells appeared deformed. The effect of the $\Delta mxiE$ mutation in the *icsA*⁺ background (BS611) on infected HeLa cells receiving STS treatment was analyzed in the Western

blot assay for caspase-3 levels. The same level of activation of caspase-3 was seen in STS-treated cells infected with this mutant as was seen in uninfected STS-treated HeLa cells (Fig. 5, lanes 2 and 6). Therefore, one or more of the genes regulated by *mxiE* are required to protect HeLa cells from STS-induced apoptosis.

Finally, BS828, a $\Delta ipgD$ mutant, was analyzed, given the fact that IpgD has been shown to lead to the activation of Akt, which is a pro-survival gene (26). As shown in Figure 8, there was no difference between HeLa cells infected with BS828 and HeLa cells infected with BS543 (*ipgD*⁺) in the apoptosis assay (Fig. 3). BS828-infected cells exposed to STS retained normal nuclei with visible nucleoli upon DAPI staining. Analysis for caspase-3 activation was performed via Western blot analysis using the $\Delta ipgD$ mutation in the *icsA*⁺ background (BS826). Again, there was no difference between HeLa cells infected with a $\Delta ipgD$ mutant and HeLa cells infected with wild-type bacteria (data not shown). These results indicate that IpgD is not essential for *S. flexneri* to protect epithelial cells from STS-induced apoptosis.

Figure 8. *Shigella flexneri* mutants analyzed in the apoptosis assay.



S. flexneri mutants analyzed in the apoptosis assay with DAPI stained images on the left and the corresponding phase contrast views on the right. All images are representatives of three independent experiments.

Discussion

Our goal in this study was to determine if *S. flexneri* infection has the ability to protect epithelial cells from apoptosis given the fact that previous work noted that HeLa cells infected with *S. flexneri* undergo a stress response yet do not die as a result of infection (21). We found that *S. flexneri* infection of HeLa cells resulted in inhibition of STS-induced apoptosis. Upon immunofluorescence analysis of 2457T-infected monolayers treated with STS, there was no detectable signal for activated caspase-3. This phenotype correlated with the consistent observations seen upon DAPI staining in which the nuclei of infected cells that were treated with STS had a healthy appearance. The Western blot results support the immunofluorescence images since 2457T-infected monolayers had significantly reduced levels of caspase-3 activation in the presence of STS compared to those for uninfected cells (Fig. 5, lane 4). Since 100% of the monolayer cannot become infected by 2457T, the uninfected HeLa cells in the monolayer became apoptotic upon STS treatment and contributed to the level of activated caspase-3 observed. A similar observation was made for monolayers of *Salmonella enterica*-infected epithelial cells (17). Therefore, these results verify that *S. flexneri* has the ability to inhibit the activation of caspase-3 in the presence of STS in order to protect HeLa cells from apoptosis. It should be noted that there is no caspase-3 activation in 2457T-infected monolayers without STS treatment (lane 3), which confirms that *Shigella* does not induce apoptosis upon normal infection of epithelial cells.

In order to identify the point of interaction that the bacterium has with the apoptosis pathway, we tested for the presence or absence of cytochrome *c* release. By determining if cytochrome *c* release occurred, we would be able to focus upstream or

downstream of this point in the apoptotic pathway, since pro-apoptotic proteins must be activated in order for cytochrome *c* release to occur. When we examined cytochrome *c* staining in infected monolayers treated with STS, we found that cytochrome *c* release does occur. The healthy, uninfected cells that did not receive STS treatment in control experiments displayed only weak staining, due to the fact that cytochrome *c* remains inside the mitochondria. The uninfected and infected cells treated with STS had strong signals, which remained in the cytoplasm of the cells, indicating that cytochrome *c* was released from the mitochondria. The staining patterns were similar to what was seen by Willhite et al. when they performed similar staining for their studies with *Helicobacter pylori* (35).

The next step was to determine if caspase-9 activation occurred, which would allow us to identify the point in the apoptosis pathway that is affected by *S. flexneri* infection. Western blot analysis revealed that monolayers infected with 2457T and treated with STS had the same levels of caspase-9 activation as did uninfected monolayers treated with STS. Densitometry analysis revealed that there was no significant difference in the activation of caspase-9 between the two treatments. Therefore, *S. flexneri* is protecting HeLa cells from STS-induced apoptosis by interfering with caspase-3 activation. Interestingly, microarray analysis by Pedron et al. found significant up-regulation of the inhibitor of apoptosis protein 1 (IAP-1) upon *Shigella* infection of epithelial cells (26). This up-regulation of IAP-1 correlates with the observations reported here, since IAP-1 inhibits caspase-3 activation directly. A similar observation was made in *Neisseria gonorrhoeae* infection of human urethral epithelium. Up-regulation of the anti-apoptotic genes *bfl-1* and *cox-2* and the c-IAP-2 gene was found to be dependent on

the *Neisseria* protein porin IB (2, 3). Therefore, up-regulation of IAP-1 by *S. flexneri* is a reasonable mechanism for the inhibition of apoptosis by the bacteria in epithelial cells.

Our observations suggest that *S. flexneri* could also inhibit the extrinsic pathway of apoptosis. If *S. flexneri* inhibits just the activation of caspase-3, it is possible that the bacteria can inhibit apoptosis that is induced via a pathway that is independent of cytochrome *c* release from the mitochondria. For example, the tumor necrosis factor family causes apoptosis through use of death receptors and the activation of caspase-8. This is typically seen when activated T cells use their Fas ligand to bind to the Fas receptor on infected target cells in order to induce apoptosis. Caspase-8 can activate caspase-3 either directly or indirectly through the activation of the pro-apoptotic protein Bid (28, 34). Thus, by inhibiting the activation of caspase-3, *S. flexneri* can protect the epithelial cells from several different apoptotic pathways to increase its survival inside the host.

To help determine the requirements for *S. flexneri* to protect HeLa cells from STS-induced apoptosis, the $\Delta ipaB$ mutant and the $\Delta mxiM$ mutant were analyzed. The $\Delta ipaB$ mutant is noninvasive, while the $\Delta mxiM$ mutant has a dysfunctional T3SS in addition to the noninvasive phenotype. Both mutants were unable to protect HeLa cells from STS-induced apoptosis, and therefore, it is shown that invasion is required for protection. The $\Delta ipaB$ mutant has a functional T3SS, and some effectors are still secreted by the bacteria upon contact with host cells (23). The data suggested that certain effectors of the T3SS needed to be inside the cytoplasm of the HeLa cells in order to protect these cells from STS-induced apoptosis.

Based on the results of the mutant analysis, we tested a $\Delta mxiE$ mutant since MxiE-regulated genes are expressed when the bacteria are present in the intracellular environment of the host cell. Some of these gene products are also secreted via the T3SS into the cytoplasm of the host cell (15, 20). DAPI staining of $\Delta mxiE$ -infected cells treated with STS showed an intermediate level of protection in that the nuclei were not healthy but also were not completely apoptotic. The shape of the nuclei and the cytoplasm appeared distorted. Western blot analysis confirmed the DAPI staining and showed that caspase-3 is activated in HeLa cells infected with the $\Delta mxiE$ mutant to the same extent as seen in the uninfected controls. These observations suggest that one or several of the MxiE-regulated genes are important for protection from apoptosis. Experiments are currently in progress to determine which MxiE-regulated genes are required for protection from STS-induced apoptosis. In addition, we cannot yet exclude the possibility that a gene not regulated by MxiE has a role in protection from apoptosis.

It was recently reported by Pendaries et al. (27) that the IpgD protein from *S. flexneri* increases phosphatidylinositol 5-monophosphate production during infection in epithelial cells. The phosphatidylinositol 5-monophosphate in turn leads to the eventual activation of the pro-survival protein Akt (27). The authors stated that IpgD was responsible for the inhibition of STS-induced apoptosis. We constructed a $\Delta ipgD$ mutant and found that it was still able to protect HeLa cells from STS-induced apoptosis. Supporting this observation is the analysis of cytochrome *c* release in infected cells. Akt is responsible for preventing the pro-apoptotic protein Bad from permeabilizing the mitochondrial membrane, which prevents cytochrome *c* release and activation of the caspase cascade (16). The presence of cytochrome *c* release and caspase-9 activation in

2457T-infected cells treated with STS in our assays indicate that any Akt activation by IpgD is not sufficient to inhibit STS-induced apoptosis. *Salmonella enterica* has also been observed to inhibit apoptosis by utilizing SopB to activate Akt (17). IpgD is the *Shigella* homolog to SopB, but there are important differences between the influences of these effectors on Akt. First, SopB sustains Akt activation for 4 hours post-infection. IpgD on the other hand activates Akt for 1 hour post-infection. The prolonged activation of Akt by *Salmonella* would result in a longer pro-survival effect on infected epithelial cells than would activation of Akt by *Shigella*. Second, a *Salmonella* Δ sopB mutant is unable to protect epithelial cells from the intrinsic pathway of apoptosis when camptothecin is used to induce apoptosis during infection. Our *Shigella* Δ ipgD mutant was able to protect epithelial cells from the intrinsic pathway when STS was used during infection. Therefore, we believe that, although Akt may have some pro-survival effects on *S. flexneri*-infected epithelial cells, this is not the main mechanism of inhibiting STS-induced apoptosis. Based on our observations, we believe that the mechanism of apoptosis inhibition by *S. flexneri* works by blocking caspase-3 activation.

In conclusion, we have found that *S. flexneri* is able to protect epithelial cells from STS-induced apoptosis by inhibiting the activation of caspase-3 despite the release of cytochrome *c* and the activation of caspase-9. Both bacterial invasion and a functional T3SS are essential for protection, and we believe that the presence of certain T3SS effectors inside the cytoplasm of the host cell is required for protection. One or several of these effectors are the proteins whose expression is regulated by MxiE, given that the Δ mxiE mutant was unable to protect HeLa cells from STS-induced apoptosis. Since *S. flexneri* is a pathogen that must find an intracellular niche inside the host to ensure

survival, one mechanism to ensure survival is the induction of apoptosis in macrophages that would otherwise kill the bacteria. More importantly, the ability of *S. flexneri* to inhibit apoptosis in epithelial cells ensures bacterial replication and survival in an intracellular niche within the host. Other pathogens such as *Salmonella*, *Chlamydia trachomatis*, and *Neisseria* also inhibit apoptosis in order to ensure survival *in vivo* (2, 3, 9, 17, 22). These organisms affect the ability of pro-apoptotic proteins to permeabilize the mitochondrial membrane and therefore prevent cytochrome *c* release. This outcome is distinct from what we report for *Shigella*-infected cells, since cytochrome *c* release and subsequent caspase-9 activation are detected with STS treatment and yet caspase-3 activation is inhibited. Therefore, *S. flexneri* is unique in that it protects epithelial cells from late-stage apoptosis by interfering with caspase-3 activation.

Acknowledgements

This work was supported by grant AI24656 from the National Institute of Allergy and Infectious Diseases.

We would also like to thank Rachel Binet, Reinaldo Fernandez, and Daniel Zurawski for technical assistance, and Dr. Cara Olsen for her help with the statistical analysis.

The opinions or assertions contained herein are the private ones of the authors and are not to be construed as official or reflecting the views of the Department of Defense or the Uniformed Services University of the Health Sciences.

References

1. **Ashe, P. C., and M. D. Berry.** 2003. Apoptotic signaling cascades. *Prog. Neuropsychopharmacol. Biol. Psychiatry.* **27**:199-214.
2. **Binnicker, M. J., R. D. Williams, and M. A. Apicella.** 2004. Gonococcal porin IB activates NF-kappaB in human urethral epithelium and increases the expression of host antiapoptotic factors. *Infect. Immun.* **72**:6408-6417.
3. **Binnicker, M. J., R. D. Williams, and M. A. Apicella.** 2003. Infection of human urethral epithelium with *Neisseria gonorrhoeae* elicits an upregulation of host anti-apoptotic factors and protects cells from staurosporine-induced apoptosis. *Cell. Microbiol.* **5**:549-560.
4. **Byrne, G. I., and D. M. Ojcius.** 2004. *Chlamydia* and apoptosis: life and death decisions of an intracellular pathogen. *Nat. Rev. Microbiol.* **2**:802-808.
5. **Chen, Y., M. R. Smith, K. Thirumalai, and A. Zychlinsky.** 1996. A bacterial invasin induces macrophage apoptosis by binding directly to ICE. *EMBO J.* **15**:3853-3860.

6. **Cherepanov, P. P., and W. Wackernagel.** 1995. Gene disruption in *Escherichia coli*: Tc^R and Km^R cassettes with the option of Flp-catalyzed excision of the antibiotic-resistance determinant. *Gene*. **158**:9-14.
7. **Datsenko, K. A., and B. L. Wanner.** 2000. One-step inactivation of chromosomal genes in *Escherichia coli* K-12 using PCR products. *Proc. Natl. Acad. Sci. U S A* **97**:6640-6645.
8. **DeFilippis, R. A., E. C. Goodwin, L. Wu, and D. DiMaio.** 2003. Endogenous human papillomavirus E6 and E7 proteins differentially regulate proliferation, senescence, and apoptosis in HeLa cervical carcinoma cells. *J. Virol.* **77**:1551-1563.
9. **Dong, F., M. Pirbhai, Y. Xiao, Y. Zhong, Y. Wu, and G. Zhong.** 2005. Degradation of the proapoptotic proteins Bik, Puma, and Bim with Bcl-2 domain 3 homology in *Chlamydia trachomatis*-infected cells. *Infect. Immun.* **73**:1861-1864.
10. **Fisher, R. A.** 1925. *Statistical methods for research workers*, 13 ed. Oliver & Loyd, London, England.

11. **Formal, S. B., G. J. Dammin, E. H. Labrec, and H. Schneider.** 1958. Experimental *Shigella* infections: characteristics of a fatal infection produced in guinea pigs. J. Bacteriol. **75**:604-610.
12. **Hilbi, H., J. E. Moss, D. Hersh, Y. Chen, J. Arondel, S. Banerjee, R. A. Flavell, J. Yuan, P. J. Sansonetti, and A. Zychlinsky.** 1998. *Shigella*-induced apoptosis is dependent on caspase-1 which binds to IpaB. J. Biol. Chem. **273**:32895-32900.
13. **Hromockyj, A. E., and A. T. Maurelli.** 1989. Identification of *Shigella* invasion genes by isolation of temperature-regulated inv::lacZ operon fusions. Infect. Immun. **57**:2963-2970.
14. **Jennison, A. V., and N. K. Verma.** 2004. *Shigella flexneri* infection: pathogenesis and vaccine development. FEMS Microbiol. Rev. **28**:43-58.
15. **Kane, C. D., R. Schuch, W. A. Day, Jr., and A. T. Maurelli.** 2002. MxiE regulates intracellular expression of factors secreted by the *Shigella flexneri* 2a type III secretion system. J. Bacteriol. **184**:4409-4419.
16. **Kennedy, S. G., E. S. Kandel, T. K. Cross, and N. Hay.** 1999. Akt/Protein kinase B inhibits cell death by preventing the release of cytochrome *c* from mitochondria. Mol. Cell. Biol. **19**:5800-5810.

17. **Knodler, L. A., B. B. Finlay, and O. Steele-Mortimer.** 2005. The *Salmonella* effector protein SopB protects epithelial cells from apoptosis by sustained activation of Akt. *J. Biol. Chem.* **280**:9058-9064.
18. **Koterski, J. F., M. Nahvi, M. M. Venkatesan, and B. Haimovich.** 2005. Virulent *Shigella flexneri* causes damage to mitochondria and triggers necrosis in infected human monocyte-derived macrophages. *Infect. Immun.* **73**:504-513.
19. **Kotloff, K. L., J. P. Winickoff, B. Ivanoff, J. D. Clemens, D. L. Swerdlow, P. J. Sansonetti, G. K. Adak, and M. M. Levine.** 1999. Global burden of *Shigella* infections: implications for vaccine development and implementation of control strategies. *Bull World Health Organ.* **77**:651-666.
20. **Le Gall, T., M. Mavris, M. C. Martino, M. L. Bernardini, E. Denamur, and C. Parsot.** 2005. Analysis of virulence plasmid gene expression defines three classes of effectors in the type III secretion system of *Shigella flexneri*. *Microbiology.* **151**:951-962.
21. **Mantis, N., M. C. Prevost, and P. Sansonetti.** 1996. Analysis of epithelial cell stress response during infection by *Shigella flexneri*. *Infect. Immun.* **64**:2474-2482.

22. **Massari, P., C. A. King, A. Y. Ho, and L. M. Wetzler.** 2003. Neisserial PorB is translocated to the mitochondria of HeLa cells infected with *Neisseria meningitidis* and protects cells from apoptosis. *Cell. Microbiol.* **5**:99-109.

23. **Menard, R., P. J. Sansonetti, and C. Parsot.** 1993. Nonpolar mutagenesis of the ipa genes defines IpaB, IpaC, and IpaD as effectors of *Shigella flexneri* entry into epithelial cells. *J. Bacteriol.* **175**:5899-5906.

24. **Navarre, W. W., and A. Zychlinsky.** 2000. Pathogen-induced apoptosis of macrophages: a common end for different pathogenic strategies. *Cell. Microbiol.* **2**:265-273.

25. **Nonaka, T., T. Kuwabara, H. Mimuro, A. Kuwae, and S. Imajoh-Ohmi.** 2003. *Shigella*-induced necrosis and apoptosis of U937 cells and J774 macrophages. *Microbiology.* **149**:2513-2527.

26. **Pedron, T., C. Thibault, and P. J. Sansonetti.** 2003. The invasive phenotype of *Shigella flexneri* directs a distinct gene expression pattern in the human intestinal epithelial cell line Caco-2. *J. Biol. Chem.* **278**:33878-33886.

27. **Pendaries, C., H. Tronchere, L. Arbibe, J. Mounier, O. Gozani, L. Cantley, M. J. Fry, F. Gaits-Iacovoni, P. J. Sansonetti, and B. Payrastre.** 2006.

PtdIns(5)P activates the host cell PI3-kinase/Akt pathway during *Shigella flexneri* infection. EMBO J. **25**:1024-1034.

28. **Reed, J. C.** 2000. Mechanisms of apoptosis. Am. J. Pathol. **157**:1415-1430.

29. **Sandlin, R. C., and A. T. Maurelli.** 1999. Establishment of unipolar localization of IcsA in *Shigella flexneri* 2a is not dependent on virulence plasmid determinants. Infect. Immun. **67**:350-356.

30. **Sansonetti, P. J., G. Tran Van Nhieu, and C. Egile.** 1999. Rupture of the intestinal epithelial barrier and mucosal invasion by *Shigella flexneri*. Clin. Infect. Dis. **28**:466-475.

31. **Schuch, R., and A. T. Maurelli.** 1999. The mxi-Spa type III secretory pathway of *Shigella flexneri* requires an outer membrane lipoprotein, MxiM, for invasion translocation. Infect. Immun. **67**:1982-1991.

32. **Steele-Mortimer, O., J. H. Brumell, L. A. Knodler, S. Meresse, A. Lopez, and B. B. Finlay.** 2002. The invasion-associated type III secretion system of *Salmonella enterica* serovar Typhimurium is necessary for intracellular proliferation and vacuole biogenesis in epithelial cells. Cell. Microbiol. **4**:43-54.

33. **Suzuki, T., K. Nakanishi, H. Tsutsui, H. Iwai, S. Akira, N. Inohara, M. Chamailard, G. Nunez, and C. Sasakawa.** 2005. A novel caspase-1/toll-like receptor 4-independent pathway of cell death induced by cytosolic *Shigella* in infected macrophages. *J. Biol. Chem.* **280**:14042-14050.
34. **Thorburn, A.** 2004. Death receptor-induced cell killing. *Cell. Signal.* **16**:139-144.
35. **Willhite, D. C., T. L. Cover, and S. R. Blanke.** 2003. Cellular vacuolation and mitochondrial cytochrome c release are independent outcomes of *Helicobacter pylori* vacuolating cytotoxin activity that are each dependent on membrane channel formation. *J Biol. Chem.* **278**:48204-48209.
36. **Zychlinsky, A., M. C. Prevost, and P. J. Sansonetti.** 1992. *Shigella flexneri* induces apoptosis in infected macrophages. *Nature.* **358**:167-169.

Chapter 3

Microarray Analysis of Shigella flexneri-Infected Epithelial Cells Identifies Host Factors Important for Apoptosis Inhibition.

Manuscript submitted as: Faherty, C.S., Merrell, D.S., Semino-Mora C., Dubois A., and Maurelli, A.T. Microarray analysis of *Shigella flexneri*-infected epithelial cells identifies host factors important for apoptosis inhibition. *BMC Genomics*. 2009.

Abstract

Background: *Shigella flexneri* inhibits apoptosis in infected epithelial cells. In order to understand the pro-survival effects induced by the bacteria, we utilized apoptosis-specific microarrays to analyze the changes in eukaryotic gene expression in both infected and uninfected cells in the presence and absence of staurosporine, a chemical inducer of the intrinsic pathway of apoptosis. The goal of this research was to identify host factors that contribute to apoptosis inhibition in infected cells.

Results: The microarray analysis revealed distinct expression profiles in uninfected and infected cells, and these changes were altered in the presence of staurosporine. These profiles allowed us to make comparisons between the treatment groups. Compared to uninfected cells, *Shigella*-infected epithelial cells, both in the presence and absence of staurosporine, showed significant induced expression of *JUN*, several members of the inhibitor of apoptosis gene family, nuclear factor κ B and related genes, genes involving tumor protein 53 and the retinoblastoma protein, and surprisingly,

genes important for the inhibition of the extrinsic pathway of apoptosis. We confirmed the microarray results for a selection of genes using *in situ* hybridization analysis.

Conclusion: Infection of epithelial cells with *S. flexneri* induces a pro-survival state in the cell that results in apoptosis inhibition in the presence and absence of staurosporine. The bacteria may target these host factors directly while some induced genes may represent downstream effects due to the presence of the bacteria. Our results indicate that the bacteria block apoptosis at multiple checkpoints along both pathways so that even if a cell fails to prevent apoptosis at an early step, *Shigella* will block apoptosis at caspase-3. Apoptosis inhibition is vital to the survival of the bacteria *in vivo*. Future characterization of these host factors is required to fully understand how *S. flexneri* inhibits apoptosis in epithelial cells.

Background

Shigella flexneri is a Gram-negative, facultative intracellular organism, and the causative agent of bacillary dysentery. Infection with *Shigella* causes an intense acute inflammatory reaction that leads to the destruction of the colonic epithelium (67). Clinical symptoms include watery diarrhea, severe abdominal pain, and bloody, mucoid stools. These symptoms of dysentery are due to the penetration of *Shigella* into colonic epithelial cells, which provide an intracellular environment for the bacteria to multiply and spread to adjacent cells (67). Entry into epithelial cells is mediated by the Ipa proteins encoded on the 220-kb virulence plasmid. Secretion of these proteins is dependent on a type III secretion system (T3SS), which is encoded by 20 genes in the *mxi-spa* locus of the

virulence plasmid. Additional T3SS effector proteins are secreted through the T3 needle when the bacteria are inside the cytoplasm of the host cell (67).

We previously demonstrated that *S. flexneri* inhibits apoptosis in epithelial cells (10). In the presence of staurosporine (STS), a chemical inducer of the intrinsic pathway of apoptosis, *S. flexneri* inhibits apoptosis by preventing the activation of caspase-3 despite the fact that both cytochrome *c* release from the mitochondria and caspase-9 activation occur (10). Given these findings, we next wanted to determine the important cellular changes that occur in epithelial cells upon infection with *S. flexneri* and subsequent exposure to STS. Previous research analyzed changes in eukaryotic gene expression due to *S. flexneri* invasion using whole genome arrays (58); however, analysis in the presence of an apoptosis inducer has not been performed. Therefore, the goal of this paper was to identify the changes in apoptosis-specific genes due to *S. flexneri* invasion both in the presence and absence of STS. This analysis will not only enhance our understanding of how *S. flexneri* survives inside epithelial cells, but also allow us to fully understand the mechanisms of protection from apoptosis by identifying the host factors involved in this process. The microarray analysis revealed distinct expression profiles in uninfected and infected cells, and these changes were altered in the presence of staurosporine. Based on these profiles, we made several comparisons between the treatment groups. Compared to uninfected cells, we found numerous alterations in host factors, including the jun oncogene, inhibitor of apoptosis gene family members, nuclear factor κ B (NF- κ B), and genes involving tumor protein 53 and the retinoblastoma protein, all of which are important for the pro-survival state of the infected cell. These data indicate that upon infection, the bacteria utilize multiple checkpoints along both pathways

to prevent apoptosis. If *Shigella* fails to inhibit apoptosis at an early step, the bacteria will block apoptosis at caspase-3. This inhibition is vital for the bacteria to survive *in vivo*.

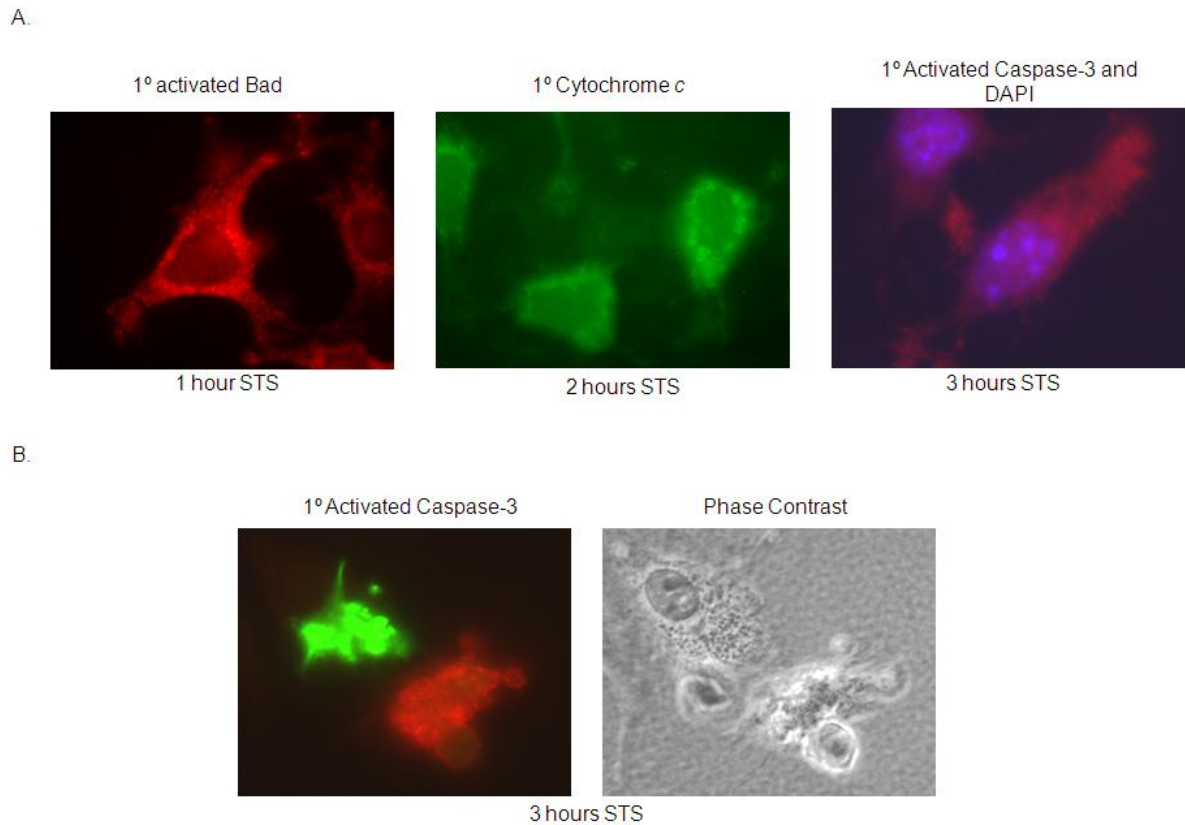
Results and Discussion

The treatments for the microarray analysis were selected based on published observations that *Shigella*-infected HeLa cells do not undergo apoptosis in the presence of STS while uninfected HeLa cells undergo apoptosis in the same conditions (10). The temporal strategy and length of STS exposure times and infection were chosen to highlight key points in the apoptosis pathway. These key points include the activation of pro-apoptotic proteins preceding damage to the mitochondria (0.5 to 1 hour STS incubation), cytochrome *c* release from the mitochondria (2 hour STS incubation), and activation of caspase-3 before significant damage to the HeLa nuclei (2.75 hour STS incubation).

To phenotypically verify that these incubation times mirrored the above expectations, we exposed uninfected HeLa cells to STS for 1, 2, or 3 hours and then performed immunofluorescence analysis (Figure 9A). After 1 hour of STS treatment, cells were stained with an antibody against the Bad protein to detect total levels of the protein (Figure 9A). Phosphorylation of Bad promotes binding to the 14-3-3 protein, which prevents the pro-apoptotic function of Bad (85). An antibody that recognizes only the phosphorylated form of Bad yielded a weak signal (data not shown). Therefore, the pro-apoptotic Bad protein was active after 1 hour of STS treatment since the dephosphorylated form of Bad was primarily detected. Next, we tested for cytochrome *c* release from the mitochondria after 2 hours of STS treatment using a weak

permeabilization treatment so only cytochrome *c* released from the mitochondria is stained and cytochrome *c* retained in the mitochondria produces only a weak signal (10). The bright signal (Figure 9A) indicates that cytochrome *c* release occurred after the 2 hours of STS treatment. Finally, caspase-3 activation and nuclear damage was assessed after 3 hours of STS treatment using an antibody that recognizes only the activated form of caspase-3 and the DAPI nuclear stain, respectively, as previously described (10). Caspase-3 activation with subsequent DNA damage was detected after 3 hours of STS treatment (Figure 9A). Control experiments verified that a 2.75 hour STS incubation time was adequate for caspase-3 activation without significant DNA damage (data not shown). In addition, to highlight our previous report that *S. flexneri* inhibits STS-induced apoptosis, we performed the apoptosis assay with a strain of bacteria expressing a green fluorescence protein (GFP) on a low copy plasmid. After the 6 hour assay, the infected cells were fixed and stained for activated caspase-3. As seen in Figure 9B, the uninfected cell is positive for activated caspase-3; whereas the adjacent infected cell only has a bright green signal due to the GFP expression by the bacteria and lacks a signal for activated caspase-3. Control experiments showed that the bacteria expressing GFP on the low copy plasmid had the same growth rate as wildtype bacteria (data not shown).

Figure 9. Immunofluorescence analysis of HeLa cells treated with staurosporine.



A. Uninfected cells stained with antibodies against key points in the STS-induced apoptosis pathway, namely Bad activation at 1 hour, cytochrome *c* release at 2 hours, and activated caspase-3 and DNA damage with DAPI nuclear staining at 3 hours STS treatment.

B. A monolayer of HeLa cells was infected with *Shigella* harboring a low copy number plasmid expressing GFP to allow green fluorescence. Left: Merged image of the monolayer for GFP and the activated form of caspase-3. Only the uninfected cells have a positive signal for caspase-3 activation. Right: Phase contrast view to visualize the bacteria in the cytoplasm of the HeLa cell.

Based on these results, we chose to examine uninfected and infected cells in the presence and absence of STS using the strategy outlined in Figure 10. The three hour incubation of Dulbecco's modified Eagle's medium (DMEM) with 50 $\mu\text{g/ml}$ gentamicin allows the intracellular population of bacteria to grow within the HeLa cells and ensures that 90% of the monolayer is infected (10). All STS treatments were matched with treatment controls in which no STS was added. After the treatments, the RNA was harvested at the indicated times, reverse transcribed, and prepared for hybridization as described in the Materials and Methods. The microarrays used are specific for apoptosis genes and contain approximately 20,000 spots representing 451 genes. The resulting microarray data were collated using the Stanford Microarray Database and utilized for pairwise analysis using the Statistical Analysis for Microarrays (SAM) algorithm and the student's two-tailed t-test to identify genes showing significant changes in expression. Supplementary Table 1 provides the data for all spots that showed statistically significant differences in the indicated pairwise analyses, and the complete data set is available at <http://smd.stanford.edu>. We performed four pairwise comparisons to identify key differences between the treatment groups, and in-depth discussion of these comparisons is provided below. Supplementary Table 2 provides the list of genes in all comparisons categorized by function and provides brief descriptions of gene function obtained from NCBI's Entrez Gene. Cluster analysis of significantly changed genes across the treatment groups revealed that the arrays segregate into two major nodes (Figure 11). These major nodes cluster uninfected cells away from infected cells. Within the uninfected node, uninfected cells treated with STS segregate away from uninfected cells that did not receive STS treatment. However, this is not the case with infected samples; STS treated

samples are interspersed with untreated samples across the node. This microarray analysis highlights clear differences in the expression of apoptotic genes in infected cells compared to uninfected cells, and interestingly, STS does not affect this pattern of apoptotic gene expression in infected cells. This analysis has provided insight into the strategies employed by *S. flexneri* to inhibit apoptosis in infected epithelial cells.

Figure 10. Schematic of the infections and treatment conditions used in this study.

The infection and STS treatment conditions were modified to analyze a time course of STS exposure and adapted from the apoptosis assay previously described (10). Briefly, *S. flexneri* was applied to a monolayer of HeLa cells and incubated at 37°C for 1 hour in Dulbecco's modified Eagle's medium (DMEM). Afterwards, the cells were washed and DMEM plus 50 µg/ml gentamicin was added to kill the extracellular bacteria and allow the intracellular bacteria to replicate. By the end of this incubation, 90% of the monolayer was infected (10). Uninfected cells received the same treatments and washes. Finally, infected and uninfected cells were washed and received DMEM plus gentamicin or DMEM plus gentamicin and 4 µM STS for 0.5, 1.0, 2.0, or 2.75 hours. After the treatments, the RNA was harvested from the cells.

Figure 10. Schematic of the infections and treatment conditions used in this study.

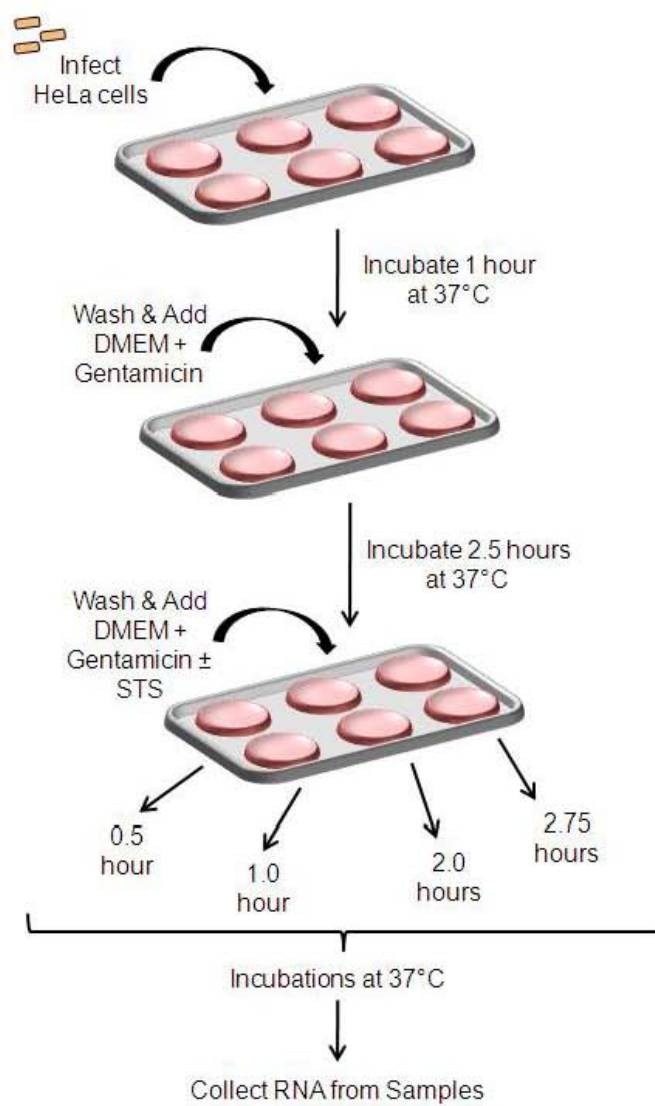
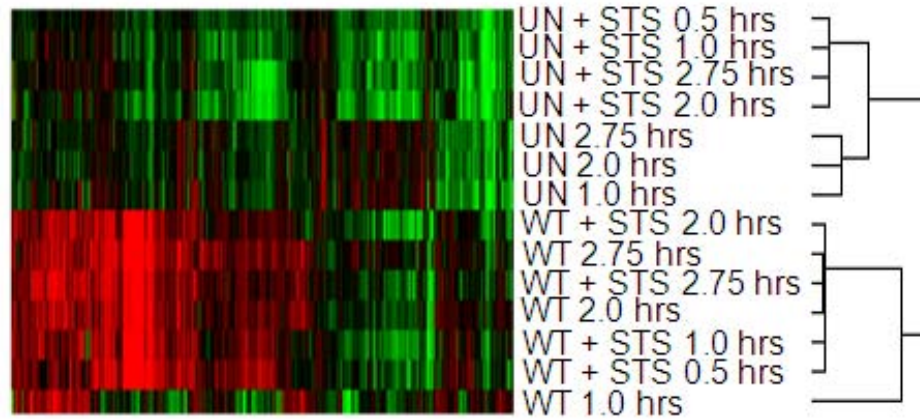


Figure 11. Cluster diagram of significant genes across treatment groups.



Cluster diagram of the genes showing statistically significant differences in uninfected (UN) or wildtype-infected (WT) HeLa cells treated with or without staurosporine (STS) for the given time points. Red and green colors represent increased or decreased expression, respectively, relative to the reference sample. Note the dendrogram shows two major nodes that segregate the majority of uninfected samples from wildtype-infected samples.

Uninfected HeLa cells with STS compared to uninfected HeLa cells.

There were 122 genes whose expression was significantly altered in uninfected cells treated with STS (USTS) versus uninfected cells (U). Interestingly, all 122 genes were repressed, which indicates that the cells receiving STS treatment turned off most gene expression during apoptotic death and suggests that the pro-apoptotic proteins already available in the cell are sufficient to induce death without *de novo* synthesis. These proteins include caspases, DNA repair enzymes, p53-associated genes, pro-apoptotic, and pro-survival genes (Supplementary Table 2).

Shigella-infected HeLa cells compared to uninfected HeLa cells.

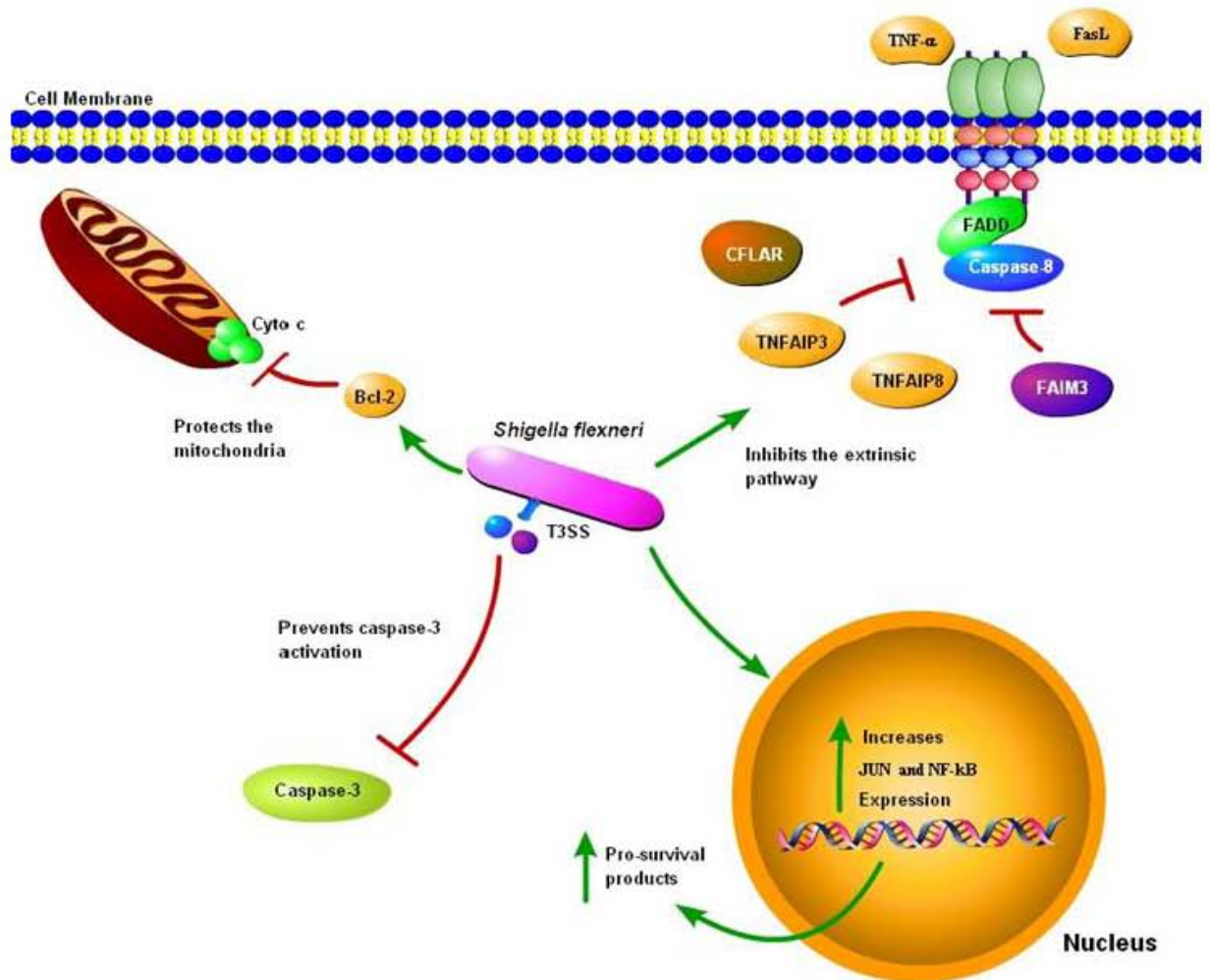
The analysis identified a total of 137 induced genes and 3 repressed genes in wildtype-infected HeLa cells (WT) compared to uninfected cells (U). In general, infected cells are in a pro-survival state compared to uninfected cells due to significant induction of various genes important for apoptosis inhibition (see Figure 12). First, there was a significant induction (17-fold) of *JUN* (also known as *c-JUN* or *AP-1*), which is a transcription factor and an oncogene (76). The p38 MAPK and JNK signaling cascades induce JUN in response to pro-inflammatory cytokines and genotoxic stress. Upon activation, JNKs translocate to the nucleus to phosphorylate and enhance the transcriptional activity of JUN (69). JUN has both pro-apoptotic and pro-survival gene targets, and it is hypothesized that the balance between these target genes is what determines whether the cell survives or undergoes apoptosis (69). Lipopolysaccharides (LPS) are the major component of the outer membrane of Gram-negative bacteria, and have been shown to induce the expression of *JUN* (2, 20). It is therefore not surprising that the induction of *JUN* is so robust in WT cells. However, we cannot rule out the

possibility that a bacterial T3SS effector protein expressed intracellularly also contributes to the induction of *JUN*. Similar induction was also seen in a previous microarray analysis of *Shigella*-infected cells (58). Below we provide evidence that WT cells are in a pro-survival state, some of which may be due to *JUN* induction. JUN targets include cyclins, E2F transcription factors, Ras-GRF1 (a guanine-nucleotide exchange factor), and p53 (32, 38, 70, 76). Given that there is a significant increase in *JUN* expression, perhaps JUN is a major contributing factor to the pro-survival state of the infected cell. Future studies involving small interfering RNA (siRNA) to knock down *JUN* expression in infected cells will allow us to determine if *JUN* induction upon infection is essential for the pro-survival state of the cell. Moreover, we predict that *S. flexneri* mutants that are unable to inhibit apoptosis may not induce *JUN* to the extent seen in WT cells.

Figure 12. Model of apoptosis inhibition by Shigella flexneri at multiple checkpoints in epithelial cells.

Infection of epithelial cells by *S. flexneri* results in several levels of protection from apoptosis. First, the bacteria prevent cytochrome *c* release from the mitochondria through the upregulation of BCL-2 proteins. Second, the extrinsic pathway of apoptosis is inhibited from *in vivo* stimuli such as TNF- α and FasL. This inhibition is most likely due to the upregulation of proteins like CFLAR, TNFAIP3, TNFAIP8, and FAIM3. Third, infection leads to the induced expression of JUN and NF- κ B, which has many pro-survival effects including the increased expression of the IAPs, the Bcl-2 family, and caspase-8 inhibitors. Finally, the bacteria prevent caspase-3 activation to provide downstream protection in the presence of strong apoptosis inducers. Through the use of T3SS effector proteins, the bacteria could directly generate mitochondrial protection, the inhibition of the extrinsic pathway, and caspase-3 inhibition. Alternatively, *S. flexneri* could indirectly produce these changes through the upregulation of pro-survival factors like JUN and NF- κ B.

Figure 12. Model of apoptosis inhibition by *Shigella flexneri* at multiple checkpoints in epithelial cells.



Surprisingly, we found multiple upregulated genes that are responsible for inhibiting apoptosis via the extrinsic pathway (Table 5 and Figure 12). This result implies that some of the apoptotic signals that occur during infection activate the extrinsic pathway of apoptosis. Signals that activate this pathway include tumor necrosis factor- α (TNF- α) and Fas ligand (30, 50). TNF- α -induced protein 8 (*TNFAIP8*) was induced in infected cells and can inhibit the TNF- α activation of caspase-8 (84). *TNFAIP3*, *FAIM3*, and *CFLAR/c-FLIP* inhibit caspase-8 activation (22, 24, 48) and all had significant induction in infected cells. Interestingly, *TNFAIP3*, also known as *A20*, was also induced in a previous microarray analysis of *Shigella*-infected cells (58). Based on the array results, we examined the ability of the *Shigella* to inhibit the extrinsic pathway of apoptosis (Figure 13). Using TNF- α -related apoptosis inducing ligand (TRAIL), which functions like TNF- α in the apoptosis assay, infected cells were able to inhibit apoptosis induction as seen upon nuclear staining. Therefore, the upregulation of genes required for the inhibition of the extrinsic pathway of apoptosis may be an important aspect for *S. flexneri* to inhibit apoptosis *in vivo*.

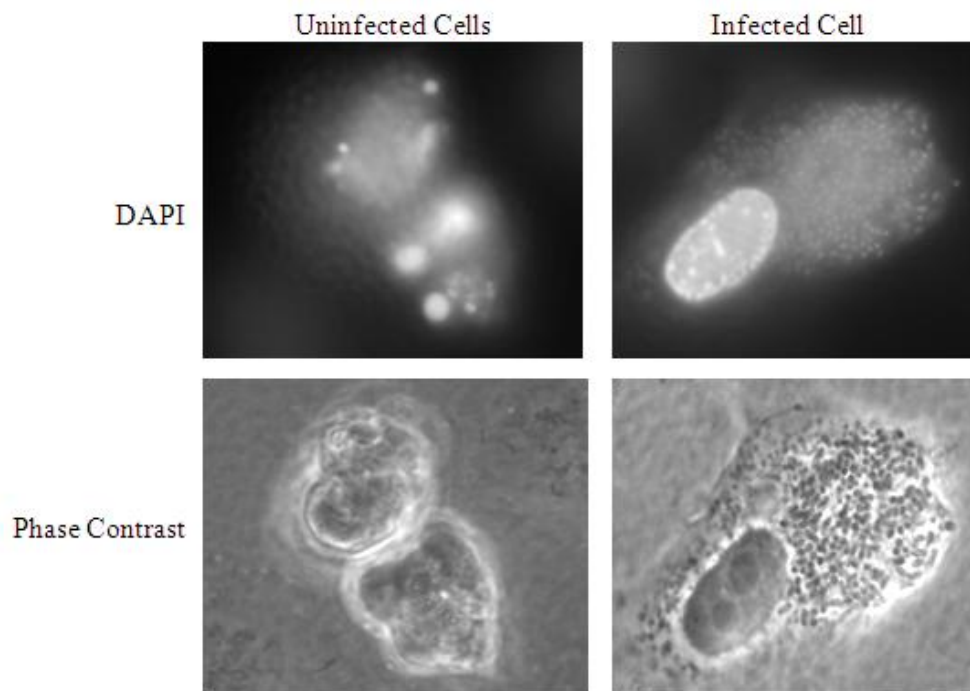
Other important genes induced in infected cells are members of the inhibitor of apoptosis (IAP) family. Expression of several IAP genes was significantly induced (Table 5). IAP upregulation has previously been observed in *Shigella*-infected cells using whole genome arrays (58). The IAP family directly inhibits caspases (45), and caspase-3 activation is inhibited in *Shigella*-infected cells in the presence of STS (10). The IAPs may be directly involved in preventing caspase-3 activation in infected cells treated with STS. On the other hand, if the IAP proteins are not directly involved in inhibition of caspase-3 activation in infected cells in the presence of STS, the induction of these genes

could still be important to enhance the pro-survival state of the infected cell. An example is the ability of cIAP-1 to inhibit TRAF2 in TNF- α -induced apoptosis (45).

Table 5. A selection of upregulated genes in wildtype-infected cells compared to uninfected cells.

Gene	Function	Fold Induction
<i>Association with the inhibition of the extrinsic pathway of apoptosis</i>		
TNFAIP3	aka A20; inhibits TNF-alpha-induced apoptosis by inhibiting caspase-8 cleavage	9.3
TNFRSF12A	functions, in part, through the NF-κB pathway to up-regulate BCL-XL and BCL-W expression for malignant cell survival	5.1
CSE1L	binds strongly to importin-alpha; highly expressed in tumor cell lines and may play a role in inhibiting TNF-mediated cell death	3.1
FAIM3	Fas apoptotic inhibitory molecule 3; inhibits caspase-8 processing	2.7
BAG4	associates with TNFR1 and death receptor-3 to negatively regulate downstream death signaling	2.6
CFLAR	CASP8 and FADD-like apoptosis regulator; aka c-FLIP; interacts with FADD and FLICE; inhibits apoptosis via human death receptors	2.5
FAIM	Fas apoptotic inhibitory molecule; pro-survival; mediates Fas resistance produced by surface Ig engagement in B cells	2.1
PEA15	a death effector domain (DED)-containing protein; inhibits both TNFRSF6 and TNFRSF1A-mediated CASP8 activity & apoptosis	2.1
TNFAIP8	tumor necrosis factor, alpha-induced protein 8; inhibits the activated form of caspase-8	2.1
<i>Interaction with caspases</i>		
BIRC4	aka XIAP; inhibits apoptosis through binding to TRAF1 and TRAF2; also inhibits caspase-3 and caspase-7	3.5
BIRC1	aka NAIP; homology to two baculoviral IAPs; suppresses apoptosis induced by various signals; binds caspase-9	3.2
BIRC5	aka survivin; with hepatitis B X-interacting protein (HBXIP) binds caspase-9; variant DeltaEx3 binds caspase-3 with BCL-2	2.8
BIRC7	aka livin; shown to interact with caspase-3, -7, & -9; degrades Smac/DIABLO	2.8

Figure 13. Infected cells resist apoptosis induction via the extrinsic pathway.



Uninfected and wildtype-infected cells analyzed in the apoptosis assay treated with TRAIL.

Top: DAPI stain of uninfected (left) and infected (right) cells. Note the uninfected cells have characteristic apoptotic nuclei while the infected cell, in which the bacteria are also stained with the DAPI, has a healthy nucleus.

Bottom: Phase contrast view of the cells. The infected cell, in which the bacteria are visible in the cytoplasm, has a healthy, round appearance while the uninfected cells are apoptotic.

Several genes that encode proteins that associate with the mitochondrial membrane were induced in WT infected cells. For example, *BCL2* was induced and is important for preventing permeabilization of the mitochondrial membrane (11). Thus, the bacteria may utilize T3SS effector proteins to increase *BCL2* expression to protect the mitochondria (Figure 12). Of note, the induction of *BCL2* does not overcome the effects of STS since cytochrome *c* release is observed in infected cells treated with STS (see below and (10)). However, STS is a strong apoptosis inducer, and the induction of *BCL2* in infected cells may be sufficient to prevent cytochrome *c* release in the absence of STS. The bacteria may encode T3SS effector proteins that target the mitochondria or pro-survival proteins, like BCL-2. These potential T3SS effectors would not be able to overcome the effects of STS, but would act as accessory proteins to enhance the pro-survival state of the cell. The increased expression of *BCL2* and other genes important for protecting the mitochondrial membrane may also be a result of other pro-survival effects (see below). Interestingly, *BECN1* expression was also induced and BECN1 has been shown to interact with BCL-2 in viral infected cells, leading to apoptosis protection (41). Therefore, the increased expression of *BCL2* and *BECN1* could promote protection of *Shigella*-infected cells from apoptosis.

Additional genes that were induced in infected cells include genes important for DNA replication and repair, and cell cycle progression (Supplementary Table 2). *XRCC4*, *XRCC5*, *ERCC2*, *RAD17*, and *RAD51*, which are all key genes in DNA replication and repair (34, 60, 62, 74), were induced. DNA damage is a signal for apoptosis (64) and maintenance of DNA integrity is an important aspect in the inhibition of apoptosis. In addition to these genes, there were also alterations in expression of genes involved in cell

cycle progression or arrest in WT infected cells. One of the few repressed genes was *SPATA4*, which may be important for the S/G2 transition (43). However, *CUL2* and *PPP2R1B* were induced, and both promote cell cycle arrest (26, 35, 39, 40). Other genes important for cell cycle progression, including *E2F3* and *TFDP2*, are induced (57, 86). As mentioned above, E2F transcription factors are regulated by JUN. The surprising changes in expression in genes that both promote and prevent cell cycle progression may reflect a complex interplay between the eukaryotic cell and the bacteria. A recent report demonstrated that the *Shigella* effector IpaB interacts with Mad2L2, leading to cell cycle arrest (27). The authors speculate that since intestinal epithelial cells undergo rapid cell turnover, the bacteria promote cell cycle arrest to maintain infection; infected cells under cell cycle arrest resist apoptosis induction, since the cells are TUNEL-negative (27). These results validate our observations that *S. flexneri* inhibits apoptosis. Conversely, cell cycle arrest can lead to apoptosis especially in the absence of the retinoblastoma tumor suppressor protein (pRb) (78). Our lab has recently reported that the *S. flexneri* effectors OspF and OspB interact with pRb to modulate the immune response (89). This interaction could also protect pRb from degradation, which would allow cell cycle arrest without leading to apoptosis. The attempt to arrest the cell cycle and the potential protection of pRb enable the bacteria to exploit cell cycle arrest and prevent apoptosis at the same time.

Finally, various genes were induced that correlate with prior observations in *S. flexneri* infection. First, *ELMO1* was induced in infected cells. The *Shigella* effector IpgB1 binds to ELMO1 to stimulate Rac1 activity, which induces membrane ruffling during invasion of epithelial cells. Therefore, IpgB1 acts as a molecular mimic of RhoG

(21), and the induction of *ELMO1* is most likely a result of the invasion process by the bacteria. Next, the *S. flexneri* effectors IpgB2 and OspB are important for nuclear factor-kappa B (NF- κ B) activation in infected cells (18, 21). The genes encoding NF- κ B and proteins required for NF- κ B activation were induced in infected cells (Supplementary Table 2 and Figure 12), including *NFKB2*. NF- κ B activation is important for inducing the expression of pro-survival proteins such as TNFAIP8 (84), TNFAIP3 (22), CFLAR (48), and IAPs (77, 88), which are induced in infected cells as mentioned above. In addition, *CARD15*, also known as *NOD2*, was upregulated in infected cells. Nod2 recognizes LPS from intracellular pathogens and activates NF- κ B (55). Even more important, Nod2 is also involved in the activation of the JNK pathway (25), which can lead to JUN activation. Therefore, NF- κ B is a significant host factor involved in inducing a pro-survival state in the infected cell. Lastly, escape from autophagy is an important aspect of *S. flexneri* infection. Atg5 binds the bacterial protein VirG/IcsA and would normally induce autophagy; however, the bacterial protein IcsB blocks Atg5 from binding VirG/IcsA (54). While there was an induction of *ATG12*, there was no subsequent induction in *ATG5* or any other gene important for autophagy. This result most likely reflects the ability of the bacteria to escape autophagy. Autophagy inhibition and apoptosis inhibition may be connected (19). Therefore, the blockage of autophagy in infected cells is likely critical for *Shigella* to survive inside epithelial cells.

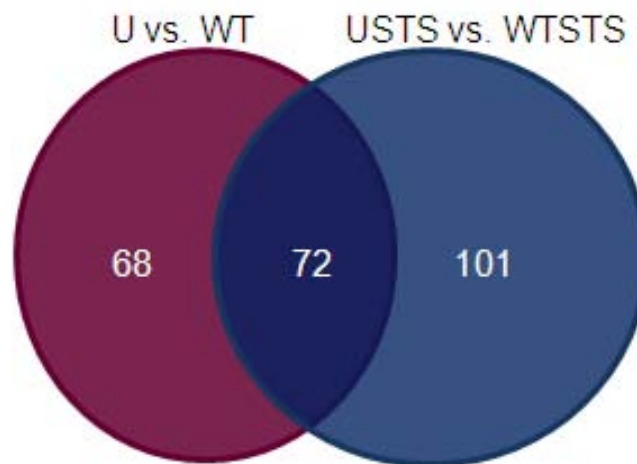
In summary, *Shigella*-infected cells are in a pro-survival state compared to uninfected cells, and a major contributing factor to this state most likely was the induction of *JUN*. Genes important for blocking the extrinsic pathway of apoptosis were also induced, in addition to the IAPs, DNA repair enzymes, and genes important for NF-

κ B activation. Moreover, the changes in gene expression seen in infected cells can be correlated to known effects of various T3SS effector proteins. The pro-survival state of infected cells may be required for apoptosis inhibition in infected cells in the presence of strong inducers like STS. At the least, the induction of these pro-survival genes may facilitate a T3SS effector protein to directly inhibit caspase-3 activation in the presence of STS.

Shigella-infected HeLa cells treated with STS compared to uninfected HeLa cells treated with STS.

There were 167 induced and 6 repressed genes in wildtype-infected cells treated with STS (WTSTS) compared to uninfected cells treated with STS (USTS). Among these, there were 72 genes that show the same differential expression, either induced or repressed, as in the U versus WT comparison (Figure 14). However, some of the levels of expression do vary. For example, *JUN* was induced even more under WTSTS conditions; a 27-fold induction was observed. This increase in induction compared to WT cells is most likely a direct result of the addition of STS to the infected cells. Interestingly, *FOSL2* or *FRA-2* was induced here but not in the U versus WT comparison. *FOSL2* is a part of the AP-1 transcription factor complex and has been shown to dimerize with *JUN* (52). Moreover, *LTBP3* was induced here but not in the U versus WT comparison. *LTBP3* is important in the activation of transforming growth factor- β (TGF- β) and has an AP-1 binding site in the promoter region (31). TGF- β can lead to cell cycle arrest, but it has also been shown to be important in tumor progression (28, 33). Thus, the increase in magnitude of *JUN* expression seen in WTSTS could lead to the induction of *FOSL2* and *LTBP3* seen in these cells.

Figure 14. Venn diagram comparing Uninfected versus Wildtype-infected to Uninfected cells treated with staurosporine versus Wildtype-infected cells treated with staurosporine.



There is a total of 140 differentially expressed genes in uninfected cells (U) compared to wildtype-infected cells (WT). Of those 140 genes, the same 72 genes were differentially expressed in uninfected cells treated with STS (USTS) compared to wildtype-infected cells treated with STS (WTSTS). The USTS vs. WTSTS comparison has a total of 173 differentially expressed genes.

Another example of increased expression due to the STS was seen in the induction of *NFKBIA*; there was approximately a 7-fold increase in WTSTS cells compared to a 3-fold increase in the U versus WT comparison. *NFKBIA* is an inhibitor of NF- κ B since it helps to trap NF- κ B in the cytoplasm (33). The induction of *NFKBIA* might be a response to the increased levels of NF- κ B due to infection, or might be a direct effect of STS. However, the induction of this gene does not affect the expression of *NFKB2* in WTSTS cells since *NFKB2* has about the same level of expression as WT cells in the U versus WT comparison.

Remarkably, approximately the same anti-apoptosis genes are induced in conditions with STS compared to the above conditions without STS suggesting the same pro-survival state of the cell was induced upon infection regardless of the presence of STS. However, there are some key differences, given the fact that the bacteria inhibit apoptosis in the presence of the strong inducer STS. The only IAP induced was *BIRC2* (Supplementary Table 2). *BIRC2* encodes cIAP1, which is involved in inhibiting caspase-8 activation (77). Interestingly, there was no induction in *BIRC4/XIAP*. Since *BIRC4/XIAP* inhibits caspase-3 activation (45), utilization of this IAP may not be important for the bacteria to inhibit caspase-3 activation in the presence of STS. Additionally, it is unlikely that the bacteria are using the XIAP already made without needing further significant production of the protein in the presence of STS over a three-hour time period. Therefore, we hypothesize that either the bacteria use a T3SS effector protein to directly inhibit caspase-3 activation in the presence of STS, or that the bacteria indirectly block caspase-3 activation by upregulation of other pro-survival genes. For example, genes required for NF- κ B activation were again induced in WTSTS cells

(Supplementary Table 2), leading to the same pro-survival effects outlined above.

Interestingly, *TRAF2* was induced in WTSTS, and this induction was not seen in the U versus WT comparison. TRAF2 is important for NF- κ B and caspase-8 activation, and is induced by NF- κ B (77). In addition, TRAF2 can activate the JNK pathway via MEKK1 leading to JUN induction (44). Also in support of protection through NF- κ B, *IER3* was induced in WTSTS cells compared to USTS cells. IER3, also known as IEX-1L, is involved in protecting cells from TNF-induced apoptosis, and IER3 is regulated by NF- κ B (82). Additional possibilities for the inhibition of caspase-3 in the presence of STS include the repression of pro-apoptotic pathways (see below). Once we identify the bacterial protein required for apoptosis inhibition, we can investigate how this protein functions in the eukaryotic cell.

There were two genes that appear in both sets of comparisons but show opposite directions of expression. First, *NALP1* was induced in U versus WT but repressed in USTS versus WTSTS. NALP1 is part of the inflammasome in which pro-inflammatory caspase-1 activation leads to interleukin-1 β (IL-1 β) processing, especially in the presence of LPS (46). NALP1 is suppressed by BCL-2 and BCL-X_L to reduce caspase-1 activation and IL-1 β production (6). *BCL2* was induced in WTSTS cells (see below). The *Shigella* effector IpaB binds and activates caspase-1 in macrophages, leading to IL-1 β secretion and cell death via pyroptosis (67). There have not been any studies regarding IpaB and caspase-1 activation in epithelial cells. While it may not be the primary method of apoptosis inhibition, NALP1 repression or inhibition of NALP1 by BCL-2 may be an important mechanism for the pro-survival state of the infected epithelial cell in the presence of STS. This finding may be a crucial explanation for the differences in

bacterial-induced cell death in macrophages and bacterial-induced cell survival in the epithelial cells. Second, *EDARADD* was repressed in U versus WT while it was induced in USTS versus WTSTS. Edaradd acts as an adaptor protein for Edar to recruit TRAF2 proteins during NF- κ B activation (23, 83). This induction of *EDARADD* possibly enhances the pro-survival effect of NF- κ B activation in the presence of STS as described above.

The comparison between USTS to WTSTS treatments revealed numerous differences in p53-associated genes and pRb-associated genes that were not seen in the U versus WT comparison (Table 6). p53 is a transcription factor and tumor suppressor, and can induce apoptosis by activating various targets that lead to mitochondrial permeabilization (49, 59). p53 itself was not altered in USTS versus WTSTS, and JUN is known to be a direct repressor of p53 (69). Therefore, the induction of *JUN* most likely had a significant effect on the expression of p53 in infected cells. However, *TP73L* or *TP63*, a homolog to p53 that can induce apoptosis by activating pro-apoptotic genes including *BAX*, *APAF1*, and *caspase-9* (59), had increased expression in WTSTS cells. The induction of *TP63* most likely lead to the increased expression of *BAX*, *APAF1*, and *caspase-9* seen in WTSTS cells. However, increased levels of these proteins and the subsequent activation of the proteins by STS had no effect on WTSTS cells since *S. flexneri* inhibits apoptosis after caspase-9 activation (10). Interestingly, p63 can induce *caspase-8* and *caspase-3* (59), but these genes were not induced in WTSTS cells. Finally, many genes, in which the gene products affect p53, were upregulated. For example, *TP53BP2* was induced in WTSTS cells. TP53BP2 is a part of the apoptosis-stimulating protein of p53 (ASPP) family of p53-interacting proteins and enhances p53 binding to

DNA for transcriptional activation of pro-apoptotic genes (66). Also, *PPP2CA*, which was induced in WTSTS cells, induces the expression of p53 and can lead to G2/M cell cycle arrest (53). *P53AIP1* was induced in WTSTS cells compared to USTS cells, and is a p53-dependent gene whose gene product binds BCL-2 to cause cytochrome *c* release from the mitochondria (47). Due to the mitochondrial permeabilization of *Shigella*-infected cells in the presence of STS, it is not surprising that these p53-regulated genes were induced. Despite the induction of p53-responsive genes, *p53* itself was not induced in WTSTS or in WT cells most likely due to significant *JUN* induction since JUN represses p53.

Table 6. A selection of upregulated genes in wildtype-infected cells with staurosporine compared to uninfected cells with staurosporine.

Gene	Function	Fold Induction
<i>Association with p53</i>		
TP53BP2	a member of the ASPP (apoptosis-stimulating protein of p53) family of p53 interacting proteins	3.3
TP73L	aka tumor protein p63; homolog to p53	3.1
JUND	member of the JUN family; a component of the AP1 TF complex; proposed to protect cells from p53-dependent senescence and apoptosis	2.8
P53AIP1	p53-regulated apoptosis-inducing protein 1; p53AIP1 regulates the mitochondrial apoptotic pathway	2.7
CUL4A	functions as an E3 ligase & with MDM2, contributes to p53 degradation; assists in nucleotide excision repair in a complex with DDB	2.6
LRDD	interacts FADD & MADD; may function as an adaptor protein in cell death-related signaling processes; a p53 effector (induces apoptosis)	2.5
NEDD8	similar to ubiquitin; conjugated to p53 via MDM2, thereby inhibiting the transcriptional activity of p53	2.2
PPP2CA	the phosphatase 2A catalytic subunit; inhibits cell growth and activates p53 & p21 (p53-responsive); overexpression leads to G2/M arrest	2.2
MDM4	contains a RING finger domain & a putative nuclear localization signal; interacts with p53 (stabilizes to counteract MDM2)	2.0
<i>Association with pRB</i>		
RBBP4	involved in chromatin remodeling & transcriptional repression associated with histone deacetylation; binds directly to pRB	3.7
JARID1A	aka RBBP2; binds with pRB for tumor suppressive functions; may interact with rhombotin-2	2.7
RBBP5	a ubiquitously expressed nuclear protein; binds pRB, which regulates cell proliferation	2.3
RBBP6	binds to unphosphorylated but not phosphorylated pRB; also binds p53; blocks suppression of adenoviral E1A protein	2.0

There were also induced genes in WTSTS cells that are responsible for suppressing p53 in addition to *JUN*. These genes include *JUND* (14), *CUL4A* (51), and *NEDD8* (1) (Supplementary Table 2). JunD, which is in the AP-1 transcription factor complex like JUN, is also important for inhibiting TNF-stimulated apoptosis. JNK increases the expression of JunD, and JunD acts with NF-κB to increase the expression of *cIAP2* (37). *GADD45* (or *GADD45A*) which is a p53-responsive gene that recognizes damaged chromatin and facilitates topoisomerase cleavage activity to cause DNA damage (7), was induced approximately 10-fold in WTSTS cells. In addition, *GADD45A* expression may be regulated by AP-1 complexes containing JunD (12). This induction may be a result of the high induction levels of the genes associated with AP-1 complexes, namely *JUN*, *JUND*, and *FOSL2*. The pro-apoptotic phenotype of *GADD45A* does not affect WTSTS cells. Another gene that is responsible for suppressing p53 and directly degrades the protein, *MDM2* (81), was induced in WTSTS cells. The induction of genes important for enhancing and suppressing p53 most likely represents an attempt by the cell to undergo apoptosis in the presence of STS, especially since p53 enhances cytochrome *c* release from the mitochondria (49). Conversely, the bacteria are inhibiting apoptosis and inducing a pro-survival state of the cell, which most likely explains the induced expression of genes responsible for suppressing p53. Interestingly, *MDM2* was induced in the U versus WT comparison in addition to the significant induction of *JUN*. The bacteria may directly upregulate *MDM2* expression or the upregulation could be a response of the eukaryotic cell to the pro-survival state seen.

pRb-associated genes occur more in the USTS versus WTSTS comparison than in the U versus WT comparison. The *RBBP4*, *RBBP5/RBQ-3*, *RBBP6*, and *JARID1A* or

RBBP2 genes were all induced in WTSTS cells and are important for pRb function (4, 36, 65, 80). In fact, *RBBP4* is repressed in cervical cancer due to human papillomavirus infection (36). *RBBP6* has been shown to bind p53, inhibit adenoviral E1A from binding pRb, and may have a ubiquitin-like domain (61). In addition, *SERPINB2*, which represses pRb pro-apoptotic signal transduction (75), was induced in WTSTS cells. As mentioned above, the bacteria may require pRb function to prevent apoptosis while attempting to cause cell cycle arrest. In support of this hypothesis, there were even more genes induced in the USTS versus WTSTS comparison that are involved in cell cycle arrest or progression than the genes induced in the U versus WT comparison. For example, *CUL1*, *CUL3*, *APPBP1*, and *ESPL1/ESPI* are induced. These genes are important for regulation of the cell cycle (8, 9, 72, 87). The observations further highlight the interplay between the bacteria attempting to arrest the cell cycle while the eukaryotic cell attempts to progress the cell cycle as described above.

Finally, there were more induced genes whose gene products are localized to the mitochondria in STS conditions (Supplementary Table 2). For example, *DIABLO* and *HTRA2* were induced in WTSTS cells and encode proteins responsible for inhibiting IAPs upon release from the mitochondria (16). The pro-apoptotic *BAX*, *BCL2L11*, *BID*, *BNIP3L*, and *BOK* proteins (16) were all induced in WTSTS cells as well. These pro-apoptotic genes do not affect the inhibition of caspase-3 by *Shigella*, especially since cytochrome *c* release occurs in the presence of STS in infected cells (10). Finally, the pro-survival *BCL2L2* or *BCL-W* and *GLRX2* (16, 29) genes, in addition to the induction of *BCL2* and *CYCS* (encodes cytochrome *c*) that also occurs in WT cells, were induced in WTSTS cells. *GLRX2* encodes glutaredoxin, which protects the mitochondria from

oxidative stress (29). The induction of these pro-survival genes most likely reflects an attempt of the infected cell to repair or maintain mitochondrial integrity during STS treatment of infected cells.

In summary, the changes in gene expression in the USTS versus WTSTS comparison were similar to the changes seen in the U versus WT comparison. Nevertheless, there were some key distinctions that include higher levels of induction of some genes, opposite expression of genes in the presence of STS, enhancement of the pro-survival state related to NF- κ B, induction of genes related to p53 and pRb, and the induction of more genes associated with the mitochondrial membrane. The majority of these changes most likely represent the pro-survival state induced by *Shigella*, and these changes were enhanced upon STS exposure. However, a few changes, including the repression of *NALP1*, may have a direct role in apoptosis inhibition by *Shigella*.

Shigella-infected HeLa cells treated with STS compared to Shigella-infected HeLa cells.

The purpose of this comparison was to measure the changes in infected cells that are required for apoptosis inhibition in the presence of STS. Surprisingly, the SAM analysis revealed no significant genes. When the less stringent student's t-test was used to analyze the data, we did find changes in gene expression (Supplementary Table 2); however, the fold changes were not as high as the other comparisons. Approximately 80% of the changes were less than two-fold and the highest induction or repression was approximately 3-fold. Thus, the array results demonstrated that there were few significant differences between the two conditions and suggested that the bacteria induce the same pro-survival state in infected cells regardless of the presence or absence of STS. Therefore, STS has no overall significant effect on infected cells. The cluster diagram in

Figure 3 supports this hypothesis since WT cells and WTSTS cells are interspersed while U cells cluster away from USTS cells. Also in support of this hypothesis, there was no change in expression of *JUN*, *BIRC2/cIAP1*, *TRAF2*, or *NFKB2*. The absence of changes in these key genes indicates that *Shigella* infection itself has a pro-survival effect on the eukaryotic cell that is not altered by the presence of STS.

Of the few additional changes seen, it is interesting to see that *CASP10* was repressed in WTSTS cells compared to WT cells. Caspase-10 is activated in the extrinsic pathway of apoptosis, and etoposide, a chemotherapeutic agent and cytotoxic drug, induces *CASP10* expression in a p53-dependent manner (17, 63). In addition, caspase-10 is activated after cytochrome *c* release to amplify caspase-9 and caspase-3 activation in the presence of etoposide. In fact, caspase-10 activation can be inhibited if cytochrome *c* release is inhibited. More importantly, a dominant-negative form of caspase-10 is able to inhibit the activation of caspase-3 in the presence of etoposide (17). Since *S. flexneri* inhibits caspase-3 activation despite cytochrome *c* release in the presence of STS, caspase-10 could be a eukaryotic target for the bacteria to utilize to interfere with caspase-3 activation and inhibit apoptosis. Alternatively, p53 inhibition could reduce caspase-10 levels, which demonstrates the importance of the inhibition of p53 activity that occurs during infection.

Finally, it is important to note that *IKBKG/NEMO* was induced in the WTSTS cells compared to WT cells (Supplementary Table 2). NEMO is the regulatory subunit of the IκB kinase (IKK) complex that, when activated, phosphorylates the IκB proteins. Phosphorylation leads to ubiquitination of IκB proteins, thereby releasing NF-κB and allowing NF-κB to enter the nucleus for transcriptional activation. In addition, cIAP1

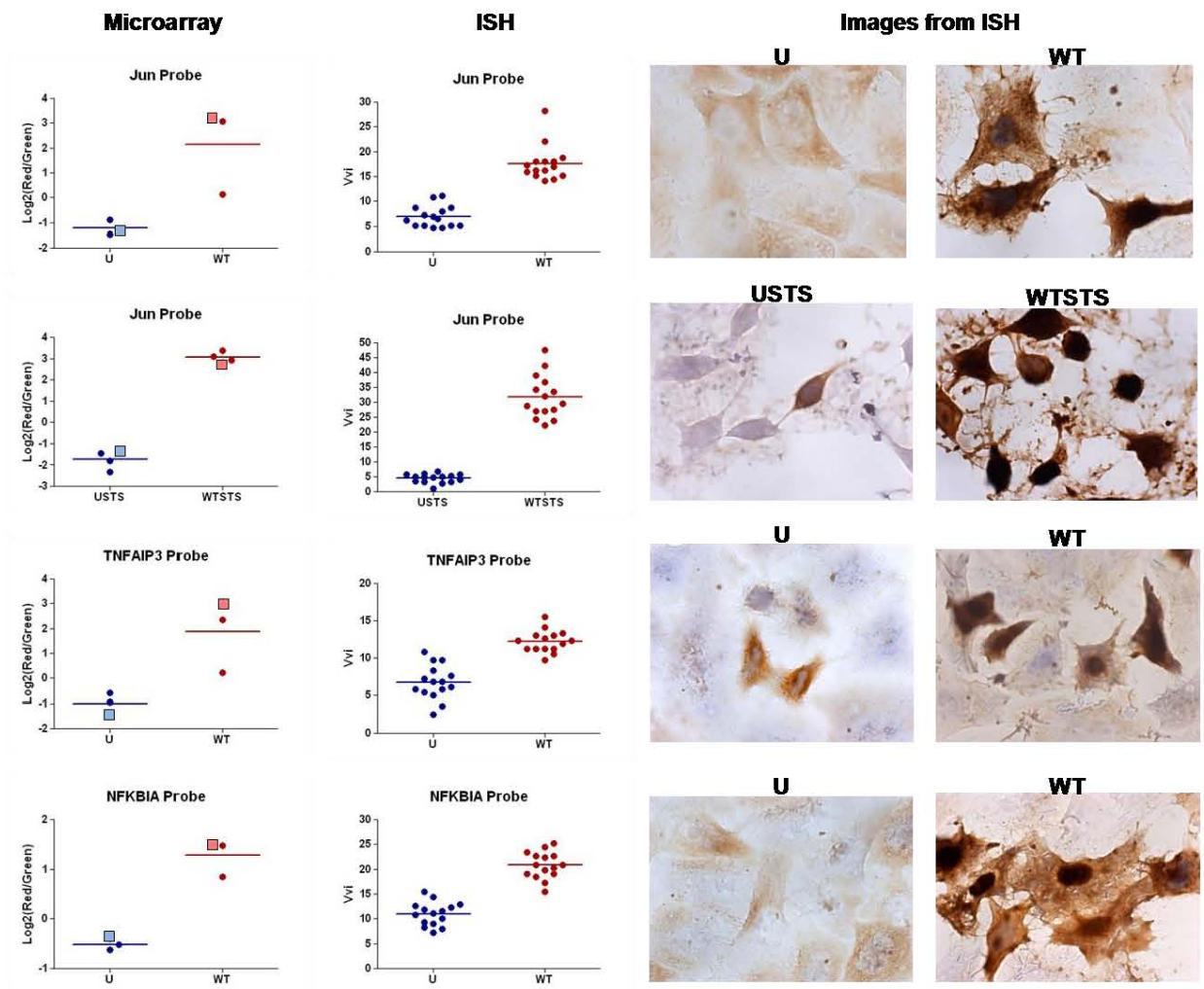
ubiquitinates NEMO in response to TNF- α stimulation, which is required for NF- κ B activation (73). The upregulation of *NEMO* is most likely a result of continued NF- κ B activation in *Shigella*-infected cells in the presence of STS. Nevertheless, this comparison highlights the fact that the infected cell is under the same pro-survival state regardless of the presence or absence of STS. This strong apoptosis inducer, therefore, has little overall effect on the infected cells.

In situ hybridization analysis to confirm the microarray results.

We used *in situ* hybridization (ISH) analysis as previously described (68) to quantify the mRNA expression of several genes and to confirm the results of the microarray analysis. ISH has been shown to be as sensitive as real-time RT-PCR (42) and is therefore an appropriate method to confirm the microarray results. Biologically independent samples were collected and analyzed with biotin-labeled probes representing genes that showed significant fold changes in the microarray results, namely *JUN*, *TNFAIP3*, and *NFKB1A*. We focused on the U versus WT comparison for each probe, but the *JUN* probe was also used for the USTS versus WTSTS comparison. Therefore, the three probes were used to analyze four sets of comparisons. As shown in Figure 15, each probe showed the same trend for the ISH analysis as was seen in the microarray analysis, namely a significant increase in expression of each gene in cells infected with bacteria as indicated by a positive, brown staining reaction. For the *JUN* probe, the same result was seen regardless of the presence of STS. All reactions utilized a control in which PBS was added in place of the probe. The controls resulted were negative for the peroxidase reaction (data not shown). Therefore, the ISH analysis validates the microarray results reported above.

Figure 15. Comparison of the microarray and in situ hybridization results.

The \log_2 of the red/green ratio for the microarray analysis is plotted on the left for the specified probe while the volumetric density (Vvi) for the *in situ* hybridization (ISH) analysis is plotted in the center for the specified probe. For the microarray analysis, the data for each time point of treatment (refer to Figure 2) are plotted with a line representing the mean of the data. The bigger, light-colored squares represent the time points that correlate with the ISH data. For the ISH, the Vvi for 15 fields at 400 \times magnification for the single time point is plotted with a line representing the mean of the data. A student's t-test was performed on the ISH data, and all p-Values were <0.0001 , indicating that there is a significant difference between uninfected cells and infected cells for the expression of each gene tested. The images on the right represent each ISH reactions for the specified treatment condition for each probe and were taken at 1000 \times magnification. U = uninfected cells, WT = infected cells, USTS = uninfected cells treated with staurosporine, and WTSTS = infected cells treated with STS.



Conclusion

The identification of the *Shigella* proteins required for the inhibition of apoptosis and the mechanism by which the proteins inhibit apoptosis will help define which changes in eukaryotic gene expression are relevant for STS inhibition. However, the changes in eukaryotic gene expression described here appear to be important for enhancing the pro-survival state of the infected cell in the absence of a strong apoptosis inducer like STS. Future studies will define the importance of the induction of certain genes. For example, siRNA studies to knock down JUN, the IAPs, or NF- κ B expression will help to determine which changes are required for apoptosis inhibition upon infection. In addition, analysis of the extrinsic pathway of apoptosis will allow us to determine if inhibition occurs prior to caspase-8 or caspase-3 activation, as well as identify which proteins in Table 5 are involved. The alterations in eukaryotic gene expression reported here are important to fully understand how *Shigella* inhibits apoptosis in epithelial cells.

There are other bacterial pathogens that inhibit apoptosis (15) and some of these pathogens have been utilized in similar microarray analyses to identify changes in eukaryotic gene expression in infected cells. Studies with *Neisseria gonorrhoeae*, which can inhibit STS-induced apoptosis at the mitochondrial level, found two to eight-fold upregulation of *BFL-1*, *COX-2*, *MCL-1*, and *cIAP2* in infected cells (5). *Mycobacterium tuberculosis* is able to induce cell death in alveolar macrophages while it can prevent apoptosis in alveolar epithelial cells. *M. tuberculosis* infection of epithelial cells results in increased expression of *BCL2* and *pRb*, decreased expression of *BAX* and *BAD*, and no change in *p53* expression despite a large increase in expression of *p53* in infected macrophages. In addition, the macrophages show significant inhibition of *pRb* (13). The

p53 and *pRb* observations are similar to the changes we report in *S. flexneri* infection of epithelial cells, both in the presence and absence of STS. Another similarity to *Shigella* infection is seen with the pathogen *Edwardsiella tarda*, which upregulates NF- κ B target genes, including *cIAP2* and *TRAF1* in macrophages (56). Finally, analysis of *Rickettsia rickettsii* infected endothelial cells in the presence of STS revealed induced expression of *TRAFs*, many genes in which the gene products localize to the mitochondria, several *IAPs*, *AKT1*, and *p53* (3). Like the above pathogens, *S. flexneri* induces similar changes in eukaryotic gene expression in order to inhibit apoptosis. However, each pathogen is unique in that it may employ a different method to inhibit apoptosis. For example, while *S. flexneri* inhibits caspase-3 activation, other pathogens like *N. gonorrhoeae* prevent mitochondrial permeabilization. Despite these differences, a common theme has emerged in that the bacteria induce a pro-survival state in infected cells, which results in similar changes in eukaryotic gene expression.

Knowing that *S. flexneri* inhibits STS-induced apoptosis at the point of caspase-3 activation (10) and given the changes in eukaryotic gene expression and resistance to TRAIL-induced apoptosis reported here, we propose that *S. flexneri* blocks apoptosis at multiple checkpoints in infected cells (Figure 12). Upon infection of epithelial cells, the bacteria either directly induce protection of the mitochondria by secreting T3SS effector proteins or indirectly protect the mitochondria by upregulating several eukaryotic genes including *JUN*, *NFKB2*, and *BCL2*. This possibility is supported by the evidence that there is no cytochrome *c* release upon normal infection with *Shigella* (10). Another level of protection induced upon infection is resistance to inducers of the extrinsic pathway of apoptosis, such as TRAIL. Upregulation of *TNFAIP3*, *TNFAIP8*, *TNFRSF12A*, *FAIM3*,

and *CFLAR* are important to inhibit caspase-8 activation, and may be direct targets of *Shigella* T3SS effector proteins or result from NF- κ B activation. It is important to inhibit apoptosis from the extrinsic pathway since many *in vivo* stimuli are present during infection such as TNF- α and Fas ligand (30, 50). Finally, the bacteria provide downstream protection and directly inhibit caspase-3 activation to prevent apoptosis, which is only evident when strong apoptosis inducers like STS are used. This downstream block provides protection if the invading *Shigella* fail to inhibit apoptosis at upstream checkpoints. While STS can overcome many of the pro-survival effects like protection of the mitochondria, the chemical cannot overcome the protection of caspase-3 cleavage induced by the bacteria. In addition, the upregulation of genes to suppress the effects of p53 enhance the pro-survival effects of the infected cell challenged with apoptosis inducers. Future experiments will determine which bacterial T3SS effector protein(s) and which eukaryotic genes are required for *S. flexneri* to inhibit apoptosis. The evidence presented here clearly shows that there are multiple steps required for *Shigella* to successfully prevent apoptosis in infected epithelial cells. Without this protection, *Shigella* would not have an efficient means of survival *in vivo*.

Materials and Methods

Bacterial strains used and growth conditions.

The strain used in the study was the wildtype *S. flexneri* serotype 2a strain 2457T. Bacteria were routinely cultured at 37°C either in Luria-Bertani broth (LB) with aeration or on tryptic soy broth plates with 1.5% agar and 0.025% Congo red (Sigma).

Immunofluorescence analysis.

After the varying STS exposures on the uninfected cells (Figure 9), cells were fixed with 3% formaldehyde (36% stock; Sigma) and 0.2% glutaraldehyde (25% stock; Sigma) in 1X PBS for 5 minutes at 4°C. Immunofluorescence analysis was performed as previously described (10). For Bad staining, a rabbit anti-Bad antibody (Cell Signaling Technology) was used in conjunction with a goat anti-rabbit immunoglobulin G (IgG) antibody conjugated to Alexa-594 (Invitrogen). An additional antibody that recognizes the phosphorylated form of Bad (phospho-Bad (Ser112), Cell Signal Technology) was also used with a goat anti-mouse IgG antibody conjugated to Alexa-594 (Invitrogen). For the cytochrome *c* release staining, the staining procedures were followed as described in the protocol provided by Molecular Probes. For the activated caspase-3 staining, a primary anti-human cleaved caspase-3 antibody (Cell Signaling Technology) was used with the same goat anti-rabbit secondary antibody above. To visualize nuclei, 5 mg/ml of 4,6-diamido- 2-phenylindole (DAPI; Molecular Probes) was diluted 1:1,000 in 1X phosphate buffered saline (PBS) and added to the monolayers for 20 min at room temperature in the dark. For all immunofluorescence experiments, antifade reagent (Molecular Probes) was added before coverslips were applied after the staining procedure. Samples were stored in the dark at 4°C and analyzed with an Olympus BX60 fluorescence microscope with an attached digital camera using X100 magnification.

Apoptosis assay and RNA isolation.

The apoptosis assay was performed in HeLa cells as previously described (10) and the various treatment conditions are provided in Figure 10. The STS exposure times were modified to reflect key points in the apoptosis pathway (see Results and

Discussion). After the apoptosis assay, the monolayers were washed with 1X PBS and RNA was isolated using TRIzol reagent. RNA was extracted from the TRIzol using chloroform, precipitated using isopropyl alcohol, and cleaned using the RNeasy kit (Qiagen). DNase treatment occurred directly on the columns, and after washes, the RNA was resuspended in 30 μ l RNase-free water. The reference RNA for all hybridizations consisted of a pooled sample of RNA isolated from normal, healthy HeLa cells. The RNA concentration of the treatments and the reference was quantitated by determining the OD₂₆₀ and the RNA integrity of all the samples was analyzed on a 1% agarose gel.

The apoptosis assay was modified to investigate the extrinsic pathway of apoptosis, which was also performed in HeLa cells using recombinant tumor necrosis factor- α related apoptosis inducing ligand (TRAIL, Calbiochem). The apoptosis assay was performed as previously described (10). Simply, TRAIL was substituted for STS in a three-hour incubation at a concentration of 3.4 μ g/ml.

Microarray hybridization and analysis.

The treatment RNA and reference RNA were concentrated to 5 μ g RNA in 12 μ l RNase-free water for cDNA synthesis. The FairPlay III kit (Stratagene) was used for preparing labeled cDNA with some modifications. 500 ng/ μ l random hexamer solution was used in the reaction, and once the cDNA was synthesized, the treatments and reference were purified using ethanol precipitation in which the samples were placed at -20°C for 1 hour. Next, the NHS-Ester containing dye coupling reaction was performed according to the protocol. The reference and treatment cDNA were subsequently indirectly labeled with Cy3 (green) and Cy5 (red) fluorophores, respectively. The samples were then purified to remove uncoupled dye, and the labeled cDNA was eluted

in 50 μ l of 10 mM Tris base, pH 8.5. The cDNA was analyzed via a spectrophotometer to determine dye incorporation and cDNA yield. The reference sample was mixed with each of the treatments so that each treatment had 1 μ g of cDNA and 1 μ g of reference cDNA. The samples were concentrated in the speed vacuum on medium heat to 44 μ l, and then 11 μ l of 10X blocking agent (7.5 μ l 10X Agilent blocking reagent, 2 μ l human COT-1 DNA (10 μ g/ μ l), 1 μ l poly d(A)₄₀₋₆₀ (8 μ g/ μ l), 1 μ l yeast tRNA (25 μ g/ μ l)) was added to the samples. The mixtures were heated to 98 °C for 2 minutes, cooled briefly, and the 2X hybridization buffer was added (HI-RPM, 55 μ l), resulting in a final volume of 110 μ l for each sample. The samples were loaded onto the ExonHit Therapeutics microarrays (451 apoptosis-specific genes) for hybridization at 65 °C. After overnight hybridization, the arrays were washed and scanned using a 4000A scanner and the GENEPIX 3.0 software.

Data were collated using the Stanford Microarray Database (71) in which spots showing obvious abnormalities were excluded from the analysis. Treatment conditions were compared to reveal changes in eukaryotic gene expression that are important for apoptosis inhibition in the presence of STS in *Shigella*-infected cells using the significance analysis of microarray (SAM) program version 2.20 and the student's t-test with a p-value cutoff of less than 0.01. The false discovery rate (FDR) of the four pairwise comparisons did not exceed 3.1%. The genes in Supplementary Table 2 were categorized by function and/or pathway using the gene descriptions provided by NCBI's Entrez Gene.

In situ hybridization analysis.

In situ hybridization (ISH) was performed as previously described (68) with some modifications to confirm the microarray results. Infections were performed in HeLa cells

with wildtype bacteria for 5.5 hours in DMEM plus 50 µg/ml gentamicin. When used, STS was applied at a 4 µM concentration for the last 2.5 hours of the assay. Uninfected cells received the same treatments and incubation times as infected cells in the appropriate comparisons. These time points were chosen to see the overall effect of infection and/or STS exposure on the cells. Afterwards, the HeLa cells were fixed with 3% formaldehyde (36% stock; Sigma) and 0.2% glutaraldehyde (25% stock; Sigma) in 1X PBS overnight at 4°C. For the ISH analysis, the probes and sequences used to generate the probes are listed in Table 7. The probe sequences were designed within the sequence of the corresponding microarray probe, and anneal to the cDNA sequence of the respective gene. All sequences are 32 nucleotides in length, and these sequences were analyzed with BLAST to ensure specificity to the gene target. All probes were synthesized in the Synthesis and Sequencing Facility, Biomedical Instrumentation Center, Uniformed Services University of the Health Sciences (USUHS; Bethesda, Maryland). The 5' end of each oligonucleotide was labeled with biotin. After probe hybridization, avidin-conjugated peroxidase and 3,3'-diaminobenzidine (DAB) tablets (Sigma) were used to detect the probes, which results in a brown reaction. Finally, the samples were counterstained with hematoxylin QS (Vector) to visualize the cells and were mounted with VectaMount.

Table 7. Probes and sequences used for the in situ hybridization experiments.

Probe	Sequence
<i>JUN</i>	5' – CCTGGGTTGAAGTTGCTGAGGTTTGCCTAGAC – 3'
<i>TNFAIP3</i>	5' – TGCGCTGGCTCGATCTCAGTTGCTCTTCTGTC – 3'
<i>NFKBIA</i>	5' – TCATGGATGATGGCCAAGTGCAGGAACGAGTC – 3'

In the data analysis, mRNA expression was quantified by a Nikon Eclipse E800 microscope as a brown reaction. Fifteen random fields were counted at 400× magnification for each preparation, according to a modification of the point-counting stereological method (79) using an intraocular reticle of 27-mm diameter, covering 3578 μm^2 (Kr409, Klarman Rulings) (68). Volumetric density (V_{vi}) analysis of the different probes was performed to measure the number of intersections of the grid that fell on the positive brown reaction. Statistical significance was determined using the student's t-test to compare treatment groups.

Author's Contributions

C.S.F. designed the experiments, collected the data, analyzed and interpreted the results, and drafted the manuscript. D.S.M. assisted in the design, execution, and data analysis for the microarray experiments, and helped draft the manuscript. C.S-M. and

A.D. assisted in the collection and interpretation of data for the *in situ* hybridization experiments. A.T.M. assisted in the experimental design and critically revised the manuscript.

Acknowledgements

We would like to thank members of the Maurelli lab for their support and input, as well as Dr. Hui Liu for assistance in the confirmation experiments and Michael Flora in the Bioinformatics Center for making the *in situ* probes. We thank the Uniformed Services University and the Henry M. Jackson Foundation for the Val Hemming Fellowship awarded to C.S.F. This work was supported by grant AI24656 from the National Institute of Allergy and Infectious Diseases. The opinions or assertions contained herein are the private ones of the authors and are not to be construed as official or reflecting the views of the Department of Defense or the Uniformed Services University of the Health Sciences.

References

1. **Abida, W. M., A. Nikolaev, W. Zhao, W. Zhang, and W. Gu.** 2007. FBXO11 promotes the Neddylation of p53 and inhibits its transcriptional activity. *J. Biol. Chem.* **282**:1797-1804.

2. **Arndt, P. G., N. Suzuki, N. J. Avdi, K. C. Malcolm, and G. S. Worthen.** 2004. Lipopolysaccharide-induced c-Jun NH2-terminal kinase activation in human neutrophils: role of phosphatidylinositol 3-Kinase and Syk-mediated pathways. *J. Biol. Chem.* **279**:10883-10891.
3. **Bechelli, J. R., E. Rydkina, P. M. Colonne, and S. K. Sahni.** 2009. *Rickettsia rickettsii* infection protects human microvascular endothelial cells against staurosporine-induced apoptosis by a cIAP(2)-independent mechanism. *J. Infect. Dis.* **199**:1389-1398.
4. **Benevolenskaya, E. V., H. L. Murray, P. Branton, R. A. Young, and W. G. Kaelin, Jr.** 2005. Binding of pRB to the PHD protein RBP2 promotes cellular differentiation. *Mol. Cell.* **18**:623-635.
5. **Binnicker, M. J., R. D. Williams, and M. A. Apicella.** 2003. Infection of human urethral epithelium with *Neisseria gonorrhoeae* elicits an upregulation of host anti-apoptotic factors and protects cells from staurosporine-induced apoptosis. *Cell. Microbiol.* **5**:549-560.
6. **Bruey, J. M., N. Bruey-Sedano, F. Luciano, D. Zhai, R. Balpai, C. Xu, C. L. Kress, B. Bailly-Maitre, X. Li, A. Osterman, S. Matsuzawa, A. V. Tersikh, B. Faustin, and J. C. Reed.** 2007. Bcl-2 and Bcl-XL regulate proinflammatory caspase-1 activation by interaction with NALP1. *Cell.* **129**:45-56.

7. **Carrier, F., P. T. Georgel, P. Pourquier, M. Blake, H. U. Kontny, M. J. Antinore, M. Gariboldi, T. G. Myers, J. N. Weinstein, Y. Pommier, and A. J. Fornace, Jr.** 1999. Gadd45, a p53-responsive stress protein, modifies DNA accessibility on damaged chromatin. *Mol. Cell. Biol.* **19**:1673-1685.
8. **Chen, Y., D. L. McPhie, J. Hirschberg, and R. L. Neve.** 2000. The amyloid precursor protein-binding protein APP-BP1 drives the cell cycle through the S-M checkpoint and causes apoptosis in neurons. *J. Biol. Chem.* **275**:8929-8935.
9. **Chestukhin, A., C. Pfeffer, S. Milligan, J. A. DeCaprio, and D. Pellman.** 2003. Processing, localization, and requirement of human separase for normal anaphase progression. *Proc. Natl. Acad. Sci. U S A* **100**:4574-4579.
10. **Clark, C. S., and A. T. Maurelli.** 2007. *Shigella flexneri* inhibits staurosporine-induced apoptosis in epithelial cells. *Infect. Immun.* **75**:2531-2539.
11. **Cory, S., and J. M. Adams.** 2002. The Bcl2 family: regulators of the cellular life-or-death switch. *Nat. Rev. Cancer.* **2**:647-656.
12. **Daino, K., S. Ichimura, and M. Neno.** 2006. Both the basal transcriptional activity of the GADD45A gene and its enhancement after ionizing irradiation are mediated by AP-1 element. *Biochim. Biophys. Acta.* **1759**:458-469.

13. **Danelishvili, L., J. McGarvey, Y. J. Li, and L. E. Bermudez.** 2003. *Mycobacterium tuberculosis* infection causes different levels of apoptosis and necrosis in human macrophages and alveolar epithelial cells. *Cell. Microbiol.* **5**:649-660.

14. **Das, M., F. Jiang, H. K. Sluss, C. Zhang, K. M. Shokat, R. A. Flavell, and R. J. Davis.** 2007. Suppression of p53-dependent senescence by the JNK signal transduction pathway. *Proc. Natl. Acad. Sci. U S A* **104**:15759-15764.

15. **Faherty, C. S., and A. T. Maurelli.** 2008. Staying alive: bacterial inhibition of apoptosis during infection. *Trends. Microbiol.* **16**:173-180.

16. **Festjens, N., M. van Gurp, G. van Loo, X. Saelens, and P. Vandenabeele.** 2004. Bcl-2 family members as sentinels of cellular integrity and role of mitochondrial intermembrane space proteins in apoptotic cell death. *Acta. Haematol.* **111**:7-27.

17. **Filomenko, R., L. Prevotat, C. Rebe, M. Cortier, J. F. Jeannin, E. Solary, and A. Bettaieb.** 2006. Caspase-10 involvement in cytotoxic drug-induced apoptosis of tumor cells. *Oncogene.* **25**:7635-7645.

18. **Fukazawa, A., C. Alonso, K. Kurachi, S. Gupta, C. F. Lesser, B. A. McCormick, and H. C. Reinecker.** 2008. GEF-H1 mediated control of NOD1 dependent NF-kappaB activation by *Shigella* effectors. PLoS Pathog. **4**:e1000228.

19. **Gozuacik, D., and A. Kimchi.** 2004. Autophagy as a cell death and tumor suppressor mechanism. Oncogene. **23**:2891-2906.

20. **Gutierrez-Venegas, G., and R. Castillo-Aleman.** 2008. Characterization of the transduction pathway involved in c-fos and c-jun expression induced by *Aggregatibacter actinomycetemcomitans* lipopolysaccharides in human gingival fibroblasts. Int. Immunopharmacol. **8**:1513-1523.

21. **Handa, Y., M. Suzuki, K. Ohya, H. Iwai, N. Ishijima, A. J. Koleske, Y. Fukui, and C. Sasakawa.** 2007. *Shigella* IpgB1 promotes bacterial entry through the ELMO-Dock180 machinery. Nat. Cell. Biol. **9**:121-128.

22. **He, K. L., and A. T. Ting.** 2002. A20 inhibits tumor necrosis factor (TNF) alpha-induced apoptosis by disrupting recruitment of TRADD and RIP to the TNF receptor 1 complex in Jurkat T cells. Mol. Cell. Biol. **22**:6034-6045.

23. **Headon, D. J., S. A. Emmal, B. M. Ferguson, A. S. Tucker, M. J. Justice, P. T. Sharpe, J. Zonana, and P. A. Overbeek.** 2001. Gene defect in ectodermal

- dysplasia implicates a death domain adapter in development. *Nature*. **414**:913-916.
24. **Hitoshi, Y., J. Lorens, S. I. Kitada, J. Fisher, M. LaBarge, H. Z. Ring, U. Francke, J. C. Reed, S. Kinoshita, and G. P. Nolan.** 1998. Toso, a cell surface, specific regulator of Fas-induced apoptosis in T cells. *Immunity*. **8**:461-471.
 25. **Hsu, Y. M., Y. Zhang, Y. You, D. Wang, H. Li, O. Duramad, X. F. Qin, C. Dong, and X. Lin.** 2007. The adaptor protein CARD9 is required for innate immune responses to intracellular pathogens. *Nat. Immunol.* **8**:198-205.
 26. **Huh, K., X. Zhou, H. Hayakawa, J. Y. Cho, T. A. Libermann, J. Jin, J. W. Harper, and K. Munger.** 2007. Human papillomavirus type 16 E7 oncoprotein associates with the cullin 2 ubiquitin ligase complex, which contributes to degradation of the retinoblastoma tumor suppressor. *J. Virol.* **81**:9737-9747.
 27. **Iwai, H., M. Kim, Y. Yoshikawa, H. Ashida, M. Ogawa, Y. Fujita, D. Muller, T. Kirikae, P. K. Jackson, S. Kotani, and C. Sasakawa.** 2007. A bacterial effector targets Mad2L2, an APC inhibitor, to modulate host cell cycling. *Cell*. **130**:611-623.
 28. **Jakowlew, S. B.** 2006. Transforming growth factor-beta in cancer and metastasis. *Cancer Metastasis Rev.* **25**:435-457.

29. **Johansson, C., C. H. Lillig, and A. Holmgren.** 2004. Human mitochondrial glutaredoxin reduces S-glutathionylated proteins with high affinity accepting electrons from either glutathione or thioredoxin reductase. *J. Biol. Chem.* **279**:7537-7543.

30. **Jung, H. C., L. Eckmann, S. K. Yang, A. Panja, J. Fierer, E. Morzycka-Wroblewska, and M. F. Kagnoff.** 1995. A distinct array of proinflammatory cytokines is expressed in human colon epithelial cells in response to bacterial invasion. *J. Clin. Invest.* **95**:55-65.

31. **Kantola, A. K., J. Keski-Oja, and K. Koli.** 2005. Induction of human LTBP-3 promoter activity by TGF-beta1 is mediated by Smad3/4 and AP-1 binding elements. *Gene.* **363**:142-150.

32. **Katabami, M., H. Donniger, F. Hommura, V. D. Leaner, I. Kinoshita, J. F. Chick, and M. J. Birrer.** 2005. Cyclin A is a c-Jun target gene and is necessary for c-Jun-induced anchorage-independent growth in RAT1a cells. *J. Biol. Chem.* **280**:16728-16738.

33. **Kiernan, R., V. Bres, R. W. Ng, M. P. Coudart, S. El Messaoudi, C. Sardet, D. Y. Jin, S. Emiliani, and M. Benkirane.** 2003. Post-activation turn-off of NF-

kappa B-dependent transcription is regulated by acetylation of p65. *J. Biol. Chem.* **278**:2758-2766.

34. **Kim, P. M., C. Allen, B. M. Wagener, Z. Shen, and J. A. Nickoloff.** 2001. Overexpression of human RAD51 and RAD52 reduces double-strand break-induced homologous recombination in mammalian cells. *Nucleic Acids Res.* **29**:4352-4360.

35. **Kipreos, E. T., L. E. Lander, J. P. Wing, W. W. He, and E. M. Hedgecock.** 1996. *cul-1* is required for cell cycle exit in *C. elegans* and identifies a novel gene family. *Cell.* **85**:829-839.

36. **Kong, L., X. P. Yu, X. H. Bai, W. F. Zhang, Y. Zhang, W. M. Zhao, J. H. Jia, W. Tang, Y. B. Zhou, and C. J. Liu.** 2007. RbAp48 is a critical mediator controlling the transforming activity of human papillomavirus type 16 in cervical cancer. *J. Biol. Chem.* **282**:26381-26391.

37. **Lamb, J. A., J. J. Ventura, P. Hess, R. A. Flavell, and R. J. Davis.** 2003. JunD mediates survival signaling by the JNK signal transduction pathway. *Mol. Cell.* **11**:1479-1489.

38. **Leaner, V. D., H. Donninger, C. A. Ellis, G. J. Clark, and M. J. Birrer.** 2005. p75-Ras-GRF1 is a c-Jun/AP-1 target protein: its up regulation results in

increased Ras activity and is necessary for c-Jun-induced nonadherent growth of Rat1a cells. *Mol. Cell. Biol.* **25**:3324-3337.

39. **Lee, T. H., M. J. Solomon, M. C. Mumby, and M. W. Kirschner.** 1991. INH, a negative regulator of MPF, is a form of protein phosphatase 2A. *Cell.* **64**:415-423.

40. **Li, H., L. L. Zhao, J. W. Funder, and J. P. Liu.** 1997. Protein phosphatase 2A inhibits nuclear telomerase activity in human breast cancer cells. *J. Biol. Chem.* **272**:16729-16732.

41. **Liang, X. H., L. K. Kleeman, H. H. Jiang, G. Gordon, J. E. Goldman, G. Berry, B. Herman, and B. Levine.** 1998. Protection against fatal Sindbis virus encephalitis by beclin, a novel Bcl-2-interacting protein. *J. Virol.* **72**:8586-8596.

42. **Liu, H., A. Rahman, C. Semino-Mora, S. Q. Doi, and A. Dubois.** 2008. Specific and sensitive detection of *H. pylori* in biological specimens by real-time RT-PCR and in situ hybridization. *PLoS One.* **3**:e2689.

43. **Liu, S. F., G. X. Lu, G. Liu, X. W. Xing, L. Y. Li, and Z. Wang.** 2004. Cloning of a full-length cDNA of human testis-specific spermatogenic cell apoptosis inhibitor TSARG2 as a candidate oncogene. *Biochem. Biophys. Res. Commun.* **319**:32-40.

44. **Liu, Z. G., H. Hsu, D. V. Goeddel, and M. Karin.** 1996. Dissection of TNF receptor 1 effector functions: JNK activation is not linked to apoptosis while NF-kappaB activation prevents cell death. *Cell.* **87**:565-576.

45. **Mace, P. D., S. Shirley, and C. L. Day.** 2009. Assembling the building blocks: structure and function of inhibitor of apoptosis proteins. *Cell. Death. Differ.* PMID: 19373243.

46. **Martinon, F., K. Burns, and J. Tschopp.** 2002. The inflammasome: a molecular platform triggering activation of inflammatory caspases and processing of proIL-beta. *Mol. Cell.* **10**:417-426.

47. **Matsuda, K., K. Yoshida, Y. Taya, K. Nakamura, Y. Nakamura, and H. Arakawa.** 2002. p53AIP1 regulates the mitochondrial apoptotic pathway. *Cancer Res.* **62**:2883-2889.

48. **Micheau, O., S. Lens, O. Gaide, K. Alevizopoulos, and J. Tschopp.** 2001. NF-kappaB signals induce the expression of c-FLIP. *Mol. Cell. Biol.* **21**:5299-5305.

49. **Mihara, M., S. Erster, A. Zaika, O. Petrenko, T. Chittenden, P. Pancoska, and U. M. Moll.** 2003. p53 has a direct apoptogenic role at the mitochondria. *Mol. Cell.* **11**:577-590.

50. **Mizuta, M., H. Nakajima, N. Mizuta, Y. Kitamura, Y. Nakajima, S. Hashimoto, H. Matsuyama, N. Shime, F. Amaya, H. Koh, A. Ishizaka, J. Magae, and S. I. Tanuma.** 2008. Fas ligand released by activated monocytes causes apoptosis of lung epithelial cells in human acute lung injury model in vitro. *Biol. Pharm. Bull.* **31**:386-390.
51. **Nag, A., S. Bagchi, and P. Raychaudhuri.** 2004. Cul4A physically associates with MDM2 and participates in the proteolysis of p53. *Cancer. Res.* **64**:8152-8155.
52. **Nishina, H., H. Sato, T. Suzuki, M. Sato, and H. Iba.** 1990. Isolation and characterization of fra-2, an additional member of the fos gene family. *Proc. Natl. Acad. Sci. U S A* **87**:3619-3623.
53. **Ofek, P., D. Ben-Meir, Z. Kariv-Inbal, M. Oren, and S. Lavi.** 2003. Cell cycle regulation and p53 activation by protein phosphatase 2C alpha. *J. Biol. Chem.* **278**:14299-14305.
54. **Ogawa, M., T. Yoshimori, T. Suzuki, H. Sagara, N. Mizushima, and C. Sasakawa.** 2005. Escape of intracellular *Shigella* from autophagy. *Science.* **307**:727-731.

55. **Ogura, Y., N. Inohara, A. Benito, F. F. Chen, S. Yamaoka, and G. Nunez.** 2001. Nod2, a Nod1/Apaf-1 family member that is restricted to monocytes and activates NF-kappaB. *J. Biol. Chem.* **276**:4812-4818.
56. **Okuda, J., Y. Arikawa, Y. Takeuchi, M. M. Mahmoud, E. Suzaki, K. Kataoka, T. Suzuki, Y. Okinaka, and T. Nakai.** 2006. Intracellular replication of *Edwardsiella tarda* in murine macrophage is dependent on the type III secretion system and induces an up-regulation of anti-apoptotic NF-kappaB target genes protecting the macrophage from staurosporine-induced apoptosis. *Microb. Pathog.* **41**:226-240.
57. **Olsson, A. Y., A. Feber, S. Edwards, R. Te Poele, I. Giddings, S. Merson, and C. S. Cooper.** 2007. Role of E2F3 expression in modulating cellular proliferation rate in human bladder and prostate cancer cells. *Oncogene.* **26**:1028-1037.
58. **Pedron, T., C. Thibault, and P. J. Sansonetti.** 2003. The invasive phenotype of *Shigella flexneri* directs a distinct gene expression pattern in the human intestinal epithelial cell line Caco-2. *J. Biol. Chem.* **278**:33878-33886.
59. **Pietsch, E. C., S. M. Sykes, S. B. McMahon, and M. E. Murphy.** 2008. The p53 family and programmed cell death. *Oncogene.* **27**:6507-6521.

60. **Post, S. M., A. E. Tomkinson, and E. Y. Lee.** 2003. The human checkpoint Rad protein Rad17 is chromatin-associated throughout the cell cycle, localizes to DNA replication sites, and interacts with DNA polymerase epsilon. *Nucleic Acids Res.* **31**:5568-5575.

61. **Pugh, D. J., E. Ab, A. Faro, P. T. Lutya, E. Hoffmann, and D. J. Rees.** 2006. DWNN, a novel ubiquitin-like domain, implicates RBBP6 in mRNA processing and ubiquitin-like pathways. *BMC Struct. Biol.* **6**:1.

62. **Reardon, J. T., H. Ge, E. Gibbs, A. Sancar, J. Hurwitz, and Z. Q. Pan.** 1996. Isolation and characterization of two human transcription factor IIH (TFIIH)-related complexes: ERCC2/CAK and TFIIH. *Proc. Natl. Acad. Sci. U S A* **93**:6482-6487.

63. **Rikhof, B., P. G. Corn, and W. S. El-Deiry.** 2003. Caspase 10 levels are increased following DNA damage in a p53-dependent manner. *Cancer Biol. Ther.* **2**:707-712.

64. **Roos, W. P., and B. Kaina.** 2006. DNA damage-induced cell death by apoptosis. *Trends Mol. Med.* **12**:440-450.

65. **Saijo, M., Y. Sakai, T. Kishino, N. Niikawa, Y. Matsuura, K. Morino, K. Tamai, and Y. Taya.** 1995. Molecular cloning of a human protein that binds to the retinoblastoma protein and chromosomal mapping. *Genomics*. **27**:511-519.

66. **Samuels-Lev, Y., D. J. O'Connor, D. Bergamaschi, G. Trigiante, J. K. Hsieh, S. Zhong, I. Campargue, L. Naumovski, T. Crook, and X. Lu.** 2001. ASPP proteins specifically stimulate the apoptotic function of p53. *Mol. Cell*. **8**:781-794.

67. **Schroeder, G. N., and H. Hilbi.** 2008. Molecular pathogenesis of *Shigella* spp.: controlling host cell signaling, invasion, and death by type III secretion. *Clin. Microbiol. Rev.* **21**:134-156.

68. **Semino-Mora, C., S. Q. Doi, A. Marty, V. Simko, I. Carlstedt, and A. Dubois.** 2003. Intracellular and interstitial expression of *Helicobacter pylori* virulence genes in gastric precancerous intestinal metaplasia and adenocarcinoma. *J. Infect. Dis.* **187**:1165-1177.

69. **Shaulian, and Karin.** 2002. AP-1 as a regulator of cell life and death. *Nat. Cell. Biol.* **4**:E131-136.

70. **Shen, Q., I. P. Uray, Y. Li, T. I. Krisko, T. E. Strecker, H. T. Kim, and P. H. Brown.** 2008. The AP-1 transcription factor regulates breast cancer cell growth via cyclins and E2F factors. *Oncogene*. **27**:366-377.

71. **Sherlock, G., T. Hernandez-Boussard, A. Kasarskis, G. Binkley, J. C. Matese, S. S. Dwight, M. Kaloper, S. Weng, H. Jin, C. A. Ball, M. B. Eisen, P. T. Spellman, P. O. Brown, D. Botstein, and J. M. Cherry.** 2001. The Stanford Microarray Database. *Nucleic Acids Res.* **29**:152-155.

72. **Singer, J. D., M. Gurian-West, B. Clurman, and J. M. Roberts.** 1999. Cullin-3 targets cyclin E for ubiquitination and controls S phase in mammalian cells. *Genes Dev.* **13**:2375-2387.

73. **Tang, E. D., C. Y. Wang, Y. Xiong, and K. L. Guan.** 2003. A role for NF-kappaB essential modifier/IkappaB kinase-gamma (NEMO/IKKgamma) ubiquitination in the activation of the IkappaB kinase complex by tumor necrosis factor-alpha. *J. Biol. Chem.* **278**:37297-37305.

74. **Thacker, J., and M. Z. Zdzienicka.** 2003. The mammalian XRCC genes: their roles in DNA repair and genetic stability. *DNA Repair (Amst)*. **2**:655-672.

75. **Tonnetti, L., S. Netzel-Arnett, G. A. Darnell, T. Hayes, M. S. Buzza, I. E. Anglin, A. Suhrbier, and T. M. Antalis.** 2008. SerpinB2 protection of

retinoblastoma protein from calpain enhances tumor cell survival. *Cancer Res.* **68**:5648-5657.

76. **Vogt, P. K.** 2001. Jun, the oncoprotein. *Oncogene.* **20**:2365-2377.

77. **Wang, C. Y., M. W. Mayo, R. G. Korneluk, D. V. Goeddel, and A. S. Baldwin, Jr.** 1998. NF-kappaB antiapoptosis: induction of TRAF1 and TRAF2 and c-IAP1 and c-IAP2 to suppress caspase-8 activation. *Science.* **281**:1680-1683.

78. **Wang, J. Y., S. Naderi, and T. T. Chen.** 2001. Role of retinoblastoma tumor suppressor protein in DNA damage response. *Acta. Oncol.* **40**:689-695.

79. **Weibel, E. R., G. S. Kistler, and W. F. Scherle.** 1966. Practical stereological methods for morphometric cytology. *J. Cell. Biol.* **30**:23-38.

80. **Witte, M. M., and R. E. Scott.** 1997. The proliferation potential protein-related (P2P-R) gene with domains encoding heterogeneous nuclear ribonucleoprotein association and Rb1 binding shows repressed expression during terminal differentiation. *Proc. Natl. Acad. Sci. U S A* **94**:1212-1217.

81. **Woods, D. B., and K. H. Vousden.** 2001. Regulation of p53 function. *Exp. Cell. Res.* **264**:56-66.

82. **Wu, M. X., Z. Ao, K. V. Prasad, R. Wu, and S. F. Schlossman.** 1998. IEX-1L, an apoptosis inhibitor involved in NF-kappaB-mediated cell survival. *Science*. **281**:998-1001.
83. **Yan, M., Z. Zhang, J. R. Brady, S. Schilbach, W. J. Fairbrother, and V. M. Dixit.** 2002. Identification of a novel death domain-containing adaptor molecule for ectodysplasin-A receptor that is mutated in crinkled mice. *Curr. Biol.* **12**:409-413.
84. **You, Z., H. Ouyang, D. Lopatin, P. J. Polver, and C. Y. Wang.** 2001. Nuclear factor-kappa B-inducible death effector domain-containing protein suppresses tumor necrosis factor-mediated apoptosis by inhibiting caspase-8 activity. *J. Biol. Chem.* **276**:26398-26404.
85. **Zha, J., H. Harada, E. Yang, J. Jockel, and S. J. Korsmeyer.** 1996. Serine phosphorylation of death agonist BAD in response to survival factor results in binding to 14-3-3 not BCL-X(L). *Cell*. **87**:619-628.
86. **Zhang, Y., and S. P. Chellappan.** 1995. Cloning and characterization of human DP2, a novel dimerization partner of E2F. *Oncogene*. **10**:2085-2093.
87. **Zheng, N., B. A. Schulman, L. Song, J. J. Miller, P. D. Jeffrey, P. Wang, C. Chu, D. M. Koepp, S. J. Elledge, M. Pagano, R. C. Conaway, J. W. Conaway,**

- J. W. Harper, and N. P. Pavletich.** 2002. Structure of the Cul1-Rbx1-Skp1-F boxSkp2 SCF ubiquitin ligase complex. *Nature*. **416**:703-709.
88. **Zou, T., J. N. Rao, X. Guo, L. Liu, H. M. Zhang, E. D. Strauch, B. L. Bass, and J. Y. Wang.** 2004. NF-kappaB-mediated IAP expression induces resistance of intestinal epithelial cells to apoptosis after polyamine depletion. *Am. J. Physiol. Cell. Physiol.* **286**:C1009-1018.
89. **Zurawski, D. V., K. L. Mummy, C. S. Faherty, B. A. McCormick, and A. T. Maurelli.** 2009. *Shigella flexneri* type III secretion system effectors OspB and OspF target the nucleus to downregulate the host inflammatory response via interactions with retinoblastoma protein. *Mol. Microbiol.* **71**:350-368.

Supplementary Table 1. Data for spots that show statistically significant differences in the indicated pairwise analyses.

Data are presented as the log₂ red to green ratio.

Uninfected vs. Uninfected + STS: 187 Spots showing statistically significant differences (SAM FDR of 3.02) between the two indicated groups.								
BIOSEQUENCE_ID	NAME	UN 1 hr	UN 2 hr	UN 2.75 hr	UN 0.5 hr STS	UN 1 hr STS	UN 2 hr STS	UN 2.75 hr STS
6321434	HS1000000260189 38599::CG4618	0.59	0.25	0.37	-0.48	-0.96	-1.95	-0.98
6301683	HS1000000005159 ADORA1	0.56	0.29	0.02	-0.72	-0.94	-1.18	-0.44
6309726	HS1000000005404 ADORA2A	1.12	1.13	1.15	0.22	0.23	-0.41	-0.31
6319060	HS1000000005895 ADRA1A	0.48	0.43	0.74	-0.65	-1.08	-1.01	-0.56
6322832	HS1000000005954 ADRA1A	0.61	0.59	0.79	-0.37	-0.67	-0.86	-0.5
6314968	HS1000000005924 ADRA1A	0.59	0.21	0.63	-0.84	-1.12	-1.6	-0.69
6312213	HS1000000006074 ADRA1A	0.43	0.52	0.24	-0.86	-1.16	-1.33	-0.58
6306227	HS1000000006094 ADRA1A	0.51	0.57	0.69	-0.73	-0.85	-0.93	-0.23
6309866	HS1000000006049 ADRA1A	0.66	0.34	0.72	-0.65	-0.82	-1.09	-0.3
6316267	HS1000000006134 ADRA1A	0.54	0.54	0.44	-0.6	-1.21	-1.29	-0.38
6301534	HS1000000006024 ADRA1A	0.42	0.32	0.31	-0.7	-1.44	-1.91	-0.67
6314698	HS1000000006004 ADRA1A	0.39	0.23	0.47	-0.6	-1.36	-1.16	-0.45
6322803	HS1000000489353 AFG3L2	0.37	0.37	0.44	-0.27	-0.73	-0.62	-0.66
6301917	HS1000000644553 AMID	0.28	0.27	0.28	-0.7	-0.75	-1.18	-1.18
6321354	HS1000000012552 ANK1	1.36	0.76	0.48	-0.52	-0.94	-0.01	-0.3
6324631	HS1000000013478 ANK3	0.54	0.08	0.21	-0.96	-1.4	-1.78	-0.79
6318896	HS1000000013285 ANK3	1.01	0.14	0.84	-0.42	-0.53	-0.77	-0.96
6311639	HS1000000013451 ANK3	0.9	0.9	1.46	-0.99	-1.67	0.26	-0.39
6322219	HS1000000017620 APAF1	-0.67	-0.37	-0.32	-1.22	-1.98	-2.22	-1.86

6316517	HS1000000019943 APOE	0.3	0.17	0.46	-0.81	-1.34	-0.94	-0.86
6323891	HS1000000020397 APP	-0.17	-0.25	0.01	-0.82	-0.97	-1.22	-1.16
6305898	HS1000000413553 APPBP1	0.2	0.21	0.44	-0.77	-1.08	-1.14	-1.1
6301763	HS1000000413615 APPBP1	0.66	0.58	1	-0.63	-0.8	-0.92	-0.35
6306179	HS1000000577126 APTX	-0.78	-0.45	-0.1	-1.22	-2.25	-1.64	-2.05
6320469	HS1000000428200 ARHGEF6	0.31	0.09	0.31	-0.61	-0.64	-1.14	-0.72
6303104	HS1000000449036 BCL2L11	-0.78	-0.84	-0.05	-1.45	-1.98	-1.77	-2.01
6308559	HS1000000532324 BCL2L13	0.39	0.76	0.25	-0.22	-1.02	-1.77	-1.09
6311548	HS1000000532119 BCL2L13	0.3	-0.13	0.31	-0.63	-0.75	-1.05	-1.13
6311159	HS1000000403011 BECN1	0.07	0.2	0.15	-0.77	-1.59	-1.36	-0.99
6311058	HS1000000403040 BECN1	0.37	1.09	1.13	-0.12	-0.36	-0.37	-0.29
6324093	HS1000000029731 BID	0.72	0.52	0.08	-1.09	-0.9	-1.14	-1.89
6300941	HS1000000029760 BID	0.09	-0.01	0.03	-0.66	-0.98	-1.16	-0.85
6322446	HS1000000029613 BID	0.2	0.34	0.31	-0.6	-0.39	-0.8	-0.73
6316912	HS1000000029721 BID	-0.03	0.29	0.09	-0.75	-1.24	-1.07	-0.63
6310983	HS1000000222616 BIRC1	0.01	-0.07	0.2	-0.71	-0.89	-0.94	-0.92
6302269	HS1000000222532 BIRC1	-0.18	-0.27	-0.21	-0.93	-1.16	-1.52	-1.33
6321002	HS1000000646739 BMF	0.49	0.28	0.35	-0.43	-1.22	-1.33	-1.07
6309867	HS1000000646757 BMF	0.39	0.5	0.4	-0.33	-0.75	-1.03	-0.39
6312926	HS1000000424606 BZRAP1	-0.24	0.52	0.86	-0.69	-1.6	-2.31	-1.17
6315668	HS1000000424637 BZRAP1	-0.54	0.75	-0.54	-1.46	-1.59	-1.74	-1.41
6308034	HS1000000035280 C6	1.68	0.39	0.3	-0.85	-0.31	-1.44	-0.76
6318221	HS1000000035600 C8B	0.72	0.15	-0.05	-0.75	-0.99	-1.48	-0.72
6319686	HS1000000035618 C8G	0.27	0.1	0.33	-0.96	-0.96	-0.38	-0.95
6304975	HS1000000035650 C8G	0.76	0.32	0.55	-0.3	-0.28	-0.37	-0.42
6320994	SA_23_P119835 CARD12	0.52	0.63	0.82	-0.57	-0.24	-1.38	-1.15
6311640	HS1000000042638 CASP3	0.56	0.25	0.46	-0.6	-0.65	-1.04	-1.22

6320978	HS1000000042663 CASP3	0.34	0.19	0.06	-0.72	-0.84	-0.99	-1.14
6303139	HS1000000043853 CASP9	0.54	0.97	0.37	-0.79	-1.69	-1.89	-0.6
6318590	HS1000000050985 CD38	0.67	0.46	0.88	-0.83	-1.45	-0.8	-1.38
6300607	HS1000000050898 CD38	-0.17	0.29	0.18	-1.21	-1.82	-2.6	-2.3
6301742	HS1000000058594 CDC42	0.51	0.66	1.21	-0.89	-0.2	-1.28	-0.92
6321269	HS10000000650197 CIAS1	0.44	0.46	0.76	-0.45	-1.03	-0.85	-0.84
6303046	HS10000000211362 CIITA	-0.43	0.57	0.16	-1.61	-1.34	-2.55	-1.87
6306628	HS10000000598129 CTNBL1	0.27	0.13	0.11	-0.5	-0.73	-0.84	-0.8
6305399	HS10000000391342 CUL1	0.19	0.76	0.81	-0.61	-0.86	-0.66	-0.55
6321367	HS10000000088577 DAP	0.26	0.1	0.19	-0.83	-1.23	-3.36	-1.93
6305631	HS10000000089173 DBC1	-0.32	-0.05	-0.45	-1.46	-1.95	-1.41	-1.86
6302523	HS10000000089528 DCC	-0.12	0.44	-0.63	-1.1	-1.58	-1.96	-1.39
6310106	HS10000000563697 DDX41	0.77	0.07	0.83	-0.35	-1.29	-0.86	-0.82
6316916	HS10000000421358 DEDD	0.66	0.32	1.08	-0.68	-0.51	-1.33	-0.35
6324110	HS10000000661729 DEDD2	0.55	0.24	0.21	-0.79	-1.1	-0.9	-0.32
6315127	HS10000000091836 DFFB	0.34	0.63	0.34	-0.52	-0.88	-1.75	-1.33
6313222	HS10000000599453 DIABLO	-0.22	-0.28	-0.13	-0.93	-1.07	-1.29	-1.06
6316843	HS10000000599315 DIABLO	-0.43	0.34	-0.29	-0.91	-1.55	-1.36	-1.47
6322342	HS10000000868202 DLL4	1.35	0.73	0.69	-0.57	-0.34	-0.26	-0.8
6304312	HS10000000417520 DNAJA3	-0.64	-0.88	-0.98	-1.82	-2.25	-2.44	-2.33
6305301	HS10000000417484 DNAJA3	-0.78	-0.71	-0.86	-1.84	-3.12	-3.99	-2.52
6308363	HS10000000417572 DNAJA3	-0.32	-0.82	-1.08	-1.72	-3.12	-3.41	-2.04
6323620	HS10000000093934 DNASE1	0.75	0.42	0.16	-0.78	-0.28	-1.42	-1.25
6317140	HS10000000094133 DNASE2	0.64	0.53	0.91	-0.69	-0.35	-0.73	-0.03
6322028	HS10000000654279 EDARADD	0.4	-0.03	0.69	-0.7	-0.91	-1.23	-0.57
6305955	HS10000000442750 ELMO1	0.36	0.6	0.11	-0.58	-0.68	-0.7	-1.37
6300435	HS10000000615289 ELMO2	0.39	0.35	0.43	-0.54	-0.61	-1.4	-0.92

6322430	HS1000000615733 ELMO2	0.02	-0.1	0.05	-0.78	-1	-1.41	-1.16
6301695	HS1000000615595 ELMO2	0.27	-0.13	0.19	-1.11	-0.78	-0.82	-1.46
6318923	HS1000000628904 ELMO3	0.65	0.1	0.6	-0.77	-1.64	-1.61	-0.64
6320588	HS1000000104903 EMP1	0.04	0.16	0.12	-1.79	-2.34	-1.91	-0.82
6305976	HS1000000105261 EMR1	0.07	0.29	0.43	-0.59	-0.99	-0.73	-0.8
6307414	HS1000000105345 EMR1	0.55	0.68	0.22	-1.02	-0.67	-1.01	-0.28
6314656	HS1000000554534 EMR2	0.28	0.31	0.26	-0.63	-0.88	-1.16	-1.16
6323641	HS1000000554564 EMR2	0.46	0.53	0.21	-0.37	-0.63	-0.58	-0.81
6309556	HS1000000554486 EMR2	0.86	-0.11	0.12	-2.03	-2.06	-1.64	-0.33
6309000	HS1000000394843 ENC1	0.59	0.58	0.36	-0.52	-1.18	-0.66	-0.51
6324721	HS1000000110150 ERCC2	0.06	0.19	0.15	-0.83	-1.21	-1.15	-0.91
6324956	HS1000000582721 FAIM	0.1	-0.01	0	-0.91	-1.26	-1.55	-1.16
6304827	HS1000000582822 FAIM	0	-0.1	-0.11	-0.87	-1.34	-1.69	-1.24
6318447	HS1000000582691 FAIM	0.06	-0.1	0.12	-0.74	-0.95	-1.35	-1.13
6303332	HS1000000422274 FAIM3	-0.05	0.44	-0.07	-1.12	-1.32	-0.99	-0.96
6314507	HS1000000422288 FAIM3	0.46	0.78	0.84	-0.61	-0.23	-0.19	-0.15
6316480	HS1000000841470 FBLN5	0.95	-0.1	0.76	-0.75	-0.84	-1.06	-0.48
6300776	HS1000000487027 GADD45G	0.86	0.91	0.64	0.17	-0.71	-0.34	-0.79
6323226	HS1000000557768 GLRX2	0.51	1.45	-0.16	-0.68	-1.22	-0.82	-0.94
6318669	HS1000000140936 GPX1	0.35	0.3	0.31	-0.92	-1.76	-1.87	-0.78
6322001	HS1000000141471 GRB2	-0.06	-0.22	-0.01	-0.79	-0.91	-1.2	-1.11
6314175	HS1000000145714 GSTT1	0.62	0.86	1.06	-0.33	-1	-1.28	-1.17
6313881	HS1000000565429 GULP1	1.47	1.29	0.84	0	-0.17	-0.08	0
6301887	HS1000000147062 GZMB	0.24	0.28	0.18	-0.36	-1.42	-1.29	-0.85
6308972	HS1000000147098 GZMM	0.21	0.07	0.07	-0.72	-1.77	-1.29	-1.54
6323660	HS1000000164309 HSPG2	0.99	0.73	0.57	-0.21	-0.17	-0.61	-0.81
6307113	HS1000000164247 HSPG2	0.52	0.82	0.63	-0.1	-1.33	-1.53	-0.62

6308098	HS1000000165370 IAPP	-0.22	-0.21	-0.08	-0.86	-1.04	-1.26	-1.14
6314816	HS1000000165701 ID1	-2.31	-1.19	-1.48	-3.44	-3.4	-4.08	-3.22
6313274	HS1000000165624 ID1	-2.6	-1.91	-1.66	-3.03	-3.24	-3.82	-3.6
6304339	HS1000000165664 ID1	-1.74	-1.45	-1.68	-2.36	-2.57	-2.86	-2.48
6303228	HS1000000411378 IER3	1.24	1.05	1.02	-0.31	-0.96	-1.1	-0.64
6313691	HS1000000411352 IER3	1.03	1.23	1.08	0	-0.67	-0.67	0
6306315	HS1000000411389 IER3	0.6	0.64	1.07	-0.18	-0.88	-1.04	-0.83
6317868	HS1000000411368 IER3	0.72	0.65	0.67	-0.32	-0.82	-1.21	-0.48
6304264	HS1000000411347 IER3	0.99	0.97	0.89	0.03	-0.58	-1.14	-0.22
6302870	HS1000000411402 IER3	0.15	0.27	0.63	-0.61	-1.94	-1.12	-0.98
6323350	HS1000000411397 IER3	1.1	0.96	0.52	-0.16	-0.36	-0.97	-0.24
6308558	HS1000000411360 IER3	0.93	1.1	0.78	-0.05	-0.49	-0.77	0.11
6318845	HS1000000411373 IER3	-0.08	0.04	0.61	-0.53	-1.22	-1.36	-1.13
6307360	HS1000000652684 IHPK3	0.47	-0.18	0.65	-0.83	-0.92	-1.49	-0.79
6310433	HS1000000395276 IKBKG	0.59	-0.13	0.41	-0.65	-0.88	-1.15	-1.53
6302521	HS1000000395110 IKBKG	0.2	0.49	0.05	-0.53	-0.86	-0.89	-0.93
6309711	HS1000000180024 ITGB2	0.71	0.66	-0.03	-0.92	-1.32	-1.97	-0.52
6312802	HS1000000180313 ITGB2	0.36	0.26	0.31	-0.4	-0.86	-0.87	-0.48
6305576	HS1000000197598 LTBP3	0.42	0.41	0.79	-0.69	-0.48	-0.82	-1.76
6300848	HS1000000389588 LTBP4	0.39	0.71	0.66	-1.6	-1.05	-1.76	-0.9
6304750	HS1000000198774 LYZ	0.29	0.34	0.32	-0.71	-1.3	-1.32	-0.93
6301126	HS1000000198769 LYZ	0.01	-0.12	0.14	-0.8	-0.77	-1.18	-1.12
6308652	HS1000000198797 LYZ	-0.12	-0.11	0.03	-0.74	-0.92	-1.06	-1.03
6319193	HS1000000740469 MATN3	0.33	0.4	0.77	-0.58	-0.51	-1.12	-0.45
6320070	HS1000000407384 MATN4	0.45	0.33	0.38	-0.64	-1.08	-1.5	-1.11
6321802	HS1000000208649 MDM2	-0.05	-0.21	-0.07	-0.87	-1.11	-1.46	-1.15
6314328	HS1000000507672 NALP1	0.38	0.54	0.96	-0.57	-0.45	-1.01	-1.22

6313153	HS1000000507511 NALP1	0.87	0.7	1.06	0.02	0	-0.32	-0.43
6305334	HS1000000647589 NALP12	0.41	-0.19	0.29	-0.48	-2.46	-2.4	-1.63
6309441	HS1000000647456 NALP12	0.42	0.28	0.75	-0.71	-0.27	-1.5	-1.38
6301773	HS1000000558791 NDUFA13	0.4	-0.07	0.11	-0.76	-1.87	-1.03	-1.64
6320171	HS1000000230807 NFKBIA	-0.43	-0.59	-0.41	-1.25	-1.87	-2.75	-2.6
6324811	HS1000000230822 NFKBIA	-0.33	-0.47	-0.63	-1.23	-1.79	-2.77	-2.91
6324383	HS1000000415751 NOL3	0.27	0.37	0.33	-0.68	-0.66	-0.62	-0.46
6305966	HS1000000232838 NOS2A	0.22	0.1	0.03	-0.6	-1.29	-1.53	-0.94
6312896	HS1000000232797 NOS2A	0.65	0.66	0.57	-0.13	-0.23	-0.78	-0.37
6307094	HS1000000234229 NPM1	0.7	0.36	0.53	-0.76	-2.21	-2.06	-1.67
6311205	HS1000000238137 OPA1	0.56	0.23	0.02	-0.71	-0.91	-1.38	-1.09
6310320	HS1000000616214 P53AIP1	0.08	0.16	0.24	-0.44	-1.62	-1.18	-1.61
6319748	HS1000000602454 PCBP4	0.38	0.43	0.69	-0.6	-0.57	-0.8	-0.86
6311088	HS1000000602329 PCBP4	1.08	1.09	0.41	-0.26	-0.07	-1.17	-0.81
6316820	HS1000000243629 PCNA	0.87	0.9	0.84	-0.14	-0.44	-0.38	0
6310260	HS1000000420310 PDCD5	1.82	1.67	1.5	0.15	0.75	-0.61	0.2
6313044	HS1000000403307 PEA15	0.85	0.22	0.96	-0.7	-0.92	-1.03	0.03
6316360	HS1000000594360 PECR	0.56	0.91	0.71	-0.2	-0.43	-1.02	-0.61
6309930	HS1000000264331 PPP2R1A	1	0.67	0.52	-0.66	-0.77	-0.65	-0.57
6301350	SA_23_P1473 PRF1	1.04	1.03	0.7	-0.38	0	0.11	-0.55
6310732	HS1000000278806 PRODH	0.48	0.73	0.75	-0.9	-0.29	-0.94	-0.28
6323849	HS1000000278783 PRODH	0.75	0.7	0.63	-0.1	-0.31	-0.48	-0.12
6324439	HS1000000430656 PTGES	0.52	0.48	0.37	-0.78	-0.21	-0.84	-0.46
6314106	HS1000000288861 PTPN6	0.2	0.18	0.37	-0.64	-1.5	-1.29	-1.05
6317433	HS1000000289167 PTPN6	-0.15	-0.02	-0.2	-1.46	-1.23	-1.11	-0.83
6306229	HS1000000294478 PTPRZ1	0.58	0.26	0.48	-0.59	-0.39	-0.47	-0.68
6324282	HS1000000294460 PTPRZ1	0.27	0.3	0.3	-0.65	-0.74	-1.45	-0.6

6314216	HS1000000419631 RABEP1	0.11	-0.32	0.31	-0.56	-1.86	-1.85	-1.45
6302276	HS1000000304951 RBBP4	-0.11	-0.04	0.16	-0.79	-0.81	-1.05	-1.09
6310442	HS1000000307023 RELA	0.17	0.56	0.28	-0.68	-1.08	-2.2	-1.43
6313588	HS1000000307349 RELA	0.47	0.59	1.21	-0.16	-1.08	-2.41	-0.98
6304469	HS1000000307244 RELA	0.17	0.3	0.23	-0.6	-0.48	-0.95	-0.72
6306238	HS1000000023200 RHOB	0.44	0.18	0.27	-0.77	-1.11	-1.27	-1.3
6305484	HS1000000023126 RHOB	0.12	0.09	0.22	-0.59	-1.44	-1.73	-2.36
6319608	HS1000000023032 RHOB	0.5	0.45	0.42	-0.45	-0.28	-0.78	-0.85
6308332	HS1000000023368 RHOB	0.35	0.41	0.3	-0.41	-0.53	-1.15	-1.15
6303350	HS1000000023101 RHOB	0.38	0.38	0.5	-0.48	-0.28	-0.88	-0.94
6313853	HS1000000608563 SEMA6A	0.69	0.25	0.43	-0.31	-0.79	-0.93	-0.63
6311920	HS1000000412962 SGPL1	0.48	0.83	0.44	-0.73	-0.9	-1.74	-0.63
6305804	HS1000000412982 SGPL1	0.08	0.12	0.46	-0.84	-2.11	-2.11	-1.15
6307807	HS1000000326034 SLIT1	0.3	0.75	0.7	-0.49	-0.71	-1.85	-0.55
6314722	HS1000000329124 SON	-0.38	0.77	0.12	-1.04	-1.41	-1.4	-1.44
6305910	HS1000000600112 SPHK2	0.08	-0.49	-0.36	-1.28	-1.08	-1.62	-1.41
6323185	HS1000000344782 TFDP1	0.45	-0.15	0.04	-1.99	-1.92	-2.05	-1.76
6324511	HS1000000164870 TNC	0.22	0.29	0.6	-0.82	-0.85	-0.27	-1.09
6303871	HS1000000164877 TNC	1	1.61	1.2	0.27	-0.66	0.34	0.04
6306200	HS1000000534493 TNFAIP8	0.4	0.57	0.39	-1.46	-0.44	-1.03	-1.38
6303717	HS1000000353517 TP53BP2	1.34	1.1	0.06	-0.03	-1	-0.68	-0.88
6309878	HS1000000430707 TP53I11	-0.3	-0.22	0.25	-1.21	-1.05	-1.76	-1.83
6301908	HS1000000401824 TP73L	0.15	0.87	0.29	-0.82	-0.86	-0.56	-0.7
6322763	HS1000000356029 TPT1	0.58	0.58	0.68	-1.33	-1.5	-0.81	0.06
6320107	HS1000000356455 TRAF2	0.88	0.48	0.45	-0.14	-0.34	-0.69	-0.49
6316153	HS1000000356934 TRAF6	0.67	0.53	0.43	-0.39	-0.27	-0.6	-0.39
6309618	HS1000000219705 TRIM37	0.77	0.2	0.06	-0.65	-1.54	-1.28	-0.66

6305582	HS1000000892631 TUBB	-0.69	0.07	-0.18	-1.33	-1.43	-1.74	-1.36
6305832	HS1000000656746 UNC5D	0.66	0.71	0.61	-0.33	-0.93	-1.09	-0.73
6308831	HS1000000370568 XRCC1	0.42	0.64	0.79	-0.21	-0.97	-0.44	-0.86
6324111	HS1000000372723 YWHAH	-0.09	-0.1	0.21	-0.9	-1.23	-1.55	-0.93
6313219	HS1000000373158 YWHAZ	0.39	0.44	0.28	-0.39	-0.71	-0.84	-0.75
6307296	HS1000000373138 YWHAZ	-0.16	-0.31	0.02	-0.88	-0.98	-1.26	-1.22

Uninfected vs. *Shigella*-infected: 210 Spots showing statistically significant differences (SAM FDR of 3.09) between the two indicated groups.

BIOSEQUENC E_ID	NAME	UN 1 hr	UN 2 hr	UN 2.75 hr	WT 1 hr	WT 2 hr	WT 2.75 hr
6320328	HS1000000615967 CIDEA	1	1.44	1.2	-0.23	-0.28	-0.41
6304553	HS1000000655170 SPATA4	1.14	1.18	1.44	-0.44	0.01	-0.31
6321567	HS1000000654347 EDARADD	1.23	0.83	1.35	-0.17	-0.5	-0.2
6316600	HS1000000434094 CELSR1	-1.59	-1.54	-1.65	0.71	0.64	0.29
6321500	HS1000000404781 CRADD	0.15	-0.07	-0.42	2.11	1.68	2.02
6313305	HS1000000565487 GULP1	0.03	-0.54	-0.66	1.67	1.52	1.67
6303592	HS1000000219700 TRIM37	-0.67	-0.39	-0.53	1.17	1.08	0.97
6307379	HS1000000307230 RELA	-0.96	-1.48	-1.46	0.35	0.74	0.49
6312694	HS1000000451589 EDIL3	0.34	0	-0.06	1.93	1.91	2.74
6321607	HS1000000023323 RHOB	-1.12	-1.04	-1.02	0.36	0.95	0.63
6301166	HS1000000028091 BCL2	-0.43	-0.04	-0.45	1.52	1.57	1.13
6304791	HS1000000230856 NFKBIA	-0.63	-0.52	-0.4	0.85	1.48	1.51
6303840	HS1000000098090 E2F3	-0.41	-0.29	-0.11	1.19	1.61	1.23
6316952	HS1000000091744 DFFA	-0.84	-1.07	-0.98	0.7	0.69	0.34
6316371	HS1000000230780 NFKBIA	-1.16	-1.22	-0.87	0.37	0.53	1.03
6306167	HS1000000355773 TPT1	-0.08	-0.23	0	1.21	1.53	1.26
6323540	HS1000000554687 EMR2	-1.74	-1.23	-0.6	0.98	0.7	0.77
6320466	HS1000000304688 JARID1A	-1.16	-1.06	-1.01	0.77	0.3	0.3

6304331	HS1000000351930 TNFAIP3	0.01	-0.2	-0.4	1.14	1.24	1.4
6312903	HS1000000371443 XRCC5	-0.22	-0.44	-0.58	0.85	1.2	1.23
6308213	HS1000000620580 AXUD1	-2.13	-1.23	-1.15	0.31	0.49	1.23
6306687	HS1000000020291 APP	-0.89	-1.37	-1.14	0.33	0.27	0.61
6311638	HS1000000565509 GULP1	-0.24	-0.48	-0.4	1.06	1.35	2.03
6311532	HS1000000088878 DAXX	-1.75	-2.12	-1.68	0.23	0.24	-0.56
6320694	HS1000000012433 ANK1	-0.41	-0.67	-0.32	1.98	0.86	2.25
6302688	HS1000000433984 TRAF4	-1.44	-0.94	-1.05	0.66	0.17	0.49
6321647	HS1000000289037 PTPN6	-0.1	-0.15	-0.45	1.12	1.17	1.63
6320929	HS1000000212327 MKI67	-1.19	-1.12	-0.98	0.17	0.06	0.16
6312357	HS1000000562561 TNFRSF12A	-0.01	-0.45	-0.63	2.39	1	2.25
6310329	HS1000000183265 JUN	-0.67	-0.55	-0.4	0.86	3.02	2.72
6314920	HS1000000626231 CARD14	-2.6	-1.74	-1.2	0.76	0.1	0.16
6318367	HS1000000183221 JUN	-2.57	-1.43	-0.14	1.03	1.6	2.67
6323200	HS1000000355993 TPT1	-0.44	-0.51	0	1.05	1.94	1.43
6310694	HS1000000617120 CARD15	-0.7	-0.34	-0.52	0.77	0.9	0.74
6320301	HS1000000451598 EDIL3	-0.58	-1.18	-0.43	0.93	0.8	1.46
6302180	HS1000000349126 TIAL1	-0.85	-0.6	-0.86	0.76	0.49	0.48
6305676	HS1000000164513 HSPG2	-0.5	-0.29	-0.94	1.59	0.87	1.06
6302505	HS1000000043640 CASP8	-0.72	0	-0.01	1.24	1.45	1.72
6315137	HS1000000042252 CASP1	-0.23	-0.6	-0.07	1.07	1.29	1.1
6302720	HS1000000202046 MAL	0.01	-0.99	-0.22	1.4	1.51	1.24
6316985	HS1000000355793 TPT1	-0.69	-0.21	-0.06	1.38	1.05	1.22
6303554	HS1000000449075 BCL2L1	-0.52	0.16	-0.15	1.33	1.21	1.65
6312270	HS1000000561883 BFAR	-2.17	-0.68	-0.8	0.75	1.18	0.96
6302658	HS1000000626228 CARD14	-0.69	-0.83	-1.19	0.33	0.91	1.27
6310779	HS1000000230592 NFKB2	-1.13	-0.9	-0.34	0.77	0.7	1.29

6303612	HS1000000019612 BIRC4	-1.49	-0.64	-0.21	1.28	1.02	1.08
6309855	HS1000000372946 YWHAZ	0.33	-0.33	0.12	1.46	2.52	3.47
6319174	HS1000000459945 MAEA	0.24	-0.62	-0.2	1.98	1.11	1.98
6323939	HS1000000183216 JUN	-1.46	-1.31	-1.4	-0.03	3.19	3.21
6316383	HS1000000023281 RHOB	-1.77	-0.99	-1.28	0.46	-0.01	0.34
6324663	HS1000000628971 ELMO3	-0.25	-0.06	-0.07	0.95	1.56	1.62
6324144	HS1000000388548 SPOP	-0.84	-1.15	0	0.88	1.28	1.67
6305056	HS1000000183304 JUN	-1.45	-0.9	-1.25	0.14	3.25	3.08
6301367	HS1000000226748 38597::CG4623	-0.71	-0.42	-0.9	2.4	0.69	1.39
6305548	HS1000000355966 TPT1	-0.17	0	-0.47	1.21	1.2	0.97
6322460	HS1000000023358 RHOB	-0.2	-0.33	-0.06	1.24	0.91	1.03
6315374	HS1000000602134 PCBP4	-1.82	-0.93	-0.82	0.75	0.41	0.48
6323266	HS1000000612988 CARD12	-0.34	-0.65	-1.06	0.92	0.87	0.63
6304443	HS1000000372801 YWHAH	-1.05	-1.18	-1.15	0.21	-0.1	0.09
6304708	HS1000000371201 XRCC4	-0.52	-0.17	-0.45	1.67	0.72	1.51
6307343	HS1000000527818 ZNF346	-0.79	-2.33	-1.81	2.29	0.56	0.35
6317119	HS1000000238640 TNFRSF11B	-0.29	-0.09	0	1.46	1.27	0.95
6300329	HS1000000480111 YME1L1	0.33	-0.66	-0.84	1.47	1.25	1.54
6300834	HS1000000627492 BIRC7	0	-0.33	-0.29	1.64	1	1.12
6302956	HS1000000858016 RPL13A	-0.56	0.36	-0.12	1.44	1.36	1.64
6306635	HS1000000027370 BAK1	-0.42	-0.32	0.2	1.6	1.4	1.04
6320575	HS1000000076594 CSE1L	-0.22	-0.67	0.25	1.11	1.62	1.65
6308624	HS1000000497886 FAF1	-1.32	-1.39	-1.73	0.37	0.66	-0.37
6308951	HS1000000420222 ATG12	-0.51	-0.3	-0.15	0.8	1.14	0.92
6319570	HS1000000017603 APAF1	-0.79	-0.64	-0.88	0.26	0.93	1
6305358	HS1000000017630 APAF1	0.09	-0.4	-0.59	0.88	1.73	1.54
6318470	HS1000000090454 GADD45A	0.14	-0.14	0.08	1.12	1.36	1.69

6323116	HS1000000219581 TRIM37	-0.54	-0.83	-1.08	0.43	0.62	0.46
6312426	HS1000000141336 GRB2	-0.75	-1.61	-1.66	0.96	0.56	0.01
6301597	HS1000000207492 MCM6	-1.48	-0.32	-0.17	2.21	1.26	1.06
6301320	HS1000000289172 PTPN6	-1.94	-0.42	-1.61	0.69	0.56	0.73
6304948	HS1000000013242 ANK3	-0.68	-0.16	-0.04	1.19	0.94	1.34
6324638	HS1000000355988 TPT1	-0.4	-1.16	0	1.09	1.31	1.18
6317993	HS1000000047477 CD2	-0.46	-0.35	0	1.25	0.96	0.94
6317595	HS1000000448900 BCL2L11	-1.51	-1.05	-1.13	0.95	0.19	0.06
6305126	HS1000000403062 BECN1	-0.7	-0.72	-0.4	0.53	0.62	0.55
6307770	HS1000000446549 THOC1	-1.88	-1.35	-0.94	0.4	0.19	0.01
6314163	HS1000000306143 RBL2	-0.67	-0.32	-0.51	0.71	0.7	1.23
6310892	HS1000000342946 TEGT	-0.35	0.13	0	1.35	1.14	1.95
6319710	HS1000000183507 JUN	-0.83	-0.81	-1.13	0.31	3.01	3.93
6312916	HS1000000022962 RHOB	-0.12	-0.21	-0.16	1.37	1.06	0.86
6310252	HS1000000351963 TNFAIP3	-0.58	-0.95	-1.44	0.23	2.37	3.03
6313732	HS1000000482385 NCKAP1	-1.48	-0.88	-0.38	1.17	0.71	0.57
6321554	HS1000000518476 SULF1	-0.3	-0.04	0	0.96	1.36	1.1
6311550	HS1000000427095 GSTO1	-0.59	-0.3	-0.45	0.63	0.98	0.7
6311538	HS1000000383696 FXR1	-0.43	-0.77	-0.41	0.5	1.4	1.19
6308351	HS1000000544530 CLUL1	-1.43	-0.83	-0.79	0.88	0.33	0.32
6305391	HS1000000334164 STAT1	-0.8	-0.31	-0.38	0.72	0.94	0.72
6302275	HS1000000446646 THOC1	0	-0.01	-0.13	1.02	1.22	0.96
6314131	HS1000000230572 NFKB2	0.2	-0.81	-0.49	1.63	0.92	1.54
6316325	HS1000000508093 CARD8	-0.18	-0.2	-0.23	1.5	1.4	0.76
6301837	HS1000000599732 SPHK2	-1.05	-1.43	-1.44	0.34	0.28	-0.27
6313876	HS1000000532205 BCL2L13	-0.25	-0.25	-0.68	0.96	0.74	0.89
6316934	HS1000000141457 GRB2	-0.1	-0.1	-0.59	0.8	1.66	1.82

6321401	HS1000000019797 APLP1	-0.52	-0.26	-0.41	0.64	1.33	0.97
6310225	HS1000000430404 BAG4	-1.06	-1.45	-0.94	0.48	0.33	-0.07
6307418	HS1000000559051 ANGPTL4	-0.05	-0.32	-0.58	2.1	0.89	1.29
6312668	HS1000000208158 MDM2	-0.32	-0.09	-0.69	0.7	1.45	1.62
6324709	HS1000000207308 MCM4	-0.32	-0.56	-0.76	0.49	0.86	0.91
6314437	HS1000000480258 YME1L1	-0.06	-0.27	-0.54	1.51	1.3	0.75
6304882	HS1000000012176 ANK1	-0.38	0.29	-0.39	2.37	1.27	1.32
6311210	HS1000000413820 TAX1BP1	-0.97	0.24	-0.63	1.57	0.95	2.44
6317728	HS1000000299590 RAD17	0	-0.47	0.14	1.05	1.44	1.98
6307224	HS1000000418662 NMI	-0.64	-0.07	-0.13	1.33	1.08	0.88
6301960	HS1000000841605 FBLN5	-0.81	-0.42	0.21	2.13	1.4	1
6315350	HS1000000307318 RELA	-1.67	-1.17	-1.95	0.5	-0.29	-0.16
6309332	HS1000000028104 BCL2	-1.56	-1.04	-1.56	0.54	0.89	-0.33
6323906	HS1000000183203 JUN	-1.6	-1.28	-0.69	0.31	1.09	2.9
6318127	HS1000000230830 NFKBIA	-0.14	-0.71	-0.24	0.69	1.52	1.85
6319463	HS1000000230575 NFKB2	-0.82	-1.07	-0.35	0.53	0.57	1.04
6321720	HS1000000322287 SIAH1	-1.56	-0.46	-1.16	0.7	0.52	0.4
6311110	HS1000000027995 BCL2	-0.86	-1.01	-1.8	0.41	0.22	0.27
6306641	HS1000000534547 TNFAIP8	-0.16	0	-0.25	0.87	1.09	0.93
6307922	HS1000000019644 BIRC5	-0.91	-1.04	-0.63	1.04	0.45	0.27
6306829	HS1000000226914 38597::CG4623	-0.11	-0.65	-0.62	0.88	1.19	0.68
6306131	HS1000000572836 CYCS	-0.07	-0.32	-0.4	2.67	1.19	1.2
6300303	HS1000000670735 DNAJB13	-0.3	-0.17	-0.53	0.67	1.17	0.96
6321712	HS1000000422283 FAIM3	-0.14	-0.01	-0.31	1.68	0.97	1.06
6317282	HS1000000772317 PROS1	-0.09	-0.53	-0.05	1.2	1.14	0.84
6306690	HS1000000101038 CELSR2	-0.4	-0.18	0	0.92	0.89	1.14
6304609	HS1000000048795 CD14	-0.09	-0.05	0	1.01	0.97	1.4

6315383	HS1000000615776 ELMO2	-2.32	-1.75	-1.85	0.37	0.4	-0.98
6313703	HS1000000615802 ELMO2	-1.86	-1.17	-0.79	0.34	0.27	0.19
6316726	HS1000000482375 NCKAP1	-1.16	-1.27	-1.03	-0.23	0.46	0.54
6305614	HS1000000183456 JUN	0	0.01	0.22	1.41	1.27	2.34
6308373	HS1000000417489 DNAJA3	-1.56	-1.2	-2.1	0.33	-0.06	-0.4
6323056	HS1000000345133 TFDP2	-0.51	-0.52	-0.29	1.38	0.86	0.59
6306184	HS1000000852760 SETX	-1.52	-0.82	-0.85	0.47	0.16	0.34
6302795	HS1000000090411 GADD45A	-0.02	-0.4	0	1.02	1.09	1.74
6323686	HS1000000183229 JUN	-1.46	-0.45	-1.4	-0.02	2.46	2.97
6311688	HS1000000023219 RHOB	-0.59	-0.8	-1.08	0.73	0.31	0.33
6315857	HS1000000141651 GRB10	-0.82	-0.48	-0.5	0.65	0.77	0.38
6307797	HS1000000434004 TRAF4	-1.45	-1.02	-0.86	0.63	-0.02	0.27
6317978	HS1000000044172 CASP10	-1.07	-0.84	-0.87	0.42	0.01	0.26
6308960	HS1000000164780 TNC	-1.18	-1.62	-1.55	0.14	0	-0.47
6312732	HS1000000558878 SH3GLB1	-1.56	-0.93	-0.46	1.11	0.53	0.4
6301911	HS1000000661786 DEDD2	-1.71	-0.74	-0.93	0.8	0.18	0.39
6304909	HS1000000532056 BCL2L13	-0.05	-0.39	-0.03	1.03	0.95	0.9
6306591	HS1000000383552 FXR1	-1.02	-0.2	-0.23	0.8	1.23	0.92
6320139	HS1000000028078 BCL2	-1.6	-0.71	-1.31	0.45	0.64	-0.07
6313993	HS1000000019946 APOE	0.39	-0.86	0.13	1.85	1.52	1.35
6319718	HS1000000670768 DNAJB13	-0.28	-0.17	0.43	1.84	1.28	1.22
6310188	HS1000000206761 MCL1	-1.38	-1.07	-0.91	0.29	0.08	-0.1
6318583	HS1000000141297 GRB2	-1.17	-1.41	-0.94	-0.03	0.2	-0.13
6307959	HS1000000013682 ANK3	-0.63	-0.37	0	1.1	0.71	1.09
6318281	HS1000000835668 ABI2	-0.11	-0.35	0	0.83	1.05	0.94
6323845	HS1000000600698 DUSP22	-0.96	-1.31	-0.33	0.31	0.87	1.56
6309514	HS1000000510962 ACIN1	-0.33	-0.08	0	1.06	1.19	0.8

6316197	HS1000000582789 FAIM	0	0.02	-0.2	0.86	0.99	1.09
6317617	HS1000000630656 TAIP-2	-1.53	-0.76	-1.62	0.52	-0.06	0.11
6324720	HS1000000628912 ELMO3	-0.2	-0.33	-0.76	0.72	0.71	0.89
6319322	HS1000000388448 SPOP	-0.11	-0.03	0	1.03	0.81	1.06
6310416	HS1000000604091 RTN4	-0.99	-0.79	-0.44	0.74	0.24	0.68
6322954	HS1000000299992 RAD23B	0	-1.21	-0.15	2.11	1.48	0.8
6308759	HS1000000245176 PDCD2	0.07	-0.52	0	1.47	1.04	1
6317701	HS1000000852719 SETX	-0.84	-1.1	-0.74	0.97	0.68	0.01
6302922	HS1000000391172 CUL2	-1.26	-1.39	-1.92	0.24	-0.24	-0.39
6317008	HS1000000626236 CARD14	-0.79	-0.66	-0.34	0.97	0.48	1.91
6303479	HS1000000197014 LTBP2	0	-0.19	-0.3	0.81	1.15	1.7
6319230	HS1000000023133 RHOB	-0.9	-1.58	-1.31	-0.23	0.16	0.37
6307727	HS1000000656599 UNC5D	-0.09	-0.32	0	0.81	1.01	0.94
6307403	HS1000000230768 NFKBIA	-0.5	-1.2	-1.38	-0.02	1.01	1.21
6308796	HS1000000608555 SEMA6A	-0.59	-1.12	-1.09	0.42	0.16	0.24
6315481	HS1000000183310 JUN	-0.45	-1.01	-0.38	0.3	2.04	2.58
6323032	HS1000000238563 TNFRSF11B	-0.97	-0.95	-1.11	1.03	0.5	-0.1
6310762	HS1000000510871 ACIN1	-1.74	-2.24	-2.12	0.18	-0.09	-1.14
6315074	HS1000000404271 CTNNA1	-0.94	-1.14	-0.68	0.25	0.31	0.07
6314063	HS1000000183549 JUN	-1.39	-1.75	-1.61	-0.68	1.66	2.64
6300373	HS1000000054918 CD97	-0.6	0.36	-0.38	1.29	1.79	0.99
6320548	HS1000000307162 RELA	-0.53	-0.45	-0.16	0.6	0.75	0.71
6308800	HS1000000307340 RELA	-1.14	-1.2	-1.64	0.16	-0.39	0.17
6303511	HS1000000145478 GSTM1	0.24	0.09	0.01	1.82	1.45	1
6324054	HS1000000307109 RELA	-0.3	-0.38	-0.18	0.59	0.95	0.77
6301065	HS1000000264580 PPP2R1B	0.11	0.38	-0.21	2.22	2.1	0.97
6318518	HS1000000740521 MATN3	-1.16	-0.58	-0.15	0.84	0.84	0.65

6306594	HS1000000230788 NFKBIA	-0.86	-0.29	-2.3	0.5	1.11	1.11
6313012	HS1000000508278 CARD8	-0.98	-0.76	-0.56	0.62	0.69	0.12
6323077	HS1000000442917 ELMO1	-0.62	-1.47	0	1.03	0.98	0.86
6317580	HS1000000210900 MGST1	-0.77	-0.03	0	0.98	1.07	1.07
6309635	HS1000000403501 PEA15	-0.73	-0.55	-0.83	0.17	0.58	0.42
6300956	HS1000000498346 CDC37	0.87	-0.14	-0.01	2.34	1.64	1.53
6309003	HS1000000383642 FXR1	0	-0.19	-0.08	1.05	1.29	0.76
6319689	HS1000000459420 TRIP	-1.4	-0.17	-1.38	0.68	0.49	0.69
6319180	HS1000000133925 GAS6	-0.75	0.18	0	1.2	1.75	1
6323292	HS1000000395145 IKBKG	-0.89	-1.18	-0.78	2.63	0.37	0.7
6302574	HS1000000451497 EDIL3	-0.05	-0.21	0	0.85	0.89	0.81
6300454	HS1000000666350 MAGI3	-0.75	-0.7	-0.69	0.73	0.08	0.82
6306828	HS1000000238406 OPA1	-2.1	-1.86	-1.74	-0.17	0.14	-1.07
6300253	HS1000000185445 KNG1	-0.08	-0.4	-1.22	0.64	1.29	1.03
6311132	HS1000000409430 CFLAR	-0.22	-0.45	-1.05	0.79	1.03	0.53
6314841	HS1000000598213 CTNBL1	0.39	0.16	0.49	1.42	1.38	2.08
6310509	HS1000000212576 MKI67	-0.46	-0.58	-0.09	0.8	0.61	1.24
6324829	HS1000000428318 ARHGEF6	-0.29	-0.04	0	0.76	1.19	1.02
6313065	HS1000000348951 TIAL1	-0.3	-0.47	-0.49	0.73	0.41	0.88
6307626	HS1000000183451 JUN	0.07	-0.18	-0.12	0.69	2.27	2.4
6303672	HS100000090441 GADD45A	0.21	0.25	-0.17	1.01	1.42	1.84
6308127	HS1000000012861 ANK3	-0.38	-1.09	-0.27	0.97	0.95	0.48
6306857	HS1000000300396 RAD51	-1.03	-0.73	-0.96	0.57	1.03	-0.05
6315693	HS1000000222631 BIRC1	-2.63	-1.35	-1.21	0.51	-0.12	-0.26
6316396	HS1000000507676 NALP1	-0.51	-0.41	0	1.07	0.75	0.74
6301782	HS1000000615345 ELMO2	-0.77	-0.94	-0.92	0.39	-0.07	0.29
6316190	HS1000000603936 RTN4	-1.87	-2.05	-1.99	0.15	0.02	-1.21

6323552	HS1000000110185 ERCC2	-1.04	-1.19	-0.94	0.62	0.1	-0.15
6313469	HS1000000544746 CLUL1	-0.28	-0.09	-0.43	0.65	0.76	0.78
6313435	HS1000000510879 ACIN1	-0.82	-0.98	-0.24	0.86	0.88	0.29

Uninfected + STS vs. *Shigella*-infected + STS: 532 Spots showing statistically significant differences (SAM FDR of 2.79) between the two indicated groups.

BIOSEQUENCE_ID	NAME	UN 0.5 hr STS	UN 1 hr STS	UN 2 hr STS	UN 2.75 hr STS	WT 0.5 hr STS	WT 1 hr STS	WT 2 hr STS	WT 2.75 hr STS
6312059	HS100000050743 5 NALP1	0.1	0.6	0.79	0.92	-1.35	-1.91	-0.64	-1.47
6300733	HS100000024513 7 PDCD1	0.13	0.4	0.62	0.24	-2.21	-1.94	-0.48	-1.92
6323228	HS100000050747 7 NALP1	0.15	0.59	0.51	0.37	-2.08	-2.17	-0.71	-1.03
6320262	HS100000039476 1 ENC1	0.58	0.21	0.47	0.43	-0.48	-1.44	-1.12	-1.98
6311853	SA_23_P163087 NID2	0.26	0.06	-1.13	-0.63	-2.24	-2.2	-2.06	-3.63
6317284	HS100000024508 8 PDCD1	0.14	0.56	0.75	0.26	-2.38	-1.94	-0.3	-2.24
6304899	HS100000010492 6 EMP1	-0.01	0.17	0.51	0.33	-0.72	-1.02	-1.31	-0.71
6307519	HS100000009405 7 DNASE1L3	0.96	0.38	1.16	0.46	-0.8	-1.36	-0.68	-0.25
6308304	HS100000009041 6 GADD45A	-0.51	-0.43	-0.75	-0.59	3.25	2.96	3.22	3.01
6305056	HS100000018330 4 JUN	-1.41	-2.33	-1.8	-1.46	3.38	3.09	2.93	2.8
6310007	HS100000018325 7 JUN	-0.43	-0.51	-0.88	-0.57	2.86	2.76	2.64	2.92
6309132	HS100000009040 7 GADD45A	-0.19	-0.34	-0.5	-0.22	2.99	2.69	2.78	2.89
6312050	HS100000009045 1 GADD45A	-0.31	-0.64	-1.02	-0.29	3.24	3.08	3.1	3.04
6319447	HS100000018340 3 JUN	-0.59	-0.91	-1.38	-0.77	3.19	2.98	2.64	3
6312847	HS100000018347 2 JUN	-0.82	-0.81	-1.46	-0.67	3.05	2.77	2.72	3.18
6310329	HS100000018326 5 JUN	-1.24	-1.04	-1.37	-0.68	3.2	2.85	2.53	2.64
6312486	HS100000018338 5 JUN	-0.47	-0.57	-0.91	-0.32	2.6	2.44	2.51	2.64
6323939	HS100000018321 6 JUN	-0.98	-1.29	-1.64	-1.27	2.27	2.46	2.9	2.14
6311267	HS100000018350 2 JUN	-0.91	-0.47	-1.03	-0.44	3.28	2.8	2.65	2.88
6304037	HS100000018328 3 JUN	-0.84	-1.46	-1.76	-1.49	3.14	2.98	2.54	2.37

6314068	HS100000018353 2 JUN	-0.8	-0.72	-1.06	-0.37	2.96	2.9	2.39	2.75
6313108	HS100000018343 5 JUN	-1.18	-0.87	-1.43	-2.3	3.41	3.2	2.9	2.9
6313649	HS100000018325 2 JUN	-0.8	-0.99	-0.87	-0.42	2.84	2.53	2.96	2.28
6310265	HS100000018323 5 JUN	-0.56	-1.01	-1.46	-0.64	3.11	2.62	2.53	2.77
6305165	HS100000018334 3 JUN	-0.69	-0.68	-1.1	-0.36	2.5	2.39	2.14	2.67
6316042	HS100000018325 8 JUN	-0.15	-0.73	-0.95	-0.76	3.38	2.77	2.68	2.69
6308395	HS100000009045 9 GADD45A	-0.92	-1.45	-1.44	-1.35	2.44	2.61	2.26	1.64
6301781	HS100000009042 9 GADD45A	-0.68	-1.06	-1.11	-1.02	2.47	2.65	2.45	1.77
6307626	HS100000018345 1 JUN	-0.57	-0.85	-1.4	-0.64	2.35	2.24	2.12	2.31
6313114	HS100000018336 5 JUN	-0.46	0.15	-0.1	-0.31	3.28	2.74	2.82	2.68
6315481	HS100000018331 0 JUN	-0.74	-0.83	-1	-1.14	2.49	1.82	1.83	1.98
6314063	HS100000018354 9 JUN	-1.64	-2.1	-2.52	-1.57	2.73	3.03	2.73	1.58
6316436	HS100000018343 6 JUN	-0.3	-0.19	-0.77	-0.4	3.39	2.96	2.51	2.67
6319195	HS100000018333 6 JUN	-0.22	-0.03	-0.55	-0.01	3.43	2.83	2.69	2.76
6306491	HS100000009040 2 GADD45A	-0.85	-1.15	-1.17	-0.8	2.52	2.6	2.45	1.63
6318367	HS100000018322 1 JUN	-1.03	-0.87	-1.07	-1.55	3.2	3.07	2.81	1.87
6318109	HS100000018352 0 JUN	-0.45	0.23	-0.74	-0.33	3.38	2.79	2.8	2.72
6318412	HS100000018349 0 JUN	-0.31	0.17	-0.5	-0.49	3.65	2.8	2.86	2.68
6318399	HS100000009039 0 GADD45A	-0.22	-0.12	-0.64	0.11	2.36	2.25	2.61	2.37
6303739	HS100000018341 2 JUN	-0.42	-0.59	-1.31	-0.18	3.46	2.87	2.39	2.88
6318155	HS100000018351 5 JUN	-0.67	-0.76	-0.8	-0.08	3.75	3.02	2.88	2.33
6303047	HS100000018329 1 JUN	-0.58	-0.22	-0.45	-0.37	2.73	2.18	1.98	1.99
6324382	HS100000035188 2 TNFAIP3	-0.08	-1.01	-0.88	-0.6	3.44	2.98	2.85	2.13
6319013	HS100000018354 5 JUN	-1.01	-0.16	-0.9	0.05	3.57	3.15	3.05	2.42
6308604	HS100000018337 7 JUN	-0.45	-0.91	-1.51	-0.64	2.38	2.11	1.74	2.19
6307121	HS100000018344 1 JUN	-0.15	-0.67	-0.51	-0.36	2.85	2.48	2.03	1.95
6323686	HS100000018322 9 JUN	-1.02	-1.11	-2.57	-0.68	3.25	3.18	2.79	2.13

6301543	HS100000018318 6 JUN	-0.89	-0.96	-2.89	-1.32	2.79	2.81	2.34	2.31
6323251	HS100000035190 7 TNFAIP3	-0.36	-0.82	-0.98	-0.98	2.99	2.18	1.73	1.96
6320061	HS100000018341 7 JUN	-0.52	-0.14	-0.69	0.35	2.87	2.27	2.34	2.51
6324919	HS100000035197 1 TNFAIP3	-0.83	-1.06	-0.54	-0.14	3.05	2.5	2.63	1.73
6323906	HS100000018320 3 JUN	-1.52	-0.94	-0.84	-1	2.6	2.49	2.25	1.17
6311290	HS100000051836 8 SULF1	0	-0.14	-0.25	0	1.94	1.97	1.52	2.16
6301416	HS100000018339 8 JUN	-0.54	-0.83	-0.84	-0.45	1.3	1.16	1.22	1
6306955	HS100000018342 2 JUN	-0.6	-0.37	-0.7	-0.21	2.9	2.24	2.12	1.58
6315205	HS100000035184 4 TNFAIP3	-0.48	-0.43	0.25	0.66	3.77	3.83	2.75	2.76
6319710	HS100000018350 7 JUN	-0.31	-0.47	-0.4	-0.36	4.05	3.48	2.23	2.35
6320856	HS100000053050 1 PPP1R15A	0.66	0.53	0.24	1.12	2.71	2.84	2.64	2.81
6324812	HS100000018355 4 JUN	-0.5	-0.36	-0.61	0.21	2.52	1.9	1.82	1.92
6320171	HS100000023080 7 NFKBIA	-1.25	-1.87	-2.75	-2.6	1.61	1.09	0.66	0.76
6314816	HS100000016570 1 ID1	-3.44	-3.4	-4.08	-3.22	-1.12	-1.34	-1.61	-1.4
6317720	HS100000053051 1 PPP1R15A	-0.22	-0.79	-1.14	-0.31	2.57	2.24	1.83	1.53
6316976	HS100000035191 2 TNFAIP3	0.09	-0.39	-0.31	0.09	3.26	2.86	2.27	1.89
6313802	HS100000023080 2 NFKBIA	-0.36	-1.03	-0.95	-0.81	2.06	1.37	1.12	1.42
6324921	HS100000018357 4 JUN	-0.02	-0.53	-0.43	-0.22	2.31	1.98	1.82	1.35
6304791	HS100000023085 6 NFKBIA	-0.87	-1.81	-2.59	-2	2.08	1.82	0.84	0.97
6311317	HS100000053051 8 PPP1R15A	-0.14	-0.35	-0.29	-0.29	1.82	1.39	1.18	1.31
6300232	HS100000035195 2 TNFAIP3	-0.07	-0.85	-1.04	0.23	3.58	3.07	2.11	2.18
6324811	HS100000023082 2 NFKBIA	-1.23	-1.79	-2.77	-2.91	1.78	1.21	0.61	0.65
6318127	HS100000023083 0 NFKBIA	-0.59	-0.46	-0.7	-0.77	2.17	1.38	1.19	1.2
6312832	HS100000051835 4 SULF1	0	0	-0.26	0.45	2.29	1.68	2.09	2.69
6306486	HS100000022692 7 38597::CG4623	-0.27	0.48	0.17	0	2.01	2.49	1.82	2.75
6321607	HS100000002332 3 RHOB	-0.73	-1.39	-1.78	-1.88	1.16	1.02	0.72	0.46
6316399	HS100000009042 4 GADD45A	-0.07	-0.09	-0.28	-0.25	0.98	1.42	1.31	1.41

6303435	HS100000067190 3 MYO18A	-0.53	-0.52	-0.74	-0.41	0.65	0.73	0.87	0.77
6308630	HS100000023084 8 NFKBIA	-0.5	-1.02	-1.17	-0.7	1.63	1.37	0.82	0.79
6317180	HS100000023079 7 NFKBIA	-0.98	-1.52	-1.77	-1.92	1.43	0.68	0.26	0.54
6306594	HS100000023078 8 NFKBIA	-1.16	-1.68	-1.64	-2.05	2.15	1.57	0.73	0.29
6315518	HS100000018348 5 JUN	-0.54	-0.99	-0.87	-0.53	1.14	0.99	1.02	0.54
6303228	HS100000041137 8 IER3	-0.31	-0.96	-1.1	-0.64	1.66	1.05	0.82	1.31
6324610	HS100000035197 6 TNFAIP3	-0.33	-0.58	-0.32	-0.02	3.16	2.44	1.88	1.42
6313274	HS100000016562 4 ID1	-3.03	-3.24	-3.82	-3.6	-1.31	-1.94	-1.65	-1.36
6305484	HS100000002312 6 RHOB	-0.59	-1.44	-1.73	-2.36	1.73	2.07	1.17	0.58
6314038	HS100000023086 9 NFKBIA	-1.51	-1.1	-2.74	-2.02	1.42	1.11	0.8	0.17
6321945	HS100000980337 6 JUND	-0.02	-0.31	-0.14	0.1	1.68	1.3	1.2	1.3
6322179	HS100000009039 8 GADD45A	-0.08	0.18	-0.02	-0.18	1.15	1.24	1.51	1.3
6314951	HS100000023081 5 NFKBIA	-0.74	-1.37	-1.61	-1.15	1.33	0.93	0.29	0.66
6308848	HS100000053049 3 PPP1R15A	0.24	-0.47	-0.47	-0.57	3.22	1.84	2.3	1.48
6313691	HS100000041135 2 IER3	0	-0.67	-0.67	0	2.22	1.55	1.42	1.32
6310252	HS100000035196 3 TNFAIP3	-0.33	-0.93	0.5	-1.47	4.01	3.51	2.98	1.47
6305480	HS100000014136 3 GRB2	-0.83	-1.11	-0.53	-0.88	0.46	0.54	0.45	0.68
6322798	HS100000002296 7 RHOB	-0.37	-0.83	-1.41	-1.93	1.93	2.21	0.92	1.04
6317024	HS100000018332 7 JUN	0.07	-0.36	-0.2	0.48	2.02	1.46	1.67	1.62
6316365	HS100000030483 1 RBBP4	0	0	-0.62	0.37	1.34	2.2	1.86	1.94
6320878	SA_23_P106002 NFKBIA	-0.56	-0.8	-1.82	-2.28	1.54	1.32	1.1	0.75
6315612	HS100000018315 9 JUN	-0.03	0.33	-0.11	0.1	1.93	1.57	1.77	1.21
6308279	HS100000023063 8 NFKB2	-0.21	-0.3	0.04	-0.31	1.14	1.24	1.06	0.88
6302688	HS100000043398 4 TRAF4	-1.26	-1.12	-0.94	-1.33	0.85	0.52	0.42	-0.02
6300406	HS100000002293 3 RHOB	-0.39	-0.53	-1.42	-1.04	1.24	0.95	0.74	0.99
6324866	HS100000020675 1 MCL1	-0.23	0.02	-0.58	-0.38	1.93	1.31	0.97	1.65
6302864	HS100000002316 0 RHOB	-0.5	-0.77	-1.55	-1.7	1.3	1.04	0.67	0.74

6305486	HS100000002290 9 RHOB	-0.43	-0.82	-1.51	-1.48	1.28	0.82	0.68	0.77
6307403	HS100000023076 8 NFKBIA	-1.17	-0.6	-1.65	-1.86	1.6	1.07	0.4	0.7
6322684	HS100000002336 6 RHOB	-0.57	-1.63	-2.38	-2.29	1.31	0.67	0.69	0.55
6310477	HS100000002335 3 RHOB	-0.48	-1.02	-1.65	-1.74	1.18	1.07	0.68	0.5
6307546	HS100000002330 1 RHOB	-0.86	-0.88	-1.81	-2.11	1.15	0.89	0.8	0.29
6314430	HS100000002332 7 RHOB	-0.39	-0.64	-1.38	-1.68	1.25	1.31	0.89	0.74
6312916	HS100000002296 2 RHOB	-0.41	-0.34	-1.03	-0.37	1.11	0.88	0.81	1.24
6301863	HS100000012809 5 FOSL2	-0.33	-0.52	-1.02	-0.55	1.17	1.13	0.59	0.95
6316707	HS100000002307 8 RHOB	-0.45	-1.11	-1.77	-1.86	1.36	0.96	0.59	0.71
6313371	HS100000018347 7 JUN	0.51	0.46	0.22	0.55	1.73	1.59	1.74	2.17
6323617	HS100000023079 2 NFKBIA	-0.99	-1.65	-4.09	-3.2	2.23	1.71	0.88	0.53
6304264	HS100000041134 7 IER3	0.03	-0.58	-1.14	-0.22	2.19	1.55	1.14	1.49
6313606	HS100000002326 2 RHOB	-0.62	-0.93	-1.69	-1.76	1.15	0.89	0.4	0.67
6310092	HS100000062627 0 CARD14	0.06	0.34	0.12	0.54	1.92	1.34	1.8	1.92
6309486	HS100000002287 7 RHOB	-0.67	-0.68	-1.49	-1.29	1.31	0.97	0.38	0.76
6307844	HS100000023430 0 NPM1	-0.92	-1.93	-0.47	-1.08	1.54	0.63	0.9	1.2
6313439	HS100000013400 6 GAS6	-0.76	-0.77	-0.67	-0.66	0.57	0.27	0.68	0.89
6314495	HS100000002330 6 RHOB	-0.55	-1.09	-1.79	-1.98	1.34	1.03	0.73	0.41
6304491	HS100000053053 1 PPP1R15A	0.56	0.58	-0.18	1.12	2.4	2.27	2.21	2.69
6310298	HS100000002309 6 RHOB	-0.43	-0.46	-1.54	-1.57	1.02	1.2	0.99	0.85
6300547	HS100000009038 2 GADD45A	-0.35	-0.25	0.19	0.02	1.66	1.13	1.22	1.31
6318183	HS100000053055 0 PPP1R15A	0.4	0.39	-0.11	0.43	1.67	1.59	1.85	2.35
6321806	HS100000023066 5 NFKB2	-0.09	-0.54	-0.36	-0.45	1.2	1.1	0.7	0.9
6303406	HS100000012816 1 FOSL2	-0.3	-0.52	-0.87	-0.65	1.07	0.89	0.48	1.11
6321793	HS100000018335 6 JUN	-0.16	0.31	-0.9	-0.14	2.42	1.66	1.6	1.42
6309855	HS100000037294 6 YWHAZ	-0.07	0.26	0.57	0.39	1.46	1.79	2.26	2.29
6306315	HS100000041138 9 IER3	-0.18	-0.88	-1.04	-0.83	1.51	1.05	0.75	0.72

6311311	HS100000025255 5 PIN1	-0.78	-0.96	-1.23	-0.82	0.7	0.21	0.67	0.23
6322639	HS100000024374 2 PCNA	-1.27	-0.52	-1.25	-0.94	1.19	0.6	1.14	0.28
6316624	HS100000002333 2 RHOB	-0.59	-1.15	-1.67	-1.94	1.14	0.86	0.45	0.35
6320300	HS100000002319 0 RHOB	-0.67	-1.09	-2.03	-2.26	1.14	0.82	0.61	0.37
6303823	HS100000018357 2 JUN	0.49	0.35	0.15	1.08	2.13	1.81	2.22	2.46
6318018	HS100000002295 5 RHOB	-0.58	-0.71	-1.53	-1.79	1.33	1.04	0.4	0.79
6324918	HS100000046960 9 SEMA4D	-0.19	-0.39	-0.44	-0.24	0.78	0.61	0.71	0.79
6324543	HS100000043757 0 ESPL1	-0.42	-1.68	-1.89	-1.17	0.88	0.45	0.53	0.83
6322331	HS100000002331 8 RHOB	-0.54	-0.61	-1.33	-1.36	0.84	0.67	0.4	0.67
6304647	HS100000053280 7 MTCH1	0	0	0.14	-0.07	1.22	1.96	1.73	2.8
6320132	HS100000043409 0 TRAF4	-0.45	0.03	0.06	0.06	1.37	0.95	1.29	1.3
6317107	HS100000002334 1 RHOB	-0.48	-0.79	-1.7	-1.79	1.14	0.9	0.68	0.47
6312026	HS100000035187 7 TNFAIP3	-0.36	-2.04	0.03	-0.28	2.98	2.77	2.09	1.12
6320181	HS100000053054 1 PPP1R15A	0	-0.17	-0.12	0.16	1.09	1.12	1.23	1.72
6324853	HS100000002313 8 RHOB	-0.85	-1.39	-1.92	-2.52	1.16	0.79	0.56	-0.1
6322993	HS100000014495 8 GSR	-0.38	-0.75	0.21	-0.42	1.05	1.82	1.54	1.04
6306902	HS100000043399 9 TRAF4	-0.97	-0.92	-1.01	-0.99	0.43	0.07	0	0.03
6322773	HS100000035194 7 TNFAIP3	-0.22	-1.2	0.14	-0.25	2.93	2.66	2.2	0.9
6309518	HS100000035378 9 TP53BP2	-0.92	-0.89	-0.65	-0.77	0.98	0.36	0.42	0.3
6307720	HS100000065426 4 EDARADD	0	0.11	-0.15	0	1.32	1.21	2.45	2.01
6302035	HS100000002308 3 RHOB	-0.43	-0.6	-1.53	-1.46	0.8	0.74	0.52	0.94
6316568	HS100000002310 8 RHOB	-0.24	-0.76	-1.59	-1.34	1.13	0.98	0.54	0.77
6319723	HS100000033433 8 STAT1	-0.2	0.38	-1	0	1.45	1.98	1.47	1.45
6319230	HS100000002313 3 RHOB	-0.63	-1.53	-2.18	-1.97	0.84	0.87	0.34	-0.04
6310285	HS100000023082 5 NFKBIA	-1.89	-2.93	-4.42	-3.81	1.05	0.36	-0.13	-1.41
6308213	HS100000062058 0 AXUD1	-1.39	-1.56	-2.33	-0.36	1.67	1.61	0.81	0.23
6302138	HS100000001990 7 APOE	-0.49	-1.15	-1.07	-0.98	0.29	0.3	0.4	0.81

6310441	HS100000041756 7 DNAJA3	-0.3	0	-0.35	0	0.81	1.61	1.12	1.29
6322632	HS100000062617 1 CARD14	-0.12	0.01	-0.18	-0.4	1.26	0.75	1.14	1.54
6315586	HS100000018327 8 JUN	-0.64	-0.83	-0.49	-0.37	1.2	0.97	1.42	0.34
6309427	HS100000085826 8 RPL13A	-0.43	-0.18	-1.33	-0.98	1.25	0.88	0.61	1.19
6318470	HS10000009045 4 GADD45A	0.01	0.69	0.38	-0.63	2.28	1.75	2.3	1.53
6323826	SA_23_P137016 Foot-and-mouth disease virus SAT	0.48	0.1	0.82	0.95	2.08	1.72	2.31	2.13
6317361	HS100000023810 0 OPA1	0	-0.07	-0.37	0	1.19	0.75	1.23	1.19
6302192	HS100000012812 6 FOSL2	-1.02	-1.47	-1.73	-1.23	0.12	0.02	-0.1	-0.29
6320565	HS10000002324 9 RHOB	-0.84	-0.88	-1.83	-2.11	1.05	0.85	0.53	-0.02
6317104	HS100000023052 5 NFKB2	0.18	0.05	0.23	0.56	1.24	1.37	1.34	1.5
6303038	HS10000002288 2 RHOB	-0.28	-0.44	-1.32	-1.17	1	0.78	0.56	0.85
6310610	HS100000018344 6 JUN	0	0.17	0.12	0	3.17	1.81	1.46	1.68
6312494	HS10000002327 6 RHOB	-0.44	-0.93	-1.63	-2.01	1.2	1.04	0.56	0.28
6304312	HS100000041752 0 DNAJA3	-1.82	-2.25	-2.44	-2.33	-0.83	-0.51	-1.15	-0.05
6316467	HS100000012816 4 FOSL2	-0.93	-1.32	-1.46	-1.22	0.18	0.07	0.11	-0.35
6313044	HS100000040330 7 PEA15	-0.7	-0.92	-1.03	0.03	1.45	0.55	0.9	1.52
6317649	HS100000008961 3 DCC	-1.92	-1.43	-1.33	-1.86	0.06	-0.37	-0.31	-0.57
6302674	HS100000018318 3 JUN	-0.12	-0.77	-1.8	-1.33	1.66	1.51	1.07	0.38
6316647	HS10000002850 5 BCL2L2	-0.45	-0.89	-1.23	-0.95	0.42	0.38	0.22	0.75
6317921	HS100000054329 1 NGFRAP1	-0.25	-0.47	-1.03	-0.39	1.12	0.79	0.59	0.75
6321016	HS100000039488 6 ENC1	-0.26	-0.51	-1.37	-0.35	0.67	1.06	1.03	0.96
6322763	HS100000035602 9 TPT1	-1.33	-1.5	-0.81	0.06	1.87	0.88	0.63	1.98
6306298	HS10000002334 0 RHOB	-0.84	-0.95	-1.86	-2.16	0.89	0.73	0.21	0.02
6319146	HS100000023084 3 NFKBIA	-0.96	-0.31	-1.42	-1.93	1.2	0.69	0.77	0.35
6312860	HS100000032614 9 SLIT1	-0.72	-0.73	-0.34	-1.15	0.82	0.54	0.32	0.61
6320153	HS10000002331 4 RHOB	-0.77	-0.91	-1.37	-1.35	0.94	0.41	0.29	-0.05
6308952	HS100000053050 6 PPP1R15A	0.2	0	-0.55	-0.22	2.65	2.27	1.83	0.81

6302658	HS100000062622 8 CARD14	-0.15	-1.22	-1.11	0.1	1.7	1.3	0.84	1.24
6324217	HS100000028903 2 PTPN6	-0.67	-0.08	-0.17	-0.54	0.75	0.9	1.11	1.71
6308617	HS100000023058 0 NFKB2	0.16	0.08	0.19	0.5	1.23	1.29	1.19	1.6
6304643	HS100000002290 4 RHOB	-0.47	-0.55	-1.07	-0.63	1.22	0.91	0.44	0.4
6306133	HS100000002334 6 RHOB	-0.52	-0.44	-1.56	-1.42	0.9	0.57	0.55	0.54
6320148	HS100000002312 7 RHOB	-0.23	-0.44	-1.47	-2.52	1.74	1.42	0.98	0.86
6322307	HS100000032606 5 SLIT1	0.03	-0.7	-0.88	-0.72	0.86	0.63	0.68	1.01
6306945	HS100000023072 5 NFKB2	-0.07	0.21	0.11	0.34	1.14	1.14	1.23	1.01
6317301	HS100000023061 4 NFKB2	0.08	0.13	0.18	0.55	1.26	1.25	1.22	1.54
6308397	HS100000002304 9 RHOB	-0.27	-0.48	-1.09	-0.27	0.83	0.77	0.58	0.94
6310583	HS100000012808 3 FOSL2	-0.89	-1.01	-1.48	-1.28	0.22	-0.12	-0.05	-0.12
6323310	HS100000002309 1 RHOB	-0.33	-0.78	-1.44	-1.9	1.28	1	0.44	0.43
6307513	HS100000012808 8 FOSL2	0.11	0.12	-0.4	-0.27	1.55	1.3	0.82	1.06
6313831	HS100000022152 8 MYBL2	-1.08	-1.49	-1	-1.24	0.37	0.1	-0.32	-0.08
6308092	HS100000024635 0 PDE1B	-0.05	-0.62	-0.46	0.01	1.55	0.65	1.04	1.57
6317608	HS100000002322 4 RHOB	-0.32	-0.57	-1.11	-0.68	0.91	0.65	0.44	0.42
6304563	HS100000001898 0 BIRC2	-0.63	-1.75	-0.41	-0.65	0.54	1.15	0.94	0.6
6320396	HS100000014686 8 GZMH	0.14	-0.28	-0.33	-0.19	1.03	0.84	1.73	2.06
6317262	HS100000059764 4 BCAP29	-0.12	0.51	0.87	0.62	1.49	2.19	1.88	2.32
6300677	HS100000060007 6 SPHK2	0.24	0.14	0.02	0.4	1.59	1.06	1.14	1.42
6322432	HS100000039058 5 CUL4A	-0.52	-0.44	-0.18	-0.11	1.58	0.59	0.88	1.1
6324684	HS100000004391 2 CASP9	-0.74	-1.05	-1.58	-1.73	-0.18	0.5	0.7	0.12
6317521	HS100000012814 4 FOSL2	-0.88	-1.15	-1.32	-1.29	0.2	-0.11	0.04	-0.33
6311071	HS100000062055 7 AXUD1	-0.34	-0.32	-1.82	-0.26	1.46	0.98	0.96	1.18
6316058	HS100000035637 6 TRAF2	-0.33	-0.42	-0.18	-0.42	0.99	0.65	0.54	0.54
6315640	HS100000002293 8 RHOB	-0.6	-0.47	-1.38	-1.5	1.3	0.99	0.37	0.28
6310320	HS100000061621 4 P53AIP1	-0.44	-1.62	-1.18	-1.61	0.14	0.46	0.17	0.44

6316413	HS100000035698 3 TRAF6	0	0.2	-0.34	0	1.13	0.87	1.06	0.93
6304450	HS100000002329 7 RHOB	-0.56	-0.74	-1.65	-1.34	1	0.42	0.45	0.14
6308584	HS100000043745 9 ESPL1	-1.19	-1	-1.44	-1.8	0.2	0.12	-0.23	-0.34
6311557	HS100000002324 2 RHOB	-0.44	-0.37	-0.95	-0.94	0.38	0.41	0.48	0.52
6323445	HS100000051825 0 SULF1	-0.02	0.45	-0.51	0.15	1.26	1.46	2.44	3.12
6310022	HS100000035183 1 TNFAIP3	-0.22	0.39	-0.27	-0.26	2.02	1.6	1.12	0.93
6308558	HS100000041136 0 IER3	-0.05	-0.49	-0.77	0.11	1.26	0.89	0.77	1.35
6313209	HS100000002333 7 RHOB	-0.59	-1.17	-1.48	-2.09	0.71	0.96	-0.02	0.15
6306131	HS100000057283 6 CYCS	-0.32	-1.72	-0.65	-0.19	1	0.85	0.89	1.03
6303668	HS100000023076 1 NFKB2	0.01	0.37	-0.01	0.02	1.27	0.89	1.08	1.38
6303215	HS100000020674 3 MCL1	-0.47	-0.78	-1.34	-0.83	1.08	0.44	0.16	0.53
6321499	HS100000039485 3 ENC1	-0.03	-0.36	-0.55	-1.02	1.37	0.95	1.08	0.46
6319608	HS100000002303 2 RHOB	-0.45	-0.28	-0.78	-0.85	0.42	0.38	0.54	0.49
6324292	HS100000002317 3 RHOB	-0.51	-0.54	-1.59	-1.49	1.32	0.84	0.39	0.26
6311486	HS100000020210 3 MAL	-0.07	0.36	-0.06	-0.36	0.91	1.06	1.51	1.71
6317142	HS100000035635 0 TRAF2	-0.14	-0.44	-0.22	-0.35	0.72	0.45	0.71	0.6
6302693	HS100000024620 4 PDE1B	-0.24	-0.56	-0.82	0.29	1.68	0.86	0.88	1.44
6317239	HS100000043059 8 PTGES	0.11	0.53	0.12	0.15	1.42	1.38	1.5	0.97
6322460	HS100000002335 8 RHOB	-0.41	-0.38	-1.64	-1.87	0.93	0.61	0.66	0.67
6305619	HS100000026442 1 PPP2R1A	-0.37	-0.34	-1	-0.86	0.59	0.52	0.32	0.74
6324765	HS100000061546 7 ELMO2	-1.31	-1.5	-0.82	-0.77	0.26	-0.17	0.21	0.24
6320456	HS100000043402 7 TRAF4	-0.63	-0.95	-2.19	-1.94	0.72	0.04	0.43	0.26
6323950	HS100000000610 6 ADRA1A	-0.69	0.22	0.41	0.11	2.15	0.99	1.84	1.56
6307797	HS100000043400 4 TRAF4	-0.9	-1.1	-0.8	-1.11	0.49	0.32	-0.04	-0.17
6313068	HS100000018339 1 JUN	-0.05	-0.35	-0.41	-0.31	1.28	0.79	0.95	0.49
6317745	HS100000035650 5 TRAF2	-0.46	-0.56	-0.66	-0.77	0.77	0.46	0.34	0.16
6303451	HS100000023055 2 NFKB2	0.1	0.05	-0.12	0.4	1.16	1.22	1.03	1.77

6324660	HS100000045596 6 NME6	0.18	0.08	0.28	0.19	0.97	0.93	1.15	0.95
6317868	HS100000041136 8 IER3	-0.32	-0.82	-1.21	-0.48	1.83	0.76	0.43	0.76
6310098	HS100000035604 7 TPT1	-1.85	-1.51	-1.54	-0.18	1	-0.07	0.53	1.18
6304746	HS100000035643 9 TRAF2	-0.25	-0.15	-0.37	-0.44	0.73	0.58	0.41	0.61
6316021	HS100000011046 4 ERCC3	-1.09	-0.87	-1.43	-0.8	-0.07	0.05	1.11	0.76
6302870	HS100000041140 2 IER3	-0.61	-1.94	-1.12	-0.98	0.98	0.6	0.74	-0.21
6313678	HS100000023085 1 NFKBIA	-0.22	-0.34	-0.53	-0.31	1.21	0.81	0.53	0.51
6320137	HS10000002305 9 RHOB	-0.17	-0.32	-0.81	-0.18	0.9	0.79	0.57	0.63
6319272	HS10000002311 3 RHOB	-0.39	-0.37	-1.45	-2.38	1.13	1.43	0.57	0.61
6324225	HS10000002314 6 RHOB	-0.56	-0.2	-1.22	-1.8	1.34	0.81	0.6	0.45
6319861	HS100000035364 6 TP53BP2	-0.56	-1.87	-1.21	-1.92	0.94	0.56	-0.27	0.25
6305336	HS10000002323 7 RHOB	-0.37	-0.37	-0.99	-0.97	0.43	0.42	0.37	0.61
6324671	HS100000020670 8 MCL1	-0.46	-0.55	-1.64	-1.67	1.15	0.64	0.41	0.25
6309050	HS100000045577 8 NME6	-0.81	-0.52	-0.41	-0.71	0.2	0.36	0.42	0.81
6305328	HS100000049503 8 DIDO1	-0.26	-0.73	-0.83	-0.71	0.9	0.45	0.17	0.65
6311688	HS10000002321 9 RHOB	-0.64	-0.8	-1.42	-1.79	1.25	0.47	0.1	0.17
6321622	HS100000008892 4 DAXX	-0.08	0	-0.33	0.23	1.05	0.73	0.99	1.13
6313821	HS10000002329 4 RHOB	-0.64	-0.86	-1.61	-1.99	0.75	0.74	0	0.06
6320095	HS100000020744 3 MCM5	0.27	0	0.06	0	0.9	1.02	1.79	1.48
6320046	HS10000002298 4 RHOB	-0.28	-0.41	-0.91	-0.86	1.02	0.87	0.17	0.62
6318938	HS100000012810 8 FOSL2	-0.11	-0.01	-0.61	-0.06	1.24	0.78	0.66	1.29
6308332	HS10000002336 8 RHOB	-0.41	-0.53	-1.15	-1.15	0.38	0.28	0.26	0.74
6309924	HS100000020674 8 MCL1	-0.1	0	-0.64	0.24	0.77	1.4	1.3	2.15
6312694	HS100000045158 9 EDIL3	-0.6	-0.33	-1	0.42	0.79	1.28	1.21	2.19
6323205	HS100000012810 3 FOSL2	-0.94	-1.16	-1.61	-1.06	0.32	-0.14	0.24	-0.38
6323350	HS100000041139 7 IER3	-0.16	-0.36	-0.97	-0.24	1.86	1.02	0.91	0.53
6304316	HS100000062627 3 CARD14	-0.47	-1.19	-1.14	-0.69	0.63	0.32	0	0.33

6324631	HS100000001347 8 ANK3	-0.96	-1.4	-1.78	-0.79	0.62	0.04	-0.31	0.75
6302663	HS100000023070 8 NFKB2	-0.24	-0.47	-0.44	0.01	0.97	0.74	0.55	1.47
6316977	HS100000002301 9 RHOB	-0.71	-1.37	-1.64	-1.94	1.1	0.93	0.07	-0.47
6303350	HS100000002310 1 RHOB	-0.48	-0.28	-0.88	-0.94	0.34	0.29	0.47	0.56
6321952	HS100000045956 7 TRIP	-0.88	-0.38	-0.54	-0.21	0.68	0.26	0.64	0.83
6323947	HS100000062633 0 CARD14	-0.12	0.48	0.22	0.22	1.34	0.91	1.38	1.36
6305341	HS100000023058 9 NFKB2	0.13	-0.38	-0.13	0.54	1.3	1.14	1.49	1.01
6302951	HS100000023082 0 NFKBIA	-0.62	-1.81	-2.21	-1.78	2.12	3.71	0.52	-0.26
6316383	HS100000002328 1 RHOB	-0.76	-1.65	-3.64	-2.91	0.43	0.85	-0.2	-0.23
6303686	HS100000054860 4 HTRA2	0	-0.01	-0.01	0	0.77	0.71	1.01	1.28
6313347	HS100000034483 3 TFDP1	-0.43	-0.26	0.15	-0.18	0.74	0.69	0.81	1.2
6313319	HS100000002318 3 RHOB	-0.45	-0.21	-0.8	-0.85	0.41	0.29	0.57	0.52
6309641	HS100000023063 5 NFKB2	-0.35	-0.59	-0.22	-0.8	1.03	0.99	0.38	0.37
6323732	HS100000030473 6 JARID1A	0.08	-0.78	-0.42	-0.71	1.09	1.19	1.24	0.24
6318733	HS100000050813 8 CARD8	0	0.43	0	0.33	0.82	1.61	1.37	1.64
6312040	HS100000058583 8 LRDD	-1.15	-0.47	-1.09	-1.42	0.13	-0.14	0.39	0.29
6320465	HS100000014183 1 GRB10	-1.17	-1.16	-1.13	-0.98	-0.19	0.34	-0.34	-0.23
6312536	HS100000004237 5 CASP1	0	0.28	-0.45	0	0.64	1.84	2.03	1.3
6317249	HS100000035634 1 TRAF2	-0.11	0.04	-0.24	-0.43	0.94	0.88	0.61	0.59
6307217	HS100000018349 5 JUN	0.02	0.06	-0.11	-0.02	1.27	0.82	0.74	0.8
6306927	HS100000002292 6 RHOB	-0.19	-0.37	-0.82	-0.77	0.99	0.97	0.18	0.61
6321263	HS100000001921 7 BIRC2	-0.05	-0.4	-0.53	-0.54	0.9	1.24	0.45	0.5
6318250	HS100000034915 2 TIAL1	0	0	-0.13	0.15	0.64	0.91	0.86	0.8
6322582	HS100000034497 9 TFDP1	-0.59	-0.85	-1.08	-1.21	0.38	0.79	-0.02	-0.05
6320981	HS100000002832 0 BCL2L1	-0.34	-1.16	-0.8	-0.48	0.17	0.34	0.63	0.72
6317221	HS100000002306 2 RHOB	-0.34	-0.45	-1.3	-1.41	1.07	0.91	0.32	0.19
6300986	HS100000018352 5 JUN	0.02	-0.45	-0.5	-0.18	1.23	0.81	0.47	0.76

6319827	HS100000021111 1 MGST1	-1.37	-1.12	-1.08	-1.7	-0.52	-0.09	-0.34	0.21
6324837	HS100000039165 6 CUL1	-0.66	-0.83	-0.72	-0.38	0.64	-0.05	0.46	0.66
6305301	HS100000041748 4 DNAJA3	-1.84	-3.12	-3.99	-2.52	-0.97	-0.8	-1.58	0.02
6319193	HS100000074046 9 MATN3	-0.58	-0.51	-1.12	-0.45	0.33	0.16	0.73	0.45
6312951	HS100000002305 4 RHOB	-0.64	-0.66	-1.54	-2.69	0.73	0.86	0.28	0.18
6302085	HS100000037058 9 XRCC1	-0.81	-0.48	-1.6	-1.16	0.03	0.39	0.28	0.16
6319537	HS100000018323 0 JUN	0.65	0.85	0.89	0.46	2.06	1.49	2.1	1.51
6301103	HS100000035638 4 TRAF2	-0.48	-0.1	-0.29	-0.26	0.65	0.42	0.5	0.84
6302873	HS100000002323 2 RHOB	-0.46	-0.25	-1.45	-1.8	1.31	0.99	0.28	0.37
6315333	HS100000066407 0 MMD2	0.41	-1.15	-0.39	0	1.18	1.17	0.94	1.97
6310294	HS100000013369 6 GAS6	0	0.18	0.75	0	0.89	2.42	2.06	1.66
6309291	HS100000062633 3 CARD14	0.37	0.53	0.19	1.08	2	1.29	1.77	2.2
6323538	HS100000018356 4 JUN	-0.03	-0.39	-0.28	0.01	1.43	0.87	0.49	1.02
6322804	HS100000002336 3 RHOB	-0.33	-0.7	-1.47	-1.43	1	0.87	0.41	-0.11
6313786	HS100000020676 8 MCL1	-0.33	-0.47	-1.35	-1.72	1.16	0.71	0.28	0.28
6306395	HS100000024373 8 PCNA	-1.44	-1.5	-1.88	-1.63	-0.98	-0.52	-0.48	-0.68
6321597	HS100000008929 8 DCC	0	-0.5	-0.66	0	0.46	0.8	1.42	1.17
6300418	HS100000035636 8 TRAF2	-0.03	0.21	0.02	0.15	0.79	0.78	0.81	0.98
6302835	HS100000018345 9 JUN	-0.03	0.03	-0.15	0.12	1.34	0.87	0.7	0.83
6310188	HS100000020676 1 MCL1	-0.61	-1.24	-1.3	-1.67	0.58	0.49	-0.1	-0.36
6320938	HS100000008884 2 DAXX	-0.78	-0.46	-0.45	-0.71	0.49	0.23	0.61	0.05
6303400	HS100000056265 0 TNFRSF12A	-1.04	0.17	-1.19	-0.31	0.78	0.75	0.77	0.75
6320541	HS100000032900 6 SON	-0.18	-0.74	-0.69	-0.66	0.77	0.12	0.44	0.5
6322050	HS100000023075 8 NFKB2	-0.03	-0.35	0	-0.08	0.84	0.81	0.58	0.6
6308363	HS100000041757 2 DNAJA3	-1.72	-3.12	-3.41	-2.04	-1.13	-1.07	-1	0.02
6316456	HS100000002320 3 RHOB	-0.5	-0.64	-1.13	-1.19	0.81	0.44	0.24	-0.13
6324864	HS100000002304 2 RHOB	-0.83	-1.37	-0.96	-1.81	0.65	0.19	0.1	-0.49

6301597	HS100000020749 2 MCM6	-0.15	0.1	0.15	0.02	0.57	1.09	1.06	1.32
6316912	HS100000002972 1 BID	-0.75	-1.24	-1.07	-0.63	0.42	-0.08	-0.15	0.39
6322685	HS100000035635 8 TRAF2	-0.15	-0.12	-0.57	-0.43	0.73	0.42	0.48	0.6
6311834	HS100000035654 6 TRAF3	-0.46	-1.11	-0.63	-0.57	0.62	-0.02	0.35	0.89
6303272	HS100000001935 3 BIRC2	0.17	0.05	0.33	0.23	1.04	1.61	1.06	0.92
6314258	HS100000035185 3 TNFAIP3	0.53	0.25	0.12	0.08	1.79	1.52	1.46	0.78
6313412	HS100000024627 6 PDE1B	-0.02	-0.3	-0.69	0	1.26	0.38	1.04	1.75
6305882	HS100000037110 0 XRCC3	-0.43	-0.47	-0.54	-0.17	0.43	0.32	0.47	0.29
6324939	HS100000041357 5 APPBP1	0	0.88	0.01	0	1.2	1.89	1.71	1.14
6303339	HS100000011032 1 ERCC2	-0.58	-1.15	-0.99	-0.72	0.69	0.39	-0.21	0.16
6322661	HS100000043404 0 TRAF4	-1.03	-0.72	-0.98	-0.71	0.3	-0.22	0.04	-0.01
6324486	HS100000035669 0 TRAF3	-0.2	0.06	-0.41	-0.01	1.07	0.92	0.44	0.91
6309567	HS100000002315 3 RHOB	-0.29	-0.39	-1.02	-0.97	0.41	0.27	0.27	0.63
6300941	HS100000002976 0 BID	-0.66	-0.98	-1.16	-0.85	0.59	0.04	-0.28	0.72
6303592	HS1000000021970 0 TRIM37	-0.12	-0.05	-0.73	0	0.58	0.77	1.08	0.8
6314294	HS100000042825 1 ARHGEF6	-0.28	0	-0.19	-0.61	0.63	1.18	0.41	1.26
6307163	HS100000039470 3 ENC1	-1.12	-0.93	0.06	-1.04	1.54	0.03	0.73	0.88
6312930	HS100000034515 5 TFDP2	-0.02	-0.77	-0.44	0.03	0.6	0.98	1.49	0.63
6323062	HS100000002291 7 RHOB	-0.43	-0.3	-1.37	-1.8	1.12	0.68	0.52	0.07
6322461	HS100000052753 6 ZNF346	-1.33	-1.59	-2.19	-1.54	-0.24	-0.91	-0.65	-0.36
6319631	HS100000002289 0 RHOB	-0.33	-0.41	-1.86	-1.79	1.07	0.9	0.25	0.19
6312162	HS100000048004 2 YME1L1	-0.03	0	-0.57	0	0.38	2.56	1.42	1.83
6321403	HS100000052470 7 SIRT1	0.12	-0.02	-0.53	-0.37	1.14	1.22	0.92	0.4
6301522	HS100000008900 6 DAXX	-0.36	-0.45	-1.23	-0.59	0.61	0.52	0.11	0.48
6306548	HS100000039163 8 CUL1	-0.52	-0.72	-0.56	-0.65	0.52	-0.12	0.36	0.67
6300892	HS100000004224 4 CASP1	-0.51	-0.22	-0.35	-0.17	0.68	0.46	0.45	1.22
6311603	HS100000002326 4 RHOB	-0.86	-1.58	-2.41	-2.9	0.39	0.42	0.15	-1.05

6315406	HS100000056361 5 DDX41	-0.36	-0.27	-0.89	-0.26	0.77	0.2	0.58	0.85
6305024	HS100000024632 2 PDE1B	-0.15	-0.17	-0.08	0.3	1.47	0.45	1.24	1.51
6311605	HS100000040184 3 TP73L	0.34	0.53	0.77	0.88	1.89	1.32	2.19	3.15
6318592	HS10000000509 9 ADORA1	0	-0.18	-0.25	-0.05	0.23	1.6	1.59	1.93
6316328	HS100000010535 2 EMR1	0.88	1.08	1.37	0	2.86	1.73	2.02	2.79
6311126	HS100000064759 7 NALP12	0.17	-0.52	-0.27	0.2	1.67	0.58	0.93	1.57
6306894	HS100000014188 0 GRB10	0.01	-0.77	-0.4	-0.1	0.95	0.4	0.82	0.74
6324828	HS100000046969 4 SEMA4D	-0.16	-0.23	-0.31	-0.43	0.99	1.33	0.61	0.3
6301045	HS100000051869 4 SULF1	0	-0.36	0.05	0	0.58	1.05	0.79	1.49
6322645	HS100000042023 9 ATG12	-0.01	0	-0.25	0	0.64	0.66	1.45	1.05
6318952	HS100000040960 5 CFLAR	-0.53	-0.31	0.26	-0.01	0.57	0.81	1.34	1.16
6318845	HS100000041137 3 IER3	-0.53	-1.22	-1.36	-1.13	0.86	0.58	0.72	-0.61
6321908	HS100000058610 2 LRDD	-0.71	-1.55	-0.69	-0.08	1.03	0.6	0.17	0.63
6304535	HS100000023071 3 NFKB2	-0.07	0.03	-0.24	-0.07	0.79	0.86	0.61	0.49
6303636	HS100000042709 9 GSTO1	-0.71	-0.84	-0.27	-0.55	1.14	0.67	-0.09	0.76
6310700	HS100000024171 7 SERPINB2	-0.93	-0.8	-0.47	-0.5	0.05	0.21	0.11	0.2
6317395	HS100000054327 6 NGFRAP1	-0.64	-1.13	-0.65	-0.68	1.15	0.95	-0.41	0.9
6320256	HS100000062624 9 CARD14	0.12	-0.13	0.08	0.07	0.85	0.69	0.69	0.69
6320211	HS100000002321 2 RHOB	-0.75	-0.95	-1.4	-1.47	0.72	0.31	0.08	-0.55
6310779	HS100000023059 2 NFKB2	-0.04	0.17	0.36	-0.14	1.31	1.34	1.1	0.62
6307113	HS100000016424 7 HSPG2	-0.1	-1.33	-1.53	-0.62	1.59	0.24	0.19	0.94
6307140	HS100000086818 1 DLL4	0.29	-0.69	-0.22	0.31	1.06	1.02	0.88	1.73
6320466	HS100000030468 8 JARID1A	-0.63	-1.16	-1.35	-0.79	0.07	-0.29	0.58	0.12
6309925	HS100000004234 6 CASP1	-0.27	0.04	-0.32	-0.03	0.72	0.5	0.65	1.06
6303991	HS100000023060 6 NFKB2	-0.05	-0.26	-0.23	-0.35	0.81	0.85	0.59	0.3
6304684	HS100000077828 1 RBBP5	-0.43	-0.39	0.23	-0.09	1.05	0.38	1.42	1.09
6308165	HS100000035181 5 TNFAIP3	-0.77	0.74	-0.03	-0.75	2.31	1.1	1.04	1.23

6306687	HS100000002029 1 APP	-0.37	-0.16	-0.13	-0.31	0.71	1.07	0.95	0.23
6322267	HS100000034901 8 TIAL1	-0.74	-0.61	-1.43	-1.06	0.4	0.24	-0.3	0.13
6312357	HS100000056256 1 TNFRSF12A	-0.08	0.48	-0.21	0.16	1.53	1.34	0.71	2.38
6324343	HS100000020866 6 MDM4	-1.28	-0.96	-0.47	-0.67	-0.1	0.07	0.29	0.47
6318724	HS100000027881 1 PRODH	-0.12	-0.12	-0.63	0.46	1.56	0.42	1.57	1.46
6316586	HS100000014146 2 GRB2	-0.44	-0.63	-0.29	-0.33	0.63	0.43	0.93	0.13
6317162	HS100000032934 9 SON	-0.35	-0.65	-0.59	-0.48	0.84	0.48	-0.06	0.7
6301886	HS100000002317 8 RHOB	-0.8	-1.65	-2.22	-3.15	0.28	0.47	-0.1	-0.95
6313818	HS100000040946 0 CFLAR	0.72	0.63	0.66	0.59	1.28	1.29	1.25	1.54
6321966	HS100000044645 5 THOC1	-1.65	-1.21	-1.05	0.2	0.13	1.04	0.66	0.61
6311064	HS100000034890 6 TIA1	-0.33	-0.27	-0.21	-0.26	0.29	0.54	0.33	0.6
6314131	HS100000023057 2 NFKB2	-0.12	-0.74	0.39	0.57	1.24	1.63	1.39	0.95
6310074	HS100000055778 9 GLRX2	-0.31	-0.71	-1.38	0	1.36	0.29	0.5	1.21
6305416	HS100000002316 5 RHOB	-0.56	-0.69	-1.66	-2.25	0.53	0.63	-0.11	-0.01
6307399	HS100000043397 1 TRAF4	-0.48	-1.59	-1.06	-0.85	0.76	0.29	-0.37	0.52
6318302	HS100000043402 2 TRAF4	-0.46	-0.87	-1.48	-0.58	0.92	0.16	-0.01	0.43
6319853	HS100000001914 9 BIRC2	-0.74	-0.16	-0.76	-1.58	0.51	1.11	0.52	0.05
6319054	HS100000043405 7 TRAF4	-1.04	-0.96	-1.18	-1.28	-0.21	-0.4	0.06	-0.51
6319268	HS100000012811 7 FOSL2	0.02	-0.19	-0.54	0.31	1.2	0.77	0.64	1.14
6321160	HS100000005092 6 CD38	-1.14	-1.77	-1.45	-1.16	-0.3	-0.63	-0.37	-0.6
6306931	HS100000066469 1 ELMOD2	-0.52	-0.88	-0.42	-1.01	0.1	0.1	0.12	0.52
6303007	HS100000023086 4 NFKBIA	-0.23	-0.06	-0.08	-0.09	0.8	0.94	0.4	0.6
6310337	HS100000037099 4 XRCC3	-0.4	-1.22	-1.27	-0.49	0.11	0.06	0.33	0.51
6324038	HS100000002320 7 RHOB	-0.83	-1.67	-2.06	-2.82	0.3	0.21	0.02	-1.07
6309930	HS100000026433 1 PPP2R1A	-0.66	-0.77	-0.65	-0.57	-0.33	0.95	0.72	0.71
6311328	HS100000042936 9 LITAF	-0.7	-0.65	-0.73	-0.63	0	-0.06	-0.13	-0.12
6301099	HS100000064459 5 AMID	-0.8	-0.32	-0.9	-0.73	0.59	0.46	-0.18	0.37

6306573	HS100000016565 2 ID1	-2.53	-2.51	-3.25	-1.64	-0.85	-1.51	-1.12	-1.15
6318448	HS100000019733 7 LTBP3	-0.24	-0.43	-0.34	0.39	1.4	0.45	0.99	1.05
6307703	HS100000023064 3 NFKB2	-0.5	-0.71	-0.06	-0.64	0.43	0.56	0.67	0.15
6316202	HS100000035634 5 TRAF2	-0.32	-0.13	-0.6	-0.17	0.46	0.35	0.5	0.74
6301042	HS100000002301 2 RHOB	-0.76	-1.74	-2.11	-3.04	0.22	0.4	-0.05	-1.02
6310062	HS100000032230 5 SIAH1	-0.65	-0.54	-0.64	-0.29	0.27	0	0.45	0.6
6320467	HS100000060066 5 DUSP22	-0.94	-0.58	-1.78	-1.11	0.32	-0.02	0.22	-0.3
6304363	HS100000004401 5 CASP9	-0.67	-0.02	-0.59	-0.05	0.22	0.82	1.85	2.12
6313440	HS100000085274 7 SETX	-0.57	0	-1.05	-0.56	0.01	0.72	1.76	2.06
6323116	HS100000021958 1 TRIM37	-0.6	-1.02	-0.24	-0.27	0.1	0.99	0.54	0.59
6322027	HS100000063069 7 TAIP-2	-0.55	-1.15	-0.66	-0.77	0.29	0.14	-0.11	-0.01
6304992	HS100000002300 2 RHOB	-0.4	-0.09	-1.58	-1.74	1.03	0.77	0.52	0.06
6323226	HS100000055776 8 GLRX2	-0.68	-1.22	-0.82	-0.94	-0.16	-0.11	0.08	-0.25
6316726	HS100000048237 5 NCKAP1	-0.26	-0.2	0.24	-0.37	0.59	0.53	0.87	1
6312803	HS100000020203 3 MAL	-0.6	-0.88	0.21	0.57	0.66	1.37	1.19	1.89
6322916	HS100000027819 9 PRLR	0	-0.29	-0.01	0	0.67	0.82	0.44	0.79
6318851	HS100000001896 8 BIRC2	-1.2	-0.48	-1.24	-0.17	0.55	1.03	0.49	-0.05
6304974	HS100000037293 6 YWHAZ	-0.73	1.22	-0.01	-0.98	1.42	1.19	1.53	2.63
6308982	HS100000002326 9 RHOB	-0.42	-0.09	-0.69	-0.89	0.42	0.18	0.44	0.66
6316985	HS100000035579 3 TPT1	0	0	-0.4	-0.38	0	2.2	2.04	1.56
6305296	HS100000043401 7 TRAF4	-0.89	-1.01	-1.04	-0.63	0.11	-0.34	-0.03	-0.13
6306245	HS100000035646 3 TRAF2	-0.12	-0.2	0.07	-0.23	0.7	0.63	0.59	0.41
6320008	HS100000012813 1 FOSL2	-0.32	-0.5	-0.41	0.02	0.65	0.3	0.44	0.75
6301787	HS100000016448 2 HSPG2	-0.08	0.15	-0.09	0.33	1.26	0.64	0.86	1.53
6321648	HS100000035641 3 TRAF2	-0.21	0.14	-0.26	-0.11	0.77	0.46	0.66	0.64
6301936	HS100000051125 0 FAIM2	-1.4	-0.98	-2.33	-1.09	-0.37	-0.1	-0.44	0.75
6321843	HS100000021133 7 CIITA	-0.31	-0.76	-0.99	-0.09	0.96	0.17	0.42	0.65

6324363	HS100000028095 9 PSEN2	-0.1	-0.4	-0.68	-0.56	0.11	0.81	0.49	0.54
6322289	HS100000026412 0 PPP2CA	-1.33	-0.7	-1.57	-1.39	0.25	-0.01	0.11	-0.75
6309240	HS100000039482 7 ENC1	-0.31	-0.16	-0.37	-0.16	0.71	0.31	0.39	0.91
6321253	HS100000040950 6 CFLAR	-0.57	0.51	-0.12	0.13	1.61	1.24	0.83	0.85
6317559	HS100000020672 6 MCL1	-0.42	-0.38	-1.51	-1.59	0.48	0.52	-0.1	0.39
6309778	HS100000039162 2 CUL1	-1.27	-0.6	-0.77	-0.61	0.12	-0.15	0.4	0.08
6300903	HS100000004228 9 CASP1	-0.26	-0.46	-0.75	-0.45	0.92	0.5	-0.05	0.86
6302067	HS100000039101 3 CUL3	-0.47	-0.17	-0.95	-0.92	0.04	0.68	0.25	0.87
6309845	HS100000064745 1 NALP12	0.2	0.04	0.43	0	0.85	1.23	0.76	1.09
6317771	HS100000030485 6 RBBP4	-0.36	0	-0.39	0	1.14	0.78	0.49	0.48
6318536	HS100000032315 7 SIPA1	-0.46	-0.65	-1.83	-0.65	1.05	-0.03	0.34	0.41
6311686	HS100000044303 7 ELMO1	-0.8	-0.81	-1.14	-1.13	-0.2	-0.44	-0.08	0.02
6302781	HS100000044649 8 THOC1	-0.61	-0.16	-0.83	-0.35	0.6	0.13	0.34	0.54
6322955	HS100000039486 9 ENC1	-0.17	-1.81	-1.78	-0.23	1.08	0.73	0.66	0
6321021	HS100000051830 9 SULF1	1.1	0.76	-0.34	1.04	1.63	2.19	1.68	2.39
6311153	HS100000087252 1 HEG1	0.57	0.15	-0.05	0.02	1.44	0.88	0.89	1.12
6317015	HS100000037302 8 YWHAZ	0	0.19	-0.81	0	0.74	0.69	1.3	0.91
6316053	HS100000023060 1 NFKB2	0.3	0.22	-0.08	0.75	1.23	1.18	1	1.41
6323344	HS100000060867 5 SEMA6A	-0.51	0.56	0.84	1.06	1.47	1.84	1.72	2.67
6317919	HS100000014188 8 GRB10	-0.08	-0.2	0.06	0.34	1.04	0.89	0.61	0.82
6320722	HS100000035646 0 TRAF2	-0.34	0.04	-0.31	-0.27	0.57	0.31	0.55	0.64
6315167	HS100000016485 7 TNC	-0.47	-0.75	-0.66	-0.71	0.66	-0.07	0.14	0.11
6322835	HS100000054452 5 CLUL1	0	-0.36	-0.36	0.49	1.09	1.01	0.59	1.07
6307260	HS100000056559 0 GULP1	0.58	0.68	-0.04	0.93	2.47	1.29	3.03	1.4
6311110	HS100000002799 5 BCL2	-0.28	-1.52	-0.54	-1.71	0.33	0.58	0.11	0.11
6301613	HS100000020670 2 MCL1	-0.78	-0.59	-1.49	-1.48	0.62	0.24	-0.01	-0.44
6309636	HS100000037074 8 XRCC1	-1.62	-0.56	-1.49	-0.68	0.5	0.03	-0.19	-0.05

6311514	HS100000014179 3 GRB10	-0.08	0.46	-0.25	-0.17	1.13	0.55	0.95	1.07
6306206	HS100000048234 6 NCKAP1	-1.34	-0.69	-1.23	-0.99	-0.6	0.39	0.15	-0.03
6301898	HS100000063066 2 TAIP-2	-0.43	-1.16	-1.17	-0.67	0.69	0.22	-0.13	-0.02
6309705	HS100000012574 4 FOXO3A	0.16	0.06	-0.32	0.31	0.95	0.99	0.6	1.16
6315060	HS100000022660 4 38597::CG4623	0	-0.05	-0.09	-0.2	0.49	0.44	0.72	0.61
6307387	HS100000051098 1 ACIN1	0.13	0.36	-0.1	-0.01	1.17	0.65	0.85	1.53
6324737	HS100000030504 4 RBBP6	0.06	-0.41	-0.53	-0.27	1.04	0.2	0.69	0.72
6324720	HS100000062891 2 ELMO3	-0.31	-0.25	-1.41	0	0.88	0.6	1.05	0.41
6311529	HS100000048010 6 YME1L1	0.31	-0.13	0.23	0.37	1.27	0.8	1.21	2.24
6313684	HS100000002802 0 BCL2	-0.66	-0.75	-0.61	-0.47	0.08	0	-0.09	0.23
6310031	HS100000035591 1 TPT1	-0.1	0	-0.21	0	0.82	0.31	1.09	1.3
6321500	HS100000040478 1 CRADD	0	0.77	0.72	0.48	1.06	1.44	2.78	2.86
6308226	HS100000020680 3 MCL1	-0.17	-0.09	-0.71	-0.19	0.76	0.48	0.34	0.64
6320006	HS100000013376 3 GAS6	0.95	2.04	0.49	0.88	2.88	1.87	2.75	2.26
6316132	HS100000041134 2 IER3	0.1	0.57	0.41	0.75	1.77	1.3	1.42	1.03
6306848	HS100000014188 5 GRB10	-0.46	-0.41	-1.35	-0.61	0.44	0.18	0.06	0.46
6316706	HS100000034898 1 TIAL1	-0.26	-0.33	-0.71	0	0.6	0.15	1.45	1.36
6302147	HS100000050764 6 NALP1	-1.22	-0.9	-1.02	-0.76	0.05	-0.15	-0.52	0.12
6317513	HS100000003159 7 BOK	-1.29	-1.73	-1.39	-1.54	-0.53	-0.62	-0.86	-0.9
6308789	HS100000052466 2 SIRT1	-0.26	-0.46	-0.42	-0.68	0.6	0.38	0.03	0.33
6321996	HS100000001091 2 ALOX15B	-0.54	-1.57	-1.92	-0.83	0.55	0.48	-0.7	0.46
6302007	HS100000062053 9 AXUD1	-0.79	-1.68	-0.58	-0.78	-0.28	0.01	0.9	0.52
6305977	HS100000016567 9 ID1	-1.49	-3.1	-3.04	-1.41	-0.68	-1.23	-0.44	-0.51
6305631	HS100000008917 3 DBC1	-1.46	-1.95	-1.41	-1.86	-0.85	-1.14	-0.44	-0.57
6308943	HS100000002752 4 BAX	-0.59	-1.06	-1	-0.46	0.44	-0.19	0.05	0.19
6315528	HS100000023083 8 NFKBIA	-0.17	-0.07	-0.07	-0.12	0.86	0.81	0.34	0.53
6309968	HS100000020470 3 MATN2	-0.61	-0.67	-0.53	-0.48	0.82	-0.13	0.32	0.3

6312219	HS100000056541 5 GULP1	-0.83	-1	-1.39	-1.05	-0.28	-0.51	-0.23	0.02
6322038	HS100000043439 8 MTL5	-0.78	-0.08	-0.4	0.76	1.81	1.1	1.2	0.7
6306339	HS100000085268 9 SETX	-0.3	-0.74	-0.52	-0.65	0.77	-0.26	0.72	0.76
6303304	HS100000023076 6 NFKB2	-0.03	0.44	0.15	0.05	1.42	1.34	1.06	0.56
6310869	HS100000003536 8 C6	-0.34	-0.74	-0.47	-1.39	0.31	0.18	0.15	0.35
6310173	HS100000020858 7 MDM2	-0.31	-0.31	-0.49	-0.43	0.26	0.21	0.11	0.29
6313475	HS100000016569 9 ID1	-3.08	-5.02	-4.05	-3.09	-1.67	-2.38	-2.37	-2.63
6302892	HS100000050837 0 CARD8	-0.22	-0.02	-0.62	-0.85	0.75	0.73	0.17	0.5
6305933	HS100000033424 6 STAT1	0	-0.73	-0.57	0.31	0.34	0.9	1.03	1.21
6308285	HS100000018346 5 JUN	-0.04	0.4	0.08	0.21	1.38	0.64	1	1.01
6308815	HS100000053052 3 PPP1R15A	0	-0.36	-1.14	-0.21	2.85	1.43	1.22	-0.01
6314692	HS100000054645 2 PD4D4	0	-0.3	-0.25	0.88	2	0.86	1.35	1.08
6315529	HS100000002287 0 RHOB	-0.62	-1.09	-1.94	-1.49	0.71	0.22	0.06	-0.77
6307139	HS100000052759 8 ZNF346	-1.06	-0.8	-1.46	-1.64	-0.43	-0.58	0.19	0.77
6322219	HS100000001762 0 APAF1	-1.22	-1.98	-2.22	-1.86	-0.13	-0.74	-1.13	-0.89
6318868	HS100000035662 5 TRAF3	-0.37	-0.35	-0.38	-0.01	0.7	0.24	0.6	0.37
6319174	HS100000045994 5 MAEA	0	0.69	0.15	0.32	1.15	0.86	1.65	2.35
6319992	HS100000022162 4 MYBL2	-0.4	-0.58	-0.65	-0.34	0.44	0.16	0.01	0.25
6302899	HS100000016563 8 ID1	-2.11	-2.46	-3.9	-1.69	-0.53	-0.78	-1.85	-0.05
6301941	HS100000045341 3 BCAP31	-0.1	-0.41	-0.88	0	0.36	0.38	1.19	0.89
6312078	HS100000044916 6 BCL2L1	-0.41	-0.65	-1.27	-1.51	0.25	0.09	-0.11	0.01
6322509	HS100000062624 4 CARD14	-0.46	-0.96	-0.5	-0.29	0.74	0.48	0.21	0
6302304	HS100000043397 4 TRAF4	0.01	-1.24	-0.32	-0.29	0.97	0.44	0.71	0.39
6323776	HS100000038376 1 FXR1	-1.55	-1.5	-0.56	-1.31	0.21	-0.32	-0.5	-0.19
6316799	HS100000053054 5 PPP1R15A	0	0.09	-0.13	0.17	0.77	0.51	0.74	1.1
6303707	HS100000021099 1 MGST1	-0.88	-0.97	-1.33	-1.1	-0.26	-0.6	-0.26	0.06
6311221	HS100000035642 3 TRAF2	-0.34	0.2	-0.57	-0.36	0.68	0.27	0.69	0.78

6310165	HS100000051848 4 SULF1	-0.14	0.02	-0.42	0.89	1.76	0.74	1.33	1.24
6306729	HS100000004229 9 CASP1	-0.25	0.06	-0.21	-0.06	0.78	0.45	0.42	0.98
6301713	HS100000040351 4 PEA15	-0.93	-0.16	0.05	-0.39	1.66	0.73	0.31	0.64
6323014	HS100000037078 5 XRCC1	-1.19	-1.04	-1.09	-0.87	-0.06	-0.51	-0.47	0.25
6311732	HS100000002299 4 RHOB	0.01	-0.26	-1.05	-0.41	0.71	0.75	0.1	0.87
6321129	HS100000083570 9 ABI2	0	-0.24	-0.74	0.53	0.58	1.69	0.78	1.3
6323801	HS100000003148 4 BNIP3L	-0.68	-2.13	-1.76	-1.15	0.08	-0.59	-0.49	0.12
6309012	HS100000054325 3 NGFRAP1	-0.07	-0.21	-1.15	-0.49	0.81	0.24	0.49	0.53
6317324	HS100000059924 1 DIABLO	-0.08	0.15	-0.67	-0.32	0.52	0.58	0.93	0.51
6319860	HS100000060429 3 RTN4	0	0.02	-0.14	0	0	2.16	1.52	2.31
6320369	HS100000002319 5 RHOB	-0.24	-0.24	-1.06	-1.13	0.53	0.77	0.33	-0.04
6324067	HS100000020886 5 MDM4	-0.5	-0.71	-0.31	-0.41	0.52	0.07	0.06	0.44
6307099	HS100000001911 1 BIRC2	0.28	0.14	0.02	0.56	0.86	1.14	0.94	0.94
6308949	HS100000014131 1 GRB2	-1.15	-0.1	-0.05	-0.76	0.66	0.2	0.64	0.59
6307524	HS100000044928 9 BCL2L11	-0.01	0.09	-0.66	-0.06	0.41	0.99	0.59	1.05
6301645	HS100000054854 0 HTRA2	-0.16	-0.2	-0.38	-0.04	0.62	0.3	0.43	0.92
6313245	HS100000002833 6 BCL2L1	-0.68	-1.17	-1.1	-0.95	-0.31	-0.39	-0.21	0.19
6309323	HS100000052471 0 SIRT1	-0.31	-0.13	-0.25	-0.33	0.58	0.62	0.41	0.14
6315077	HS100000022722 2 NEDD8	-0.47	-0.25	-0.35	0	-0.07	1.09	1.06	1.22
6324517	HS100000027798 7 PRLR	-0.1	-1.24	-0.79	-0.48	0.53	0.2	0.4	0.15
6307370	HS100000002314 8 RHOB	-0.57	-0.5	-2.66	-1.72	1	0.63	-0.19	-0.24
6315708	HS100000085267 4 SETX	-0.1	-0.29	-0.09	-0.37	0.52	0.59	0.44	0.24
6323271	HS100000004247 8 CASP2	-1.65	-0.93	-1.48	-2.05	0.21	-0.38	0.28	-1.15
6307144	HS100000019880 5 LYZ	-0.81	-0.99	-1.31	-1.02	-0.27	-0.57	-0.21	0.05
6322880	HS100000030719 0 RELA	-0.24	-1.38	-0.85	-0.16	0.55	0.56	0.46	0.08
6313231	HS100000037108 3 XRCC3	-0.11	-0.29	-0.39	0.06	0.91	0.37	0.4	1.18

<i>Shigella</i>-infected vs. <i>Shigella</i>-infected + STS: 93 Spots showing statistically significant differences (pValue < 0.01) between the two indicated groups.								
BIOSEQUENC E_ID	NAME	WT 1 hr	WT 2 hr	WT 2.75 hr	WT 0.5 hr STS	WT 1 hr STS	WT 2 hr STS	WT 2.75 hr STS
6319954	HS1000000604123 RTN4	-0.42	-0.46	-0.56	-0.29	-0.21	-0.12	-0.2
6307488	HS1000000604143 RTN4	-0.34	-0.37	-0.48	-0.1	-0.06	-0.17	-0.13
6312490	HS1000000498283 CDC37	-0.3	-0.17	-0.22	0.12	0.08	0.01	0.14
6322877	HS1000000101046 CELSR2	-0.54	-0.58	-0.7	-0.34	-0.31	-0.17	-0.33
6312365	HS1000000300038 RAD23B	-0.36	-0.29	-0.17	0.16	0.04	-0.1	0.12
6319535	HS1000000603917 RTN4	-0.47	-0.43	-0.59	-0.18	-0.04	-0.22	-0.22
6308817	HS1000000564010 DDX41	-0.04	0.01	0.07	0.47	0.29	0.31	0.34
6312351	HS1000000421647 DEDD	-0.48	-0.39	-0.4	-0.15	-0.14	-0.15	0.11
6302330	HS1000000604373 RTN4	-0.48	-0.55	-0.59	-0.3	-0.2	-0.2	-0.08
6316672	HS1000000206721 MCL1	-0.47	-0.47	-0.63	-0.24	-0.1	-0.3	-0.05
6306519	HS1000000101292 CELSR2	-0.71	-0.57	-0.68	-0.36	-0.38	-0.21	-0.23
6300527	HS1000000858080 RPL13A	0.02	0.04	0.07	0.36	0.39	0.58	0.6
6318737	HS1000000278856 PRODH	0.23	0.23	0.27	0.7	0.63	0.8	0.66
6301221	HS1000000563794 DDX41	-0.8	-0.9	-0.82	-0.22	-0.33	-0.34	-0.6
6321606	HS1000000027655 BAX	-0.02	-0.31	-0.2	0.35	0.16	0.51	0.26
6323336	HS1000000226530 38597::CG4623	-0.57	-0.34	-0.32	0.12	0.13	0.18	-0.08
6321594	HS1000000858068 RPL13A	-0.17	0	-0.04	0.46	0.3	0.41	0.57
6309811	HS1000000429610 LITAF	-0.07	-0.32	-0.3	0.37	0.32	0.33	0.1
6310315	HS1000000429267 LITAF	-0.1	-0.26	-0.31	0.38	0.33	0.35	0.18
6301109	HS1000000140910 GPX1	-0.65	-0.55	-0.55	-0.01	0.11	0.02	-0.3
6315550	HS1000000410206 HDAC3	-0.43	-0.67	-0.45	0.12	0.15	-0.04	-0.06
6311527	HS1000000140995 GPX1	-0.66	-0.43	-0.4	0.19	0.23	0.06	-0.21
6302235	HS1000000260513 POR	-0.14	-0.09	0	0.56	0.61	0.42	0.39
6321385	HS1000000110645 ERCC3	-0.7	-0.81	-0.62	-0.02	-0.1	-0.06	-0.36
6313664	HS1000000232856	-0.36	-0.75	-0.61	0.3	0.5	0.04	-0.11

	NOS2A							
6321759	HS1000000278824 PRODH	-0.15	-0.03	-0.22	1	0.63	0.53	0.37
6308567	HS1000000395304 IKBKG	-0.93	-1.05	-0.91	0.17	-0.03	-0.42	-0.33
6322513	HS1000000390917 CUL3	-0.59	-0.45	-0.21	0.35	0.48	0.8	0.12
6300457	HS1000000238227 OPA1	1.1	1.44	1.45	2.4	2.22	3.19	2.25
6303536	HS1000000507369 NALP1	0.07	0.33	0.13	-1.12	-1.05	-1.96	-0.94
6324332	HS1000000469481 UNC13B	-0.36	0.26	-0.16	-0.81	-1.73	-1.9	-1.61
6312427	HS1000000005263 ADORA2A	0.23	0.34	0.06	-1.17	-1.18	-1.54	-0.82
6302495	HS1000000647480 NALP12	-0.03	-0.43	-0.14	-1.51	-1.79	-1.95	-0.89
6316950	HS1000000387531 NME5	0.3	0.06	0.1	-1.66	-0.99	-1.38	-0.67
6314827	HS1000000017527 APAF1	0.11	-0.57	-0.28	-1.73	-1.15	-1.83	-1.55
6310560	HS1000000424551 BZRAP1	-0.47	-1.13	-0.62	-2.09	-2.44	-1.82	-1.61
6317978	HS1000000044172 CASP10	0.42	0.01	0.26	-0.88	-0.89	-1.33	-0.9
6313065	HS1000000348951 TIAL1	0.73	0.41	0.88	-0.74	-0.05	-0.85	-0.08
6302956	HS1000000858016 RPL13A	1.44	1.36	1.64	-0.13	0.54	0.42	0.68
6312561	HS1000000110326 ERCC2	0.26	0.03	0.21	-1.15	-0.53	-0.95	-1.01
6309764	HS1000000047500 CD2	0.53	0.44	0.83	0	-0.94	-0.69	-0.24
6320803	HS1000000650122 CIAS1	-0.04	-0.52	-0.36	-1.54	-1.55	-1.27	-1.07
6314273	HS1000000226884 38597::CG4623	0.77	0.34	0.38	-0.77	-0.62	-0.6	-0.22
6324203	HS1000000343381 TEGT	0.44	0.34	0.54	-0.83	-0.85	-0.61	-0.12
6322830	HS1000000391264 CUL2	0.71	0.37	0.89	0	-0.65	-0.49	-0.38
6309258	HS1000000194858 LIMS1	0.67	1.22	1.03	-0.17	0	-0.19	0.37
6315742	HS1000000577358 APTX	1.05	0.63	1.06	-0.36	-0.16	-0.02	0.34
6302370	HS1000000345222 TFDP2	0.49	0.78	1	0	-0.04	-0.54	-0.23
6305631	HS1000000089173 DBC1	0.26	0.17	0.19	-0.85	-1.14	-0.44	-0.57
6317055	HS1000000241743 SERPINB2	0.49	0.63	1.03	-0.06	-0.21	-0.63	-0.01
6301280	HS1000000372941 YWHAZ	0.97	1.42	1.27	0	0.52	0.3	0.31
6323960	HS1000000630651	0.39	0	0.47	-0.64	-0.62	-0.36	-0.97

	TAIP-2							
6300655	HS1000000232792 NOS2A	0.82	0.49	0.42	-0.27	-0.5	-0.52	-0.12
6312303	HS1000000388355 SPOP	-0.07	-0.27	0.18	-1.04	-1.09	-0.89	-0.85
6322456	HS1000000307195 RELA	1.09	0.99	0.82	0	0.25	-0.16	0.25
6308234	HS1000000401833 TP73L	0.93	0.85	0.92	-0.03	-0.38	0.2	0.3
6311205	HS1000000238137 OPA1	0.27	-0.2	-0.08	-1.03	-0.81	-1.11	-0.55
6316871	HS1000000353704 TP53BP2	-0.01	0.16	0.09	-0.58	-1.06	-0.9	-0.49
6323282	HS1000000148489 HDAC1	0.52	0.43	0.21	-0.73	-0.27	-0.53	-0.26
6306392	HS1000000616230 P53AIP1	0.25	0.32	-0.1	-0.68	-0.37	-0.77	-0.88
6309614	HS1000000420227 ATG12	0.53	0.6	0.26	-0.34	-0.48	-0.51	-0.07
6317327	HS1000000366217 VDAC1	0.88	0.59	0.57	-0.32	-0.36	-0.06	0.21
6315231	HS1000000647381 NALP12	0.41	0.67	0.37	0	-0.45	-0.45	-0.2
6301746	HS1000000119702 EFEMP1	-0.16	-0.31	-0.54	-1.09	-1.39	-1.03	-0.87
6316429	HS1000000617229 CARD15	0.13	-0.02	0.32	-0.82	-0.38	-0.47	-0.72
6300641	HS1000000379223 USP7	0.9	0.63	0.65	0	0	-0.3	0.33
6318691	HS1000000413966 TAX1BP1	0.67	0.63	0.87	0.12	-0.01	0.28	-0.27
6311035	HS1000000013220 ANK3	0.01	-0.3	-0.29	-0.89	-0.92	-0.97	-0.74
6315915	HS1000000243729 PCNA	0.57	0.39	0.51	-0.35	-0.33	0.05	-0.15
6307763	HS1000000006009 ADRA1A	0.98	0.67	0.79	-0.18	0.07	0.22	0.42
6316126	HS1000000065949 CIDEA	-0.37	-0.37	-0.33	-1.03	-0.97	-1.32	-0.79
6323803	HS1000000371496 XRCC5	0.61	0.82	0.46	0	-0.2	0.13	0
6314453	HS1000000092069 DFFB	-0.05	0.13	0.18	-0.85	-0.53	-0.23	-0.61
6322468	HS1000000695796 CGB	0.16	-0.1	-0.09	-0.7	-0.89	-0.35	-0.56
6304096	HS1000000042759 CASP4	0.2	0.3	0.41	-0.03	-0.49	-0.16	-0.33
6310586	HS1000000344882 TFDP1	0.55	0.38	0.39	-0.13	0.09	-0.29	-0.12
6324708	HS1000000695829 CGB	-0.1	-0.15	0.12	-0.43	-0.73	-0.62	-0.56
6322902	HS1000000510976 ACIN1	0	-0.08	0.1	-0.44	-0.36	-0.46	-0.69
6300759	HS1000000185453	-0.05	-0.27	0	-0.81	-0.47	-0.49	-0.63

	KNR1							
6309758	HS1000009806236 CGB5	-0.06	-0.11	-0.17	-0.75	-0.72	-0.46	-0.47
6313703	HS1000000615802 ELMO2	0.34	0.27	0.19	-0.32	-0.27	-0.08	-0.11
6322207	HS1000000259935 38599::CG4618	0.21	0.38	0.31	-0.14	-0.2	-0.25	-0.03
6309822	HS1000000289152 PTPN6	-0.32	-0.16	-0.38	-0.97	-0.68	-0.57	-0.74
6315182	HS1000000384536 DPF3	0.04	0.11	-0.1	-0.27	-0.53	-0.37	-0.52
6311306	HS1000000043001 CASP6	-0.09	0.04	-0.16	-0.44	-0.54	-0.52	-0.43
6305963	HS1000000089209 DBC1	0.63	0.45	0.43	0	0	0.1	0.28
6312476	HS1000000615500 ELMO2	-0.22	-0.19	-0.31	-0.51	-0.78	-0.53	-0.75
6322229	HS1000000356533 TRAF3	0.11	0.11	-0.01	-0.16	-0.33	-0.21	-0.41
6317397	HS1000000615617 ELMO2	-0.03	-0.13	-0.23	-0.47	-0.56	-0.53	-0.32
6320593	HS1000000615821 ELMO2	-0.19	-0.28	-0.17	-0.49	-0.61	-0.51	-0.55
6316253	HS1000000145080 GSTA1	-0.3	-0.44	-0.27	-0.67	-0.56	-0.63	-0.73
6318442	HS1000000532373 BCL2L13	0.06	0.09	0.04	-0.12	-0.35	-0.17	-0.27
6308117	HS1000000615868 ELMO2	-0.38	-0.23	-0.3	-0.56	-0.67	-0.66	-0.47

Supplementary Table 2. Lists of genes in all comparisons categorized by function.

Induction or repression refers to the changes in gene expression in the second treatment relative to the first treatment for each comparison. Underlined is repressed; **Bold** is induced. (Variant) refers to a separate probe for the same gene.

Comparison 1	Comparison 2	Comparison 3	Comparison 4
U vs USTS	U vs WT	USTS vs WTSTS	WT vs WTSTS
All repressed	Induced unless <u>underlined</u>	Induced unless <u>underlined</u>	Repressed unless bold
Caspases			
CASP3	CASP1	CASP1	CASP10
CASP9	CASP10	CASP2	CASP4
	CASP8	CASP9	CASP6
Caspase-3 Substrates			
DCC	DFFA	DCC	DFFB
DFFB	MCL1 (variant)	MCL1 (variant)	MCL1 (variant)
	TAX1BP1		TAX1BP1
Interaction with caspases			
APAF1	APAF1	APAF1	APAF1
BIRC1	BIRC1	BIRC2	NALP1
CARD12	BIRC4	CRADD	NALP12
NALP1	BIRC5	NALP1 (variant)	
NALP12	BIRC7	<u>NALP1 (variant)</u>	
	CARD12	NALP12	
	CRADD		
	NALP1		
Localized or targeted to the mitochondria			
AFG3L2	BAK1	BAX	BAX
BCL2L11	BCL2	BCL2	BCL2L13
BCL2L13	BCL2L11	BCL2L1	OPA1 (variant)
BID	BCL2L13	BCL2L11	OPA1 (variant)
BMF	BFAR	BCL2L2	PRODH
DIABLO	CYCS	BID	VDAC1

DNAJA3	DNAJA3	BNIP3L
GLRX2	MAL	BOK
OPA1	MGST1	CYCS
PRODH	OPA1	DIABLO
	SH3GLB1	DNAJA3
	YME1L1	GLRX2
		HTRA2
		MAL
		MGST1
		MTCH1
		OPA1
		PRODH
		YME1L1

Pro-apoptotic genes

AMID	ACIN1	ACIN1	ACIN1
APOE	APOE	ALOX15B	CD2
APP	APP	AMID	CIDEA
CTNNBL1	AXUD1	APOE	DBC1
DBC1	<u>CIDEA</u>	APP	ELMO2
EDARADD	CTNNBL1	AXUD1	NOS2A
ELMO2	DAXX	BCAP31	RTN4
ELMO3	DUSP22	DAXX	TAIP-2
IAPP	<u>EDARADD</u>	DBC1	TIAL1
IHPK3	ELMO2	DIDO1	TRAF3
PDCD5	ELMO3	<u>DNASE1L3</u>	UNC13B
TRAF6	FAF1	DUSP22	
	GRB10	EDARADD	
	GSTM1	ELMO2	
	MAGI3	ELMO3	
	NCKAP1	FOXO3A	
	NMI	GRB10	
	PDCD2	NCKAP1	
	PROS1	NGFRAP1	
	RBL2	<u>PDCD1</u>	
	RTN4	PDCD4	
	SIAH1	PPP1R15A	
	STAT1	RTN4	
	TAIP-2	SIAH1	
	TIAL1	STAT1	
	TNFRSF11B	TAIP-2	
	TRIP	TIA1	
	ZNF346	TIAL1	

TRAF3
TRAF6
TRIP
ZNF346

p53 and p53 associated genes

ENC1	MDM2	CUL4A	HDAC1
MDM2	PCBP4	ENC1 (variant)	LITAF
P53AIP1	UNC5D	<u>ENC1 (variant)</u>	P53AIP1
PCBP4		LITAF	TP53BP2
PTGES		LRDD	TP73L
TP53BP2		MDM2	USP7
TP53I11		MDM4	
TP73L		NEDD8	
UNC5D		P53AIP1	
		PPP2CA	
		PSEN2	
		PTGES	
		TP53BP2	
		TP73L	

DNA Repair, DNA metabolic process, or Response to DNA damage

APTX	ERCC2	ERCC2	APTX
DNASE1	RAD17	ERCC3	ERCC2
DNASE2	RAD23B	ID1	ERCC3
ERCC2	RAD51	PCNA	PCNA
ID1	SETX	PPP2R1A	RAD23B
PCNA	XRCC4	SETX	XRCC5
PPP2R1A	XRCC5	SIRT1	
RBBP4		XRCC1	
XRCC1		XRCC3	

Induction of Apoptosis by Extracellular Signals

ADORA1	DEDD2	ADORA1	ADORA2A
ADORA2A		ADRA1A	ADRA1A
ADRA1A		CD38	DEDD
CD38			
DAP			
DEDD			
DEDD2			
NDUFA13			

Anti-apoptosis

FAIM	ANGPTL4	ATG12	ATG12
FAIM3	APLP1	CFLAR	CGB
GPX1	ATG12	EDIL3	CGB5
IER3	BAG4	FAIM2	EFEMP1
NOL3	CFLAR	FXR1	GPX1
NPM1	CSE1L	GAS6	GSTA1
PEA15	EDIL3	GSR	MCL1 (variant)
PTPRZ1	FAIM	GSTO1	POR
SGPL1	FAIM3	IER3	RPL13A (variant)
SON	FXR1	MAEA	RPL13A (variant)
SPHK2	GAS6	MCL1 (variant)	SPOP
TNFAIP8	GSTO1	NPM1	TEGT
TPT1	MAEA	PDE1B	YWHAZ
TRAF2	MCL1 (variant)	PEA15	
YWHAH	PEA15	PRLR	
YWHAZ	RPL13A	RPL13A	
	SPHK2	SON	
	SPOP	SPHK2	
	TEGT	TNFAIP3	
	TNFAIP3	TNFRSF12A	
	TNFAIP8	TPT1	
	TNFRSF12A	TRAF2	
	TPT1	TRAF4	
	TRAF4	YWHAZ	
	YWHAH		
	YWHAZ		

Cell Cycle Progression

APPBP1	CDC37	APPBP1	CDC37
CUL1	CUL2	CUL1	CUL2
DDX41	E2F3	CUL3	CUL3
PTPN6	MCM4	DDX41	DDX41
TFDP1	MCM6	ESPL1	DPF3
	MKI67	FOSL2	HDAC3
	PPP2R1B	MCM5	PTPN6
	PTPN6	MCM6	TFDP1
	<u>SPATA4</u>	MTL5	TFDP2
	TFDP2	MYBL2	
	THOC1	PIN1	
		PTPN6	
		TFDP1	
		TFDP2	
		THOC1	

Cell Adhesion, structure, or extracellular matrix

ANK1	ABI2	ABI2	ANK3
ANK3	ANK1	ANK3	CELSR2
EMP1	ANK3	<u>EMP1</u>	LIMS1
EMR1	CELSR1	EMR1	
EMR2	CELSR2	HSPG2	
FBLN5	EMR2	MATN2	
HSPG2	FBLN5	MATN3	
ITGB2	HSPG2	<u>NID2</u>	
MATN3	MATN3		
MATN4			
TUBB			

NF- κ B Pathway

CIAS1	IKBKG	NFKB2	CIAS1
IKBKG	NFKB2	NFKBIA	IKBKG
NFKBIA	NFKBIA	RELA	RELA
RELA	RELA		

Akt Pathway

BECN1	BECN1	TNC
TNC	TNC	

TGF-beta Pathway

LTBP3	LTBP2	LTBP3
LTBP4	SULF1	MYO18A
		SULF1

Ras/Rho/Rac or GTPases

ARHGEF6	ARHGEF6	ARHGEF6
CDC42	CTNNAL1	ELMO1
ELMO1	ELMO1	GRB2
GRB2	GRB2	RHOB
RABEP1	RHOB	SIPA1
RHOB		

p38/JNK Pathway

GADD45G	GADD45A	GADD45A
	JUN	JUN
		JUND

pRB Pathway

	JARID1A	JARID1A RBBP4 RBBP5 RBBP6 SERPINB2	SERPINB2
Complement or Immune Response			
C6	CARD14	C6	CARD15
C8B	CARD15	CARD14	KNG1
C8G	CARD8	CARD8	NOS2A
CIITA	CD14	CIITA	
GULP1	CD2	GULP1	
GZMB	CD97	GZMH	
GZMM	GULP1	LYZ	
LYZ	KNG1	SEMA4D	
NOS2A			
PRF1			
Unknown			
BZRAP1	CLUL1	BCAP29	BZRAP1
DLL4	DNAJB13	CLUL1	NME5
GSTT1	SEMA6A	DLL4	38599::CG4618
PECR	TRIM37	ELMOD2	38597::CG4623 (variant)
SEMA6A	38599::CG4618	HEG1	38597::CG4623 (variant)
SLIT1		MMD2	
TRIM37		NME6	
38599::CG4618		SEMA6A	
		SLIT1	
		TRIM37	
		38597::CG4623	

Gene Functions for Each Comparison

U vs USTS

All genes are repressed

Caspases

CASP3 Effector caspase

CASP9 Initiator caspase that activates caspase-3

Caspase-3 Substrates

DCC deleted in colorectal carcinoma protein; cleaved by caspase-3 & induces apoptosis

DFFB DNA fragmentation factor (DFF) B subunit; triggers both DNA fragmentation and chromatin

condensation during apoptosis

Interaction with caspases

APAF1	upon binding cytochrome c and dATP, this protein forms the apoptosome; binds & activates caspase-9
BIRC1	aka NAIP; homology to two baculovirus inhibitor of apoptosis proteins; suppresses apoptosis induced by various signals
CARD12	In Ced4 family and can induce apoptosis; In <i>C. elegans</i> , binds & activates Ced3, an initiator caspase, via CARD domain.
NALP1	Interacts strongly with caspase 2 and weakly with caspase 9. Overexpression induces apoptosis in cells
NALP12	Implicated in the activation of proinflammatory caspases (e.g., CASP1) via their involvement in inflammasomes

Localized or targeted to the mitochondria

AFG3L2	This gene encodes a protein localized in mitochondria and closely related to paraplegin
BCL2L11	apoptosis facilitator; binds Bcl-2 and is induced by the transcription factor foxO3a
BCL2L13	BCL2-like 13 (apoptosis facilitator); aka Bcl-Rambo; pro-apoptotic; induces cyto c release
BID	heterodimerizes with either agonist BAX or antagonist BCL2; mediates mitochondrial damage induced by caspase-8 (CASP8)
BMF	This protein contains a single BCL2 homology domain 3 (BH3); binds BCL2 proteins and function as an apoptotic activator
DIABLO	Encodes an inhibitor of apoptosis protein (IAP)-binding protein; released from mitochondria
DNAJA3	maintenance of mitochondrial integrity
GLRX2	a mitochondrial oxidoreductase; prosurvival through PI-3-kinase-Akt signaling pathway; involved the activation NF- κ B & Bcl-2
OPA1	A component of the mitochondrial network; a major organizer of the mitochondrial inner membrane; loss causes apoptosis
PRODH	A mitochondrial proline dehydrogenase which catalyzes the first step in proline catabolism; pro-apoptotic

Pro-apoptotic genes

AMID	Significant homology to NADH oxidoreductases and the apoptosis-inducing factor PDCD8/AIF. Overexpression induces apoptosis
APOE	Possibly pro-apoptotic; Apolipoprotein E, essential for the normal catabolism of triglyceride-rich lipoprotein constituents
APP	amyloid beta (A4) precursor protein; pro-apoptotic, but most observations w/ neurons
CTNBL1	unknown function; the C-terminal portion of the protein has been shown to possess apoptosis-inducing activity
DBC1	deleted in bladder cancer 1; possible tumor suppressor functions
EDARADD	a death domain-containing protein that acts as an adaptor to link EDAR to downstream signaling pathways (TNF-receptor associated)
ELMO2	interacts with the dedicator of cyto-kinesis 1 protein; phagocytosis of apoptotic cells
ELMO3	The protein encoded by this gene is similar to a <i>C. elegans</i> protein that functions in phagocytosis of apoptotic cells and in cell migration
IAPP	Islet, or insulinoma, amyloid polypeptide (IAPP, or amylin); may induce apoptotic cell-death in particular cultured cells
IHPK3	This gene encodes a protein that belongs to the inositol phosphokinase (IPK) family; enhances IFN- β apoptotic signals
PDCD5	programmed cell death 5; exact function is not defined, this protein is thought to play an early and universal role in apoptosis
TRAF6	activates NF- κ B, p38, & JNK; binds to active caspase-8 upon TCR stimulation and facilitates its movement into lipid rafts

p53 and p53 associated genes

ENC1	a p53-induced gene
------	--------------------

MDM2	Overexpression of this gene can result in excessive inactivation of tumor protein p53; functions as an E3 ubiquitin ligase
P53AIP1	p53-regulated apoptosis-inducing protein 1; p53AIP1 regulates the mitochondrial apoptotic pathway
PCBP4	This gene is induced by the p53; can suppress cell proliferation by inducing apoptosis and cell cycle arrest in G(2)-M.
PTGES	glutathione-dependent prostaglandin E synthase; induced by p53, and may be involved in TP53 induced apoptosis.
TP53BP2	a member of the ASPP (apoptosis-stimulating protein of p53) family of p53 interacting proteins
TP53I11	induced by p53; proapoptotic
TP73L	aka tumor protein p63; homolog to p53
UNC5D	unc-5 homolog D; amplifies p53-dependent apoptotic response

DNA Repair, DNA metabolic process, or Response to DNA damage

APTX	aprtaxin; may play a role in single-stranded DNA repair
DNASE1	This protein is stored in the zymogen granules of the nuclear envelope and functions by cleaving DNA in an endonucleolytic manner
DNASE2	located in the lysosome, hydrolyzes DNA under acidic conditions & mediates the breakdown of DNA during erythropoiesis & apoptosis
ERCC2	involved in transcription-coupled nucleotide excision repair; defects in gene may lead to cancer
ID1	helix-loop-helix protein; forms heterodimers w/ TFs - can inhibit DNA binding and transc. activation; role in cell growth & differentiation
PCNA	proliferating cell nuclear antigen; ↑ processivity of leading strand synthesis during DNA rep; involved in RAD6-dependent DNA repair
PPP2R1A	protein phosphatase 2 (formerly 2A), regulatory subunit A , alpha isoform; implicated in the negative control of cell growth and division
RBBP4	involved in the homologous recombination and repair of DNA
XRCC1	Involved in repair of DNA single-strand breaks due to ionizing radiation & alkylating agents

Induction of Apoptosis by Extracellular Signals

ADORA1	an adenosine receptor that belongs to the G-protein coupled receptor 1 family; type A1 receptors inhibit adenylyl cyclase
ADORA2A	Extracellular adenosine induces apoptosis by mitochondrial damage & caspase activation via A(2a) adenosine receptors
ADRA1A	Alpha-1-adrenergic receptors (alpha-1-ARs); activate mitogenic responses and regulate growth and proliferation of many cells
CD38	"ADP-ribosylation of CD38 can induce apoptosis in CD38-expressing cells"; functions as an ADP-ribosyl cyclase cADPR hydrolase
DAP	death associated protein; a positive mediator of programmed cell death that is induced by interferon-gamma
DEDD	a scaffold protein for death receptors that directs CASP3 to certain substrates & facilitates their ordered degradation during apoptosis
DEDD2	role in death receptor-induced apoptosis & targets CASP8 & CASP10 to the nucleus; degrades intermediate filaments during apoptosis
NDUFA13	NALP proteins, such as NALP2, are involved in the activation of caspase-1 by Toll-like receptors

Anti-apoptosis

FAIM	Fas apoptotic inhibitory molecule; pro-survival; mediates Fas resistance produced by surface Ig engagement in B cells
FAIM3	Fas apoptotic inhibitory molecule 3; inhibits caspase-8 processing
GPX1	Glutathione peroxidase functions in the detoxification of hydrogen peroxide; protects from CD95-induced apoptosis in breast cancer cells
IER3	protection of cells from Fas- or TNF-alpha-induced apoptosis; involved in ERK survival and ERK activation

NOL3	nucleolar protein 3 (apoptosis repressor with CARD domain); interacts with caspase-2, -8 to inhibit apoptosis
NPM1	nucleolar protein; shuttles to cytoplasm; multiple functions - ribosomal protein assembly & transport, regulation of tumor suppressor ARF
PEA15	a death effector domain (DED)-containing protein; inhibits both TNFRSF6- and TNFRSF1A-mediated CASP8 activity & apoptosis.
PTPRZ1	a member of the receptor type protein tyrosine phosphatase family; induced in gastric cancer cells,
SGPL1	sphingosine-1-phosphate lyase 1; genetic changes affecting intestinal sphingosine-1-phosphate metabolism may correlate with cancer
SON	SON DNA binding protein; may also be involved in protecting cells from apoptosis and in pre-mRNA splicing
SPHK2	sphingosine kinase 2; acts as a second messenger to regulate proliferation and survival
TNFAIP8	tumor necrosis factor, alpha-induced protein 8; inhibits the activated form of caspase-8 (which inhibits BID and casp3)
TPT1	tumor protein, prosurvival, interacts w/ MCL1, others; involved in calcium binding and microtubule stabilization
TRAF2	associates with TRAF1 to interact with IAPs; interacts with TRADD to ensure recruitment of IAPs for direct inhibition of caspases
YWHAH	in 14-3-3 family; 14-3-3 binds to Bad to prevent Bad from translocating to the mitochondria to displace Bcl-xL
YWHAZ	in 14-3-3 family; interacts with IRS1 protein, suggesting a role in regulating insulin sensitivity

Cell Cycle Progression

APBP1	aka NEDD8 activating enzyme E1 subunit 1; required for cell cycle progression through the S/M checkpoint
CUL1	cell cycle arrest; required for G1 to G0 transition or apoptosis pathway
DDX41	DEAD (Asp-Glu-Ala-Asp) box polypeptide 41; putative RNA helicase
PTPN6	protein tyrosine phosphatase (PTP) family; signaling molecule that regulates cell growth, differentiation, mitotic cycle
TFDP1	transcription factor; associates with E2F; controls transcriptional activity of genes involved in cell cycle progression from G1 to S phase

Cell Adhesion, structure, or extracellular matrix

ANK1	key roles in cell motility, activation, proliferation, contact and the maintenance of specialized membrane domains
ANK3	link integral membrane proteins to spectrin-actin cytoskeleton; roles in cell motility, activation, proliferation, & contact
EMP1	adhesion molecule, possibly associates with EGF
EMR1	resembles G protein-coupled hormone receptors (7TM receptors); has six EGF-like modules; possible adhesive properties
EMR2	Cell attachment; TM7 receptor family expressed predominantly by cells of the immune system
FBLN5	promotes adhesion of endothelial cells through interaction of integrins and the RGD motif; may play a role in vascular development
HSPG2	Heparan sulfate proteoglycan; a major component of basement membranes; may stabilize other molecules; involved in cell adhesion
ITGB2	integrin, beta 2; cell adhesion as well as cell-surface mediated signalling; prosurvival
MATN3	thought to be involved in the formation of filamentous networks in the extracellular matrices of various tissues
MATN4	thought to be involved in the formation of filamentous networks in the extracellular matrices of various tissues
TUBB	tubulin; pro-survival

NF-kB Pathway

CIAS1	interacts with apoptosis-associated speck-like protein containing a CARD; may function as an activator of NF-kappaB
IKBKKG	encodes the regulatory subunit of the IKK complex to activates NF-kappaB -- for inflammation, immunity, cell survival, & other pathways
NFKBIA	NF-kappaB activation inhibitor (traps NF-kB in cytoplasm)
RELA	the p65 unit of the NF-kB heterodimer
Akt Pathway	
BECN1	associates with Bcl-2; prosurvival; may be required for autophagy
TNC	tenascin C; TnC-mediated adhesion can promote cell survival through Akt in human chondrosarcoma cells
TGF-beta Pathway	
LTBP3	latent transforming growth factor beta binding protein 3; activates TGF-beta and localizes to the ECM
LTBP4	binding protein 4; activates TGF-beta and localizes to the ECM
Ras/Rho/Rac or GTPases	
ARHGEF6	Rac/Cdc42 guanine nucleotide exchange factor (GEF) 6; activate the Ras-like family of Rho proteins by exchanging bound GDP for GTP
CDC42	a small GTPase of the Rho-subfamily; can regulate actin polymerization through its direct binding to N-WASP to activate Arp2/3 complex
ELMO1	Activates Rac-1, which also occurs in Shigella infection
GRB2	binds the epidermal growth factor receptor; has SH2/SH3 domains; involved in Ras signaling; may promoter tumor growth
RABEP1	RAB GTPase binding effector protein 1; interacts with the GTP form of Rab5; required for membrane docking and fusion of endosomes
RHOB	Ras homolog gene family, member B; tumor suppressor; negative regulator of Ras signaling pathways
p38/JNK Pathway	
GADD45G	↑ with stressful growth arrest conditions & DNA-damaging agents; mediates activation of the p38/JNK pathway via MTK1/MEKK4 kinase
Complement or Immune Response	
C6	C6 is a component of complement cascade; part of the MAC
C8B	C8 beta is one of the three subunits that comprise the component 8 (C8) of the complement, part of MAC
C8G	C8G is one of the three polypeptides that constitute C8
CIITA	located in the nucleus and acts as a positive regulator of MHC II gene transcription; upregulated by IFN-γ; downregulated in tumors
GULP1	adaptor protein required for engulfment of apoptotic cells by phagocytes; clearance of apoptotic cells is critical during inflammation
GZMB	granzyme B; crucial for the rapid induction of target cell apoptosis by CTL in cell-mediated immune response.
GZMM	granzyme M; cleaves DNA damage sensor enzyme poly(ADP-ribose) polymerase to prevent cellular DNA repair and force apoptosis
LYZ	LYZ encodes human lysozyme, whose natural substrate is the bacterial cell wall peptidoglycan ; anti-microbia
NOS2A	nitric oxide synthase 2A (inducible, hepatocytes); antimicrobial and antitumoral activities
PRF1	similar to complement C9; a key effector molecule for T-cell- and natural killer-cell-mediated cytotoxicity
Unknown	
BZRAP1	benzodiazapine receptor (peripheral) associated protein 1; potential role as important molecular adaptors

DLL4	Drosophila delta gene homology; encodes Notch ligands, EGF repeats, and a transmembrane domain
GSTT1	(GST) theta 1 (GSTT1); catalyze the conjugation of reduced glutathione to a variety of electrophilic and hydrophobic compounds
PECR	peroxisomal trans-2-enoyl-CoA reductase
SEMA6A	sema domain, transmembrane domain (TM), and cytoplasmic domain, (semaphorin) 6A
SLIT1	slit homolog 1 (Drosophila)
TRIM37	tripartite motif (TRIM) family; The TRIM motif includes zinc-binding domains, a RING finger region, a B-box motif and a coiled-coil domain
38599::CG4618	Drosophila melanogaster gene CG4618; unknown

U vs WT

Mostly induced unless underlined for repression

Caspases

CASP1	Cleaves & activates interleukin-1, a cytokine involved in the processes such as inflammation, septic shock, and wound healing
CASP10	Cleaves and activates caspases 3 and 7, and the protein itself is processed by caspase 8
CASP8	Involved in the extrinsic pathway; activates caspase-3 and Bid, which leads to mitochondrial permeabilization

Caspase-3 Substrates

DFFA	a subunit of DNA fragmentation factor (DFF); a caspase-3 substrate & triggers DNA fragmentation during apoptosis
MCL1	The alternatively spliced shorter gene product (isoform 2) promotes apoptosis and is death-induced; cleaved by caspase-3
TAX1BP1	Tax1 binding protein 1; inhibits TNF-alpha-induced apoptosis with A20; is cleaved by caspase-3, -6, & -7

Interaction with caspases

APAF1	upon binding cytochrome c and dATP, this protein forms the apoptosome; binds & activates caspase-9
BIRC1	aka NAIP; homology to two baculovirus IAPs; suppresses apoptosis induced by various signals; binds caspase-9
BIRC4	aka XIAP; inhibits apoptosis through binding to TRAF1 and TRAF2; also inhibits caspase-3 and caspase-7.
BIRC5	aka survivin; with hepatitis B X-interacting protein (HBXIP) binds caspase-9; varinat DeltaEx3 bind caspase-3 with Bcl-2
BIRC7	aka Livin; shown to interact with caspase-3, -7, & -9; degrades Smac/DIABLO
CARD12	In Ced4 family and can induce apoptosis; In C. elegans, binds & activates Ced3, an initiator caspase, via CARD domain.
CRADD	recruits caspase 2 to the cell death signal complex that includes TNFR1A, RIP kinase, and other CARD domain-containing proteins
NALP1	Interacts strongly with caspase 2 and weakly with caspase 9. Overexpression induces apoptosis in cells

Localized or targeted to the mitochondria

BAK1	accelerates the opening of VDAC to reduce membrane potential & release cyto c; interacts with p53 after exposure to cell stress
BCL2	an integral outer mitochondrial membrane protein that blocks apoptotic death
BCL2L11	apoptosis facilitator; binds Bcl-2 and is induced by the transcription factor foxO3a
BCL2L13	BCL2-like 13 (apoptosis facilitator); aka Bcl-Rambo; pro-apoptotic; induces cyto c release
BFAR	inhibits Bax-induced cell death; interacts with Bcl-2, Bcl-X(L), & DED-containing procaspases; suppresses Fas-induced apoptosis

CYCS	cytochrome c, a component of the electron transport chain in mitochondria; also involved in initiation of apoptosis
DNAJA3	maintenance of mitochondrial integrity
MAL	a highly hydrophobic integral membrane protein; shown to induce cytochrome c release by interacting with mitochondria
MGST1	catalyzes the conjugation of glutathione to electrophiles; localized to the ER & mitochondria to protect from oxidative stress
OPA1	A component of the mitochondrial network; a major organizer of the mitochondrial inner membrane; loss causes apoptosis
SH3GLB1	aka Bif-1: Bif-1 is an important component of the mitochondrial pathway for apoptosis as a novel Bax/Bak activator
YME1L1	localized in the mitochondria; may play a role in mitochondrial protein metabolism & may be involved in mitochondrial pathologies

Pro-apoptotic genes

ACIN1	not involved in DNA condensation; a role in internucleosomal DNA cleavage during apoptosis; phosphorylation inhibits
APOE	Possibly pro-apoptotic; Apolipoprotein E, essential for the normal catabolism of triglyceride-rich lipoprotein constituents
APP	amyloid beta (A4) precursor protein; pro-apoptotic, but most observations w/ neurons
AXUD1	localizes to the nucleus; induced in response to elevated levels of axin; possible tumor suppressor function
<u>CIDEC</u>	<u>cell death-inducing DFFA-like effector c; a novel family of cell death-inducing DFF45-like effectors (CIDEs); promote apoptosis</u>
CTNBL1	unknown, but the C-terminal portion of the protein has been shown to possess apoptosis-inducing activity
DAXX	may regulate apoptosis; interacts with Fas; in the nucleus, is a potent transcription repressor; associates with centromeres in G2 phase
DUSP22	dual specificity phosphatase 22; A MAPK phosphatase that may be a tumor suppressor
<u>EDARADD</u>	<u>a death domain-containing protein that acts as an adaptor to link EDAR to downstream signaling pathways (TNF-receptor associated)</u>
ELMO2	interacts with the dedicator of cyto-kinesis 1 protein; phagocytosis of apoptotic cells
ELMO3	The protein encoded by this gene is similar to a C. elegans protein that functions in phagocytosis of apoptotic cells and in cell migration
FAF1	Fas associated factor 1; binds to FAS antigen and can initiate apoptosis or enhance apoptosis initiated through FAS antigen
GRB10	a growth factor receptor-binding protein; overexpression inhibits tyrosine kinase activity leading to growth suppression
GSTM1	a glutathione S-transferase; belongs to the mu class; functions in the detoxification of electrophilic compounds, including carcinogens
MAGI3	localize to tight junctions; possibly involved in tumor suppression; HPV E6 proteins target MAGI-3 for degradation
NCKAP1	NCK-associated protein 1 ;Found to induce apoptosis in neuronal cells
NMI	interacts with NMYC and CMYC (two members of the oncogene Myc family), and other TFs, and STATs; may prevent tumor growth
PDCD2	programmed cell death 2; expression repressed by BCL6 as seen in certain cancers
PROS1	a plasma protein; cofactor for activated protein C (for anticoagulation); also stimulates phagocytosis of apoptotic cells
RBL2	retinoblastoma-like 2; possible tumor suppressor functions
RTN4	reticulons; associated with ER; a potent neurite outgrowth inhibitor, may block the regeneration of the CNS
SIAH1	an E3 ligase; involved in ubiquitination and proteasome-mediated degradation of specific proteins; implicated in induction of apoptosis
STAT1	a member of the STAT protein family; induces apoptosis in response to IFN- γ and TNF- α

TAIP-2	cysteine-serine-rich nuclear protein 3; possible positive regulation of apoptosis; positive regulation of transcription
TIAL1	an RNA-binding protein; represses cyto c biosynthesis during stress; induces DNA fragmentation in permeabilized cells
TNFRSF11B	an osteoblast-secreted decoy receptor that functions as a negative regulator of bone resorption; inhibits osteoclastogenesis
TRIP	interacts with TRAF2, inhibits TRAF2-mediated nuclear factor kappa-B, subunit 1 activation required for protection against apoptosis
ZNF346	a nucleolar, zinc finger protein that binds to dsRNA or RNA/DNA hybrids; expression potentially induces apoptosis in murine fibroblast cells

p53 and p53 associated genes

MDM2	Overexpression of this gene can result in excessive inactivation of tumor protein p53; functions as an E3 ubiquitin ligase
PCBP4	This gene is induced by the p53; can suppress cell proliferation by inducing apoptosis and cell cycle arrest in G(2)-M.
UNC5D	unc-5 homolog D; amplifies p53-dependent apoptotic response

DNA Repair, DNA metabolic process, or Response to DNA damage

ERCC2	involved in transcription-coupled nucleotide excision repair; defects in gene may lead to cancer
RAD17	recruits the RAD1-RAD9-HUS1 onto chromatin after DNA damage; phosphorylation promotes the DNA-damage-induced cell cycle G2 arrest
RAD23B	involved in the nucleotide excision repair; possible role in DNA damage recognition in base excision repair
RAD51	in a complex other RAD51 proteins & XRCC2 to catalyze homologous pairing between ss- & dsDNA; a role in recombinational repair of DNA
SETX	contains a DNA/RNA helicase domain & may be involved in both DNA & RNA processing; involved in DNA repair.
XRCC4	with DNA ligase IV & DNA protein kinase, repairs dsDNA breaks by non-homologous end joining & the completion of V(D)J recombination
XRCC5	the DNA-binding component of the DNA-dependent protein kinase & associates with XRCC4 and DNA ligase

Induction of Apoptosis by Extracellular Signals

DEDD2	role in death receptor-induced apoptosis & targets CASP8 & CASP10 to the nucleus; degrades intermediate filaments during apoptosis
-------	--

Anti-apoptosis

ANGPTL4	an angioprotein involved in regulating glucose homeostasis, lipid metabolism, and insulin sensitivity; pro-survival in endothelial cells
APLP1	a membrane-associated glycoprotein that is cleaved by secretases & may act as transcriptional activator; ↑ in tumors
ATG12	involved in autophagy, which is a process of bulk protein degradation through delivery to lysosomes; provides nutrients through recycling
BAG4	associates TNFR1 and death receptor-3 to negatively regulate downstream death signaling
CFLAR	CASP8 and FADD-like apoptosis regulator; aka FLIP; interact with FADD & FLICE; inhibits apoptosis via human death receptors
CSE1L	binds strongly to importin-alpha; highly expressed in tumor cell lines and may play a role in inhibiting TNF-mediated cell death
EDIL3	an integrin ligand; mediates angiogenesis; acts as an angiogenic factor in the context of tumor formation; accelerates tumor growth
FAIM	Fas apoptotic inhibitory molecule; pro-survival; mediates Fas resistance produced by surface Ig engagement in B cells
FAIM3	Fas apoptotic inhibitory molecule 3; inhibits caspase-8 processing
FXR1	an RNA binding protein; interacts with FMR1 and FXR2; associate with polyribosomes; overexpressed in squamous cell carcinomas.
GAS6	a gamma-carboxyglutamic acid (Gla)-containing protein; may stimulate cell proliferation; may

	play a role in thrombosis
GSTO1	GST, omega class; shown to translocate to the nucleus in progression of cancer cells in esophageal adenocarcinoma
MAEA	mediates attachment of erythroblasts to MΦ to promote terminal maturation & enucleation of erythroblasts by suppressing apoptosis
MCL1	The alternatively spliced longer gene product (isoform 1) enhances cell survival by inhibiting apoptosis
PEA15	a death effector domain (DED)-containing protein; inhibits both TNFRSF6- and TNFRSF1A-mediated CASP8 activity & apoptosis.
RPL13A	encodes a ribosomal protein that is a component of the 60S subunit; in the L13P family of ribosomal proteins; located in the cytoplasm
SPHK2	upregulates sphingosine-1-phosphate (SPP), which has diverse biological functions to regulate proliferation and survival
SPOP	recruits DAXX to Cul3 to promote degradation of Daxx
TEGT	a Bax inhibitor; resides in ER; regulates calcium homeostasis
TNFAIP3	aka A20; inhibits TNF-alpha-induced apoptosis by inhibiting caspase-8 cleavage; shown to act with TAX1BP1
TNFAIP8	tumor necrosis factor, alpha-induced protein 8; inhibits the activated form of caspase-8 (which inhibits BID and casp3)
TNFRSF12A	functions, in part, through the NF-κB pathway to up-regulate BCL-XL & BCL-W expression for malignant cell survival
TPT1	tumor protein, prosurvival, interacts w/ MCL1, others; involved in calcium binding and microtubule stabilization
TRAF4	unlike other TRAFs, does not bind TNFR1, TNFR2, Fas or CD40; upregulated in tumors (also unique); may be involved in cell migration
YWHAH	in 14-3-3 family; 14-3-3 binds to Bad to prevent Bad from translocating to the mitochondria to displace Bcl-xL
YWHAZ	in 14-3-3 family; interacts with IRS1 protein, suggesting a role in regulating insulin sensitivity

Cell Cycle Progression

CDC37	a molecular chaperone in cell signal transduction; with Hsp90 associates with IKK (during NF-κB activation) & Akt (prosurvival)
CUL2	a negative regulator of the cell cycle (causes arrest); required for programmed transitions from the G1 to G0 phase or apoptotic pathway
E2F3	E2F transcription factor 3; role in cell cycle control; a target of DNA tumor viruses; binds pRB in a cell-cycle dependent manner; ↑ in cancer
MCM4	member of mini-chromosome maintenance protein complex; phosphorylated by CDC2 kinase to reduce the DNA helicase activity
MCM6	part of MCM complex; with MCM2, 4 and 7 proteins, has DNA helicase activity, and may act as a DNA unwinding enzyme
MKI67	a nuclear protein that is associated with and may be necessary for cellular proliferation; increased in cancer/tumors
PPP2R1B	β isoform of the constant regulatory subunit A of protein phosphatase 2, which negatively controls cell growth; ↑ in tumors/cancers
PTPN6	protein tyrosine phosphatase (PTP) family; signaling molecule that regulates cell growth, differentiation, mitotic cycle
<u>SPATA4</u>	<u>may accelerate S to G2 phase transition in MCF7 cells; may be a testis-specific apoptosis candidate oncogene</u>
TFDP2	E2F dimerization partner 2; modulates the function of E2F in cell cycle regulation and oncogenesis
THOC1	in the transcription/export complex; regulates transcriptional elongation by linking RNA polymerase II with RNA processing factors

Cell Adhesion, structure, or extracellular matrix

ABI2	may control actin polymerization in protrusions; potential regulator of motility; implicated in Rac-dependent cytoskeletal reorganization
------	---

ANK1	key roles in cell motility, activation, proliferation, contact and the maintenance of specialized membrane domains
ANK3	link integral membrane proteins to spectrin-actin cytoskeleton; roles in cell motility, activation, proliferation, & contact
CELSR1	part of the cadherin superfamily; located at the plasma membrane; involved in contact-mediated communication; neural-specific
CELSR2	part of the cadherin superfamily; located at the plasma membrane; involved in contact-mediated communication
EMR2	Cell attachment; TM7 receptor family expressed predominantly by cells of the immune system
FBLN5	promotes adhesion of endothelial cells through interaction of integrins and the RGD motif; may play a role in vascular development
HSPG2	Heparan sulfate proteoglycan; a major component of basement membranes; may stabilize other molecules; involved in cell adhesion
MATN3	thought to be involved in the formation of filamentous networks in the extracellular matrices of various tissues
NF-κB Pathway	
IKBKG	encodes the regulatory subunit of the IKK complex to activates NF-kappaB -- for inflammation, immunity, cell survival, & other pathways
NFKB2	nuclear factor of kappa light polypeptide gene enhancer in B-cells 2 (p49/p100)
NFKBIA	NF-kappaB activation inhibitor (traps NF- κ B in cytoplasm)
RELA	the p65 unit of the NF- κ B heterodimers
Akt Pathway	
BECN1	associates with Bcl-2; prosurvival; may be required for autophagy
TNC	tenascin C; TnC-mediated adhesion can promote cell survival through Akt in human chondrosarcoma cells
TGF-beta Pathway	
LTBP2	TGF-beta binding protein; a member of the TGF-beta latent complex; a structural component of microfibrils; and a role in cell adhesion
SULF1	a heparan sulfate 6-O-endosulfatase; a TGF-beta1-responsive gene both; possibly a negative regulator of TGF-beta1-induced fibrogenesis
Ras/Rho/Rac or GTPases	
ARHGEF6	Rac/Cdc42 guanine nucleotide exchange factor (GEF) 6; activate the Ras-like family of Rho proteins by exchanging bound GDP for GTP
CTNNAL1	may modulate Rho pathway signaling in vivo by providing a scaffold for the Lbc Rho guanine nucleotide exchange factor
ELMO1	Activates Rac-1, which also occurs in Shigella infection
GRB2	binds the epidermal growth factor receptor; has SH2/SH3 domains; involved in Ras signaling; may promoter tumor growth
RHOB	Ras homolog gene family, member B; tumor suppressor; negative regulator of Ras signaling pathways
p38/JNK Pathway	
GADD45A	↑ with DNA damage; mediates activation of the p38/JNK pathway via MTK1/MEKK4 kinase; interacts with PCNA to prevent cell growth
JUN	c-jun; oncogene; interacts directly DNA sequences to regulate gene expression (transcriptional activation); overexpressed in cancers
pRB Pathway	
JARID1A	aka RBBP2; binds with pRB for tumor suppressive functions; may interact w/ rhombotin-2
Complement or Immune Response	
CARD14	belongs to MAGUK & CARD families; when expressed in cells activated NF- κ B & induced the phosphorylation of Bcl10
CARD15	aka NOD2; involved in immune response to intracellular bacterial LPS by recognizing the muramyl dipeptide (MDP) & activates NFKB

CARD8	acts as an adaptor molecule that inhibit NFκB activation, & activate CASP1-dependent IL1B secretion and apoptosis; in the inflammasome
CD14	a surface protein expressed on monocytes/macrophages; binds LPS (triggers inflammation) & apoptotic cells (for phagocytosis)
CD2	expressed on T & NK cells; binds with CD58 on epithelial cells, leading to IL-8 synthesis and TNFα release
CD97	a receptor on surface of activated leukocytes involved in cell adhesion & signaling processes early after leukocyte activation; ↑ in tumors
GULP1	adaptor protein required for engulfment of apoptotic cells by phagocytes; clearance of apoptotic cells is critical during inflammation
KNG1	plays role in assembly of the plasma kallikrein; anti-adhesive properties in vitronectin-dependent adhesion, which leads to apoptosis
Unknown	
CLUL1	clusterin-like 1 (retinal); unknown
DNAJB13	belongs to the evolutionarily conserved DNAJ/HSP40 family of proteins; unknown (may inhibit human testis spermatogenesis apoptosis)
SEMA6A	sema domain, transmembrane domain (TM), and cytoplasmic domain, (semaphorin) 6A
TRIM37	tripartite motif (TRIM) family; The TRIM motif includes zinc-binding domains, a RING finger region, a B-box motif and a coiled-coil domain
38599::CG4618	Drosophila melanogaster gene CG4618; unknown

USTS vs WTSTS

Mostly induced unless underlined for repression

Caspases

CASP1	Cleaves & activates interleukin-1, a cytokine involved in the processes such as inflammation, septic shock, and wound healing
CASP2	permeabilizes mitochondria; activation occurs in a complex that contains PIDD, whose expression is induced by p53
CASP9	Initiator caspase that activates caspase-3

Caspase-3 Substrates

DCC	deleted in colorectal carcinoma protein; cleaved by caspase-3 & induces apoptosis
MCL1	The alternatively spliced shorter gene product (isoform 2) promotes apoptosis and is death-induced; cleaved by caspase-3

Interaction with caspases

APAF1	upon binding cytochrome c and dATP, this protein forms the apoptosome; binds & activates caspase-9
BIRC2	aka cIAP1; inhibits apoptosis by binding to TRAF1 & TRAF2; binds but does not inhibit caspases; degrades Smac/DIABLO
CRADD	recruits caspase 2 to the cell death signal complex that includes TNFR1A, RIP kinase, and other CARD domain-containing proteins
NALP1	Interacts strongly with caspase 2 and weakly with caspase 9. Overexpression induces apoptosis in cells
<u>NALP1</u>	<u>Interacts strongly with caspase 2 and weakly with caspase 9. Overexpression induces apoptosis in cells</u>
NALP12	Implicated in the activation of proinflammatory caspases (e.g., CASP1) via their involvement inflammasomes

Localized or targeted to the mitochondria

BAX	interacts with, & ↑ the opening of, VDAC, which leads to the loss in membrane potential & release of cytochrome c; regulated by p53
BCL2	an integral outer mitochondrial membrane protein that blocks apoptotic death

BCL2L1	aka Bcl-xL; located at the outer mitochondrial membrane; regulates VDAC opening; anti-apoptotic
BCL2L11	apoptosis facilitator; binds Bcl-2 and is induced by the transcription factor foxO3a
BCL2L2	localized to the outer mitochondrial membrane; inhibits Bad, Bax, and Bik; expression induced by Akt
BID	heterodimerizes with either agonist BAX or antagonist BCL2; mediates mitochondrial damage induced by caspase-8 (CASP8)
BNIP3L	targeted to the mitochondria for cyto c release; interacts with Bcl-2 & Bcl-xL (both prosurvival); adenoviral protein E1B inhibits
BOK	localizes to the mitochondria & induces cytochrome c release upon DNA damage & subsequent p53 induction
CYCS	cytochrome c, a component of the electron transport chain in mitochondria; also involved in initiation of apoptosis
DIABLO	Encodes an inhibitor of apoptosis protein (IAP)-binding protein; released from mitochondria
DNAJA3	maintenance of mitochondrial integrity
GLRX2	a mitochondrial oxidoreductase; prosurvival through PI-3-kinase-Akt signaling pathway; involved in activation NF- κ B & Bcl-2
HTRA2	localized to mitochondrial inner membrane; inhibits XIAP when released with cyto c; also localizes to ER & nucleus
MAL	a highly hydrophobic integral membrane protein; shown to induce cytochrome c release by interacting with mitochondria
MGST1	catalyzes the conjugation of glutathione to electrophiles; localized to the ER & mitochondria to protect from oxidative stress
MTCH1	has two proapoptotic isoforms, both of which are imported into the mitochondrial OM ; induces cytochrome c release
OPA1	A component of the mitochondrial network; a major organizer of the mitochondrial inner membrane; loss causes apoptosis
PRODH	A mitochondrial proline dehydrogenase which catalyzes the first step in proline catabolism; pro-apoptotic
YME1L1	localized in the mitochondria; may play a role in mitochondrial protein metabolism & may be involved in mitochondrial pathologies

Pro-apoptotic genes

ACIN1	not involved in DNA condensation; a role in internucleosomal DNA cleavage during apoptosis; phosphorylation inhibits
ALOX15B	a lipoygenase; decreased in cancer/tumors;
AMID	significant homology to NADH oxidoreductases and the apoptosis-inducing factor PDCD8/AIF. Overexpression induces apoptosis
APOE	Possibly pro-apoptotic; Apolipoprotein E, essential for the normal catabolism of triglyceride-rich lipoprotein constituents
APP	amyloid beta (A4) precursor protein; pro-apoptotic, but most observations w/ neurons
AXUD1	localizes to the nucleus; induced in response to elevated levels of axin; possible tumor suppressor function
BCAP31	a transmembrane protein of the ER; cleaved by casp8, inducing mitochondrial fission through ER calcium signals, enhancing cyto c release
DAXX	may regulate apoptosis; interacts with Fas; in the nucleus, is a potent transcription repressor; associates with centromeres in G2 phase
DBC1	deleted in bladder cancer 1; possible tumor suppressor functions
DIDO1	a cytoplasmic protein that translocates to the nucleus upon apoptotic signal activation (in mice); upregulated by apoptotic signals
<u>DNASE1L3</u>	<u>hydrolyzes DNA, is not inhibited by actin, and mediates the breakdown of DNA during apoptosis</u>
DUSP22	dual specificity phosphatase 22; A MAPK phosphatase that may be tumor suppressors
EDARADD	a death domain-containing protein that acts as an adaptor to link EDAR to downstream signaling pathways (TNF-receptor associated)

ELMO2	interacts with the dedicator of cyto-kinesis 1 protein; phagocytosis of apoptotic cells
ELMO3	The protein encoded by this gene is similar to a <i>C. elegans</i> protein that functions in phagocytosis of apoptotic cells and in cell migration
FOXO3A	in the forkhead family of TFs; inhibited by Akt; when activated, translocates to the nucleus & induces cell death genes (e.g. Fas ligand)
GRB10	a growth factor receptor-binding protein; overexpression inhibits tyrosine kinase activity leading to growth suppression
NCKAP1	NCK-associated protein 1 ;Found to induce apoptosis in neuronal cells
NGFRAP1	mediates apoptosis in response to nerve growth factor by interacting with the death domain of neurotrophin receptor p75NTR
<u>PDCD1</u>	<u>in Ig superfamily; induced in the thymus when anti-CD3 Abs are injected & large numbers of thymocytes undergo apoptosis (in mice)</u>
PDCD4	localized to the nucleus in proliferating cells; expression modulated by cytokines in NK and T cells; possible tumor suppressor
PPP1R15A	GADD34; increased following stressful growth arrest conditions & treatment w/ DNA-damaging agents; response is correlated w/ apoptosis
RTN4	reticulons; associated with ER; a potent neurite outgrowth inhibitor, may block the regeneration of the CNS
SIAH1	an E3 ligase; involved in ubiquitination and proteasome-mediated degradation of specific proteins; implicated in induction of apoptosis
STAT1	a member of the STAT protein family; induces apoptosis in response to IFN- γ and TNF- α
TAIP-2	cysteine-serine-rich nuclear protein 3; possible positive regulation of apoptosis; positive regulation of transcription
TIA1	possesses nucleolytic activity against CTL cells; possibly pro- apoptotic as it induces DNA fragmentation in CTL targets
TIAL1	an RNA-binding protein; represses cyto c biosynthesis during stress; induces DNA fragmentation in permeabilized cells
TRAF3	component of the LT β R signaling complex, which inhibits NF- κ B activation & induces cell death; target of EBV LMP1 protein
TRAF6	activates NF- κ B, p38, & JNK; binds to active caspase-8 upon TCR stimulation and facilitates its movement into lipid rafts
TRIP	interacts with TRAF2, inhibits TRAF2-mediated nuclear factor kappa-B, subunit 1 activation required for protection against apoptosis
ZNF346	a nucleolar, zinc finger protein that binds to dsRNA or RNA/DNA hybrids; expression potently induces apoptosis in murine fibroblast cells

p53 and p53 associated genes

CUL4A	functions as an E3 ligase & with MDM2, contributes to p53 degradation; assists in nucleotide excision repair in a complex with DDB
ENC1	a p53-induced gene; encodes an actin binding protein
<u>ENC1</u>	<u>a p53-induced gene; encodes an actin binding protein</u>
LITAF	LPS-induced TNF α factor = a DNA-binding protein & can mediate TNF α expression by direct binding to TNF α promoter; induced by p53
LRDD	interacts FADD & MADD; may function as an adaptor protein in cell death-related signaling processes; a p53 effector (induces apoptosis)
MDM2	Overexpression of this gene can result in excessive inactivation of tumor protein p53; functions as an E3 ubiquitin ligase
MDM4	contains a RING finger domain & a putative nuclear localization signal; interacts with p53 (stabilizes to counteract MDM2)
NEDD8	similar to ubiquitin; conjugated to p53 via MDM2, thereby inhibiting the transcriptional activity of p53
P53AIP1	p53-regulated apoptosis-inducing protein 1; p53AIP1 regulates the mitochondrial apoptotic pathway
PPP2CA	the phosphatase 2A catalytic subunit; inhibits cell growth & activates p53 & p21 (p53-responsive); overexpression leads to G2/M arrest

PSEN2	presenilin 2; triggers apoptosis via p53, which also down-regulates the anti-apoptotic presenilin 1
PTGES	glutathione-dependent prostaglandin E synthase; induced by p53, and may be involved in TP53 induced apoptosis.
TP53BP2	a member of the ASPP (apoptosis-stimulating protein of p53) family of p53 interacting proteins
TP73L	aka tumor protein p63; homolog to p53

DNA Repair, DNA metabolic process, or Response to DNA damage

ERCC2	involved in transcription-coupled nucleotide excision repair; defects in gene may lead to cancer
ERCC3	ATP-dependent DNA helicase; functions in nucleotide excision repair; also is the 89 kDa subunit of TF2 to function in class II transcription
ID1	helix-loop-helix protein; forms heterodimers w/ TFs - can inhibit DNA binding and transc. activation; role in cell growth & differentiation
PCNA	proliferating cell nuclear antigen; ↑ processivity of leading strand synthesis during DNA rep; involved in RAD6-dependent DNA repair
PPP2R1A	protein phosphatase 2 (formerly 2A), regulatory subunit A , alpha isoform; implicated in the negative control of cell growth and division
SETX	contains a DNA/RNA helicase domain & may be involved in both DNA & RNA processing; involved in DNA repair.
SIRT1	sirtuin protein; repair of DNA breaks; deacetylates the DNA repair factor Ku70, which sequesters Bax away from mitochondria; inhibits p53
XRCC1	Involved in repair of DNA single-strand breaks due to ionizing radiation & alkylating agents
XRCC3	RecA/Rad51-related protein family; participates in homologous recombination to maintain chromosome stability & repair DNA damage

Induction of Apoptosis by Extracellular Signals

ADORA1	an adenosine receptor that belongs to the G-protein coupled receptor 1 family; type A1 receptors inhibit adenylyl cyclase
ADRA1A	Alpha-1-adrenergic receptors (alpha-1-ARs); activate mitogenic responses and regulate growth and proliferation of many cells
CD38	"ADP-ribosylation of CD38 can induce apoptosis in CD38-expressing cells"; functions as an ADP-ribosyl cyclase cADPR hydrolase

Anti-apoptosis

ATG12	involved in autophagy, which is a process of bulk protein degradation through delivery to lysosomes; provides nutrients through recycling
CFLAR	CASP8 and FADD-like apoptosis regulator; aka FLIP; interact with FADD & FLICE; inhibits apoptosis via human death receptors
EDIL3	an integrin ligand; mediates angiogenesis; acts as an angiogenic factor in the context of tumor formation; accelerates tumor growth
FAIM2	inhibits fas-induced apoptosis; may interact with proteins of Bcl-2 family
FXR1	an RNA binding protein; interacts with FMR1 and FXR2; associate with polyribosomes; overexpressed in squamous cell carcinomas.
GAS6	a gamma-carboxyglutamic acid (Gla)-containing protein; may stimulate cell proliferation; may play a role in thrombosis
GSR	Malignant lung tumors (squamous cell carcinoma and adenocarcinoma) had increased activity of this enzyme
GSTO1	GST, omega class; shown to translocate to the nucleus in progression of cancer cells in esophageal adenocarcinoma
IER3	protection of cells from Fas- or TNF-alpha-induced apoptosis; involved in ERK survival and ERK activation
MAEA	mediates attachment of erythroblasts to MΦ to promote terminal maturation & enucleation of erythroblasts by suppressing apoptosis
MCL1	The alternatively spliced longer gene product (isoform 1) enhances cell survival by inhibiting apoptosis
NPM1	nucleolar protein; shuttles to cytoplasm; multiple functions - ribosomal protein assembly & transport, regulation of tumor suppressor ARF

PDE1B	possibly pro-survival - inhibition induced apoptosis; PDE1B2 plays a role in differentiated macrophages by regulating cGMP levels
PEA15	a death effector domain (DED)-containing protein; inhibits both TNFRSF6- and TNFRSF1A-mediated CASP8 activity & apoptosis.
PRLR	prolactin receptor; induced in cancer/tumors; prolactin is a growth factor that stimulates Jak2, Stat5, & Erk1/2
RPL13A	encodes a ribosomal protein that is a component of the 60S subunit; in the L13P family of ribosomal proteins; located in the cytoplasm
SON	SON DNA binding protein; may also be involved in protecting cells from apoptosis and in pre-mRNA splicing
SPHK2	sphingosine kinase 2; acts as a second messenger to regulate proliferation and survival
TNFAIP3	aka A20; inhibits TNF-alpha-induced apoptosis by inhibiting caspase-8 cleavage; shown to act with TAX1BP1
TNFRSF12A	activates NFκB signaling pathway & this upregulates BCL-XL and BCL-W expression in malignant glioblastoma cells
TPT1	tumor protein, prosurvival, interacts w/ MCL1, others; involved in calcium binding and microtubule stabilization
TRAF2	associates with TRAF1 to interact with IAPs; interacts with TRADD to ensure recruitment of IAPs for direct inhibition of caspases
TRAF4	unlike other TRAFs, does not bind TNFR1, TNFR2, Fas or CD40; upregulated in tumors (also unique); may be involved in cell migration
YWHAZ	in 14-3-3 family; interacts with IRS1 protein, suggesting a role in regulating insulin sensitivity

Cell Cycle Progression

APBP1	aka NEDD8 activating enzyme E1 subunit 1; required for cell cycle progression through the S/M checkpoint
CUL1	cell cycle arrest; required for G1 to G0 transition or apoptosis pathway
CUL3	component of a ubiquitin E3 ligase that is essential for mitotic division; ubiquitinates DAXX with SPOP (the adaptor protein)
DDX41	DEAD (Asp-Glu-Ala-Asp) box polypeptide 41; putative RNA helicase
ESPL1	separase; separates sister chromatids by cleaving cohesin Rad21 during the metaphase-to-anaphase transition; may be an oncogene
FOSL2	encode leucine zipper proteins that can dimerize with proteins of the JUN family, thereby forming the TF complex AP-1; ↑ in tumors
MCM5	MCM family of chromatin-binding proteins; ↑ G0 to G1/S phase transition of the cell cycle; interacts with Stat1 for trans. activation
MCM6	part of MCM complex; with MCM2, 4 and 7 proteins, has DNA helicase activity, and may act as a DNA unwinding enzyme
MTL5	metallothionein-like protein; may play a role in regulation of cell growth & differentiation; may be important for meiosis of germ cells
MYBL2	a TF involved in cell cycle progression; activates cell division cycle 2, cyclin D1, and insulin-like growth factor-binding protein 5 genes
PIN1	encodes an essential nuclear peptidylprolyl cis-trans isomerase involved in regulation of mitosis; depletion induces apoptosis
PTPN6	protein tyrosine phosphatase (PTP) family; signaling molecule that regulates cell growth, differentiation, mitotic cycle
TFDP1	transcription factor; associates with E2F; controls transcriptional activity of genes involved in cell cycle progression from G1 to S phase
TFDP2	E2F dimerization partner 2; modulates the function of E2F in cell cycle regulation and oncogenesis
THOC1	in the transcription/export complex; regulates transcriptional elongation by linking RNA polymerase II with RNA processing factors

Cell Adhesion, structure, or extracellular matrix

ABI2	may control actin polymerization in protrusions; potential regulator of motility; implicated in Rac-dependent cytoskeletal reorganization
------	---

ANK3	link integral membrane proteins to spectrin-actin cytoskeleton; roles in cell motility, activation, proliferation, & contact
<u>EMP1</u>	<u>adhesion molecule, possibly associates with EGF</u>
EMR1	resembles G protein-coupled hormone receptors (7TM receptors); has six EGF-like modules; possible adhesive properties
HSPG2	Heparan sulfate proteoglycan; a major component of basement membranes; may stabilize other molecules; involved in cell adhesion
MATN2	in family involved in the formation of filamentous networks in the ECM of tissues; binds collagen I, fibrillin-2, but unknown function
MATN3	thought to be involved in the formation of filamentous networks in the extracellular matrices of various tissues
<u>NID2</u>	<u>found to be ubiquitous component of basement membrane zones underneath developing epithelia of most of the major organ systems</u>
NF-κB Pathway	
NFKB2	nuclear factor of kappa light polypeptide gene enhancer in B-cells 2 (p49/p100)
NFKBIA	NF-kappaB activation inhibitor (traps NF- κ B in cytoplasm)
RELA	the p65 unit of the NF- κ B heterodimer
Akt Pathway	
TNC	tenascin C; TnC-mediated adhesion can promote cell survival through Akt in human chondrosarcoma cells
TGF-beta Pathway	
LTBP3	latent transforming growth factor beta binding protein 3; activates TGF-beta and localizes to the ECM
MYO18A	aka TIAF1; induced by TGF β ; inhibits the cytotoxic effects of TNF α & overexpressed TNF receptor adaptors TRADD, FADD, and RIP
SULF1	a heparan sulfate 6-O-endosulfatase; a TGF-beta1-responsive gene both; possibly a negative regulator of TGF-beta1-induced fibrogenesis
Ras/Rho/Rac or GTPases	
ARHGEF6	Rac/Cdc42 guanine nucleotide exchange factor (GEF) 6; activate the Ras-like family of Rho proteins by exchanging bound GDP for GTP
ELMO1	Activates Rac-1, which also occurs in Shigella infection
GRB2	binds the epidermal growth factor receptor; has SH2/SH3 domains; involved in Ras signaling; may promoter tumor growth
RHOB	Ras homolog gene family, member B; tumor suppressor; negative regulator of Ras signaling pathways
SIPA1	a mitogen induced GTPase activating protein (GAP) with activity for Ras-related regulatory proteins Rap1 and Rap2
p38/JNK Pathway	
GADD45A	↑ with DNA damage; mediates activation of the p38/JNK pathway via MTK1/MEKK4 kinase; interacts with PCNA to prevent cell growth
JUN	c-jun; oncogene; interacts directly DNA sequences to regulate gene expression (transcriptional activation); overexpressed in cancers
JUND	member of the JUN family; a component of the AP1 TF complex; proposed to protect cells from p53-dependent senescence & apoptosis
pRB Pathway	
JARID1A	aka RBBP2; binds with pRB for tumor suppressive functions; may interact with rhombotin-2
RBBP4	involved in chromatin remodeling & transcriptional repression associated with histone deacetylation; binds directly to pRB
RBBP5	a ubiquitously expressed nuclear protein; binds pRB, which regulates cell proliferation
RBBP6	binds to underphosphorylated but not phosphorylated pRB; also binds p53; blocks suppression of adenoviral E1A protein
SERPINB2	SerpinB2 is a cell survival factor that modulates pRb repression of proapoptotic signal

transduction

Complement or Immune Response

C6	C6 is a component of complement cascade; part of the MAC
CARD14	belongs to MAGUK & CARD families; when expressed in cells activated NF- κ B & induced the phosphorylation of Bcl10
CARD8	acts as an adaptor molecule that inhibit NFKB activation, & activate CASP1-dependent IL1B secretion and apoptosis; in the inflammasome
CIITA	located in the nucleus and acts as a positive regulator of MHC II gene transcription; upregulated by IFN- γ ; downregulated in tumors
GULP1	adaptor protein required for engulfment of apoptotic cells by phagocytes; clearance of apoptotic cells is critical during inflammation
GZMH	expressed in NK cells; directly cleaves ICAD (for DNA fragmentation) & Bid (cyto c release) in target cells; important for pathogen clearance
LYZ	LYZ encodes human lysozyme, whose natural substrate is the bacterial cell wall peptidoglycan ; anti-microbia
SEMA4D	modifies CD40-CD40L B-cell signaling by augmenting B-cell aggregation and survival and down-regulating CD23 expression

Unknown

BCAP29	B-cell receptor-associated protein 29; unknown
CLUL1	clusterin-like 1 (retinal); unknown
DLL4	Drosophila delta gene homology; encodes Notch ligands, EGF repeats, and a transmembrane domain
ELMOD2	ELMO/CED-12 domain containing 2; unknown
HEG1	HEG homolog 1 (zebrafish); unknown
NME6	non-metastatic cells 6, protein expressed in (nucleoside-diphosphate kinase); unknown
SEMA6A	sema domain, transmembrane domain (TM), and cytoplasmic domain, (semaphorin) 6A
SLIT1	slit homolog 1 (Drosophila)
TRIM37	tripartite motif (TRIM) family; The TRIM motif includes zinc-binding domains, a RING finger region, a B-box motif and a coiled-coil domain
38597::CG4623	Dmel\CG4623; unknown

WT vs WTSTS

Mostly repressed unless **bold** for induction**Caspases**

CASP10	Cleaves and activates caspases 3 and 7, and the protein itself is processed by caspase 8
CASP4	cleaves & activates its own precursor protein, as well as caspase 1 precursor; can interact with TRAF6, triggered by LPS
CASP6	processed by caspase-7, -8, & -10; cleaves laminin A; regulated by p53

Caspase-3 Substrates

DFFB	DNA fragmentation factor (DFF) B subunit; triggers both DNA fragmentation and chromatin condensation during apoptosis
MCL1	The alternatively spliced shorter gene product (isoform 2) promotes apoptosis and is death-induced; cleaved by caspase-3
TAX1BP1	Tax1 binding protein 1; inhibits TNF-alpha-induced apoptosis with A20; is cleaved by caspase-3, -6, & -7

Interaction with caspases

APAF1	upon binding cytochrome c and dATP, this protein forms the apoptosome; binds & activates caspase-9
-------	--

NALP1	Interacts strongly with caspase 2 and weakly with caspase 9. Overexpression induces apoptosis in cells
NALP12	Implicated in the activation of proinflammatory caspases (e.g., CASP1) via their involvement in inflammasomes

Localized or targeted to the mitochondria

BAX	interacts with, & ↑ the opening of, VDAC, which leads to the loss in membrane potential & release of cytochrome c; regulated by p53
BCL2L13	BCL2-like 13 (apoptosis facilitator); aka Bcl-Rambo; pro-apoptotic; induces cyto c release
OPA1	A component of the mitochondrial network; a major organizer of the mitochondrial inner membrane; loss causes apoptosis
OPA1	A component of the mitochondrial network; a major organizer of the mitochondrial inner membrane; loss causes apoptosis
PRODH	A mitochondrial proline dehydrogenase which catalyzes the first step in proline catabolism; pro-apoptotic
VDAC1	a major mitochondrial outer-membrane transporter; role in energy production by controlling metabolite traffic

Pro-apoptotic genes

ACIN1	not involved in DNA condensation; a role in internucleosomal DNA cleavage during apoptosis; phosphorylation inhibits
CD2	Ligation of MHC-I together with CD2 augmented growth inhibition and enhanced the level of apoptosis
CIDEA	shown to activate apoptosis (mice); inhibited by the DNA fragmentation factor DFF45 but not by caspase inhibitors
DBC1	deleted in bladder cancer 1; possible tumor suppressor functions
ELMO2	interacts with the dedicator of cyto-kinesis 1 protein; phagocytosis of apoptotic cells
NOS2A	nitric oxide synthase 2A (inducible, hepatocytes); antimicrobial and antitumoral activities
RTN4	reticulons; associated with ER; a potent neurite outgrowth inhibitor, may block the regeneration of the CNS
TAIP-2	cysteine-serine-rich nuclear protein 3; possible positive regulation of apoptosis; positive regulation of transcription
TIAL1	an RNA-binding protein; represses cyto c biosynthesis during stress; induces DNA fragmentation in permeabilized cells
TRAF3	component of the LTβR signaling complex, which inhibits NF-κB activation & induces cell death; target of EBV LMP1 protein
UNC13B	expressed in the kidney; is upregulated by hyperglycemia, which increases the levels of diacylglycerol (induces apoptosis)

p53 and p53 associated genes

HDAC1	histone deacetylase 1; component of the histone deacetylase complex; it deacetylates/inactivates p53
LITAF	LPS-induced TNFα factor = a DNA-binding protein & can mediate TNFα expression by direct binding to TNFα promoter; induced by p53
P53AIP1	p53-regulated apoptosis-inducing protein 1; p53AIP1 regulates the mitochondrial apoptotic pathway
TP53BP2	a member of the ASPP (apoptosis-stimulating protein of p53) family of p53 interacting proteins
TP73L	aka tumor protein p63; homolog to p53
USP7	role in transcriptional regulation, DNA replication, & apoptosis; deubiquitinates p53 for p53 stabilization

DNA Repair, DNA metabolic process, or Response to DNA damage

APTX	apratxin; may play a role in single-stranded DNA repair
ERCC2	involved in transcription-coupled nucleotide excision repair; defects in gene may lead to cancer
ERCC3	ATP-dependent DNA helicase; functions in nucleotide excision repair; also is the 89 kDa subunit of TF2 to function in class II transcription

PCNA	proliferating cell nuclear antigen; ↑ processivity of leading strand synthesis during DNA rep; involved in RAD6-dependent DNA repair
RAD23B	involved in the nucleotide excision repair; possible role in DNA damage recognition in base excision repair
XRCC5	the DNA-binding component of the DNA-dependent protein kinase & associates with XRCC4 and DNA ligase

Induction of Apoptosis by Extracellular Signals

ADORA2A	Extracellular adenosine induces apoptosis by mitochondrial damage & caspase activation via A(2a) adenosine receptors
ADRA1A	Alpha-1-adrenergic receptors (alpha-1-ARs); activate mitogenic responses and regulate growth and proliferation of many cells
DEDD	a scaffold protein for death receptors that directs CASP3 to certain substrates & facilitates their ordered degradation during apoptosis

Anti-apoptosis

ATG12	involved in autophagy, which is a process of bulk protein degradation through delivery to lysosomes; provides nutrients through recycling
CGB	chorionic gonadotropin, beta polypeptide; may act as a tumor-stimulating growth factor
CGB5	chorionic gonadotropin, beta polypeptide 5; expressed in tumors/cancers
EFEMP1	EGF-containing fibulin-like extracellular matrix protein 1; upregulation is associated with pancreatic adenocarcinoma
GPX1	Glutathione peroxidase functions in the detoxification of hydrogen peroxide; protects from CD95-induced apoptosis in breast cancer cells
GSTA1	encodes a glutathione S-transferase in the alpha class.; metabolizes bilirubin; protects cells from ROS & the products of peroxidation
MCL1	The alternatively spliced longer gene product (isoform 1) enhances cell survival by inhibiting apoptosis
POR	an ER membrane oxidoreductase; binds FAD and FMN, to allow it to donate electrons directly from NADPH to P450 enzymes
RPL13A	encodes a ribosomal protein that is a component of the 60S subunit; in the L13P family of ribosomal proteins; located in the cytoplasm
RPL13A	encodes a ribosomal protein that is a component of the 60S subunit; in the L13P family of ribosomal proteins; located in the cytoplasm
SPOP	recruits DAXX to Cul3 to promote degradation of Daxx
TEGT	a Bax inhibitor; resides in ER; regulates calcium homeostasis
YWHAZ	in 14-3-3 family; interacts with IRS1 protein, suggesting a role in regulating insulin sensitivity

Cell Cycle Progression

CDC37	a molecular chaperone in cell signal transduction; with Hsp90 associates with IKK (during NF-κB activation) & Akt (prosurvival)
CUL2	a negative regulator of the cell cycle (causes arrest); required for programmed transitions from the G1 to G0 phase or apoptotic pathway
CUL3	component of a ubiquitin E3 ligase that is essential for mitotic division; ubiquitinates DAXX with SPOP (the adaptor protein)
DDX41	DEAD (Asp-Glu-Ala-Asp) box polypeptide 41; putative RNA helicase
DPF3	a tissue-specific anchor between histone acetylations as well as methylations and chromatin remodeling
HDAC3	has histone deacetylase activity & represses transcription; can also down-regulate p53 function
PTPN6	protein tyrosine phosphatase (PTP) family; signaling molecule that regulates cell growth, differentiation, mitotic cycle
TFDP1	transcription factor; associates with E2F; controls transcriptional activity of genes involved in cell cycle progression from G1 to S phase
TFDP2	E2F dimerization partner 2; modulates the function of E2F in cell cycle regulation and oncogenesis

Cell Adhesion, structure, or extracellular matrix

ANK3 link integral membrane proteins to spectrin-actin cytoskeleton; roles in cell motility, activation, proliferation, & contact

CELSR2 **part of the cadherin superfamily; located at the plasma membrane; involved in contact-mediated communication; unknown**

LIMS1 involved in integrin signaling; found in focal adhesion plaques; may play a role in integrin-mediated cell adhesion or spreading

NF-κB Pathway

CIAS1 interacts with apoptosis-associated speck-like protein containing a CARD; may function as an activator of NF-κappaB

IKBKKG **encodes the regulatory subunit of the IKK complex to activate NF-kappaB -- for inflammation, immunity, cell survival, & other pathways**

RELA the p65 unit of the NF-κB heterodimers

pRB Pathway

SERPINB2 SerpinB2 is a cell survival factor that modulates pRb repression of proapoptotic signal transduction

Complement or Immune Response

CARD15 aka NOD2; involved in immune response to intracellular bacterial LPS by recognizing the muramyl dipeptide (MDP) & activates NFκB

KNG1 plays role in assembly of the plasma kallikrein; anti-adhesive properties in vitronectin-dependent adhesion, which leads to apoptosis

NOS2A nitric oxide synthase 2A (inducible, hepatocytes); antimicrobial and antitumoral activities

Unknown

BZRAP1 benzodiazapine receptor (peripheral) associated protein 1; potential role as important molecular adaptors

NME5 non-metastatic cells 5, protein expressed in (nucleoside-diphosphate kinase); unknown

38599::CG4618 Drosophila melanogaster gene CG4618; unknown

38597::CG4623 Dmel\CG4623; unknown

38597::CG4623 Dmel\CG4623; unknown

Chapter Four

Spa15 of Shigella flexneri is Secreted Through the Type-III Secretion System and Prevents Staurosporine-Induced Apoptosis.

Manuscript submitted as: Faherty, C.S. and Maurelli, A.T. Spa15 of *Shigella flexneri* is secreted through the type-III secretion system and prevents staurosporine-induced apoptosis. *Infection and Immunity*. 2009.

Abstract

Shigella flexneri is a gram negative, facultative intracellular pathogen that invades the colonic epithelium and causes bacillary dysentery. We previously demonstrated that *S. flexneri* inhibits staurosporine-induced apoptosis in infected epithelial cells and that a $\Delta mxiE$ mutant is unable to inhibit apoptosis. Therefore, we hypothesized that a MxiE-regulated gene was responsible for protection of epithelial cells from apoptosis. Analysis of all MxiE-regulated genes yielded no mutants that lacked the ability to prevent apoptosis. Spa15, which is defined as a type-III secretion system chaperone, was analyzed since it associates with MxiE. A $\Delta spa15$ mutant was unable to prevent staurosporine-induced apoptosis. C-terminal hemagglutinin-tagged *spa15* was secreted by *S. flexneri* within two hours in the Congo red secretion assay, and secretion was dependent on the type-III secretion system. Spa15 was also secreted by *Shigella* in infected epithelial cells as verified by immunofluorescence analysis. Spa15 secretion was decreased in the $\Delta mxiE$ mutant, which demonstrates why this mutant is unable to prevent

staurosporine-induced apoptosis. Our data are the first to show that Spa15 is secreted in a type-III secretion system-dependent fashion, and the absence of Spa15 in the $\Delta spa15$ mutant results in the loss of protection from staurosporine-induced apoptosis in epithelial cells. Thus, Spa15 contributes to the intracellular survival of *Shigella* by blocking apoptosis in the infected host cell.

Introduction

Shigella flexneri is a gram-negative, facultative intracellular pathogen that causes bacillary dysentery. Clinical symptoms of disease include watery diarrhea, severe abdominal pain, and bloody stools (38). Disease is a result of the ability of the pathogen to invade the colonic epithelium. Once *S. flexneri* enters the colon, the bacteria transit through M cells and encounter resident macrophages. The bacteria escape the macrophages by inducing cell death, and subsequently invade epithelial cells at the basolateral face (18). Proinflammatory signaling and a subsequent efflux of polymorphonuclear cells (PMNs) into the infected tissue allow the bacteria to invade more epithelial cells at the basolateral pole while the PMNs contribute to the disease severity by causing local tissue destruction (18). Once inside the cytoplasm of the host cell, *S. flexneri* induces actin polymerization which allows the bacteria to move to adjacent cells without the need to enter the extracellular environment (5). The epithelial cells provide the bacteria with an intracellular niche to multiply and spread to adjacent cells.

S. flexneri virulence requires a 220-kb virulence plasmid that encodes a type-III secretion system (T3SS), the Ipa proteins essential for entry into the host cells, and other

effector proteins. The T3SS is comprised of a needle complex that has a seven-ringed basal body and a protruding needle. The needle complex delivers proteins directly to the host cell from the bacterial cytoplasm (13). Temperature regulation of the genes on the virulence plasmid allows the needle complex to be synthesized and assembled at 37°C. The secretion of proteins is induced upon contact of the bacteria with the host cell. The Ipa proteins mediate entry of the bacteria into the epithelial cell through localized actin depolymerization and membrane engulfment. After engulfment, the bacteria are inside a vacuole that is subsequently lysed, allowing the bacteria to enter the cytoplasm of the host cell (38). Once inside the cytoplasm, the bacteria spread and secrete additional effector proteins. These proteins are encoded by genes that are scattered throughout the 220-kb virulence plasmid and are subsequently secreted through the T3SS for post-invasion virulence (6).

We previously showed that *S. flexneri* inhibits staurosporine (STS)-induced apoptosis in epithelial cells by preventing the activation of caspase-3, a key protein in apoptotic cell death, and that a $\Delta mxiE$ mutant is unable to prevent STS-induced apoptosis (7). MxiE is a transcriptional activator that induces the expression of approximately 20 bacterial genes when the bacteria are inside the cytosol of the host cell. The subsequent protein products are secreted through the T3SS (21, 24). We therefore hypothesized that a MxiE-regulated gene is responsible for protection. In this study, we analyzed all of the MxiE-regulated genes and found that none were required to inhibit STS-induced apoptosis. We also analyzed a $\Delta spa15$ mutant since Spa15 associates with MxiE (34). This report describes the inability of a $\Delta spa15$ mutant to prevent STS-induced apoptosis and demonstrates, for the first time, that Spa15 is secreted through the T3SS. Spa15 was

originally described as a T3SS chaperone and a co-anti-activator to MxiE (33, 34). We are proposing a new, third function in which Spa15 is involved in apoptosis inhibition in epithelial cells since Spa15 is secreted by the T3SS and the $\Delta spa15$ mutant is unable to prevent apoptosis in epithelial cells.

Materials and Methods

Bacterial strains and growth conditions.

The strains of *S. flexneri* used are listed in Table 8. Bacteria were routinely cultured at 37°C either in Luria-Bertani broth (LB) with aeration or on tryptic soy broth (TSB) plates with 1.5% agar and 0.025% Congo red (Sigma). Antibiotics were used at the following concentrations: kanamycin, 50 µg/ml; streptomycin, 50 µg/ml; chloramphenicol, 5 µg/ml; and ampicillin, 100 µg/ml.

Strain and plasmid construction.

BS902 was constructed using the λ red linear recombination method as previously described (7). PCR was used to amplify a kanamycin resistance cassette gene (*kan*) from pKD4 (Table 8) with 5' and 3' overhangs identical to the 5' and 3' regions of *spa15* internal to the start and stop codons (Table 9). Kanamycin resistant recombinants were purified and screened via PCR using primers (Table 9) that annealed approximately 70 base pairs upstream and downstream of the *spa15* coding region to detect the size difference due to the insertion of the kanamycin cassette. Next, this mutant was used as the donor strain for transduction of 2457T using P1L4, and selection for kanamycin resistance.

Table 8. Strains and plasmids used in this study.

Strain/Plasmid	Description	Source/Reference
<i>S. flexneri</i> strains		
2457T	Wild-type serotype 2a	12
BS611	2457T/ $\Delta mxiE2::aphA-3$	21
BS613	BS611/ pRRS13 ($P_{lac}mxiE^+$)	21
BS652	2457T/ $\Delta spa47::aadA$	Lab stock
BS766	2457T transformed with pKM208	7
BS902	2457T/ $\Delta spa15::aphA-3$	This study
BS904	BS902 transformed with pBSKS-spa15	This study
BS905	2457T transformed with pSpa15-2HA	This study
BS906	BS611 transformed with pSpa15-2HA	This study
BS907	BS613 transformed with pSpa15-2HA	This study
BS908	BS652 transformed with pSpa15-2HA	This study
BS909	2457T transformed with pMxiE-2HA	This study
BS914	BS902 transformed with pSpa15-2HA	This study
<i>E. coli</i> strains		
DH5 α	<i>endA1 hsdR17 supE44 thi-1 recA1 gyrA96 relA1</i> ($\Delta lacIZYA-argF$) U169 <i>deoR</i> ($\Phi 80 \Delta lac \Delta [lacZ]$ <i>M15</i>)	16

Plasmids

pKD4	oriR6K, <i>bla</i> , <i>aphA-3</i>	9
pKM208	Temperature-sensitive <i>red</i> -, <i>gam</i> -, <i>lacI</i> -expressing plasmid driven by P_{Tac} promoter, <i>bla</i>	9
pBSKS(-)	pBluescript cloning vector, <i>bla</i>	Stratagene
pBSKS-spa15	<i>spa15</i> cloned into pBSKS	This study
pDZ1	Cloning intermediate for 2HA fusions, <i>cat</i>	44
pSpa15-2HA	<i>spa15</i> cloned into pDZ1, <i>cat</i>	This study
pMxiE-2HA	<i>mxiE</i> cloned into pDZ1, <i>cat</i>	This study

Table 9. Primers used in this study.

Purpose	Forward Primer		Reverse Primer	
	Name	Sequence	Name	Sequence
Amplify	S15kanF	5' – AGTAACAT	S15kanR	5' – TAAGACCC
<i>aphA-3</i>		TAATTTAGTTC		CATTTAAGATTT
cassette for		AATTAGTTAGA		CCATCCTCTGAT
<i>spa15</i>		GATAGTCTTTT		AAAACATCATGC
deletion		CACGATTGGTG		AGAATCTCATA
		TGTAGGCTGGA		TGAATACCTCCT
		GCTGCTTC – 3'		TAG – 3'
Confirm	Spa15F2	5' – GTTATATCT	Spa15R2	5' – CCAATCGA
$\Delta spa15$		ATGCTGAGATT		AACATCGCTAA
deletion		G – 3'		G – 3'
Cloning of	spaF	5' – GATC <u>GGTA</u>	spaR2	5' – GATC <u>GGAT</u>
<i>spa15</i> into		<u>CC</u> ATGAGTAAC		<u>CC</u> ATTATAAGA
pBSKS		ATTAATTTAGT		CCCCATTTAAG
		TC – 3'		ATTTC – 3'
Sequence	pBSKF	5' – AGCGGATA	pBSKR	5' – GTTTTCCC
<i>spa15</i> in		ACAATTTCACA		AGTCACGACGT
pBSKS		CAGGAAAC – 3'		TG – 3'

Cloning of <i>spa15</i> into pDZ1	spaF	5' – GATC <u>GGTA</u> <u>CCATGAGTAAC</u> ATTAATTTAGT TC – 3'	spaR	5' – GATC <u>AGAT</u> <u>CTTAAGACCCC</u> ATTTAAGATTTC – 3'
Cloning of <i>mxiE</i> into pDZ1	mxiE2HAF	5' – CTAG <u>GGTA</u> <u>CCATGGAAGGG</u> TTTTTTTTTGTGTC CG – 3'	mxiE2HAR	5' – AGATC <u>GG</u> <u>ATCCAATTTTTT</u> CATTTATTTTTT TCAC – 3'
Sequence <i>spa15</i> and <i>mxiE</i> in pDZ1	pDZ1F	5' – CTGGGTTG AAGGCTCTCAA G – 3'	pDZ1R	5' – TCAGCCCCA TACGATATAAG – 3'

The restriction enzyme sites are underlined.

Additional primers listed in Table 9 were used to construct the pBSKS-*spa15*, pSpa15-2HA, and pMxiE-2HA plasmids. *spa15* was amplified by colony PCR using Platinum Taq DNA polymerase high fidelity (Invitrogen) and cloned into pGEM-T (Promega) according to the manufacturers' protocols. Subsequently, *spa15* was subcloned into pBSKS (Stratagene) via the Acc65I and BamHI restriction enzyme sites using T4 DNA ligase (New England Biolabs). The ligation reaction was transformed into *E. coli* DH5α for production of the new plasmid, pBSKS-*spa15*. The *spa15* insert sequence was verified with primers that anneal outside the multiple cloning site (MCS) of

the vector. pBSKS-*spa15* was subsequently transformed into BS902 to generate BS904. To create C-terminal HA tags of *spa15* and *mxiE*, vector pDZ1 was used. pDZ1 contains two hemagglutinin (HA) epitopes and is a low-copy vector with a pACYC184 origin of replication (44). *spa15* and *mxiE* were amplified by colony PCR as mentioned above, cloned into pGEM-T, and subcloned into pDZ1 using *Acc65I* and *BglIII* for *spa15*, and *Acc65I* and *BamHI* for *mxiE*. The ligation reactions were transformed into *E. coli* DH5 α for production of the new plasmids pSpa15-2HA and pMxiE-2HA. The inserts were sequenced using primers that anneal outside the MCS of pDZ1. The plasmids were transformed into the various strains listed in Table 1 and selected on medium with the appropriate antibiotic.

Virulence assays.

The invasion, plaque, and apoptosis assays were performed as previously described (7, 17, 31). Briefly for the apoptosis assay, bacterial cultures were grown to mid-log phase, washed in 1X phosphate buffered saline (PBS), resuspended in 1X Dulbecco's modified Eagle's medium (DMEM), and applied to a semi-confluent monolayer of HeLa cells. The plates were centrifuged at 3,000 rpm for 10 min at 37°C to facilitate the invasion process by allowing the bacteria to make contact with the HeLa cells. The plates were incubated at 37°C with 5% CO₂ for 30 min. The cells were then washed with 1X PBS, DMEM plus 50 μ g/ml gentamicin was added, and the plates were incubated for 3 hours at 37°C with 5% CO₂. Cells were then washed again, and DMEM plus 50 μ g/ml gentamicin and 4 μ M STS (Calbiochem) was added for an additional 3 hours. After the assay, the cells were processed for immunofluorescence or Western blot analysis.

Congo red secretion assay.

The Congo red secretion assay was used to identify the proteins secreted by the bacteria through the T3SS, and was performed as previously described (4). Briefly, bacteria were grown to mid-log phase, resuspended in 1X PBS, and Congo red (CR) was added to a final concentration of 30 µg/ml. The bacteria were incubated at 37°C for 30 minutes for secretion of early T3SS proteins, or at one hour intervals for secretion of late T3SS effector proteins (40). After incubation, the bacteria were pelleted by centrifugation, the supernatant was collected and filtered through a 0.22 µm filter, and stored at -20°C. The proteins in the supernatant represent the secreted proteins and were concentrated by trichloroacetic acid (TCA) precipitation. TCA pellets were resuspended in 50 µl sodium dodecyl sulfate (SDS) loading buffer for protein analysis and stored at -20°C. The bacterial pellets, representing the nonsecreted proteins, were resuspended in 500 µl of SDS loading buffer and stored at -20°C.

Immunofluorescence and Western blot analysis.

The same procedures were followed for immunofluorescence or Western blot analysis as previously described (7). For the immunofluorescence analysis, infected HeLa monolayers were fixed with 1X PBS with 3% formaldehyde (36% stock; Sigma) and 0.2% glutaraldehyde (25% stock; Sigma). To visualize nuclei, 5 mg/ml of 4,6-diamido-2-phenylindole (DAPI; Molecular Probes) was diluted 1:1,000 in 1X PBS. To detect activated caspase-3, a rabbit anti-human cleaved caspase-3 antibody (Cell Signaling Technologies) was used with a secondary goat-anti-rabbit immunoglobulin G (IgG) antibody conjugated to Alexa 488 (Invitrogen). To measure secretion of the hemagglutinin (HA)-tagged Spa15, infected cells were stained with a mouse monoclonal

anti-HA antibody (Covance) followed by a goat anti-mouse IgG antibody conjugated to Alexa 488 (Invitrogen). After the staining procedure, antifade reagent (Molecular Probes) was applied to all samples, which were then overlaid with coverslips and stored at 4°C in the dark.

For Western blot analyses, each sample was resolved by SDS-polyacrylamide gel electrophoresis (PAGE), and Coomassie blue staining verified equal loading of total protein for all samples. Caspase-3 was detected with rabbit anti-human caspase-3 or cleaved caspase-3 antibodies (Cell Signaling Technology) followed by a donkey anti-rabbit IgG antibody conjugated to horseradish peroxidase (Amersham Biosciences). The HA-tagged Spa15 was detected using a mouse monoclonal anti-HA antibody in a 1:1,000 dilution with a sheep anti-mouse IgG antibody conjugated to horseradish peroxidase (Amersham Biosciences). IpaB and IpaC were detected with mouse monoclonal anti-IpaB (1:20,000 dilution) and anti-IpaC (1:5,000 dilution) antibodies as previously described (30). The same secondary antibodies were used as with the anti-HA antibody. Western blots were developed using the Visualizer developing system (Upstate Cell Signaling Solutions) according to the protocol provided, and the blots were imaged using a Fuji Intelligent Dark Box with Fujinon lens and Image Reader LAS-3000 software (Fuji) on the chemiluminescence setting in increment mode at 10-second intervals. Densitometry comparisons were made using the Image Gauge V4.22 software provided.

Statistical analysis.

The densitometry results for the caspase-3 Western blot were analyzed using Tukey's analysis of variance (ANOVA) post hoc test on the SPSS program, version 12.0.1 for Windows. For the strain comparison in the Congo red secretion assay, the

ratios of Spa15 secretion in wildtype bacteria (strain BS905) to the $\Delta mxiE$ mutant (strain BS906) and to the *mxiE* complemented strain (strain BS907) were compared. A repeated measures ANOVA was performed using Tukey's post-hoc analysis for all time-points on the SPSS program version 12.0.1 for Windows. Ratios were analyzed on a log scale to comply with the assumptions of ANOVA, and the summaries are reported as geometric mean ratios relative to BS905, averaging across three repetitions.

Results

Identifying spa15 as the anti-apoptosis gene.

We constructed deletion mutants in most of the MxiE-regulated genes or utilized a strain of *E. coli* expressing the *Shigella* entry region (SER), which contains all of the genes necessary for epithelial cell invasion (26). We did not find any MxiE-regulated genes that were responsible for apoptosis protection (Table 10). All of the mutants and the *E. coli* strain prevented STS-induced apoptosis (data not shown). Therefore, we hypothesized that the protective gene/protein is either *mxiE* itself or a protein that associates with MxiE, namely IpgC, OspD1, or Spa15. IpgC is a co-activator needed for the induction of MxiE-regulated genes while OspD1 and Spa15 have been described as anti-activators of MxiE (34, 35). A $\Delta ipgC$ mutant was not invasive and was not further pursued. OspD1 was eliminated as a candidate since the *E. coli* strain carrying the SER blocks apoptosis and *ospD1* is not located within the SER (6). The *spa15* gene was a likely candidate since it is located within the SER and encodes a T3SS chaperone that has the ability to bind to several T3SS effector proteins (6, 33). Therefore, we constructed BS902, a $\Delta spa15$ mutant of wildtype *S. flexneri* strain 2457T. The mutant showed a

slightly (10%) reduced entry efficiency, similar to published data on a $\Delta spa15$ mutant constructed in *S. flexneri* strain M90T (33). In addition, the mutant produced plaque sizes about half the size as wildtype bacteria in the plaque assay (data not shown).

Table 10. *Shigella* genes analyzed that had no effect on apoptosis protection.

MxiE-regulated genes		Genes in which the products associate with Spa15	
<u>Deletion mutants</u>	<u>Via <i>E. coli</i> strain¹</u>	<u>Deletion mutants</u>	<u>Via <i>E. coli</i> strain¹</u>
<i>ospB</i> ²	<i>ipaH_1</i>	<i>ipaA</i>	<i>ospC2</i>
<i>ospC1</i>	<i>ipaH_2</i>	<i>ipgB1</i>	<i>ospC3</i>
<i>ospD3</i>	<i>ipaH_5</i>	<i>ospB</i>	<i>ospD1</i>
<i>ospE1</i>	<i>ipaH_7</i>		<i>ipgB2</i>
<i>ospE2</i>			
<i>ospF</i>			
<i>ospG</i>			
<i>virA</i>			
<i>ospE1</i> and <i>ospE2</i> ³			
<i>ospC1</i> , <i>ospB</i> , and <i>ospF</i> ⁴			
<i>ipaH1.4</i>			
<i>ipaH2.5</i>			
<i>ipaH4.5</i>			
<i>ipaH7.8</i>			
<i>ipaH9.8</i>			
<i>ipaH_4</i>			

¹ = The *E. coli* strain expresses the *Shigella* entry region and invades epithelial cells (see text).

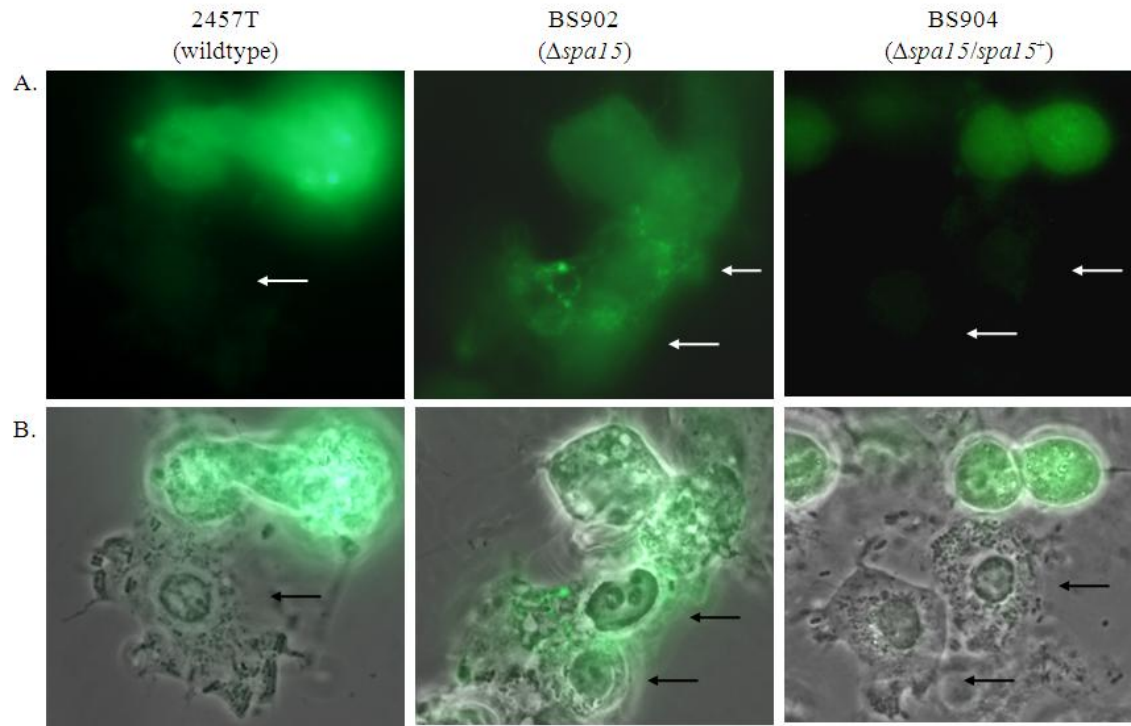
² = Gene product also associates with Spa15.

³ = Double mutant analyzed.

⁴ = Triple mutant analyzed.

BS902 was next analyzed in the apoptosis assay and was found to be unable to prevent STS-induced apoptosis as confirmed by immunofluorescence analysis for activated caspase-3 (Fig. 16). Interestingly, the mutant also appeared to induce apoptosis in infected cells and closely neighboring uninfected cells even without STS present. DAPI staining of the nuclei of these cells showed classic signs of apoptosis with shape distortion, DNA fragmentation, and/or chromatin condensation (Fig. 17). Complementation of the $\Delta spa15$ mutant (BS904) restored protection in the apoptosis assay (Fig. 16). The inability of BS902 to prevent STS-induced apoptosis was verified in a Western blot analysis for caspase-3 activation (Fig. 18A). Densitometry analysis revealed there was a significant increase in caspase-3 activation in BS902-infected monolayers treated with STS compared to both 2457T-infected and BS904-infected monolayers treated with STS (Fig. 18B). In addition, the Western blot demonstrates that BS902-infected cells were apoptotic even in the absence of STS as evidenced by the presence of the 17 kD band (lane 5). Lanes of uninfected cells, wildtype-infected cells (2457T), or cells infected with the *spa15* complemented strain (BS904) did not have bands at 17 kD when STS was absent (Lanes 1, 3, and 7). In lanes 4 and 8, infected cells treated with STS have some caspase-3 activation since 90% of the monolayer is infected and the remaining 10% of cells in the monolayer are uninfected and sensitive to STS. This level of activation is expected and similar to what was seen in Figure 16 in which the uninfected cells in the population have a positive signal for caspase-3.

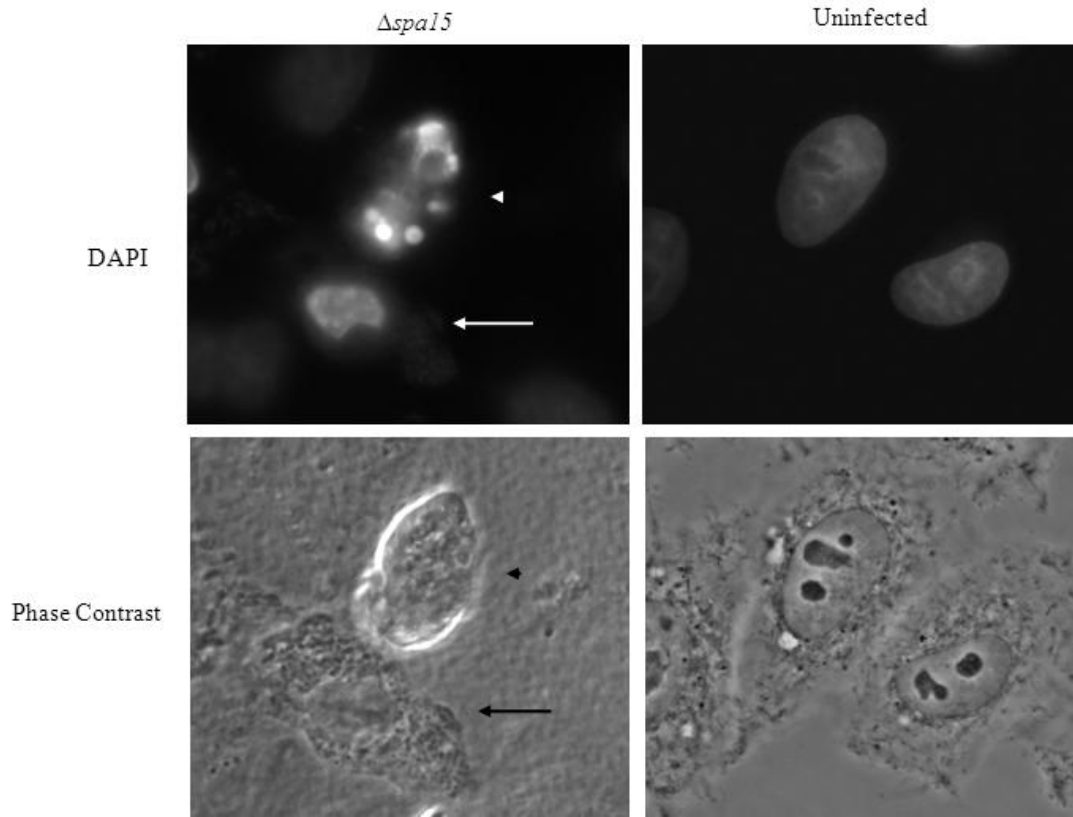
Figure 16. The $\Delta spa15$ mutant cannot prevent caspase-3 activation in HeLa monolayers treated with staurosporine.



A. Activated caspase-3 (green) immunofluorescence of monolayers infected with 2457T (left), BS902 (center), and BS904 (right). Activated caspase-3 is not present in cells infected with 2457T or BS904, but is present in uninfected cells and cells infected with BS902. Arrows point to infected cells. All images were taken with a 100 \times objective.

B. Merged image of the immunofluorescence images from panel A and phase contrast view to visualize the bacteria inside the cells. Images are representative of three repeated experiments. All images were taken with a 100 \times objective.

Figure 17. BS902-infected cells are apoptotic upon normal infection.



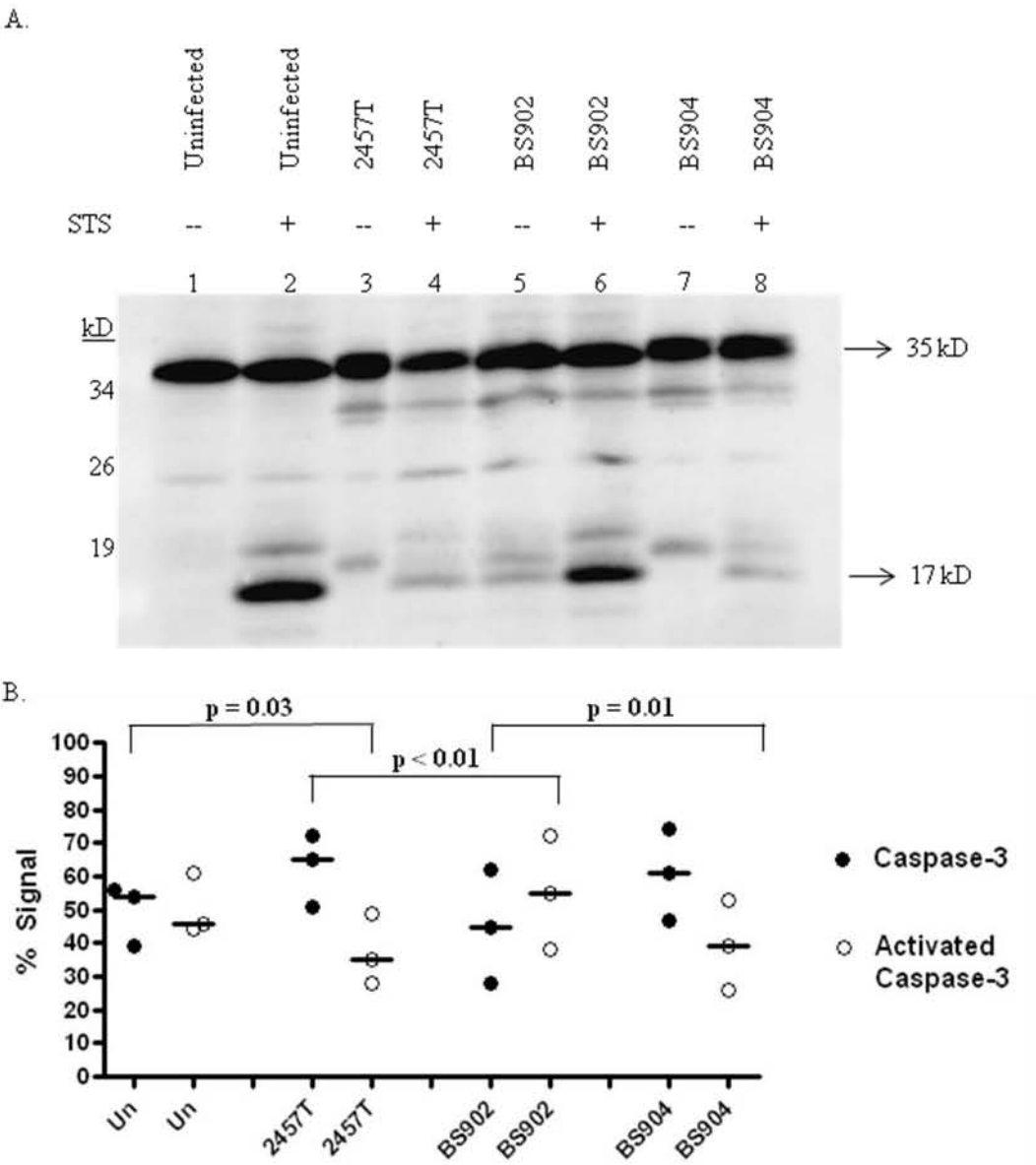
HeLa monolayers were infected with the $\Delta spa15$ mutant (BS902) without STS for 6 hours. Top: DAPI staining reveals altered nuclear shape, chromatin condensation, and DNA fragmentation of the nuclei in infected cells (arrow) and in closely neighboring uninfected cells (arrow head). On the other hand, uninfected nuclei have a normal, round shape and visible nucleoli. Bottom images are the phase contrast views to visualize the bacteria inside the cells. Images are representative of three repeated experiments. All images were taken with a 100 \times objective.

Figure 18. Western blot analysis for caspase-3 activation.

A. Whole-cell lysates were separated by SDS-PAGE and analyzed by immunoblotting with antibodies to recognize the full-length, inactive form of caspase-3 (35 kD) and the large fragment (17 kD) resulting from cleavage during activation. There are some extra bands at approximately 33 and 18 kD in lanes containing bacterial strains. These bands are *Shigella* proteins that cross-react with the anti-caspase-3 antibodies in the Western blot. Adsorption of the antibody significantly reduced the intensity of the bands, but was not able to remove them completely (data not shown).

B. Densitometry analysis of the caspase-3 Western blot with the percent (%) total caspase-3 signal represented on the y-axis. The graph is the scatter plot of the amount of inactive caspase at 35 kD (closed circles) compared to the amount of activated caspase-3 (open circles) at 17 kD for each treatment of three repeated experiments. The line represents the median value for each protein in each treatment. P-values were determined using Tukey's analysis of variance post hoc test with normalization of the data to the mean of the gels. "Un" represents uninfected HeLa cells while infected monolayers are represented by the strain number used in the treatment groups. All groups were treated with STS.

Figure 18. Western blot analysis for caspase-3 activation.



Finally, we constructed mutations in *ipaA* and *ipgB1* since the gene products are known to associate with Spa15 and are secreted into epithelial cells (32, 33, 41). The mutants had reduced invasion efficiencies as previously described (32, 41). We found that neither *ipaA* nor *ipgB1* were required for apoptosis inhibition since both of the mutants protected in the apoptosis assay (data not shown). The four other proteins that associate with Spa15 were ruled out as candidate protective proteins since the genes encoding these proteins are not present in the *E. coli* strain expressing the SER (Table 10). Therefore, the $\Delta spa15$ mutant was the only strain besides the $\Delta mxiE$ mutant that was unable to protect HeLa cells in the apoptosis assay.

Spa15 is secreted into the cytoplasm of the host cell.

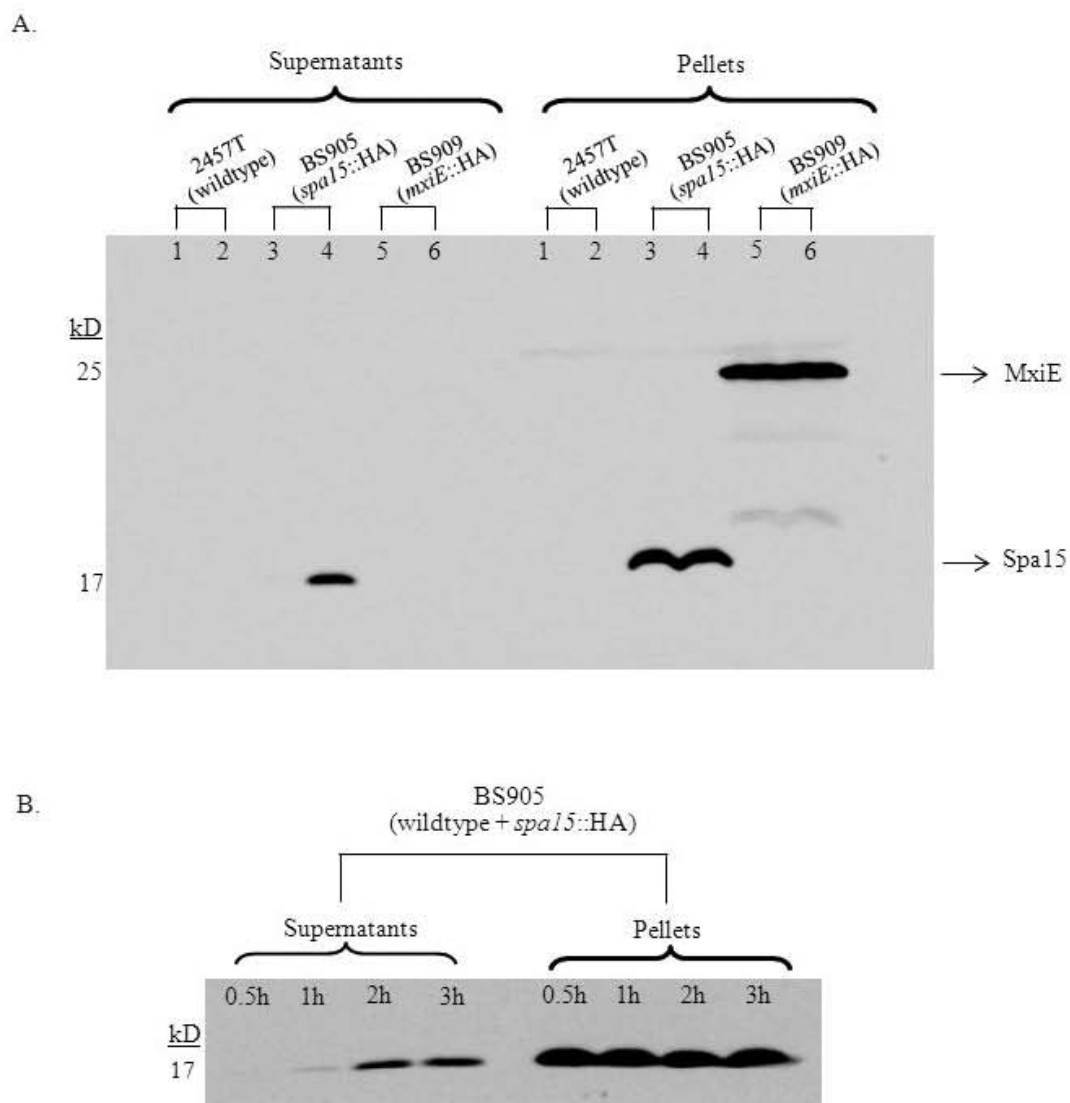
We reasoned that in order to inhibit apoptosis, the bacterial proteins need to be secreted into the cytoplasm of the epithelial cell. Therefore, we constructed C-terminal hemagglutinin (HA) tags of *spa15* and *mxiE*, and looked for secretion of these proteins in the Congo red (CR) secretion assay. After construction the sequences were verified, and the plasmids encoding the tagged *spa15* and *mxiE* were transformed into 2457T producing strains BS905 and BS909, respectively. The CR assay was performed at time points of 30 minutes and 2.5 hours to determine if protein secretion could be seen within the first 30 minutes like the Ipa proteins or if secretion required longer incubation times. Using an antibody against the HA tag, we found that MxiE was not secreted at either 30 minutes or 2.5 hours (Fig. 19A). However, Spa15 was secreted by 2.5 hours in the CR assay despite the absence of detectable secretion in the first 30 minutes (Fig. 19A).

Figure 19. Spa15 is secreted in the Congo red secretion assay.

A. Western blot analysis was performed for the hemagglutinin (HA) tag on Spa15 and MxiE in supernatant and pellet samples from the Congo red secretion assay. 2457T alone at 30 minutes (Lane 1) and 2.5 hours (Lane 2) served as a negative control for the anti-HA antibody. 2457T + pSpa15-2HA plasmid (strain BS905) did not secrete the tagged version of Spa15 at 30 minutes (3) but did secrete at 2.5 hours (4). 2457T + pMxiE-2HA plasmid (strain BS909) did not secrete the tagged version of MxiE at either 30 minutes (5) or 2.5 hours (6). The data are representative of three independent experiments.

B. Time course of Spa15 secretion in the Congo red assay. Secretion in 2457T harboring the pSpa15-2HA plasmid (strain BS905) in the Congo red assay was performed at 0.5 hour, 1 hour, 2 hours, and 3 hours.

Figure 19. *Spa15* is secreted in the Congo red secretion assay.



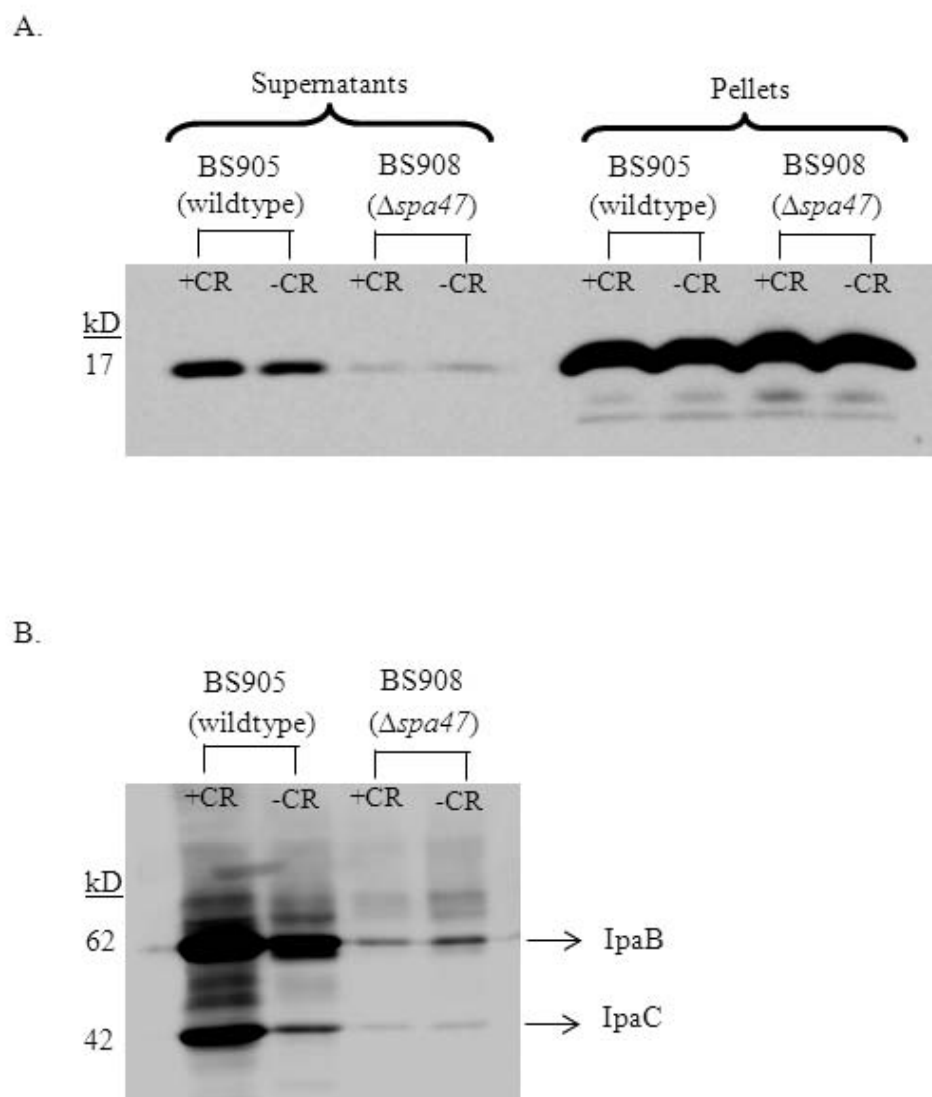
To further define Spa15 secretion, we performed a time course in wildtype bacteria (BS905) in the CR assay, and collected samples at 30 minutes, 1 hour, 2 hours, and 3 hours. We found that Spa15 was only slightly secreted by 1 hour and significantly secreted by 2 hours in the CR assay (Fig. 19B). To determine if Spa15 secretion is dependent on the T3SS and CR inducible like other effectors, we transformed the pSpa15-2HA plasmid into a $\Delta spa47$ mutant (BS908) and performed the CR assay. Spa47 is the ATPase that provides energy for the T3SS, and a $\Delta spa47$ mutant is unable to secrete T3 effectors (39, 42). Western blot analysis demonstrated that there was no Spa15 secretion in the $\Delta spa47$ mutant at 2.5 hours (Fig. 20A). In addition, the secretion of Spa15 like other T3 effectors was inducible with CR since there was a reduction in Spa15 secretion in BS905 when CR was absent (Fig. 20A). This pattern of CR-inducible secretion is the same for known *Shigella* T3SS effectors. To demonstrate that the secretion of Spa15 is similar to other T3SS effector proteins, we blotted the same samples for secretion of IpaB and IpaC and found the same pattern of secretion as Spa15 (Fig 20B). Therefore, Spa15 is secreted in a CR-inducible, T3SS-dependent fashion.

Figure 20. Spa15 secretion requires the type-III secretion system.

A. Secretion of Spa15 in 2457T harboring the pSpa15-2HA plasmid (strain BS905) with (1) and without (2) Congo red compared to the secretion of Spa15 in the $\Delta spa47$ mutant harboring the pSpa15-2HA plasmid (strain BS908) with (3) and without (4) Congo red. All samples were taken at the 2.5 hour time-point. Western blot analysis against the HA tag indicated secretion is dependent on the T3SS and CR inducible. These results are representative of three repeated experiments.

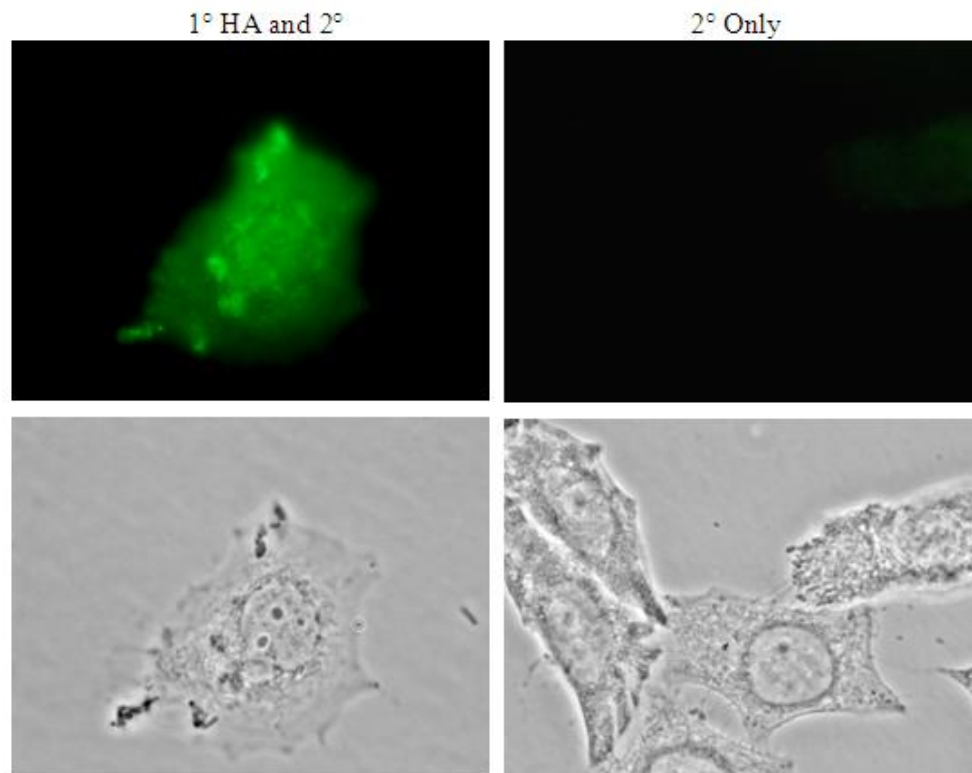
B. The supernatants from (A) were blotted and analyzed with antibodies to IpaB (62 kD) and IpaC (42 kD).

Figure 20. *Spa15* secretion requires the type-III secretion system.



Finally, to determine if secretion of the HA-tagged Spa15 in the CR assay also occurred in infected HeLa cells, BS905 was used in an infection assay in which the intracellular bacterial population was allowed to grow for three hours in the presence of gentamicin to kill any extracellular bacteria. We chose the three hour time-point since this is when we apply STS in the apoptosis assay. Therefore, the protective bacterial factor should be present in the cytoplasm of the host cell by three hours for apoptosis inhibition to occur. The infected monolayers were fixed and stained with the primary anti-HA antibody and counterstained with a secondary antibody conjugated to Alexa fluor 488. There was a strong signal with the anti-HA antibody concentrated around the bacteria and distributed throughout the HeLa cell cytoplasm, indicating that Spa15 was secreted inside epithelial cells by three hours post-infection (Fig. 21).

Figure 21. Spa15 is secreted into the cytoplasm of infected epithelial cells.



Immunofluorescence (top) and phase-contrast views (bottom) of HeLa cells infected with BS905 at 3 hours post-infection are shown. The HA signal is concentrated around the bacteria and distributed throughout the cytoplasm of the host cell indicating that Spa15 is secreted during infection. There was no significant signal above background when the infected HeLa cells were stained only with the secondary antibody (right). All images were taken with a 100× objective.

Spa15 secretion is delayed in the $\Delta mxiE$ mutant.

Since the $\Delta mxiE$ mutant is unable to prevent STS-induced apoptosis, we hypothesized that the secretion of Spa15 in this mutant was altered. We performed a time course in the CR assay comparing Spa15 secretion in 2457T harboring the pSpa15-2HA plasmid (BS905) to secretion in the $\Delta mxiE$ mutant harboring the pSpa15-2HA plasmid (BS906) at 1.5, 2.0, and 2.5 hours. We chose these time points since secretion occurs by 2 hours in wildtype bacteria. As seen in Figure 22A, secretion of Spa15 is significantly reduced in BS906 compared to BS905. After complementation of the $\Delta mxiE$ mutation in the presence of the pSpa15-2HA plasmid (BS907), secretion of Spa15 was restored to wildtype levels (Fig. 22A). We verified equal loading of protein in all samples by both Coomassie staining of total protein (data not shown) and analyzing the secretion of IpaB since IpaB secretion is not affected by the $\Delta mxiE$ mutation (Fig. 22B). As shown, the same amount of IpaB was secreted at all time points in all strains. Figure 22C is a graph of the densitometry analysis of Spa15 secretion in which the geometric mean ratios of secretion are plotted. The amount of Spa15 secretion was standardized to the amount of IpaB secretion for each sample. Relative to BS905, there was a significant difference in Spa15 secretion between BS906 and BS907 across all time points, with a p-Value less than 0.001. In addition, Spa15 secretion was consistently decreased in BS906 relative to BS905 since the values fall below the black line. The p-Value for these data, as determined by a repeated measures ANOVA using Tukey's post-hoc analysis, is equal to 0.01. Spa15 secretion in BS907 was consistently increased relative to BS905 since the values are above the black line. The p-Value for these data is 0.002. The reduced secretion in the $\Delta mxiE$ mutant most likely explains why this mutant is unable to inhibit

STS-induced apoptosis, and the data suggest that the levels of MxiE determine the amount of Spa15 secretion.

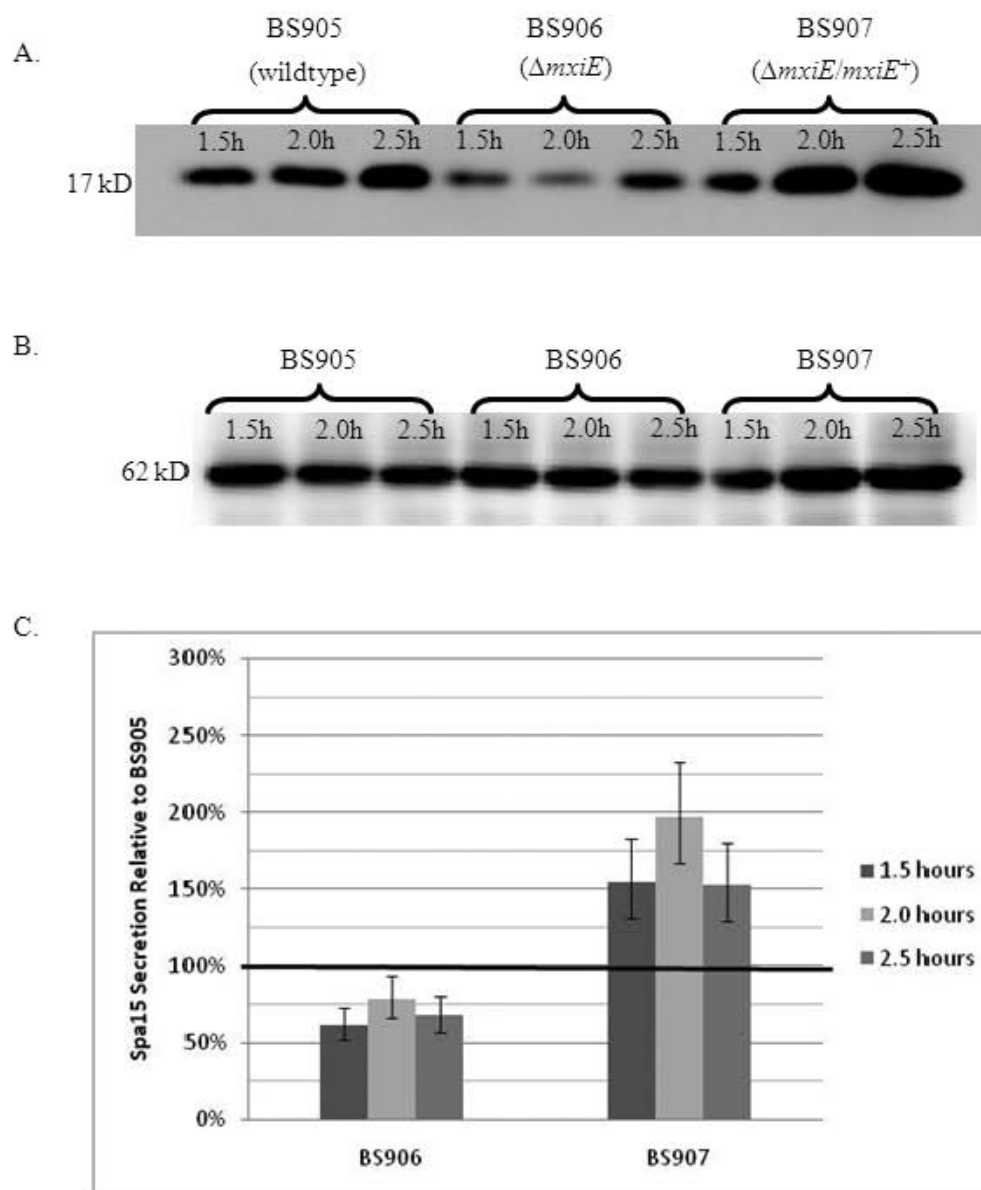
Figure 22. Spa15 secretion in the $\Delta mxiE$ mutant.

A. Time course of Spa15 (17 kD) secretion in BS905 (wildtype) compared to secretion of Spa15 in BS906 ($\Delta mxiE$) and BS907 ($\Delta mxiE/mxiE^+$). The Congo red assay was performed at 1.5, 2.0, and 2.5 hours, and Western blot analysis was performed against the HA tag. This Western blot represents three independent experiments.

B. The samples from panel A were blotted for IpaB secretion to confirm equal loading of total protein.

C. Densitometry analysis of Spa15 secretion in BS905, BS906, and BS907. The geometric mean ratios of Spa15 secretion from the Western blot in panel A in BS906 and BS907 is plotted relative to the secretion of Spa15 in BS905 (set at 100% and represented by the black line). The amount of Spa15 secretion was standardized to the amount of IpaB secretion in panel B for each sample. Error bars represent the standard error for the three repeated experiments. A repeated measures ANOVA using Tukey's post-hoc analysis demonstrated that the p-Value for Spa15 secretion in BS906 relative to BS905 is 0.01. The p-Value for Spa15 secretion in BS907 relative to BS905 is 0.002. The p-Value for the difference in Spa15 secretion between BS906 and BS907 is <0.001.

Figure 22. *Spa15* secretion in the $\Delta mxiE$ mutant.



Discussion

We have identified *spa15* as the *S. flexneri* gene required for the inhibition of apoptosis in epithelial cells. Given that the $\Delta mxiE$ mutant is unable to prevent STS-induced apoptosis (7), we were surprised to discover that none of the MxiE-regulated genes were required for protection. The repertoire of MxiE-regulated genes has been extensively categorized (3, 21, 24, 27); these genes have a 17 base pair sequence defined as the MxiE box that is upstream of the promoter (27). Therefore, we are confident that Table 10 represents all of the MxiE-regulated genes in *S. flexneri*. Complementation of the $\Delta mxiE$ mutation in strain BS613 restored apoptosis protection (data not shown), which led us to investigate proteins known to associate with MxiE to explain the $\Delta mxiE$ mutant phenotype. Spa15 associates with MxiE and has been described as a co-anti-activator for MxiE to prevent early transcriptional activation of MxiE-regulated genes (34). The $\Delta spa15$ mutant was unable to inhibit apoptosis, even in the absence of STS, while complementation with *spa15*⁺ restored protection. The small plaque size (data not shown) also suggests that the bacteria are unable to prevent apoptosis in the absence of STS. As the cells become apoptotic, the bacteria are most likely exposed to the extracellular environment where gentamicin is present during the plaque assay (31). Subsequently, the bacteria are killed by the antibiotic and the plaques fail to develop fully.

The closely neighboring uninfected cells that were apoptotic in monolayers infected with the $\Delta spa15$ mutant in the absence of STS could be due to the cytokine expression of the infected cells. Epithelial cells secrete many cytokines, especially TNF- α , interleukin-1 α (IL-1 α), and IL-6 (11). TNF- α , IL-1 α , and IL-6 secretion has been

reported during *Shigella* infection (1, 23), and *Chlamydia*-infected epithelial cells have been shown to secrete these cytokines as well (19). TNF- α induces apoptosis via the extrinsic pathway, and a combination of IL-1 α and TNF- α induces apoptosis in epithelial cells (43). IL-6 protects the colonic epithelium during *Citrobacter rodentium* infection, and IL-6 induces the expression of anti-apoptotic genes *BCL-xL*, *MCL-1*, *cIAP-2*, and *BCL-3* (8). We have never observed apoptosis in neighboring uninfected cells in the absence of STS when wildtype bacteria are used to infect the epithelial cells. We hypothesize that the $\Delta spa15$ mutant-infected cells are releasing more TNF- α and/or IL-1 α , which, in turn, induces apoptosis in neighboring uninfected cells. Another possibility is that $\Delta spa15$ mutant-infected cells are releasing less IL-6. Therefore, it is possible that *Shigella* not only protects cells that it infects, but also protects closely neighboring uninfected cells. This pro-survival effect on neighboring cells is ideal for the bacteria since *Shigella* eventually spreads to adjacent cells during infection.

Spa15 has been described as a T3SS chaperone based on the necessity of Spa15 to be present for secretion of several proteins (34). These target proteins include IpaA, IpgB1, IpgB2, OspB, OspC2, OspC3, OspD1, and MxiE (15, 33, 34). None of the secreted target proteins were required to inhibit apoptosis (Table 10). Therefore, the only mutants that were unable to inhibit STS-induced apoptosis were the $\Delta mxiE$ mutant and the $\Delta spa15$ mutant. This result led us to investigate whether MxiE, Spa15, or both proteins were secreted through the T3SS. We suspected that MxiE is not secreted given that it is a transcriptional activator and that a previous report showed that MxiE is not secreted by 30 minutes in the CR assay (34). However, for both proteins, we wanted to determine if secretion occurred at later time points as was observed for some T3SS

effectors (40). We chose the 2.5-hour time point since we apply STS at 3 hours post-infection in the apoptosis assay (7). If the proteins are secreted and inhibit apoptosis, significant secretion must therefore occur prior to 3 hours post-infection. We constructed an HA-tagged version of Spa15 and determined that it was functional as evidenced by complementation in BS914. BS914 invaded HeLa cells at wildtype levels and protected in the apoptosis assay (data not shown) verifying that the HA tag does not interfere with Spa15 function. Afterwards, we detected secretion of HA-tagged Spa15 in the CR assay.

This report is the first to demonstrate that Spa15 is secreted by the T3SS. We were able to detect Spa15 secretion because we assayed for the tagged protein and we analyzed later time points in the CR secretion assay. A previous report only analyzed Coomassie stained protein gels for secreted products of *S. flexneri* M90T and a $\Delta spa15$ mutant at the 30 minute time point (34). It is therefore not surprising that secretion of Spa15 was not detected prior to our work. One could argue that sample processing after the CR assay resulted in the appearance of secretion, perhaps due to lysis of the bacteria. The absence of Spa15 secretion in the $\Delta spa47$ mutant argues against this scenario since Spa15, like IpaB and IpaC, remained in the pellet fraction and was not secreted due to the absence of Spa47. In addition, the HA tag does not cause secretion of an otherwise nonsecreted protein since the HA-tagged MxiE was not secreted. We are therefore confident that Spa15 is secreted into epithelial cells based on the CR assay and the immunofluorescence analysis of Spa15 secretion in infected epithelial cells (Figure 21).

Since Spa15 is the anti-apoptosis factor and is secreted, we hypothesized that the $\Delta mxiE$ mutant did not prevent STS-induced apoptosis because Spa15 secretion was altered. We detected a significant decrease in Spa15 secretion in the $\Delta mxiE$ mutant

(Figure 22). Secretion was restored above wildtype levels when the $\Delta mxiE$ mutation was complemented (BS907), which is verified by the fact that BS613 inhibits STS-induced apoptosis (data not shown). The comparison of Spa15 secretion between strains BS905, BS906, and BS907 is valid since the HA tag does not interfere with function. Therefore, not enough Spa15 is secreted from the $\Delta mxiE$ mutant in order for this strain to inhibit apoptosis in the presence of STS. Interestingly, epithelial cells infected with the $\Delta mxiE$ mutant never appeared apoptotic in the absence of STS (data not shown). The low levels of Spa15 secreted by the $\Delta mxiE$ mutant are most likely sufficient to inhibit apoptosis during infection but insufficient to inhibit apoptosis in the presence of a strong apoptosis inducer like STS.

Based on our data, it appears that the levels of MxiE affect the amount of Spa15 that is secreted. With MxiE absent in strain BS906, Spa15 cannot bind to MxiE to prevent early activation of MxiE-regulated genes. Spa15 secretion above wildtype levels in BS907 suggests that when more MxiE is present, more Spa15 is needed to prevent early transcriptional activation of MxiE-regulated genes. Once this higher amount of Spa15 is released from MxiE, Spa15 is available for secretion by the T3SS. It is also possible that MxiE contributes to the stability of Spa15. The absence of MxiE may cause Spa15 to remain attached to another protein, possibly OspD1, which would reduce the level of Spa15 secretion in the $\Delta mxiE$ mutant. Future studies analyzing how MxiE modulates the secretion of Spa15 are clearly needed.

Most T3SS chaperones bind to one or two targets and are encoded next to the genes for these targets. For example, *ipgC* is immediately upstream of *ipaB* and *ipaC* on the virulence plasmid, and IpgC binds to both IpaB and IpaC to prevent early association

of these proteins (29). *spa15* is an atypical chaperone since it is encoded in the middle of the *mxi-spa* operon and the genes that encode the Spa15 targets are scattered throughout the 220 kb virulence plasmid (6, 33). Homology searches with BLAST revealed several homologues to Spa15 in other pathogens including InvB from *Salmonella enterica* subspecies *enterica* serovar Typhimurium, SpaK from *S. enterica* subspecies *enterica* serovar Paratyphi A, BsaR from several *Burkholderia* species, and YsaK from *Yersinia enterocolitica*. At least two of the homologues, InvB and YsaK, are also atypical T3SS chaperones in that they bind to many targets and are not encoded near the genes for those targets (25, 33). These homologues are similar in structure, and there are six conserved residues in the chaperones that define a binding motif (25). Given the sequence identities and similarities, it is possible that some of the homologues are also secreted into eukaryotic cells. The percent identity between Spa15 and the homologues is approximately 30%. It remains to be seen if the homologues have additional functions. These T3SS chaperones may truly represent a new, unique class of chaperones.

During apoptosis cytochrome *c* release from the mitochondria results in caspase-9 activation and subsequent caspase-3 activation (2). Given that *S. flexneri* inhibits STS-induced apoptosis prior to caspase-3 activation despite the release of cytochrome *c* and caspase-9 activation, we believe there are a few likely eukaryotic targets for Spa15 to directly inhibit caspase-3 (Figure 23). First, Spa15 could bind directly to caspase-3 and block the cleavage site. Alternatively, Spa15 could associate with caspase-9 to prevent it from activating caspase-3. This association would not prevent caspase-9 from being activated by the apoptosome (2) but would prevent the activated form of caspase-9 from cleaving caspase-3. Finally, Spa15 could enhance the binding of an inhibitor of apoptosis

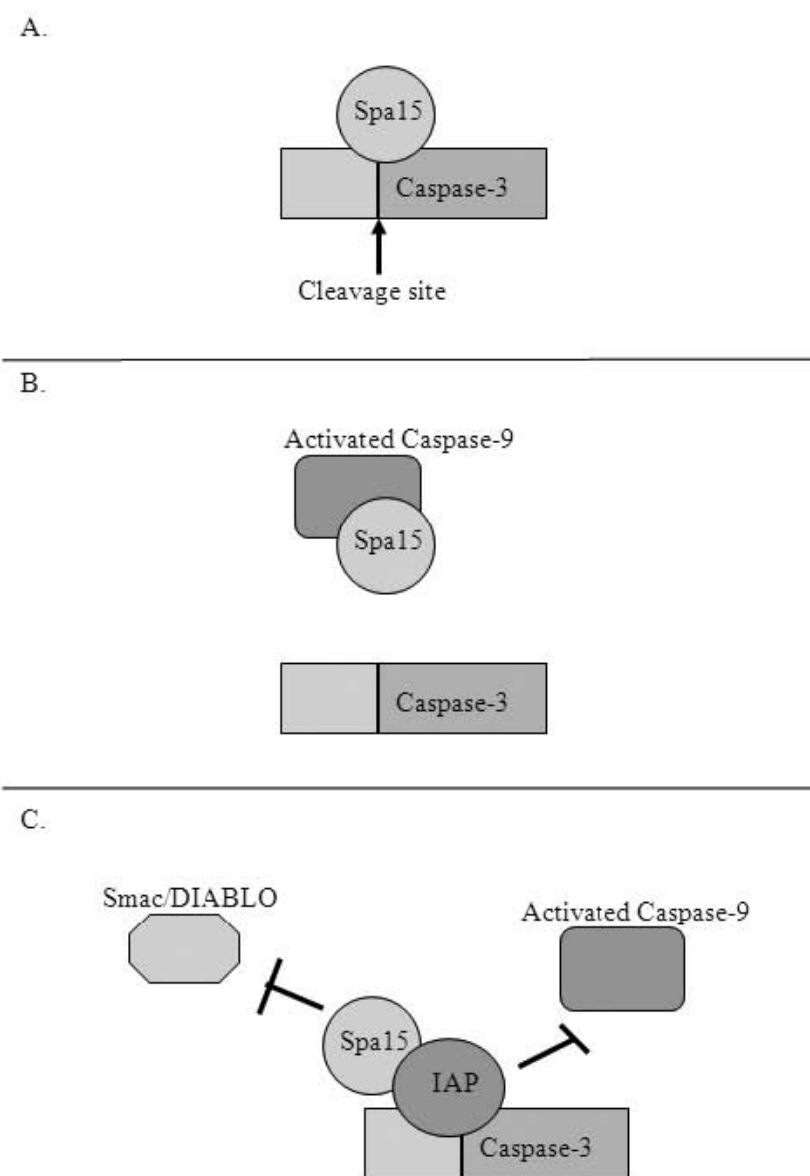
protein (IAP) to caspase-3. This enhanced binding would prevent the dissociation of the IAP from caspase-3 by proteins like Smac/Diablo that are released from the mitochondria (10). The binding of Spa15 to an IAP would also prevent activated caspase-9 from cleaving caspase-3 since the caspase-3 cleavage site would be blocked by the IAP. We are in the process of identifying potential eukaryotic targets through protein interaction screens.

Figure 23. Model of Spa15 function in the eukaryotic cell.

Since caspase-3 activation is inhibited in infected cells in the presence of STS, there are three scenarios in which Spa15 could be involved to inhibit caspase-3 activation. Spa15 could:

- A. Bind directly to caspase-3 to prevent cleavage and activation.
- B. Inhibit the activated form of caspase-9 to prevent caspase-3 activation.
- C. Enhance the binding of an inhibitor of apoptosis protein (IAP) to caspase-3. This enhanced binding would prevent Smac/Diablo from dissociating the IAP from caspase-3 and prevent caspase-9 from activating caspase-3.

Figure 23. Model of Spa15 function in the eukaryotic cell.



In conclusion, we have identified Spa15 as the anti-apoptosis factor that inhibits apoptosis in epithelial cells during *S. flexneri* infection. Of equal importance, we were able to demonstrate for the first time that Spa15 is secreted through the T3SS and has effector function in addition to being a T3SS chaperone. Prevention of epithelial cell apoptosis is important for the bacteria to survive inside the host. During infection, many apoptosis stimuli are present. These stimuli include the cytokines tumor necrosis factor- α (20) and Fas ligand (36), leukocyte elastases (14), and the transmigration of polymorphonuclear cells across the colonic epithelium (22) that occurs during *Shigella* infection (28). If *S. flexneri* is unable to prevent epithelial cell apoptosis and the infected cells die, the bacteria will be exposed to the extracellular environment that is infiltrated with immune cells. In fact, *in vivo* studies have verified that only immune cells are apoptotic during *Shigella* infection (36, 37, 45). Therefore, the inhibition of epithelial cell apoptosis is vital for *S. flexneri* to establish a replicative niche inside the host in order to survive.

Acknowledgements

This work was supported by grant AI24656 from the National Institute of Allergy and Infectious Diseases. We would like to thank the Henry M. Jackson Foundation and the Uniformed Services University for the Val Hemming Fellowship awarded to C.S.F, as well as the Graduate Education Office at USU for additional stipend support. We also thank members of the Maurelli lab for their technical assistance, and Dr. Cara Olsen for help with the statistical analysis. The opinions or assertions contained herein are the private ones of the authors and are not to be construed as official or reflecting the views

of the Department of Defense or the Uniformed Services University of the Health Sciences.

References

1. **Arondel, J., M. Singer, A. Matsukawa, A. Zychlinsky, and P. J. Sansonetti.** 1999. Increased interleukin-1 (IL-1) and imbalance between IL-1 and IL-1 receptor antagonist during acute inflammation in experimental Shigellosis. *Infect. Immun.* **67**:6056-6066.
2. **Ashe, P. C., and M. D. Berry.** 2003. Apoptotic signaling cascades. *Prog. Neuropsychopharmacol. Biol. Psychiatry.* **27**:199-214.
3. **Ashida, H., T. Toyotome, T. Nagai, and C. Sasakawa.** 2007. *Shigella* chromosomal IpaH proteins are secreted via the type III secretion system and act as effectors. *Mol. Microbiol.* **63**:680-693.
4. **Bahrani, F. K., P. J. Sansonetti, and C. Parsot.** 1997. Secretion of Ipa proteins by *Shigella flexneri*: inducer molecules and kinetics of activation. *Infect. Immun.* **65**:4005-4010.
5. **Bernardini, M. L., J. Mounier, H. d'Hauteville, M. Coquis-Rondon, and P. J. Sansonetti.** 1989. Identification of icsA, a plasmid locus of *Shigella flexneri* that

governs bacterial intra- and intercellular spread through interaction with F-actin. Proc. Natl. Acad. Sci. U S A **86**:3867-3871.

6. **Buchrieser, C., P. Glaser, C. Rusniok, H. Nadjari, H. D'Hauteville, F. Kunst, P. Sansonetti, and C. Parsot.** 2000. The virulence plasmid pWR100 and the repertoire of proteins secreted by the type III secretion apparatus of *Shigella flexneri*. Mol. Microbiol. **38**:760-771.
7. **Clark, C. S., and A. T. Maurelli.** 2007. *Shigella flexneri* inhibits staurosporine-induced apoptosis in epithelial cells. Infect. Immun. **75**:2531-2539.
8. **Dann, S. M., M. E. Spehlmann, D. C. Hammond, M. Iimura, K. Hase, L. J. Choi, E. Hanson, and L. Eckmann.** 2008. IL-6-dependent mucosal protection prevents establishment of a microbial niche for attaching/effacing lesion-forming enteric bacterial pathogens. J. Immunol. **180**:6816-6826.
9. **Datsenko, K. A., and B. L. Wanner.** 2000. One-step inactivation of chromosomal genes in *Escherichia coli* K-12 using PCR products. Proc. Natl. Acad. Sci. U S A **97**:6640-6645.
10. **Ekert, P. G., and D. L. Vaux.** 2005. The mitochondrial death squad: hardened killers or innocent bystanders? Curr. Opin. Cell. Biol. **17**:626-630.

11. **Fahey, J. V., T. M. Schaefer, J. Y. Channon, and C. R. Wira.** 2005. Secretion of cytokines and chemokines by polarized human epithelial cells from the female reproductive tract. *Hum. Reprod.* **20**:1439-1446.

12. **Formal, S. B., G. J. Dammin, E. H. Labrec, and H. Schneider.** 1958. Experimental *Shigella* infections: characteristics of a fatal infection produced in guinea pigs. *J. Bacteriol.* **75**:604-610.

13. **Ghosh, P.** 2004. Process of protein transport by the type III secretion system. *Microbiol. Mol. Biol. Rev.* **68**:771-795.

14. **Ginzberg, H. H., P. T. Shannon, T. Suzuki, O. Hong, E. Vachon, T. Moraes, M. T. Abreu, V. Cherepanov, X. Wang, C. W. Chow, and G. P. Downey.** 2004. Leukocyte elastase induces epithelial apoptosis: role of mitochondrial permeability changes and Akt. *Am. J. Physiol. Gastrointest. Liver. Physiol.* **287**:G286-298.

15. **Hachani, A., L. Biskri, G. Rossi, A. Marty, R. Menard, P. Sansonetti, C. Parsot, G. T. Van Nhieu, M. L. Bernardini, and A. Allaoui.** 2008. IpgB1 and IpgB2, two homologous effectors secreted via the Mxi-Spa type III secretion apparatus, cooperate to mediate polarized cell invasion and inflammatory potential of *Shigella flexneri*. *Microbes Infect.* **10**:260-268.

16. **Hanahan, D.** 1983. Studies on transformation of *Escherichia coli* with plasmids. J. Mol. Biol. **166**:557-580.
17. **Hromockyj, A. E., and A. T. Maurelli.** 1989. Identification of *Shigella* invasion genes by isolation of temperature-regulated inv::lacZ operon fusions. Infect. Immun. **57**:2963-2970.
18. **Jennison, A. V., and N. K. Verma.** 2004. *Shigella flexneri* infection: pathogenesis and vaccine development. FEMS Microbiol. Rev. **28**:43-58.
19. **Johnson, R. M.** 2004. Murine oviduct epithelial cell cytokine responses to *Chlamydia muridarum* infection include interleukin-12-p70 secretion. Infect. Immun. **72**:3951-3960.
20. **Jung, H. C., L. Eckmann, S. K. Yang, A. Panja, J. Fierer, E. Morzycka-Wroblewska, and M. F. Kagnoff.** 1995. A distinct array of proinflammatory cytokines is expressed in human colon epithelial cells in response to bacterial invasion. J. Clin. Invest. **95**:55-65.
21. **Kane, C. D., R. Schuch, W. A. Day, Jr., and A. T. Maurelli.** 2002. MxiE regulates intracellular expression of factors secreted by the *Shigella flexneri* 2a type III secretion system. J. Bacteriol. **184**:4409-4419.

22. **Le'Negrate, G., E. Selva, P. Auberger, B. Rossi, and P. Hofman.** 2000. Sustained polymorphonuclear leukocyte transmigration induces apoptosis in T84 intestinal epithelial cells. *J. Cell. Biol.* **150**:1479-1488.
23. **Le-Barillec, K., J. G. Magalhaes, E. Corcuff, A. Thuizat, P. J. Sansonetti, A. Phalipon, and J. P. Di Santo.** 2005. Roles for T and NK cells in the innate immune response to *Shigella flexneri*. *J. Immunol.* **175**:1735-1740.
24. **Le Gall, T., M. Mavris, M. C. Martino, M. L. Bernardini, E. Denamur, and C. Parsot.** 2005. Analysis of virulence plasmid gene expression defines three classes of effectors in the type III secretion system of *Shigella flexneri*. *Microbiology.* **151**:951-962.
25. **Lilic, M., M. Vujanac, and C. E. Stebbins.** 2006. A common structural motif in the binding of virulence factors to bacterial secretion chaperones. *Mol. Cell.* **21**:653-664.
26. **Maurelli, A. T., B. Baudry, H. d'Hauteville, T. L. Hale, and P. J. Sansonetti.** 1985. Cloning of plasmid DNA sequences involved in invasion of HeLa cells by *Shigella flexneri*. *Infect. Immun.* **49**:164-171.

27. **Mavris, M., P. J. Sansonetti, and C. Parsot.** 2002. Identification of the cis-acting site involved in activation of promoters regulated by activity of the type III secretion apparatus in *Shigella flexneri*. J. Bacteriol. **184**:6751-6759.
28. **McCormick, B. A., A. M. Siber, and A. T. Maurelli.** 1998. Requirement of the *Shigella flexneri* virulence plasmid in the ability to induce trafficking of neutrophils across polarized monolayers of the intestinal epithelium. Infect. Immun. **66**:4237-4243.
29. **Menard, R., P. Sansonetti, C. Parsot, and T. Vasselon.** 1994. Extracellular association and cytoplasmic partitioning of the IpaB and IpaC invasins of *S. flexneri*. Cell. **79**:515-525.
30. **Mills, J. A., J. M. Buysse, and E. V. Oaks.** 1988. *Shigella flexneri* invasion plasmid antigens B and C: epitope location and characterization with monoclonal antibodies. Infect. Immun. **56**:2933-2941.
31. **Oaks, E. V., M. E. Wingfield, and S. B. Formal.** 1985. Plaque formation by virulent *Shigella flexneri*. Infect. Immun. **48**:124-129.
32. **Ohya, K., Y. Handa, M. Ogawa, M. Suzuki, and C. Sasakawa.** 2005. IpgB1 is a novel *Shigella* effector protein involved in bacterial invasion of host cells. Its

activity to promote membrane ruffling via Rac1 and Cdc42 activation. J. Biol. Chem. **280**:24022-24034.

33. **Page, A. L., P. Sansonetti, and C. Parsot.** 2002. Spa15 of *Shigella flexneri*, a third type of chaperone in the type III secretion pathway. Mol. Microbiol. **43**:1533-1542.

34. **Parsot, C., E. Ageron, C. Penno, M. Mavris, K. Jamoussi, H. d'Hauteville, P. Sansonetti, and B. Demers.** 2005. A secreted anti-activator, OspD1, and its chaperone, Spa15, are involved in the control of transcription by the type III secretion apparatus activity in *Shigella flexneri*. Mol. Microbiol. **56**:1627-1635.

35. **Pilonieta, M. C., and G. P. Munson.** 2008. The chaperone IpgC copurifies with the virulence regulator MxiE. J. Bacteriol. **190**:2249-2251.

36. **Raqib, R., C. Ekberg, P. Sharkar, P. K. Bardhan, A. Zychlinsky, P. J. Sansonetti, and J. Andersson.** 2002. Apoptosis in acute shigellosis is associated with increased production of Fas/Fas ligand, perforin, caspase-1, and caspase-3 but reduced production of Bcl-2 and interleukin-2. Infect. Immun. **70**:3199-3207.

37. **Sansonetti, P. J., J. Arondel, J. R. Cantey, M. C. Prevost, and M. Huerre.** 1996. Infection of rabbit Peyer's patches by *Shigella flexneri*: effect of adhesive or

invasive bacterial phenotypes on follicle-associated epithelium. *Infect. Immun.* **64**:2752-2764.

38. **Schroeder, G. N., and H. Hilbi.** 2008. Molecular pathogenesis of *Shigella* spp.: controlling host cell signaling, invasion, and death by type III secretion. *Clin. Microbiol. Rev.* **21**:134-156.

39. **Tamano, K., S. Aizawa, E. Katayama, T. Nonaka, S. Imajoh-Ohmi, A. Kuwae, S. Nagai, and C. Sasakawa.** 2000. Supramolecular structure of the *Shigella* type III secretion machinery: the needle part is changeable in length and essential for delivery of effectors. *EMBO J.* **19**:3876-3887.

40. **Toyotome, T., T. Suzuki, A. Kuwae, T. Nonaka, H. Fukuda, S. Imajoh-Ohmi, T. Toyofuku, M. Hori, and C. Sasakawa.** 2001. *Shigella* protein IpaH(9.8) is secreted from bacteria within mammalian cells and transported to the nucleus. *J. Biol. Chem.* **276**:32071-32079.

41. **Tran Van Nhieu, G., A. Ben-Ze'ev, and P. J. Sansonetti.** 1997. Modulation of bacterial entry into epithelial cells by association between vinculin and the *Shigella* IpaA invasin. *EMBO J* **16**:2717-2729.

42. **Venkatesan, M. M., J. M. Buysse, and E. V. Oaks.** 1992. Surface presentation of *Shigella flexneri* invasion plasmid antigens requires the products of the spa locus. *J. Bacteriol.* **174**:1990-2001.

43. **Wright, K., G. Kolios, J. Westwick, and S. G. Ward.** 1999. Cytokine-induced apoptosis in epithelial HT-29 cells is independent of nitric oxide formation. Evidence for an interleukin-13-driven phosphatidylinositol 3-kinase-dependent survival mechanism. *J. Biol. Chem.* **274**:17193-17201.

44. **Zurawski, D. V., C. Mitsuhashi, K. L. Mumy, B. A. McCormick, and A. T. Maurelli.** 2006. OspF and OspC1 are *Shigella flexneri* type III secretion system effectors that are required for postinvasion aspects of virulence. *Infect. Immun.* **74**:5964-5976.

45. **Zychlinsky, A., K. Thirumalai, J. Arondel, J. R. Cantey, A. O. Aliprantis, and P. J. Sansonetti.** 1996. In vivo apoptosis in *Shigella flexneri* infections. *Infect. Immun.* **64**:5357-5365.

Chapter Five

Discussion

Preface

Shigella flexneri is a facultative, intracellular pathogen that must adapt to the host environment in order to replicate and survive. It has been well-established since the 1960s that *Shigella* invades the colonic epithelium and replicates inside epithelial cells (12, 30). Studies aimed to understand how the pathogen survives *in vivo* led to the discovery that *S. flexneri* induces a rapid cell death in macrophages using IpaB in order to escape the adverse environment inside the immune cells. This cell death in macrophages also allows the pathogen to gain access to the basolateral pole of the colonic epithelium for invasion (6, 31). Previous research demonstrated that the bacteria do not induce cell death in epithelial cells despite the presence of IpaB (16, 29). In fact, researchers do not understand how the bacteria differentiate between macrophages, the cells that are detrimental to the bacteria, and epithelial cells, the cells that allow the bacteria to replicate and survive inside the host. In order to understand how the *Shigella* reacts to different cellular environments, it was first important to demonstrate that the bacteria behave differently in epithelial cells and can actually inhibit cell death. The hypothesis of this dissertation is based on previous literature and states that *Shigella* inhibits apoptosis in epithelial cells in order to establish a replicative niche inside the host.

In order to test this hypothesis, the first aim was to demonstrate that *S. flexneri* can inhibit apoptosis in epithelial cells. The development of the apoptosis assay allowed for the inhibition of apoptosis to be observed and provided a platform to determine how the bacteria inhibit apoptosis, which addressed the second aim of this thesis. The microarray analysis provided further understanding of the changes in eukaryotic gene expression upon infection that is vital for *Shigella* to inhibit apoptosis in epithelial cells. Finally, the identification of the *Shigella* factor responsible for apoptosis inhibition addressed the third aim of this dissertation and identified a new T3SS effector protein.

Discussion and Significance of Findings

Shigella flexneri inhibits apoptosis in epithelial cells.

The only research with regards to the induction of cell death performed in epithelial cells prior to this dissertation demonstrated that *S. flexneri* does not induce a rapid cell death in epithelial cells as the bacteria do in macrophages. Despite the presence of a stress response in infected epithelial cells, the cells are viable and intact up to four hours post-infection (16). This viability is in contrast to macrophages that are induced into a rapid cell death by two hours post-infection (10). Since the bacteria appear in close proximity to the mitochondria in epithelial cells (16), it was possible that the bacteria actively inhibit apoptosis given that the mitochondria are a key factor in apoptosis induction (26). No analysis on the proteins involved in apoptosis was performed in infected cells prior to this work.

I developed the apoptosis assay to determine if *S. flexneri* could inhibit apoptosis in epithelial cells. In this assay STS is used as an apoptosis inducer so analysis of the entire pathway can be performed, from the activation of pro-apoptotic proteins upstream of the mitochondria, to cytochrome *c* release, to caspase activation, and to the phenotypic signs of apoptosis, namely nuclear and cytoplasmic changes. Despite cytochrome *c* release and caspase-9 activation in the presence of STS in *Shigella*-infected cells, the bacteria are able to inhibit caspase-3 activation. The absence of apoptosis in *Shigella*-infected epithelial cells is in agreement with *in vivo* studies that characterized the apoptotic cells present during infection. Only immune cells were found to be apoptotic (25, 27, 33), which verifies that *Shigella* is preventing apoptosis in epithelial cells.

Not only is this research the first demonstration that *Shigella* can inhibit apoptosis in epithelial cells, *Shigella* is the first bacterial pathogen identified to inhibit apoptosis downstream of cytochrome *c* release. As outlined in chapter one, many bacterial pathogens can inhibit apoptosis; however, these bacteria utilize different mechanisms to prevent cytochrome *c* release from the mitochondria (4). Prevention of cytochrome *c* release is an ideal strategy, especially for obligate intracellular pathogens, since the mitochondrial membrane is permeabilized during cytochrome *c* release. The damaged mitochondria can no longer generate energy, and therefore, mitochondrial integrity is vital for the survival of eukaryotic cells (11). For obligate intracellular pathogens, cytochrome *c* release could be very detrimental to the survival of the pathogen. For example, the developmental cycle of the obligate intracellular pathogen *Chlamydia* ranges from 48 to 72 hours (18). It is not until late in infection when *Chlamydia* can differentiate from the growing replicative bodies (RBs) to the infectious form of elementary bodies (EBs). At this point, the EBs lyse

the eukaryotic cell in order to spread to new cells for replication and eventual transmission to a new host (18). If *Chlamydia* inhibited apoptosis after cytochrome *c* release from the mitochondria, the *Chlamydial* life cycle would be jeopardized since cytochrome *c* release damages the mitochondria and prevents the cell from generating more energy.

Consequently, *Chlamydia* would not be able to survive inside the host cell and RBs would not differentiate into EBs. As the non-infectious RB form of *Chlamydia* is released from the dying cell, the bacteria cannot infect new host cells and, thus, the infection cycle is aborted. Therefore, *Chlamydia* inhibits apoptosis prior to cytochrome *c* release from the mitochondria (23) to ensure that the host cell remains viable for completion of the *Chlamydial* life cycle.

Even though cytochrome *c* release occurs in *Shigella* infected cells in the presence of STS, there was no cytochrome *c* release upon normal infection in epithelial cells. The cytochrome *c* release detected in the apoptosis assay is due to the STS. Therefore, it is not the goal of *Shigella* to induce cytochrome *c* release upon infection. However, in scenarios in which cytochrome *c* release does occur, *S. flexneri* is able to overcome this challenge and prevent apoptosis by inhibiting caspase-3 activation. In addition, the ability to inhibit caspase-3 activation provides protection from both the intrinsic pathway and extrinsic pathways of apoptosis since caspase-3 is activated in both pathways (26). During *Shigella* infection TNF- α and Fas ligand are present in the rectal mucosa to activate the extrinsic pathway of apoptosis while the transmigration of PMN cells across the colonic epithelium, which occurs during *Shigella* infection (17), induces the intrinsic pathway of apoptosis in the epithelial cells (7, 13, 25). Therefore, there is a necessity for *S. flexneri* to inhibit both

pathways of apoptosis. The most efficient way to inhibit both pathways is at the point of caspase-3 activation.

The microarray analysis provides further insights into apoptosis inhibition.

The microarray analysis provided an in-depth examination of the changes in apoptosis-specific gene expression upon infection. Some of the observations, such as the induction of *JUN* and genes encoding the members of the IAP family were also observed in a previous study with *Shigella* using whole genome arrays (22). However, this previous study did not analyze the changes in eukaryotic gene expression in the presence of an apoptosis inducer like STS. The comparisons between uninfected cells treated with STS to infected cells treated with STS identified changes in gene expression that may be important for apoptosis inhibition by *Shigella*. For example, genes associated with p53 repression and pRb function were altered in infected cells compared to uninfected cells only when STS was present. Future experiments are needed to verify these observations and determine the role of these eukaryotic genes in apoptosis inhibition by *Shigella*.

The microarray study also was designed to compare infected cells and infected cells treated with STS. Interestingly, there was no significant difference in the two treatment groups as seen in the lack of a significant SAM analysis and the cluster diagram presented in Figure 11 in chapter three. This observation was actually quite surprising since it was expected that important differences would be obtained. Upon further consideration however, it would be inefficient for *Shigella* to induce changes in response to the presence of an apoptotic inducer. First, there are multiple inducers present during the course of infection as described above. Second, apoptosis inducers act quickly on cellular targets. The bacteria would have to rapidly identify and overcome these changes within the host

cell. If the bacteria induce pro-survival changes at the onset of infection regardless of the type of apoptosis inducer and regardless of the time at which the inducer is encountered, then *Shigella* would have a more efficient means of inhibiting cell death and surviving. Thus, the microarray data have provided a new direction to approach the understanding of apoptosis inhibition with regards to *Shigella* pathogenesis. The bacteria are not inhibiting apoptosis by reacting to the presence of apoptosis inducers. Instead, *Shigella* induces pro-survival changes at the onset of infection in the likely scenario that different inducers of apoptosis will eventually be encountered.

The microarray observations led to the model presented in chapter three that *S. flexneri* inhibits apoptosis at multiple checkpoints along the apoptotic pathways in epithelial cells. This work demonstrates that there are multiple effects upon infection, and that *Shigella* has evolved to overcome the multiple efforts by the host to induce apoptosis in infected cells. If these mechanisms fail in the presence of strong apoptosis inducers like STS, then the bacteria can provide late-stage protection by inhibiting caspase-3 activation. This multi-faceted approach is similar to other bacterial pathogens. For example, *Chlamydia*, *Neisseria*, *Anaplasma*, *Rickettsia*, *Coxiella*, and *Bartonella* use several methods to inhibit apoptosis as mentioned in chapter one. Therefore, it appears that there is a common theme among bacteria that can inhibit apoptosis, and further investigation of this multi-faceted approach could greatly enhance our understanding of apoptosis inhibition by bacterial pathogens.

The changes in eukaryotic gene expression observed in the microarray study can be further explored. For example, additional studies can confirm the increases in *BCL-2* expression and determine if this induced expression is responsible for the lack of

cytochrome *c* release upon normal infection. These studies could lead to the identification of another *Shigella* protein that binds to the mitochondria or to BCL-2 to prevent cytochrome *c* release. Moreover, the effects of NF- κ B and the jun oncogene induction in infected cells should be analyzed. Small inhibitory RNA (siRNA) studies to knock down expression of these eukaryotic factors, or the use of inhibitors, prior to or during *Shigella* infection may reveal the role of both NF- κ B and jun activation during *Shigella*-mediated apoptosis inhibition. Studies that define the importance of the observations made from the microarray experiment will enhance our understanding into how *Shigella* implements a pro-survival state in infected epithelial cells.

While it is important to confirm the effects of NF- κ B and jun induction, it is equally important to determine how the bacteria induce the expression of both eukaryotic factors. The Gram-negative cell surface component lipopolysaccharide (LPS) activates the NF- κ B pathway through the Toll-like receptor 4 (TLR4) during infection (7, 19), and NF- κ B activation by LPS might be an explanation as to how *Shigella* induces a pro-survival state in the infected epithelial cells (4). However, the pro-survival state due to NF- κ B activation may not be mediated by LPS as suggested by two studies. First, Binnicker et al. (3) utilized purified lipooligosaccharide (LOS) from *Neisseria gonorrhoeae* and applied it to the surface of host cells. LOS is similar to LPS except that it does not have repeating O-polysaccharides (24). Despite this difference, LOS is still a strong TLR4 activator that leads to NF- κ B activation (20, 24). There is no increase in the expression of the pro-survival gene *Bfl-1* in cells exposed to LOS that is seen upon infection with *Neisseria*, and *Bfl-1* induction is important for the inhibition of apoptosis by *N. gonorrhoeae*. Additionally, infection of host cells with an LOS mutant results in

the same induced expression of *Bfl-1* that occurs during infection with wildtype bacteria (3, 4). Binnicker et al. hypothesized that different bacterial products could promote the formation of different Rel/NF- κ B complexes during activation. These different complexes may interact with different transcription factors and regulatory proteins to control the transcription of an entirely distinct set of genes (3, 4). Second, *Legionella pneumophila* inhibits apoptosis in macrophages through NF- κ B activation during intracellular growth. Live, extracellular *L. pneumophila* and formalin-killed bacteria do not trigger NF- κ B activation or apoptosis inhibition (1). The *Legionella* study provides further evidence that the anti-apoptotic phenotype induced by pathogens through NF- κ B activation is not mediated by LPS (4). The same scenario could be true for jun since LPS has also been shown to be responsible for the induction of jun expression (2, 5).

Therefore, future studies need to determine if *S. flexneri* activates NF- κ B via LPS or through another T3SS effector protein. These studies may require the use of pulldown experiments in which eukaryotic proteins serve as bait for identifying interacting *Shigella* proteins. Additional studies could utilize LPS mutants of *Shigella* to determine if the same levels of NF- κ B activation are achieved, or if the same pro-survival genes are induced upon infection compared to wildtype bacteria. If the same levels of activation are seen with the LPS mutants, then an additional bacterial protein is required for the pro-survival effects that are dependent upon NF- κ B activation. *Shigella* could be the third pathogen identified to activate a pro-survival state through NF- κ B activation that is independent of LPS. The identification of the *Shigella* effector responsible for NF- κ B activation could assist researchers in identifying other bacterial proteins important for NF- κ B activation. These studies will not only be important for understanding apoptosis

inhibition in *Shigella* infection, but will also enhance our understanding of how pathogens utilize NF- κ B to induce a pro-survival state in the infected cell.

The microarray analysis in chapter three also revealed significant upregulation of eukaryotic genes that are responsible for inhibiting the extrinsic pathway of apoptosis. Furthermore, data presented in that chapter demonstrated that *S. flexneri* can inhibit apoptosis when an inducer of the extrinsic pathway, TNF- α -related apoptosis inducing ligand (TRAIL), was used. Future studies need to investigate if inhibition of the extrinsic pathway occurs prior to caspase-8 or caspase-3 activation. Only the lack of caspase-3 activation may be observed, and this would most likely be due to the inhibition by Spa15 since only caspase-3 inhibition is seen upon STS exposure. If the lack of caspase-8 activation is observed, this inhibition could be due to the upregulation of *TNFAIP8*, *TNFAIP3*, *FAIM3*, and/or *CFLAR/c-FLIP* observed from the microarray analysis. On the other hand, the lack of caspase-8 activation could be a direct result of another *Shigella* T3SS effector protein binding to and inhibiting the cleavage of caspase-8. In order to approach the investigation of the extrinsic pathway, Western blot analysis should first be performed to identify the point in the pathway that is inhibited in infected cells in the presence of TRAIL. Second, Western blot analysis could identify if eukaryotic proteins responsible for inhibiting the extrinsic pathway, for example *TNFAIP8*, *FAIM3*, or *CFLAR*, are increased in the presence or absence of TRAIL in infected cells. Finally, and depending on the results, protein interaction studies could identify which *Shigella* effector proteins bind to any relevant eukaryotic targets required for inhibition of the extrinsic pathway. The analysis of the extrinsic pathway may have the same results as the intrinsic pathway in that TRAIL may function like STS and overcome upstream pro-survival effects

but not caspase-3 activation. Alternatively, *Shigella* may use different T3SS effector proteins to inhibit the extrinsic pathway of apoptosis. No matter the method employed by the bacteria, these studies will allow us to appreciate the extent as to which *S. flexneri* evolved to survive within epithelial cells inside the host.

Identification of the Shigella factor responsible for apoptosis inhibition.

The identification of Spa15 as the *S. flexneri* factor responsible for the inhibition of STS-induced apoptosis is a significant finding. Initially, the results suggested that a MxiE-regulated gene was required to inhibit STS-induced apoptosis in epithelial cells since a $\Delta mxiE$ mutant did not inhibit STS-induced apoptosis. However, extensive analysis utilizing various deletion mutants and an *E. coli* strain expressing the *Shigella* entry region (SER) led to the identification of Spa15 as the protective factor in *S. flexneri*. More importantly, this dissertation successfully demonstrated for the first time that Spa15 is secreted through the T3SS and into the cytoplasm of the host cell. A previous study did not detect Spa15 secretion since the report only analyzed Coomassie stained protein gels for secreted proteins at the 30 minute time point (19). The longer incubation time in the CR assay and the sensitivity of the HA antibody detection in the Western blot analysis were optimal conditions required to detect Spa15 secretion. The identification of Spa15 as the anti-apoptosis factor is significant for *Shigella* pathogenesis since Spa15 is a new T3SS effector protein that functions in epithelial cells. In addition, the fact that Spa15 is secreted is also important for other bacterial pathogens which encode Spa15 homologues. At least two of these homologues, InvB from *S. enterica* subspecies *enterica* serovar Typhimurium and YsaK from *Yersinia enterocolitica*, are also atypical chaperones in that they are not encoded near the genes encoding the target proteins (14, 19). Moreover, the homologues

are similar in structure, have the six conserved residues that define the binding motif to the bacterial targets, and are 30% identical to Spa15 (14). Therefore, it is possible that these homologues are also secreted through the T3SS. Given that the identity is 30%, the homologues may not have a similar function as Spa15, and the proteins may not even be secreted. However, if the homologues are secreted, these proteins could represent a new class of bacterial effector proteins that are defined as chaperones and secreted to have effector function inside host cells.

While the $\Delta spa15$ mutant does not inhibit apoptosis and complementation restores protection, experiments are needed to verify that Spa15 alone is both necessary and sufficient to inhibit apoptosis. This verification requires transfection experiments in which *spa15* would be cloned into a eukaryotic expression vector for expression in HeLa cells. Once expression is verified, the HeLa cells can be exposed to STS, and analyzed to determine if apoptosis is blocked in the HeLa cells expressing *spa15*. DAPI staining will allow comparisons of the nuclei of transfected cells after STS exposure to the nuclei of untransfected cells or cells transfected with an empty vector after STS exposure. The results will give an indication as to whether *spa15* expression is inhibiting apoptosis if the nuclei are healthy in transfected cells while the nuclei of untransfected cells or cells transfected with the empty vector are apoptotic. Verification of apoptosis inhibition can occur by analyzing the transfected cells for caspase-3 activation after STS treatment via Western blot analysis. A population of *spa15* transfected cells should not have activated caspase-3 in the presence of STS. It is possible that Spa15 alone is not sufficient for apoptosis inhibition. The extensive mutant and strain analysis ruled out the contribution of most *Shigella* genes. If another factor is required in addition to Spa15, it would have to be a

gene located within the SER. The mutant analysis and secretion data have demonstrated that Spa15 is necessary for apoptosis inhibition. The transfection experiments will determine if Spa15 alone is sufficient to inhibit apoptosis in epithelial cells.

In order to determine the function of Spa15 in epithelial cells, the eukaryotic binding partner of Spa15 needs to be identified. The model of eukaryotic binding partners presented in chapter four suggests that there are three likely scenarios for Spa15 to directly prevent caspase-3 activation. The possibilities include direct binding to caspase-3 to prevent cleavage, binding to caspase-9 in such a way that allows activation but prevents subsequent caspase-3 activation, or binding to an inhibitor of apoptosis protein (IAP) to prevent caspase-3 activation. For the identification of the eukaryotic binding partner, *spa15* can be cloned into an expression vector to generate a tag fusion for the purification of the Spa15 protein. This protein can be subsequently used in pull-down experiments against HeLa cell lysates in order to identify a binding partner. A caveat to consider is that the placement of a tag on the N-terminus of Spa15 may interfere with folding and/or function of the protein. Therefore, the tag could be placed on the C-terminus of Spa15 for proper folding and function. This option should be considered given that the $\Delta spa15$ mutant could be complemented with the C-terminal hemagglutinin-tagged version of *spa15*. Therefore, this HA tag could be utilized in the pull-down experiments. Additional considerations include potential protein modifications of Spa15 by the eukaryotic cell. For example, Spa15 could be phosphorylated by the epithelial cell, and this phosphorylation may be required for Spa15 to bind to a eukaryotic protein. One method to overcome this obstacle would be to transform a high-copy plasmid with the tagged version of Spa15 into wildtype *S. flexneri*, and use this strain to infect HeLa cells. The tagged-Spa15 would be secreted

into and modified by the epithelial cells. This strategy will have the benefit of potentially co-purifying the eukaryotic binding partner from the HeLa lysate. If co-purification cannot be obtained, the modified Spa15 could still be purified and used in subsequent pull-down experiments against a HeLa lysate. Once the eukaryotic binding partner is identified, protein interaction studies in which N-terminal and C-terminal truncations of Spa15 and the eukaryotic target will define the important domains required for the binding and interaction of the two proteins. The future studies in this area are important to understand how Spa15 functions in epithelial cells to inhibit apoptosis.

As outlined in chapter four, the $\Delta mxiE$ mutant did not prevent STS-induced apoptosis due to the reduced secretion of Spa15 compared to wildtype bacteria. In addition, complementation of the $\Delta mxiE$ mutation with a high-copy plasmid results in increased secretion of Spa15. Spa15 is a co-anti-activator of MxiE to prevent early transcriptional activation of MxiE-regulated genes (21). The differential secretion data suggest that Spa15 secretion is controlled by MxiE, and experiments designed to determine why Spa15 secretion is reduced in the $\Delta mxiE$ mutant are clearly needed. This reduced amount of Spa15 secretion may occur because Spa15 remains bound to OspD1, which is also involved in the anti-activation of MxiE (21). The binding of Spa15 to OspD1 in the $\Delta mxiE$ mutant would inhibit or reduce Spa15 secretion. When there is an overabundance of MxiE in the $\Delta mxiE/mxiE^+$ complemented strain, more Spa15 may be needed to prevent early transcriptional activation of MxiE-regulated genes. This higher amount of Spa15 would then be released from MxiE during transcriptional activation and secreted. There is a possibility that the levels of MxiE might dictate Spa15, and possibly even OspD1, expression. Through Western blot analysis, Spa15 expression in the $\Delta mxiE$ mutant strain

could be compared to both the wildtype strain and the $\Delta mxiE/mxiE^+$ complemented strain. The expression levels of Spa15 were not analyzed since the secretion analysis was performed in wildtype bacteria with the pSpa15-2HA plasmid. The expression of the HA-tagged Spa15 was controlled by the promoter on the plasmid and not by the native promoter for the T3SS operon. Expression studies would therefore require the use of a Spa15 antibody or a promoter fusion assay to adequately assess the expression pattern of Spa15 from the native promoter in the T3SS operon. The aforementioned studies will establish how MxiE affects the secretion and possibly expression of Spa15 to ascertain why Spa15 secretion is reduced in the $\Delta mxiE$ mutant.

Additional Studies

The disparate response of Shigella to macrophages and epithelial cells.

The results of this dissertation have provided the basis for additional studies to enhance our understanding of *S. flexneri* pathogenesis. As mentioned in the introduction chapter, *Shigella* induces a rapid cell death in macrophages through the use of the effector IpaB binding to and activating caspase-1. In addition to being required for invasion of epithelial cells, IpaB is required for post-invasion virulence and therefore must be present in the cytoplasm of these cells (29). *Shigella* does not induce a cell death in epithelial cells as it does in macrophages. The identification of the eukaryotic binding partner of Spa15 may enhance our understanding of this paradox, but additional research is clearly needed. First, Spa15 is significantly secreted by 2 hours in the CR assay. The data suggest that an adequate level of Spa15 is not present in macrophages to have a protective effect since macrophages are killed rapidly by the bacteria. In one study, almost 60% of macrophages

were killed by 2 hours post-infection while another study detected cell death in approximately 40% of macrophages 90 minutes after infection (10, 32). Therefore, Spa15 secretion in macrophages should be examined. If Spa15 is not secreted adequately, it may be due to the expression of *spa15* in the macrophages. Lucchini et al. found in a microarray analysis that the expression of *Shigella* T3SS operon containing *spa15* is reduced approximately 10-fold throughout the entire infection in macrophages compared broth culture (15). The reduced expression of *spa15* in macrophages can be confirmed by Western blot analysis, and it would be interesting to establish if the presence of Spa15 in macrophages delays or inhibits IpaB-mediated cell death. In order to perform these studies, the $\Delta spa15$ mutant complemented with the pBSKS-*spa15* plasmid in which *spa15* is under the control of a *lac* promoter could be used to infect macrophages. The high copy number of the plasmid and the constitutive expression from the *lac* promoter would significantly increase Spa15 expression. The progression of cell death can then be analyzed and compared to wildtype bacteria. If macrophage cell death is reduced and/or delayed with the $\Delta spa15/spa15^+$ complemented strain, then Spa15 interferes with IpaB-mediated pyroptosis of macrophages. Therefore, *Shigella* must reduce the level of Spa15 expression in order to effectively kill and escape from the macrophages. If cell death is not reduced with the $\Delta spa15/spa15^+$ complemented strain, then Spa15 does not interfere with IpaB-mediated pyroptosis of macrophages.

In order to further understand the differences between macrophages and epithelial cells with regards to Spa15 expression and secretion by *Shigella*, the level of caspase-1 expression and activation in epithelial cells needs to be analyzed. Studies have not identified whether IpaB activates caspase-1 in infected epithelial cells or if the same level

of caspase-1 activation occurs in infected epithelial cells as it does in infected macrophages. Caspase-1 expression and activation have been detected in epithelial cells (9, 28); and therefore, it is available for cleavage and activation by IpaB during *Shigella* infection. As mentioned above, IpaB is present in the cytoplasm of epithelial cells during infection (29). The fact that *Shigella* induces cell death in macrophages while it induces a pro-survival state in epithelial cells may be attributed to the secretion and expression of Spa15. However, the lack of caspase-1 activation in infected epithelial cells may also be important for *Shigella* to maintain the pro-survival state. Future studies should investigate the role of IpaB inside the cytoplasm of the epithelial cell. If caspase-1 is not activated by IpaB in epithelial cells, perhaps there is another function for IpaB. Determination of an alternative function will require additional experiments, possibly through protein interaction studies. Differences in the function of IpaB between macrophages and epithelial cells may lead to studies investigating how *Shigella* differentiates the two eukaryotic cell types. These studies will enhance our understanding of how *S. flexneri* survives *in vivo*.

*In vivo conditions and apoptotic stimuli*³.

The analyses performed throughout this dissertation have relied on tissue culture cells and chemical apoptosis inducers like STS. These conditions were needed to characterize apoptosis inhibition by *S. flexneri* but future experiments should aim to use physiologically relevant conditions. First, primary colonic epithelial cells could be used to confirm the anti-apoptosis observations made in HeLa cells. These primary cells are

³Excerpt adapted from the review article: Faherty, C.S. and A.T. Maurelli. Staying alive: bacterial inhibition of apoptosis during infection. *Trends in Microbiology*. 2008 April;16(4):173-80.

not only relevant to *Shigella* infection, but have the added benefit of not being immortalized like tissue culture cells. Immortalized cell lines are cancer cells, and these cells are already in an anti-apoptotic state. While STS is able to overcome this state in the HeLa cells, the use of primary colonic cells could identify additional pro-survival changes induced by the bacteria upon infection. In addition, the effects of TNF- α , IL-1 α , and IL-6 on neighboring epithelial cells during infection as discussed in chapter four could be analyzed in colonic epithelial cells. Second, physiologically relevant apoptosis inducers should be used in future experiments since these inducers occur during *Shigella* infection. As mentioned in chapter four, TNF- α and Fas ligand are present to activate the extrinsic pathway of apoptosis during infection while the transmigration of PMN cells across the colonic epithelium induces apoptosis in the epithelial cells (8, 13, 25). These conditions can be replicated in the laboratory setting and used to analyze the ability of *S. flexneri* to inhibit apoptosis in colonic epithelial cells. Reproducing physiological conditions is not only possible but important to facilitate an appropriate understanding of apoptosis inhibition during infection.

Conclusion

S. flexneri is a unique pathogen and has evolved to overcome many challenges from the host in order to survive *in vivo*. Extensive progress has been made to analyze how *S. flexneri* inhibits apoptosis in epithelial cells. This work has demonstrated for the first time that *Shigella* can inhibit apoptosis in epithelial cells, and *Shigella* is the only bacterial pathogen identified thus far that prevents caspase-3 activation directly. Second, the microarray analysis provided new insights into apoptosis inhibition by *S. flexneri*. The pro-

survival changes induced by the bacteria occur upon infection, and *Shigella* uses a multi-faceted approach to inhibit both pathways of apoptosis. Finally, the identification of Spa15 as the anti-apoptotic factor demonstrated for the first time that this bacterial protein is secreted through the T3SS.

Future experiments are needed to enhance our understanding of apoptosis inhibition by *S. flexneri*. These investigations include protein interaction studies, secretion and expression analyses, examination of the extrinsic pathway of apoptosis and NF- κ B activation, and utilization of physiologically-relevant conditions in experiments. The future experiments will lead to significant gains in the understanding of *Shigella* pathogenesis, which include the determination of how the bacteria differentiate macrophages from epithelial cells. This research can also lead to the development of novel therapeutics that would prevent *Shigella* from inhibiting apoptosis. If the bacteria cannot prevent apoptosis, *Shigella* will be exposed to the extracellular environment that is infiltrated by immune cells. In addition, the Δ *spa15* mutant may serve as a novel vaccine candidate since this strain is unable to avoid the immune system by surviving inside an intracellular niche. Future experiments could also benefit other researchers in understanding how bacterial pathogens inhibit apoptosis in host cells. Bacterial pathogens inhibit apoptosis to survive *in vivo*. In order to effectively treat and prevent infections, it is vital to understand the survival mechanisms of these pathogens.

References

1. **Abu-Zant, A., S. Jones, R. Asare, J. Suttles, C. Price, J. Graham, and Y. A. Kwaik.** 2007. Anti-apoptotic signalling by the Dot/Icm secretion system of *L. pneumophila*. *Cell. Microbiol.* **9**:246-264.

2. **Arndt, P. G., N. Suzuki, N. J. Avdi, K. C. Malcolm, and G. S. Worthen.** 2004. Lipopolysaccharide-induced c-Jun NH2-terminal kinase activation in human neutrophils: role of phosphatidylinositol 3-Kinase and Syk-mediated pathways. *J. Biol. Chem.* **279**:10883-10891.

3. **Binnicker, M. J., R. D. Williams, and M. A. Apicella.** 2004. Gonococcal porin IB activates NF-kappaB in human urethral epithelium and increases the expression of host antiapoptotic factors. *Infect. Immun.* **72**:6408-6417.

4. **Faherty, C. S., and A. T. Maurelli.** 2008. Staying alive: bacterial inhibition of apoptosis during infection. *Trends Microbiol.* **16**:173-180.

5. **Gutierrez-Venegas, G., and R. Castillo-Aleman.** 2008. Characterization of the transduction pathway involved in c-fos and c-jun expression induced by *Aggregatibacter actinomycetemcomitans* lipopolysaccharides in human gingival fibroblasts. *Int. Immunopharmacol.* **8**:1513-1523.

6. **Jennison, A. V., and N. K. Verma.** 2004. *Shigella flexneri* infection: pathogenesis and vaccine development. *FEMS Microbiol. Rev.* **28**:43-58.
7. **Jiang, Q., S. Akashi, K. Miyake, and H. R. Petty.** 2000. Lipopolysaccharide induces physical proximity between CD14 and toll-like receptor 4 (TLR4) prior to nuclear translocation of NF-kappa B. *J. Immunol.* **165**:3541-3544.
8. **Jung, H. C., L. Eckmann, S. K. Yang, A. Panja, J. Fierer, E. Morzycka-Wroblewska, and M. F. Kagnoff.** 1995. A distinct array of proinflammatory cytokines is expressed in human colon epithelial cells in response to bacterial invasion. *J. Clin. Invest.* **95**:55-65.
9. **Kolinska, J., V. Lisa, J. A. Clark, H. Kozakova, M. Zakostelecka, L. Khailova, M. Sinkora, A. Kitanovicova, and B. Dvorak.** 2008. Constitutive expression of IL-18 and IL-18R in differentiated IEC-6 cells: effect of TNF-alpha and IFN-gamma treatment. *J. Interferon. Cytokine Res.* **28**:287-296.
10. **Koterski, J. F., M. Nahvi, M. M. Venkatesan, and B. Haimovich.** 2005. Virulent *Shigella flexneri* causes damage to mitochondria and triggers necrosis in infected human monocyte-derived macrophages. *Infect. Immun.* **73**:504-513.
11. **Kroemer, G., L. Galluzzi, and C. Brenner.** 2007. Mitochondrial membrane permeabilization in cell death. *Physiol. Rev.* **87**:99-163.

12. **LaBrec, E. H., H. Schneider, T. J. Magnani, and S. B. Formal.** 1964. Epithelial cell penetration as an essential step in the pathogenesis of bacillary dysentery. *J. Bacteriol.* **88**:1503-1518.
13. **Le'Negrate, G., E. Selva, P. Auberger, B. Rossi, and P. Hofman.** 2000. Sustained polymorphonuclear leukocyte transmigration induces apoptosis in T84 intestinal epithelial cells. *J. Cell. Biol.* **150**:1479-1488.
14. **Lilic, M., M. Vujanac, and C. E. Stebbins.** 2006. A common structural motif in the binding of virulence factors to bacterial secretion chaperones. *Mol. Cell.* **21**:653-664.
15. **Lucchini, S., H. Liu, Q. Jin, J. C. Hinton, and J. Yu.** 2005. Transcriptional adaptation of *Shigella flexneri* during infection of macrophages and epithelial cells: insights into the strategies of a cytosolic bacterial pathogen. *Infect. Immun.* **73**:88-102.
16. **Mantis, N., M. C. Prevost, and P. Sansonetti.** 1996. Analysis of epithelial cell stress response during infection by *Shigella flexneri*. *Infect. Immun.* **64**:2474-2482.

17. **McCormick, B. A., A. M. Siber, and A. T. Maurelli.** 1998. Requirement of the *Shigella flexneri* virulence plasmid in the ability to induce trafficking of neutrophils across polarized monolayers of the intestinal epithelium. *Infect. Immun.* **66**:4237-4243.
18. **Miyairi, I., and G. I. Byrne.** 2006. *Chlamydia* and programmed cell death. *Curr. Opin. Microbiol.* **9**:102-108.
19. **Page, A. L., P. Sansonetti, and C. Parsot.** 2002. Spa15 of *Shigella flexneri*, a third type of chaperone in the type III secretion pathway. *Mol. Microbiol.* **43**:1533-1542.
20. **Palsson-McDermott, E. M., and L. A. O'Neill.** 2004. Signal transduction by the lipopolysaccharide receptor, Toll-like receptor-4. *Immunology.* **113**:153-162.
21. **Parsot, C., E. Ageron, C. Penno, M. Mavris, K. Jamoussi, H. d'Hauteville, P. Sansonetti, and B. Demers.** 2005. A secreted anti-activator, OspD1, and its chaperone, Spa15, are involved in the control of transcription by the type III secretion apparatus activity in *Shigella flexneri*. *Mol. Microbiol.* **56**:1627-1635.
22. **Pedron, T., C. Thibault, and P. J. Sansonetti.** 2003. The invasive phenotype of *Shigella flexneri* directs a distinct gene expression pattern in the human intestinal epithelial cell line Caco-2. *J. Biol. Chem.* **278**:33878-33886.

23. **Pirbhai, M., F. Dong, Y. Zhong, K. Z. Pan, and G. Zhong.** 2006. The secreted protease factor CPAF is responsible for degrading pro-apoptotic BH3-only proteins in *Chlamydia trachomatis*-infected cells. *J. Biol. Chem.* **281**:31495-31501.

24. **Pridmore, A. C., G. A. Jarvis, C. M. John, D. L. Jack, S. K. Dower, and R. C. Read.** 2003. Activation of toll-like receptor 2 (TLR2) and TLR4/MD2 by *Neisseria* is independent of capsule and lipooligosaccharide (LOS) sialylation but varies widely among LOS from different strains. *Infect. Immun.* **71**:3901-3908.

25. **Raqib, R., C. Ekberg, P. Sharkar, P. K. Bardhan, A. Zychlinsky, P. J. Sansonetti, and J. Andersson.** 2002. Apoptosis in acute shigellosis is associated with increased production of Fas/Fas ligand, perforin, caspase-1, and caspase-3 but reduced production of Bcl-2 and interleukin-2. *Infect. Immun.* **70**:3199-3207.

26. **Reed, J. C.** 2000. Mechanisms of apoptosis. *Am. J. Pathol.* **157**:1415-1430.

27. **Sansonetti, P. J., J. Arondel, J. R. Cantey, M. C. Prevost, and M. Huerre.** 1996. Infection of rabbit Peyer's patches by *Shigella flexneri*: effect of adhesive or invasive bacterial phenotypes on follicle-associated epithelium. *Infect. Immun.* **64**:2752-2764.

28. **Satoh, Y., Y. Ishiguro, H. Sakuraba, S. Kawaguchi, H. Hiraga, S. Fukuda, and A. Nakane.** 2009. Cyclosporine Regulates Intestinal Epithelial Apoptosis via TGF- β Related Signaling. *Am. J. Physiol. Gastrointest. Liver Physiol.* PMID: 19608730.

29. **Schuch, R., R. C. Sandlin, and A. T. Maurelli.** 1999. A system for identifying post-invasion functions of invasion genes: requirements for the Mxi-Spa type III secretion pathway of *Shigella flexneri* in intercellular dissemination. *Mol. Microbiol.* **34**:675-689.

30. **Voino-Tasenetsky, M. V., and T. N. Khavkin.** 1964. A study of the intraepithelial localization of dysentery-causing agents by means of fluorescent antibodies. *J. Microbiol.* **12**:98-100.

31. **Zychlinsky, A., B. Kenny, R. Menard, M. C. Prevost, I. B. Holland, and P. J. Sansonetti.** 1994. IpaB mediates macrophage apoptosis induced by *Shigella flexneri*. *Mol. Microbiol.* **11**:619-627.

32. **Zychlinsky, A., M. C. Prevost, and P. J. Sansonetti.** 1992. *Shigella flexneri* induces apoptosis in infected macrophages. *Nature.* **358**:167-169.

33. **Zychlinsky, A., K. Thirumalai, J. Arondel, J. R. Cantey, A. O. Aliprantis, and P. J. Sansonetti.** 1996. *In vivo* apoptosis in *Shigella flexneri* infections. Infect. Immun. **64**:5357-5365.